PROCEEDINGS OF IGY SYMPOSIUM

VOL. I

February 13-16, 1961, New Delhi

COUNCIL OF SCIENTIFIC & INDUSTRIAL RESEARCH
NEW DELHI

27

CFTRI Experiment STATION
Dy/ACC No. 388
Date...26.7.76
Gill Road LUDHIANA-3.

PROCEEDINGS OF
IGY SYMPOSIUM

PROCEEDINGS OF IGY SYMPOSIUM

VOL. I

February 13-16, 1961, New Delhi

Under the auspices of

INDIAN NATIONAL COMMITTEE FOR IGY
PHYSICAL RESEARCH COMMITTEE OF CSIR
RADIO RESEARCH COMMITTEE OF CSIR

COUNCIL OF SCIENTIFIC & INDUSTRIAL RESEARCH
NEW DELHI

© 1962
COUNCIL OF SCIENTIFIC & INDUSTRIAL RESEARCH
NEW DELHI, INDIA

A(F) N62.1

Scientific & Research Library
No. 271
7 JAN 1985
C.F.T.R.I. Experiment Station. LUDHIANA-6

PRINTED AT THE CATHOLIC PRESS, RANCHI, INDIA

PREFACE

The Council of Scientific & Industrial Research organized a symposium at the National Physical Laboratory, New Delhi, in February 1961 under the Chairmanship of the late Prof. K. S. Krishnan to discuss the scientific results of the International Geophysical Year (IGY) work done in India. Papers on various geophysical subjects were presented and discussed at the symposium and the Council has arranged to publish the papers in two volumes. In this first volume, papers and abstracts of papers relating to Ionospheric morphology and true height profiles; Ionospheric drift; Ionospheric absorption; Solar terrestrial relationships; and other related topics have been included. Some of the papers which were presented have already been published in scientific journals; and only abstracts of them are included. The present volume is to be followed by a second one in which papers on Meteorology; Geomagnetism; Aurora and airglow; Cosmic rays; Oceanography; Outer space; Seismology; and Nuclear radiation will be published.

Thanks are due to Dr A. P. Mitra for collecting and preparing the papers for publication.

K. R. Ramanathan
Chairman
Indian National Committee of the IGY

Ahmedabad
August 10, 1962

ABBREVIATIONS USED

CRPL	Central Radio Propagation Laboratory, Boulder (Colorado)
CSAGI	Special Committee of the International Geophysical Year
CRNA	Cosmic Radio Noise Absorption
CW	Continuous Wave
DPDT	Double Pole Double Throw
EMT	Eastern Mean Time
IGC	International Geophysical Cooperation
IGY	International Geophysical Year
RWD	Regular World Days
SC	Sudden Commencement
SCNA	Sudden Cosmic Noise Absorption
SD	Sidereal Day
SEA	Sudden Enhancement of Atmospherics
s.f.e.	solar flare effect
SID	Sudden Ionospheric Disturbances
SPA	Sudden Phase Anomaly
SWF	Short Wave Fade-out
SWI	Special World Intervals
WMI	World Meteorological Intervals

CONTENTS

PREFACE v

Advances in Ionosphere and Aeronomy during IGY 1
A. P. MITRA

IONOSPHERIC MORPHOLOGY AND TRUE HEIGHT PROFILES

Ionospheric Observations at Tiruchirapalli 40
S. RANGASWAMY & C. S. R. RAO

Ionosphere over Trivandrum: Part II — Ionospheric Observations during 1957–59 48
CH. SATYANARAYANMURTHY

Determination of Loss Coefficient in F Region from True Height Profiles over Delhi 57
K. K. MAHAJAN & A. P. MITRA

A Note on Changes of Maximum of Ionization of F_1 Layer Associated with Sunspot Activity 64
C. S. G. K. SETTY & I. R. KAMAL

Ionosphere over Trivandrum: Part I — Total Electron Content in the Ionosphere (*Abstract*) 70
C. S. R. RAO & T. N. RANGANATHAN

Ionosphere over Trivandrum: Part III — Profiles and Electron Distribution in the Ionosphere (*Abstract*) 70
C. S. R. RAO & S. C. BOSE

IONOSPHERIC DRIFT

A New Ionospheric Drift Recorder 72
B. RAMACHANDRA RAO & R. RAGHAVA RAO

Height Variation of Anisotropy and Drift of Irregularities in the Ionosphere 80
B. RAMACHANDRA RAO & K. V. V. RAMANA

Effects of Moving Anisometric Irregularities in F Region of Ionosphere 85
R. N. SINGH

Horizontal Drift in the Ionosphere over Delhi (*Abstract*) ... 95
S. N. MITRA, K. K. VIJ & P. DASGUPTA

Study of Horizontal Drifts in the E Region at Waltair (*Abstract*)... 96
R. RAGHAVA RAO & B. RAMACHANDRA RAO

Simultaneous Study of Drifts at Different Levels in the Ionosphere by Spaced Receiver Method (*Abstract*) 96
E. BHAGIRATHA RAO & B. RAMACHANDRA RAO

Statistical Analysis of Fading of a Single Downcoming Wave (*Abstract*) 97
P. DASGUPTA & K. K. VIJ

IONOSPHERIC ABSORPTION

Results of Cosmic Noise Observations at Delhi on 22·4 Mc/s. ... 98
K. A. SARADA & A. P. MITRA

Ionospheric Absorption Using Cosmic Radio Noise on 25 Mc/s. at Ahmedabad 117
R. V. BHONSLE

Ionospheric Absorption over Delhi during IGY and IGC ... 132
M. K. RAO, S. C. MAZUMDAR & S. N. MITRA

Ionospheric Absorption on 2·5/2·6 Mc/s. at Ahmedabad ... 142
J. S. SHIRKE

Collision Frequency Measurements in Ionosphere at Waltair ... 149
K. V. V. RAMANA & B. RAMACHANDRA RAO

Effect of Magnetic Activity on Night-time Absorption 155
K. V. V. RAMANA, Y. V. RAMANA MURTY & B. RAMACHANDRA RAO

Diurnal Variation of Absorption on 5·65 Mc/s. at Waltair (*Abstract*) ... 157
B. RAMACHANDRA RAO & K. V. V. RAMANA

SOLAR TERRESTRIAL RELATIONSHIPS

Sudden Cosmic Radio Noise Absorption Associated with Solar Flares 158
K. A. SARADA & A. P. MITRA

Effect of Solar Flares on E Region Drifts at Waltair 171
R. RAGHAVA RAO & B. RAMACHANDRA RAO

Effect of Geomagnetic Disturbances on F_2 Layer of the Ionosphere in Low and Middle Latitudes 176
K. M. KOTADIA & K. R. RAMANATHAN

CONTENTS

Geomagnetic Disturbance Effects in Equatorial E_s 197
B. N. BHARGAVA & R. V. SUBRAHMANYAN

Effect of Magnetic Activity on E Region Drifts at Waltair ... 202
R. RAGHAVA RAO & B. RAMACHANDRA RAO

Effect of Magnetic Activity on Horizontal Drifts in F_2 Region ... 205
B. RAMACHANDRA RAO, E. BHAGIRATHA RAO &
Y. V. RAMANA MURTY

Some Characteristics of Enhanced Solar Radio Emission at 28·6 Mc/s. 212
M. KRISHNAMURTHI & S. RAMAKRISHNA

A Study of Sudden Enhancement of Atmospherics on 27 kc/s. Band (*Abstract*) 218
M. W. CHIPLONKAR & R. N. KAREKAR

Changes in the Electron Density Distribution in the Ionosphere over Ahmedabad Associated with Solar Flares and Magnetic Storms: Part I — July 10–20, 1959 (*Abstract*) 218
S. S. DEGAONKAR

Spread F and Geomagnetic Activity (*Abstract*) 219
C. V. S. RAO & S. N. MITRA

Geomagnetic Field and Ionospheric Drift (*Abstract*) 219
S. N. MITRA & K. K. VIJ

Magnetic Storms and Cosmic Radio Noise on 25 Mc/s. at Ahmedabad (*Abstract*) 220
R. V. BHONSLE & K. R. RAMANATHAN

IONOSPHERIC IRREGULARITIES

Variation of Angle of Arrival of Downcoming Radio Waves and Irregularities in the Ionosphere 221
S. S. BANERJEE & P. K. MUKHERJEE

Focussing Effects due to Large Scale Irregularities in F_2 Layer ... 233
G. SIVARAMA SASTRY, T. SESHAGIRI RAO &
M. KRISHNAMURTHI

Ionospheric Propagation of Atmospherics (*Abstract*) 237
M. W. CHIPLONKAR & M. S. HATTIANGADI

A Directional Study of Atmospherics for Climatology (*Abstract*) ... 238
M. W. CHIPLONKAR & T. A. RAJU

On the Law of Propagation of Atmospherics on 175 kc/s. (*Abstract*) 238
M. W. CHIPLONKAR & T. A. RAJU

Flutter Fading of Short Wave Radio Signals in Equatorial Regions and its Connection with Spread Echoes, Magnetic Storms and the Radiation Belt (*Abstract*) 239
CHAMAN LAL

APPENDICES 240

AUTHOR INDEX 246

Advances in ionosphere and aeronomy during IGY

A. P. MITRA

National Physical Laboratory
New Delhi

Some of the major advances in ionosphere and aeronomy during the IGY have been discussed under the following heads: (i) the high atmosphere, including atmospheric models deduced from observations involving rockets and satellites, (ii) the ionosphere, with reference to the characteristics of the polar and the equatorial ionosphere obtained by ionosondes and other techniques, and the outer ionosphere as deduced from experiments involving satellite transmission, cosmic radio noise and incoherent scatter, (iii) some new techniques such as the whistlers, the cosmic radio noise and the Argus project, (iv) solar flares and ionospheric ionization, and (v) physics of the ionosphere.

As in the other fields of geophysics, the IGY work on ionosphere has been considerable and achievements many. It is well to remember that during the first Polar Year the ionosphere was unknown, and during the second, the technique of exploration of the ionosphere had only recently been developed. There was no automatic equipment available, and the kind of information that we now get in a modern routine ionogram had to be pieced together from several observations. Nevertheless, certain discoveries were made of which mention may be made of the phenomena of ionospheric disturbances in polar latitudes, as an example.

In the twenty-five years that followed the second Polar Year, automatic equipments have been devised for obtaining quick ionograms at a predetermined schedule, new techniques have been developed for studying drifts and absorption in the ionosphere; and the techniques of radio astronomy have been employed for studying the regions beyond the maximum of the F_2 region, normally inaccessible to terrestrial radio techniques, now known as outer ionosphere, and the whistlers have been discovered and studied.

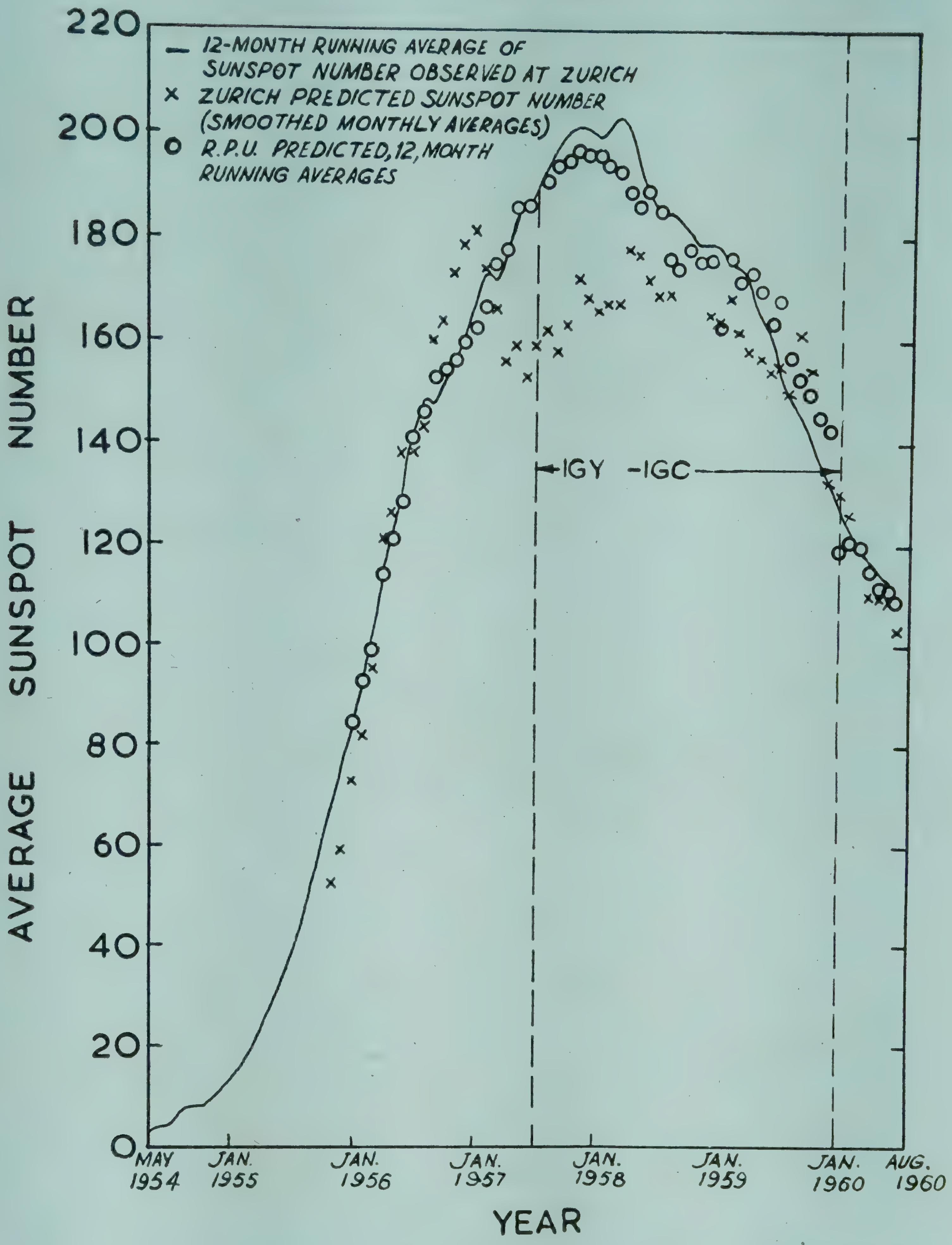

Fig. 2 — Details of present sunspot cycle and predictions from Zürich and NPL, Delhi

previous sunspot cycles covering a period of over 200 years, and the periods for the IGY–IGC and the first two Polar Years are indicated. The great difference in the sunspot activity between the IGY–IGC and the Polar Years may be noted.

In Fig. 2 the present sunspot cycle and the periods of the IGY and the IGC are shown in greater detail. It will be noticed that during the entire

TABLE 2 — SUNSPOT NUMBERS AND FREQUENCY OF LARGE STORMS SINCE LAST QUIET SUN OF 1954

	1954	1955	1956	1957	1958	1959	1960	TOTAL
Sunspot number	4	38	142	190	185	159	142	—
Storms with highest K_p of 7	2	2	9	12	12	7	9	53
Storms with highest K_p of 8	—	3	7	5	4	7	3	29
Storms with highest K_p of 9	—	—	1	6	3	2	2	14
All	2	5	17	23	19	16	14	96

period of 2½ years during the IGY and IGC, unusually high solar activity was maintained. The 12-month running average sunspot number never went below 180 during this period and was around 200 for a substantial portion of the time. The monthly average sunspot number varied over the range 125–205.

Predictions of the sunspot number made at Zürich and at the Radio Propagation Unit of New Delhi are also indicated in the figure.

As a result of the high solar activity, solar flares and magnetic storms occurred in great numbers during this period. Dodson and Hedeman[1] reported that during the period July 1957 to December 1958, a total of 6762 flares were observed, of which 835 were of class 1^-, 5389 of class 1, 497 of class 2 and 41 of class 3 and 3^+. Magnetic storms were also numerous, many of them severe. Kodaikanal reported 69 magnetic storms during the IGY–IGC of which 14 were classified as ‘ severe ’. Five of these occurred in September 1957 alone and three in July 1959. July 1959, in particular, was a period of great disturbance and a subject of coordinated international study. Bartels[2] noted that of the 96 large storms (having highest K_p values of 7 and above) that occurred during the seven years since the last quiet sun of 1954, 23 occurred in 1957 alone. Similarly, of the 14 storms having highest K_p values of 9 that occurred during this period, 6 occurred in 1957 (Table 2).

THE HIGH ATMOSPHERE

There have been revolutionary advances in upper atmospheric physics, arising principally from the successful launching of satellites and also to some extent, from the greatly increased frequency of rocket soundings during the IGY and IGC. These advances have been responsible for: (i) increased accuracy in the determination of atmospheric density at heights below 200 km.; and (ii) extension of density values from the pre-IGY values of 200 km. to 1700 km. in the post-IGY/IGC era.

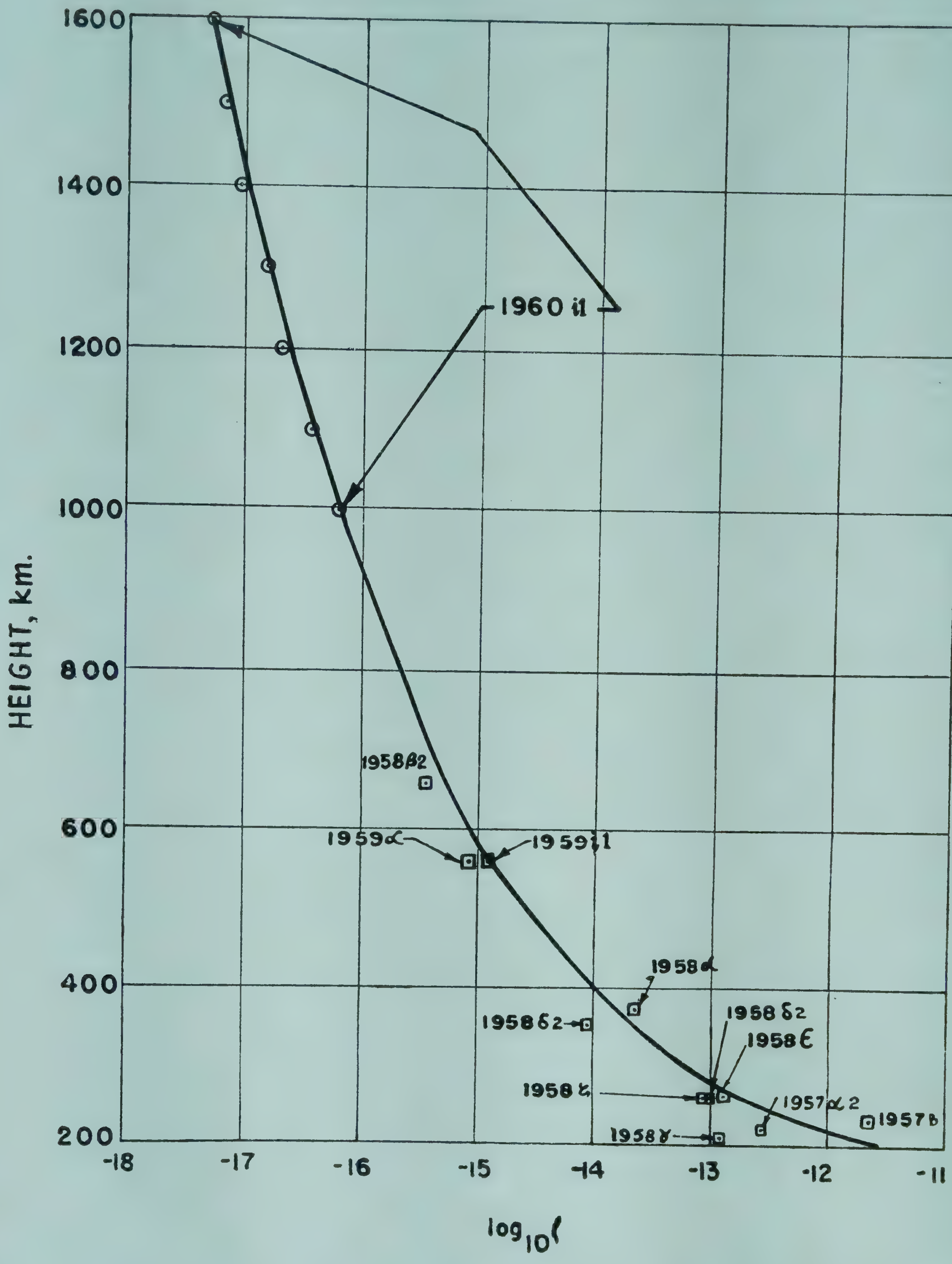

FIG. 3 — DENSITY VALUES OBTAINED FROM OBSERVATIONS OF DIFFERENT SATELLITES AS A FUNCTION OF HEIGHT

The density values obtained from satellites have depended principally on the observations of the changes in the orbital elements caused by satellite drag; and refer to heights somewhat above the perigee heights of the satellites. Both U.S.S.R. and U.S. satellites have been used. The U.S.S.R. satellites launched during this period orbited at somewhat lower altitudes

TABLE 3 — DENSITY VALUES CALCULATED FROM DIFFERENT SATELLITES OBSERVATIONS

HEIGHT km.	DENSITY g./cm.^{3}	SATELLITE	AUTHOR(S)
220	$1{\cdot}3\times10^{-13}$	1958 γ	Sterne[3]
228	$2{\cdot}8\times10^{-13}$	1957 α2	Schilling & Sterne[4]
233	$2{\cdot}2\times10^{-12}$	1957 β	Schilling & Sterne[4]
260	$1{\cdot}0\times10^{-13}$	1958 δ2	Krassovsky[5]
260	$9{\cdot}0\times10^{-14}$	1958 δ	Groves[6]
263	$1{\cdot}3\times10^{-13}$	1958 ε	Schilling & Whitney[7]
355	$8{\cdot}8\times10^{-15}$	1958 δ2	Schilling & Whitney[7]
368	$1{\cdot}4\times10^{-14}$	1958 α	Schilling & Sterne
558	$8{\cdot}8\times10^{-16}$	1959 α	Groves
560	$1{\cdot}2\times10^{-15}$	1959 *i*1	Martin & Priester[8]
656	$3{\cdot}5\times10^{-16}$	1958 β2	Jachhia[13]
1000	$6{\cdot}6\times10^{-17}$	1960 *i*1	Romer[12]
1100	$3{\cdot}6\times10^{-17}$		
1200	$2{\cdot}1\times10^{-17}$		
1300	$1{\cdot}4\times10^{-17}$		
1400	$9{\cdot}3\times10^{-18}$		
1500	$6{\cdot}8\times10^{-18}$		
1600	$5{\cdot}2\times10^{-18}$		

than the U.S. satellites, and have therefore yielded density values over a wide range of heights. The satellites used for this purpose were Sputnik I (1957 α2), Sputnik II (1957 β), Explorer I (1958 α), Vanguard I (1958 β2), Sputnik III (1958 δ2), Explorer IV (1958 ε), Vanguard II (1959 α1), Discoverer VI (1959 ζ) and Explorer VII (1959 *i*1). The perigee heights and the corresponding densities are outlined in Table 3 and are also given in Fig. 3. The lowest perigee height, amongst these satellites, is that of Explorer III (228 km.) and the highest that of Vanguard I (656 km.). The more recent results of Echo I are also included in the table, although the Echo satellite was a post-IGY event, because these results have extended density values greatly in excess of these heights (to 1700 km.).

Such determinations, for which already a voluminous literature[3–10] exists, indicate that, for heights above 200 km., the atmospheric density is appreciably higher, on the average, than was thought of before satellite drag data became available. In Fig. 4, the atmospheric models given by a number of authors for the height range 200–700 km. are given and the pre-IGY model of Hulbert[11] (extrapolated to 700 km.) is shown for comparison. The model marked CIRA 1961[12] needs special mention: this was prepared recently by a specially constituted COSPAR committee and representing aeronomists from all major scientific groups. In contrast, the density distributions below 200 km. show little changes from the pre-IGY values (Fig. 5).

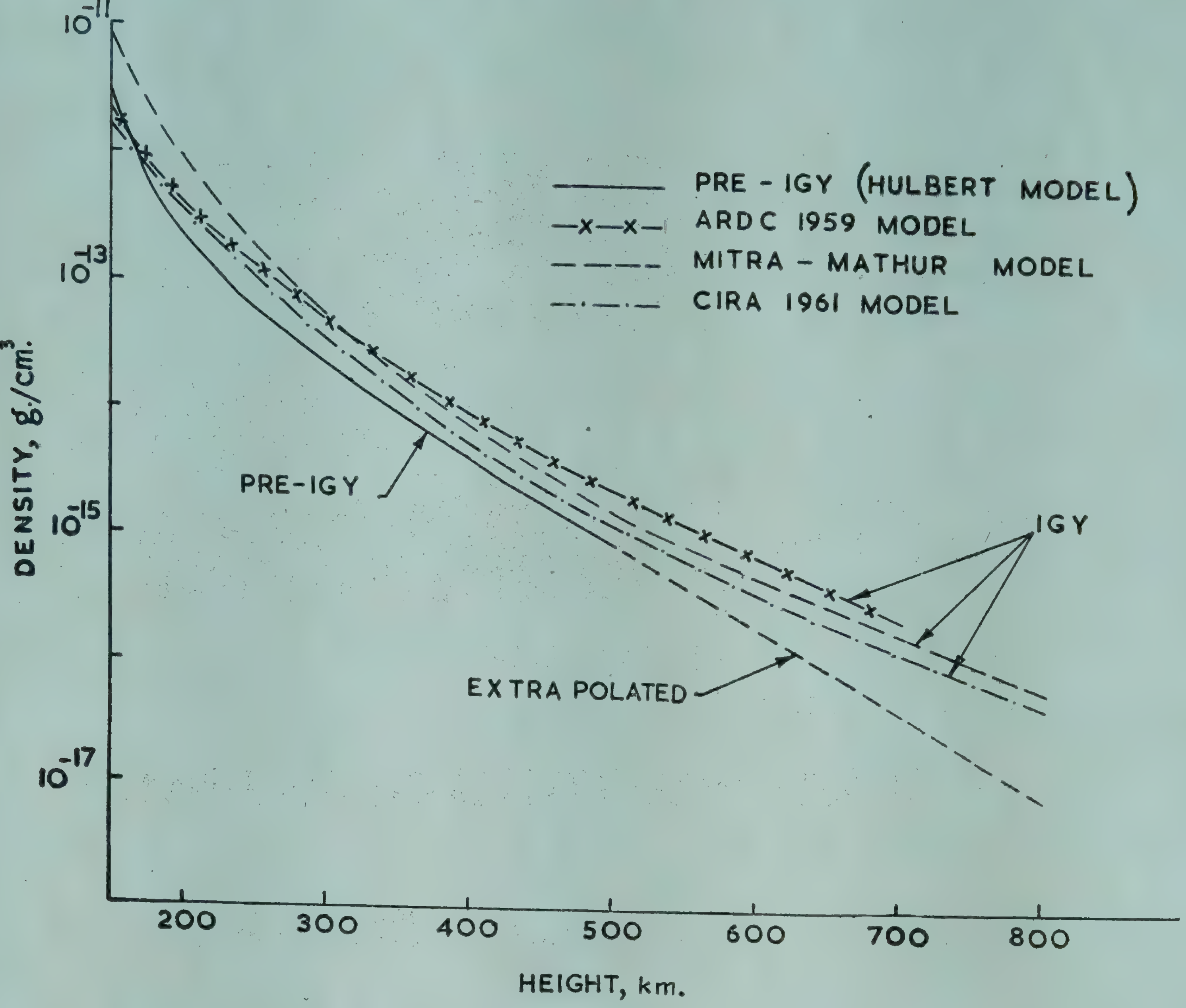

FIG. 4 — THEORETICAL DENSITY MODELS FOR THE UPPER ATMOSPHERE FOR HEIGHTS 150–800 KM. BASED ON ROCKETS AND SATELLITE MEASUREMENTS (PRE-IGY MODEL IS SHOWN FOR COMPARISON)

What we have discussed above may be called ‘ average ’ values. At high altitudes, atmospheric density is found to have an appreciable diurnal and annual variation, although no definite variation of air density with latitude (except for a possible increase of about 60 per cent over the winter pole) has been observed.

The diurnal variation is small for altitudes below 280 km., but the magnitude of the variation increases at greater heights. As a result of diurnal heating, the maximum density occurs about two hours after midday and the minimum about two hours before sunrise. The maximum and minimum density models as given in CIRA 1961 are shown in Fig. 6. These models refer to the period 1958–59 and hence to relatively high solar activity. It has been observed that the atmospheric density is very sensitive to solar activity and all accelerations of the satellite with perigee heights between 200 and 1600 km. show a good correlation with the flux of the solar decimeter radiation (3–30 cm.)[13] (Fig. 7). The effect increases at greater altitudes: comparison between the variations of orbital acceleration of Vanguard I and Sputnik III, during 1500 revolutions (about 5 months) over the period April

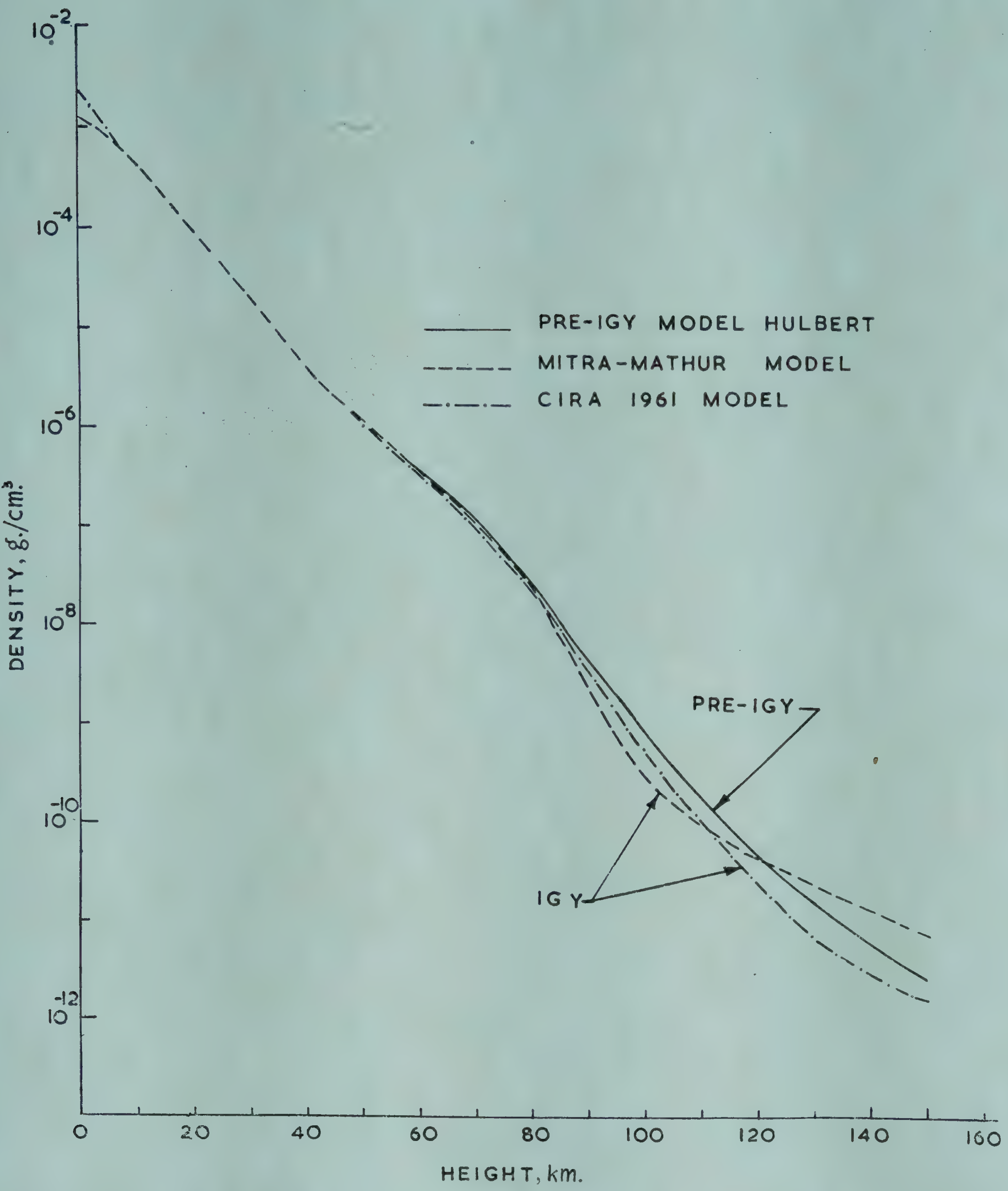

FIG. 5 — DENSITY DISTRIBUTIONS IN THE UPPER ATMOSPHERE BELOW 150 KM.

to December 1958, indicates a variation of ±50 per cent for Vanguard with perigee around 650 km., and ±20 per cent for Sputnik III with perigee around 250 km. According to Nicolet[14], such variations must result from a change in the atmospheric conditions below 150 km., due to heat conducted from higher levels where ultraviolet radiation is absorbed, and perhaps in addition from a variation in the heat flow coming from the top of the atmosphere. Nicolet estimates the heat flow to be of the order of 0·15 erg cm.$^{-2}$ sec.$^{-1}$. Increase in atmospheric density due to corpuscular heating following major solar flares has also been observed[15] (Fig. 8).

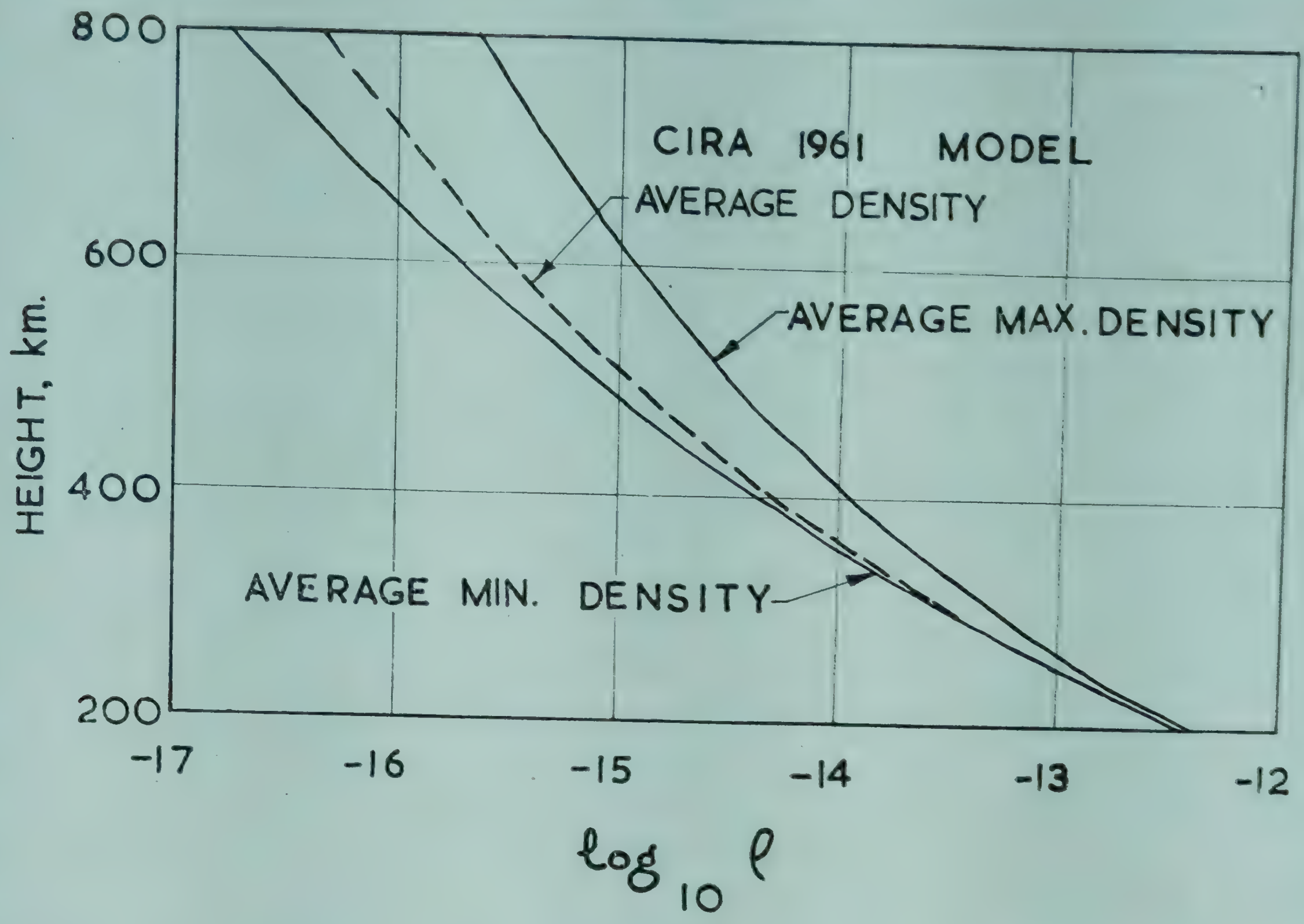

Fig. 6 — Maximum and minimum densities in the upper atmosphere as given by the COSPAR International Reference Atmosphere (CIRA 1961)

Composition. At low altitudes the atmosphere consists principally of O_2 and N_2 in the ratio 0·2683 : 1, the mean molecular weight being 28·966. Molecular oxygen is substantially dissociated at heights above 90 km., and molecular nitrogen at somewhat greater heights, thus altering the mean molecular weight at heights above 90 km. The distribution of the various atmospheric constituents will depend on the distribution of molecular and atomic oxygen in the dissociation region, on the distribution of temperature and on the level of diffusive separation. Molecular weight and temperature above 100 km. are the least known quantities.

The composition of the high atmosphere can be evaluated by direct sampling, atmospheric absorption of solar radiation, and use of mass spectrometer. The second method[16,17], in particular, has been used with great success in determining the distribution of atomic oxygen in the important region of 90–110 km. The method is based on measurements made by photon counters using the different wavelength ranges: in one, the counter is sensitive only to the band 1425–1500 Å near the centre of a Hartley band of molecular oxygen; in the other, the counter is sensitive to a band of X-rays, 45–55 Å, for which the absorption coefficient (air) is $2{\cdot}2\text{–}3\times10^{-19}$ cm.²/sec. The radiation in 1425–1500 Å is only absorbed by molecular oxygen, and so the intensity of the radiation at any height is a measure of the total oxygen content above this height. Results obtained at New Mexico and

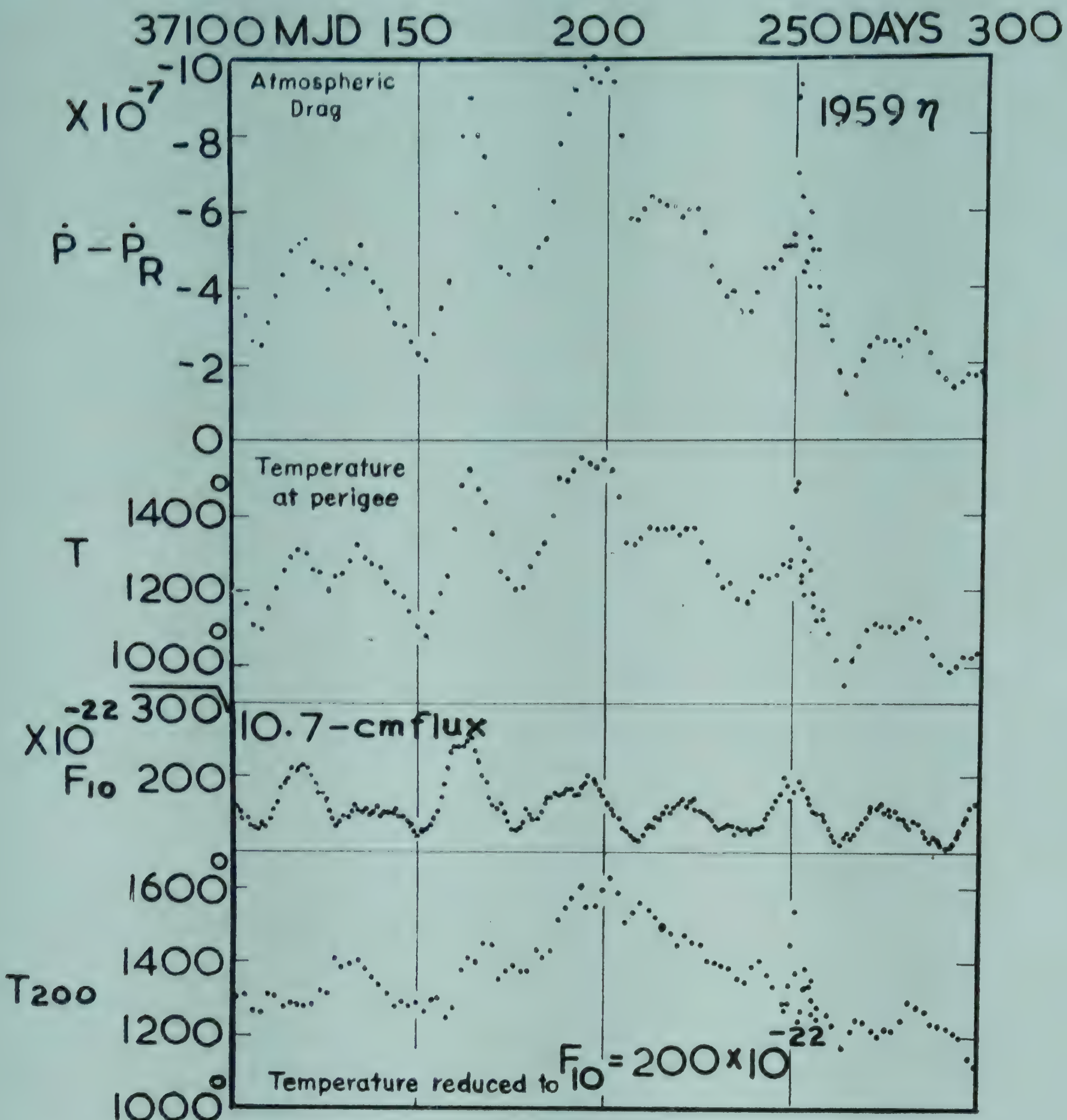

FIG. 7 — SATELLITE 1959 η: ATMOSPHERIC DRAG, TEMPERATURE T(°K.), 10·7 CM. FLUX F_{10} AND TEMPERATURE T_{200} REDUCED TO STANDARD FLUX $F_{10} = 200$, DURING A PERIOD OF LIVELY '27-DAY' FLUCTUATIONS

Fort Churchill are shown in Fig. 9. In the same figure results of a theoretical study by Nicolet[16] involving the photochemistry of oxygen in the lower ionosphere are also indicated. It will be observed that molecular oxygen is rapidly dissociated at heights above 80 km., and that at a height of 110 km., the ratio of the particle density of atomic oxygen to the particle density of molecular oxygen, $n(O)/n(O_2)$ may have a value around 2.

The question of determining the level at which diffusive separation of the atmospheric constituents occurs is very important, for at heights above this level each constituent will be distributed according to its own scale height, thus causing a filtering out of the heavier constituents. Mass spectrometers flown by Townsend and co-workers in three Aerobee-Hi firings just before

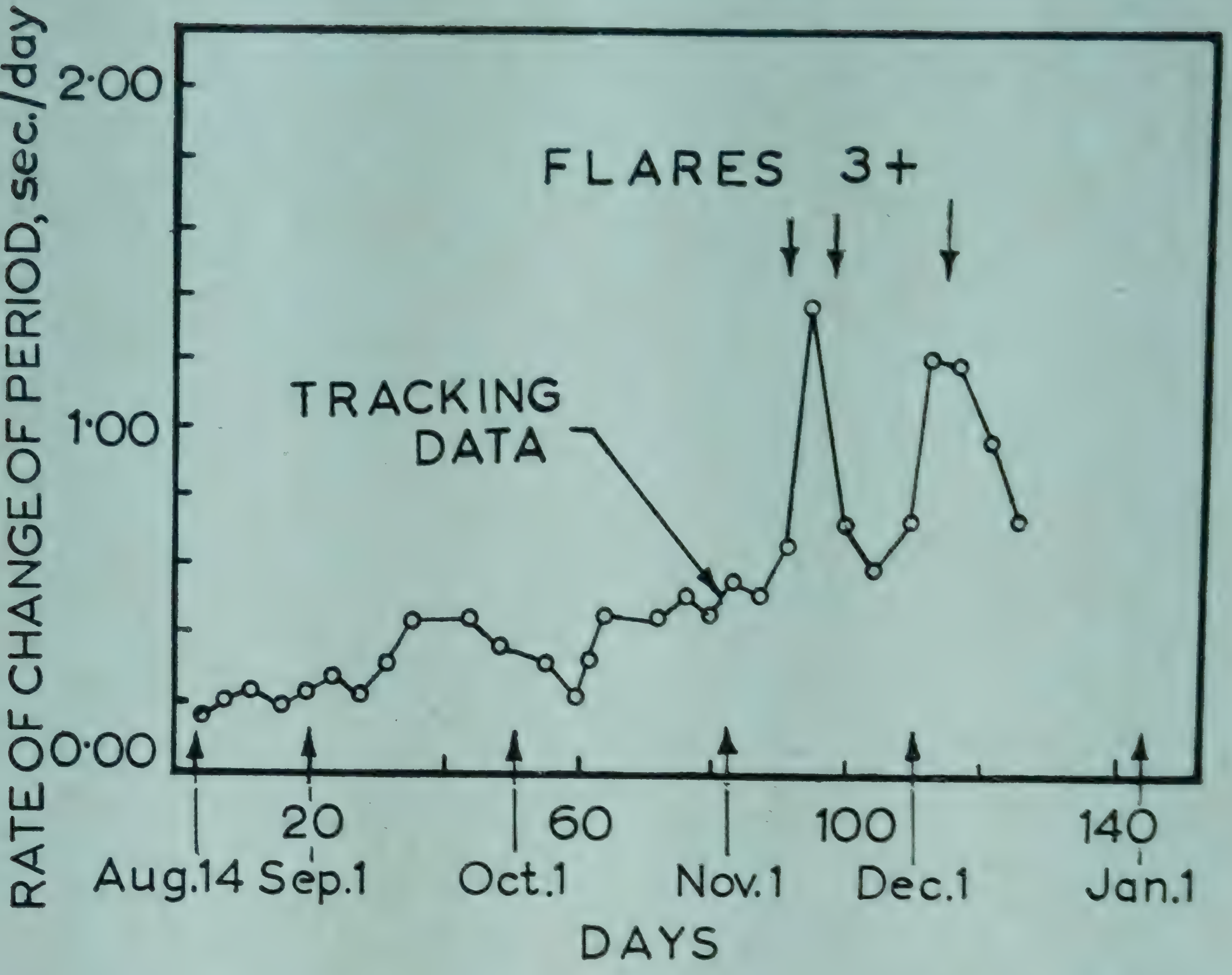

Fig. 8 — Sudden increases in the rate of change of orbital period of Echo I in late November and early December 1960, with the occurrence of strong flare activity on the sun

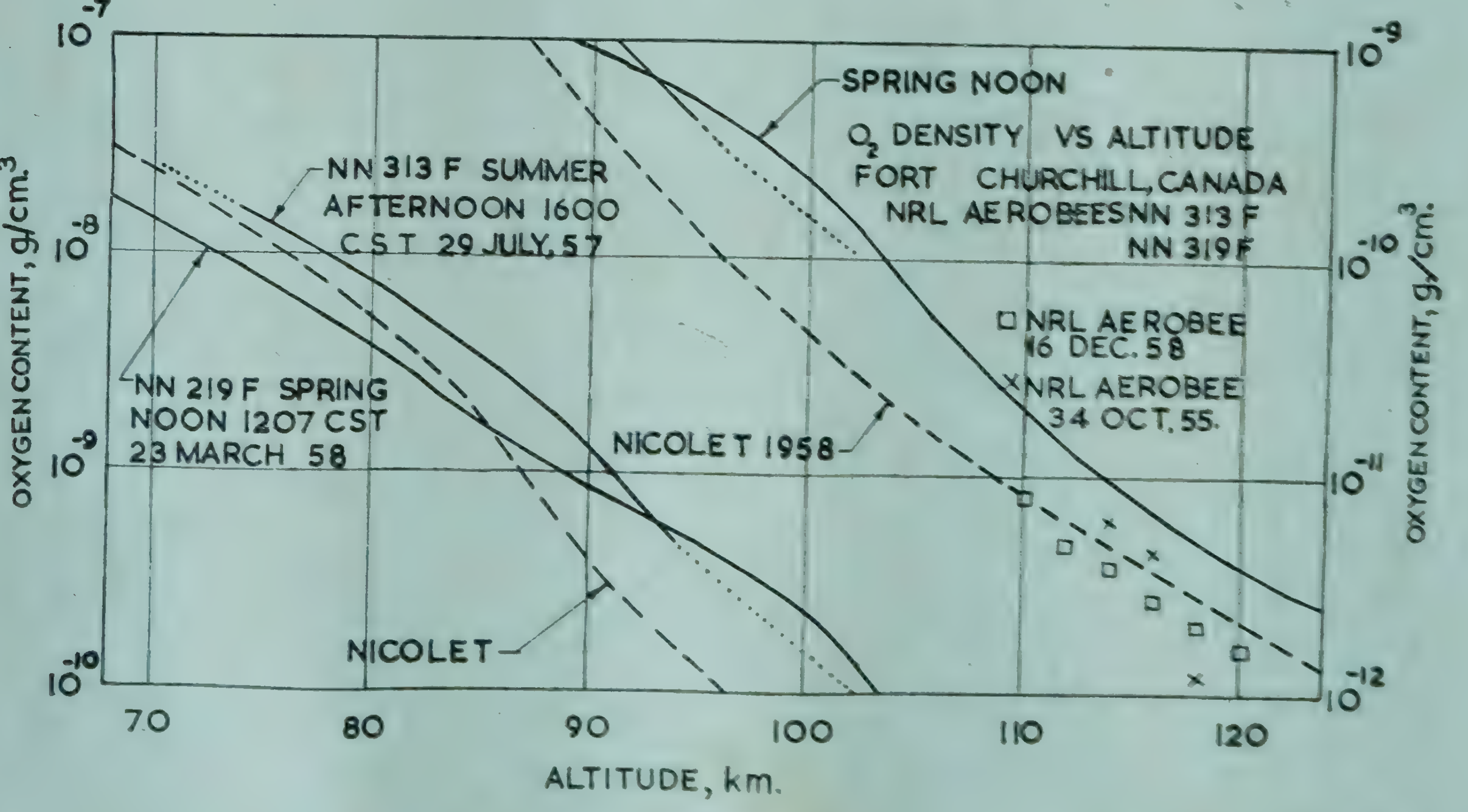

Fig. 9 — Distribution of molecular oxygen in the upper atmosphere obtained from rocket observations

and during the IGY showed that separation of argon relative to nitrogen becomes effective at altitudes between 100 and 120 km.

It has previously been indicated that the most uncertain parameters in the high atmosphere are the mean molecular weight (m), and the atmospheric temperature (T). The scale height (H) being a function of both m and T ($H = kT/mg$), any determination of the scale height from experimental data, such as density profiles, only indicates how (T/m) varies, but does not provide independent values for T and m. Theoretical interpretations from different authors have varied, depending principally on the assumptions of diffusive separation. The COSPAR Working Group on Reference Atmosphere, recognizing the uncertainties in molecular weight, proposed the following approximate values:

Altitude, *km.*	Molecular weight
100	28·966 (sea level value)
200	27·00
400	20·00
600	16·00
800	16·00

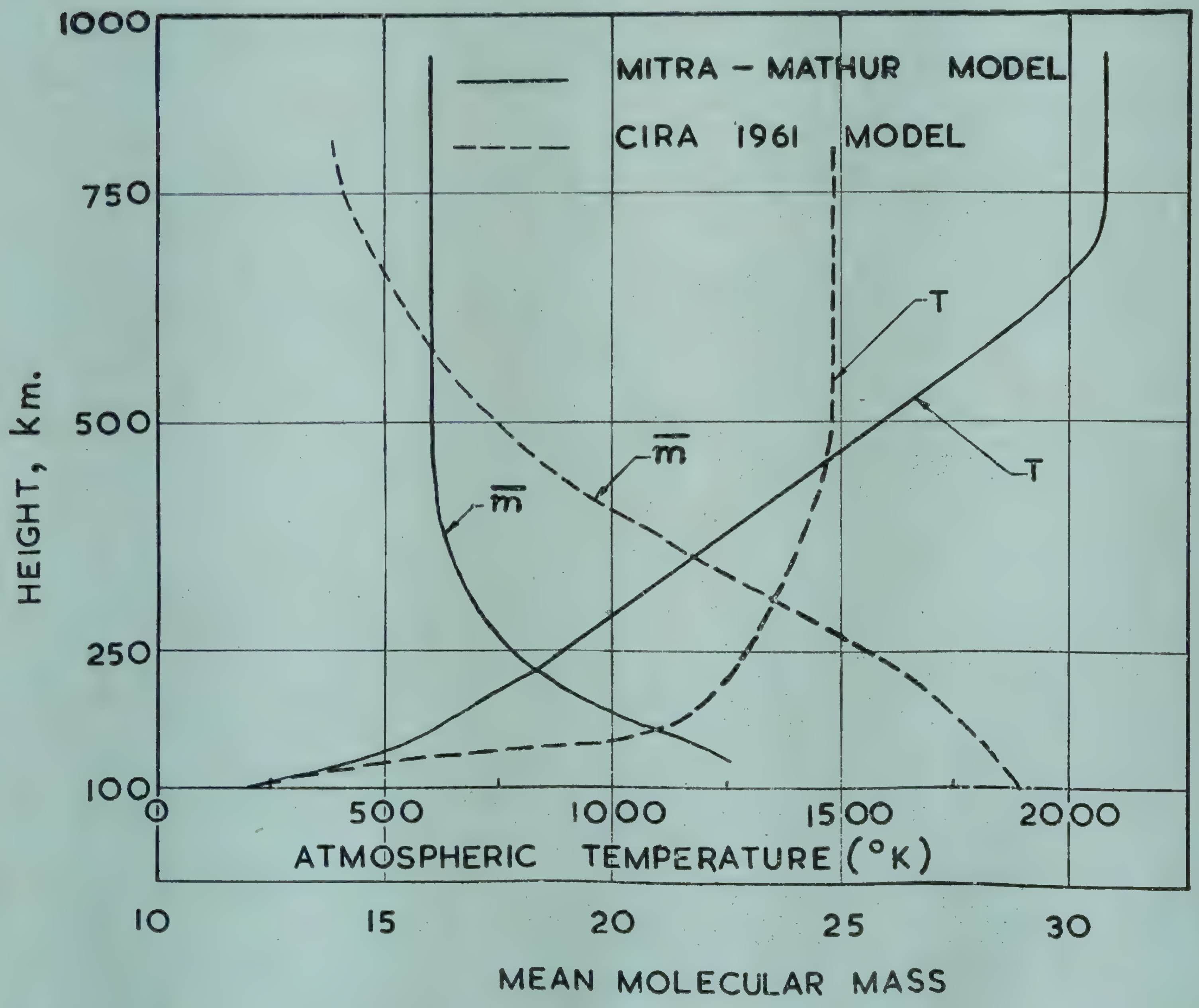

FIG. 10 — DISTRIBUTION OF MEAN MOLECULAR MASS AND TEMPERATURE IN THE HIGH ATMOSPHERE FOR TWO MODELS: CIRA 1961, AND MITRA-MATHUR MODEL

TABLE 4 — MOLECULAR WEIGHT AND TEMPERATURE OF ATMOSPHERE AT 500 km.

CONDITION	MOL. WT	TEMPERATURE °*K*.	REFERENCE
Minimum	16·59	1186	CIRA 1961
	17·90	1180	Nicolet
	15·62	1050	Kallman-Bijl
Average	16·00	1591	Mathur & Mitra
	17·48	1474	Nicolet
	18·32	1580	Kallman-Bijl
	16·85	1389	CIRA 1961
Maximum	17·41	1811	CIRA 1961
	21·78	2030	Nicolet
	17·76	1828	Kallman-Bijl

The detailed variations of m and T for the CIRA 1961 model and for the model recently prepared by Mathur and Mitra based on satellite data are shown in Fig. 10. A comparison of the values of m and T at 500 km. as given in CIRA 1961 and those obtained by various investigations is given in Table 4.

From the table it can be seen that while the atmospheric temperature might vary by nearly 1000° over a 24-hr period, the uncertainty for the average value is less than 200°K. For $\bar{m}$, the uncertainty is around 20 per cent. A difference of less than 200°K. is well within the variation expected from changes in the intensity of solar radiation.

Above 500 km., the uncertainties in $\bar{m}$ and T increase. At 800 km., a molecular weight of 14 ± 1 has been found. This implies presence of helium and/or hydrogen at these heights.

If $\bar{m}$ and T are known, then one may easily obtain the distribution of the major atmospheric constituents. The distributions derived by Mathur and Mitra for average conditions are given in Fig. 11.

THE IONOSPHERE

A considerable part of the IGY investigations was directed towards the study of ionic composition of the ionization profiles in the various regions of the ionosphere and their variations with the time of the day and season. Ionospheric characteristics in special geographical areas, for example, the equator and the poles, received special attention. In this field, achievements have been many and varied, and it will not be possible to indicate

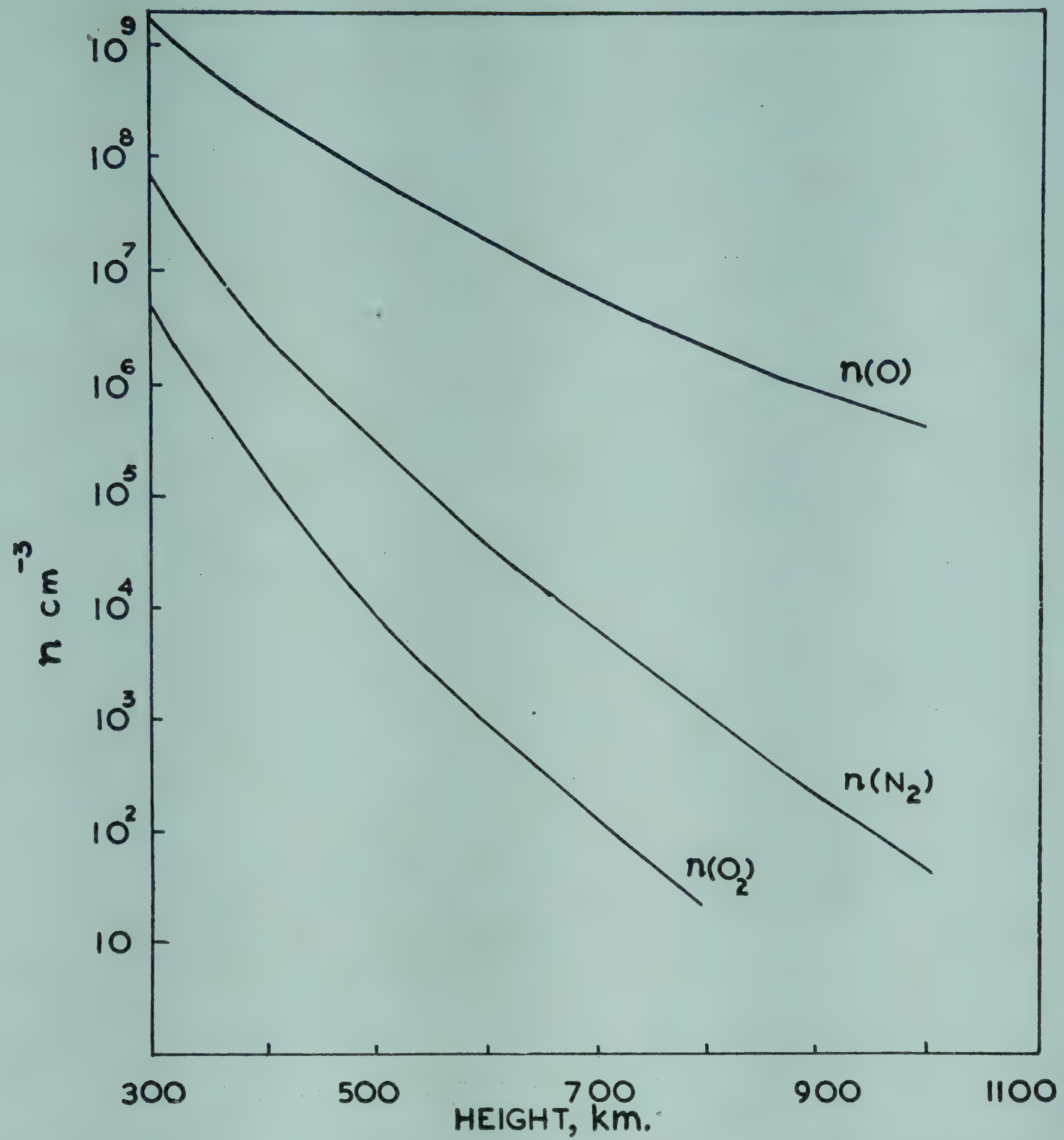

FIG. 11 — DISTRIBUTION OF ATMOSPHERIC CONSTITUENTS FOR HEIGHTS 300–1000 KM. FOR THE MITRA-MATHUR MODEL

all the major developments in this article. Instead, we shall outline some of the IGY developments in the following aspects: (i) Nature of ion composition up to 1000 km., based principally on rocket and satellite measurements using mass spectrometers; (ii) polar and equatorial phenomena; and (iii) the outer ionosphere.

Ion Composition. Information on ion composition in the ionospheric regions has for a long time been inadequate. The present situation, however, has considerably improved with recent measurements of ion composition by Bennet RF mass spectrometers flown in rockets and satellites[19,20]. The rocket measurements extended to some 200 km. At higher heights satellite-borne

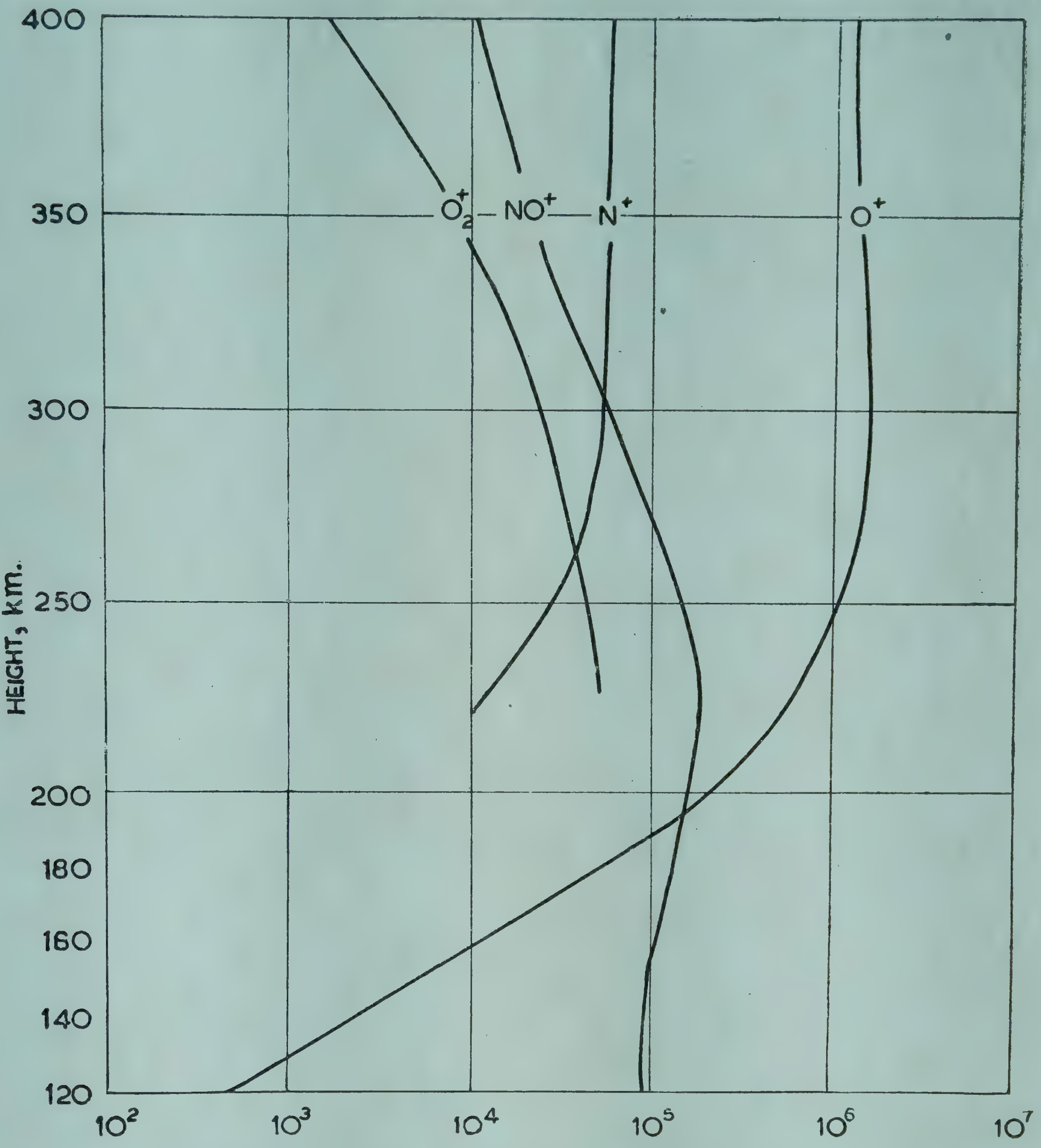

FIG. 12 — ION COMPOSITION FROM ROCKETS AND SATELLITE MEASUREMENTS

RF mass spectrometers have been used: Russian measurements involving Sputnik III (1958 δ2) covered altitudes from 225 to 980 km. in the latitude range from 27° to 65°N during day-time. From both the U.S. and the U.S.S.R. observations, the following conclusions have been made:

(i) The positive ions present are: N^+, O^+, H_2O^+, N_2^+, NO^+ and O_2^+.

(ii) In the E region of the ionosphere (100–150 km.) nitric oxide (although a negligible neutral atmospheric constituent) is the predominant positive ion (density of the order of 3×10^5). There is an apparent diurnal effect, $n(NO^+)/n(O_2^+)$ being larger during the day.

(iii) In the F region, the predominant ion is O^+.

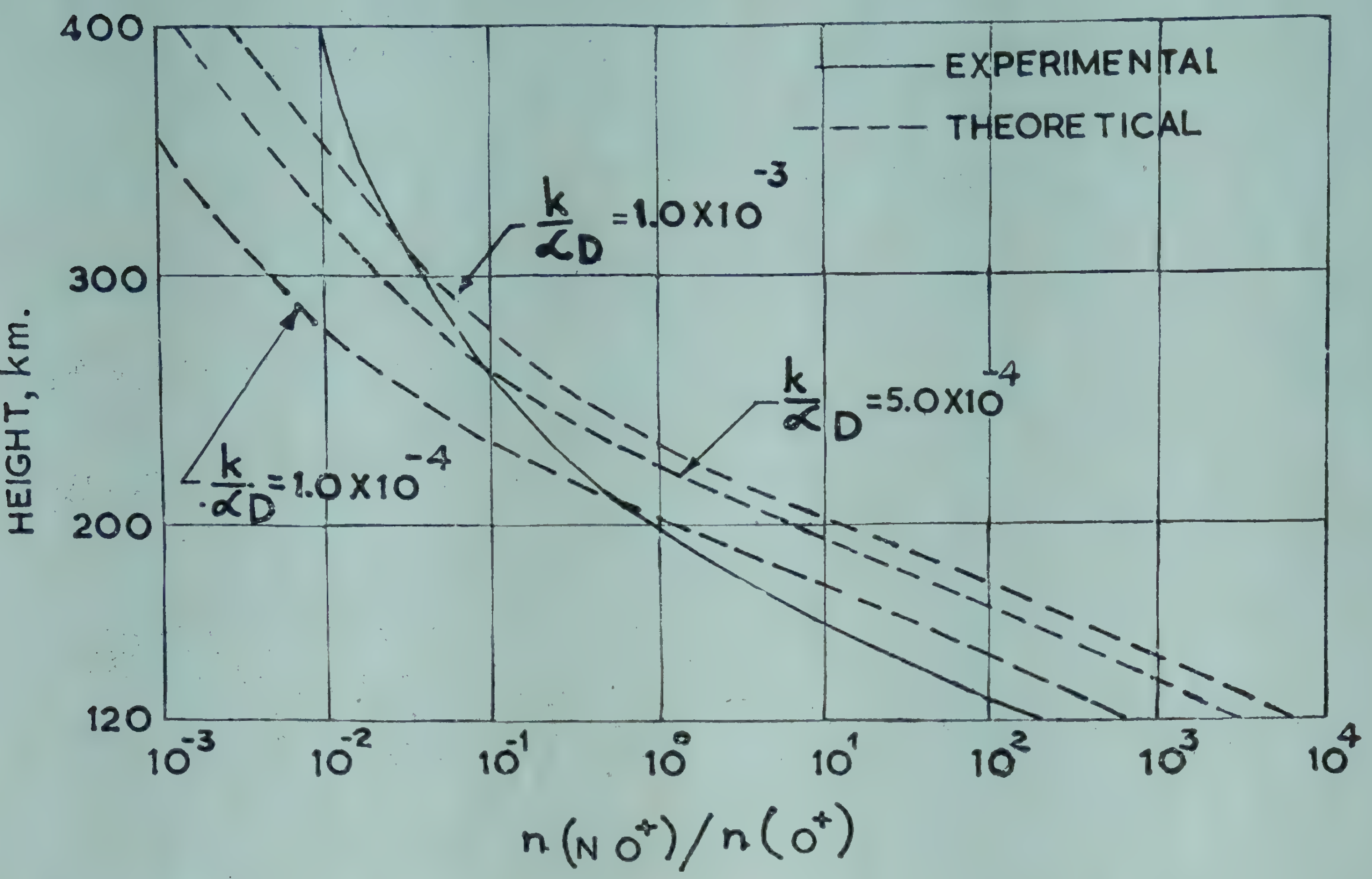

FIG. 13 — COMPARISON OF THE EXPERIMENTALLY DEDUCED VALUES OF THE RATIO $n(NO^+)/n(O^+)$ WITH THEORETICAL COMPUTATIONS

(iv) As altitude increases from 100 to 200 km., the order of relative abundance of positive ions changes from (O_2^+, NO^+) at 100 km. to (NO^+, O_2^+, O^+) at 150 km. and finally to (O^+, NO^+, O_2^+) at 200 km. The relative abundance of ions computed from Russian observations is given in Fig. 12.

Of these conclusions the most remarkable is the preponderance of NO^+ in the E region, and the apparent diurnal effect. The most likely process for the production of NO^+ appears to be the ion-atom interchange process:

$$O^+ + N_2 \longrightarrow NO^+ + N(k) \tag{1}$$

followed by the dissociative recombination of NO^+

$$NO + e \longrightarrow N + O(\alpha_D) \tag{2}$$

Under equilibrium conditions $n(NO^+)/n(O^+)$ would then be given by

$$\frac{n(NO^+)}{n(O^+)} = \frac{kn(N_2)}{\alpha_D(NO^+)} \simeq \frac{kn(N_2)}{\alpha_D Ne} \tag{3}$$

The most recent value for k is that of Longstroth and Hasted and is $4{\cdot}7 \times 10^{-12}$ cm.³/sec. The value of $\alpha_D(NO)$ is not known, but is likely to be of the order $10^{+8\pm1}$ cm.³/sec., so that $n(NO^+)/n(O^+)$ is given by

$$\frac{n(NO^+)}{n(O^+)} = 5 \times 10^{-4\pm1} \frac{n(N_2)}{Ne} \tag{4}$$

TABLE 5 — NUMBER OF IONOSPHERIC STATIONS, VERTICAL SOUNDINGS AND COSMIC NOISE MEASURING EQUIPMENTS IN POLAR AND EQUATORIAL REGIONS

REGION	TOTAL IONOSPHERIC STATIONS	VERTICAL SOUNDINGS	COSMIC NOISE
Arctic	51	37	6
Antarctic	18	18	1
Equatorial	51	42	3
India	12	8	2
World	284	177	14

A comparison of the experimentally observed values of the ratio $n(NO^+)/n(O^+)$ with those obtained from Equation (4) for different values of k/α_D is given in Fig. 13. It will be noted that a close correspondence can be achieved by assigning a value around 1×10^{-4} for the ratio k/α_D. This would indicate a value of 5×10^{-8} cm.^{3}/sec. for α_D.

The above considerations also help in understanding the diurnal effect. The day-to-night variation in the ion ratio can be caused by the variation in the neutral atmospheric density or, more specifically, in $n(N_2)$. Since day-time atmospheric density is known to be higher than the night-time density, the ion ratio is also expected to be higher.

Polar and Equatorial Phenomena. The polar and equatorial regions naturally received a great amount of attention during the IGY, and in both, many new stations were set up, especially in the Antarctic. Table 5 gives the number of ionospheric stations, vertical incidence soundings and cosmic noise measuring equipments in polar and equatorial regions during the IGY.

Polar Regions. The arctic ionosphere is a highly complex region, in which the normal ionic layers are continually distorted by appreciable fluxes of incoming solar particles by strong atmospheric turbulence and auroral currents. As a result, the radio propagation characteristics in this region are highly variable.

Apart from its practical interest in the improvement in HF polar communication circuits, the arctic ionosphere provides unusual opportunities for studying the nature and magnitude of solar particles which are continually impinging on the arctic ionosphere, specially during disturbed conditions. Further, due to long night hours in winter, the arctic ionosphere can provide better information on ionospheric loss processes than the ionosphere at lower latitudes.

One of the most remarkable discoveries in the polar regions is the Polar Cap Absorption (PCA), discovered during the IGY by the cosmic radio noise method. PCA occurs within a few hours after the flare, covering the entire polar cap, reaches maximum within a few hours, then decays slowly during the following few days. After a day or two, a sudden commencement of magnetic storm almost invariably follows often accompanied by intense auroral activity. At high latitude stations ($\Phi > 75°$), the maximum of absorption is reached usually before the sudden commencement of geomagnetic storm (SSC). At lower latitudes ($\Phi = 60$–$75°$), the PCA event is generally weaker, spreading to the auroral zone before the SSC. These events were first noted at the time of the great cosmic ray producing flare of February 23, 1956[21,22], but many have since been observed[23]. It is believed that these events are a result of ionization of the polar atmosphere by fast protons in the energy range of 10–100 MeV. emitted from the sun after a solar flare.

Balloon observations[21–23] of cosmic rays have confirmed the presence of proton flux during PCA events. Many such balloon flights have been made at both high and middle latitudes, especially at the University of Minnesota and the State University of Iowa. Since in most cases the energies are not high enough to reach the ground level, PCA events are observed considerably more frequently than ground level flare-associated cosmic ray events.

The exact nature of ionization charges in the polar ionosphere during Polar Blackouts is naturally of great interest. Such measurements were made by Jackson and Seddon[24]. Unusually high electron densities were found to occur in the D region, mainly between 60 and 80 km. There were no changes in the E and F regions.

In contrast to the Polar Blackout the normal polar ionosphere does not appear to have been studied adequately although such studies offer great promise. Results of some preliminary analysis of vertical incidence soundings[25] made in the Antarctica (using the following U.S.-operated stations: Pole, Byrd, Little America, Ellsworth and Wilkes) indicate the following unusual features:

(i) For Wilkes (66°S) and Ellsworth (78°S) stations, f_0F_2 reaches maximum around midday in conformity with temperate latitude stations, but for Little America (78°S) and Byrd, the maximum occurs in the evening and for the Pole, the diurnal variation is weak with maximum occurring in the early morning hours.

(ii) In July, the minimum f_0F_2 over the Pole is greater than that over any other station, although its atmosphere at this time is not illuminated below about 450 km.

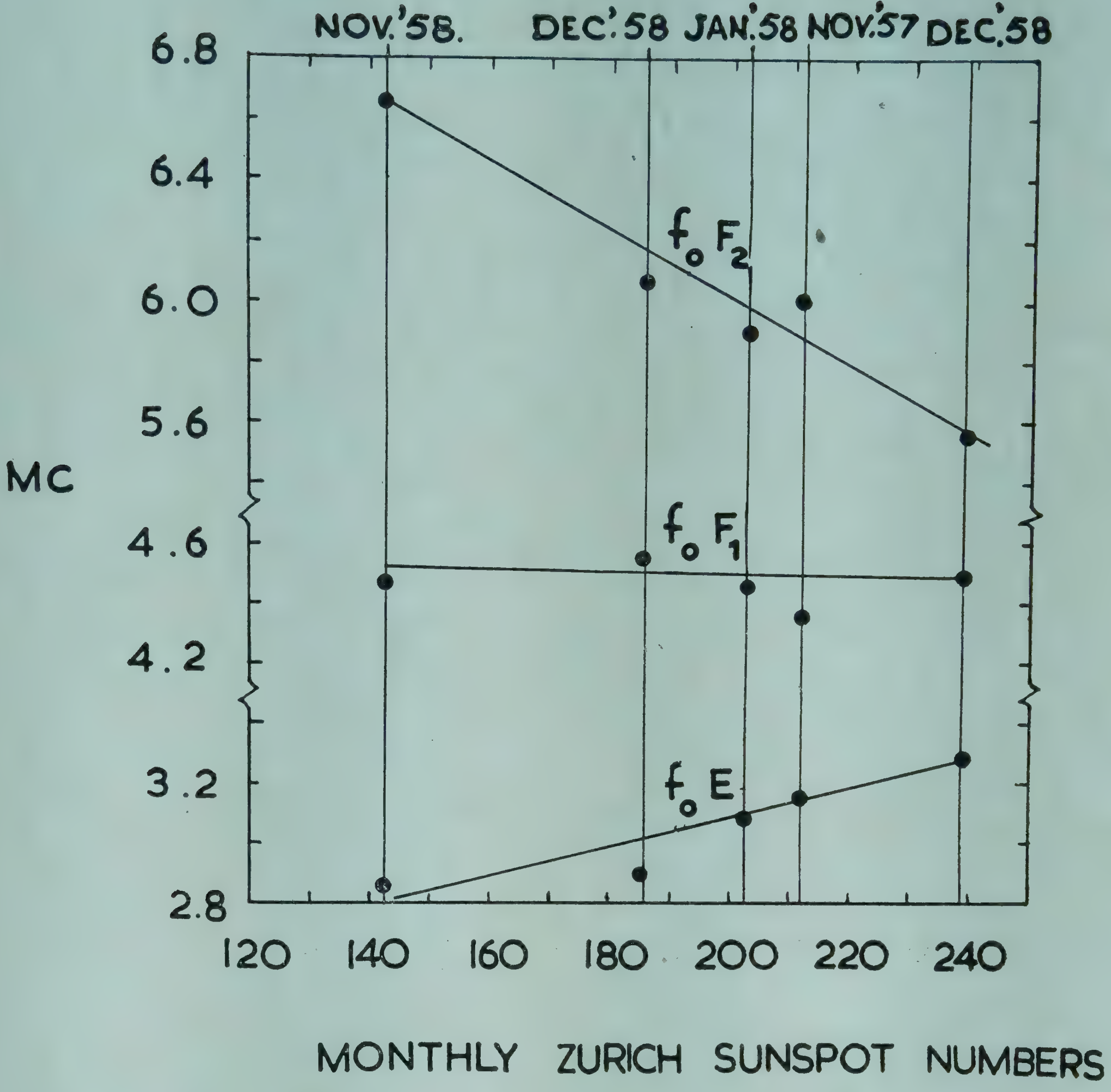

Fig. 14 — Variations of ionospheric critical frequencies over the Pole as a function of sunspot number

(iii) The summer-time daylight behaviour of f_0E, f_0F_1 and f_0F_2 over the Pole when plotted against Zürich sunspot number shows some curious features. While f_0E increases with sunspot number in the normal way, f_0F_1 is virtually unaffected and f_0F_2 decreases (Fig. 14).

Equatorial Regions. The equatorial ionosphere is defined by $20° < \Phi > 0°$ and is characterized by several outstanding anomalies. One of the most important is the geomagnetic anomaly belt which lies within the dip values of $\pm 30°$. The belt appears as a trough in f_0F_2 near noon-time, shows a 'bite-out' in f_0F_2 in the diurnal curve, and exhibits special types of E_s and spread F. During the IGY, there existed three main chains of equatorial stations. These were the Indian, South American and African chains, lying roughly around 75°E, 75°W and 0° longitude zones respectively. The stations are listed in Table 6.

TABLE 6 — STATIONS IN EQUATORIAL IONOSPHERIC CHAINS

Indian		South American		African	
Station	Long. Zone	Station	Long. Zone	Station	Long. Zone
Delhi (18·7°N)		Bogota (15·9°N)		Ibadan (10·4°N)	
Banaras (15·1°N)		Pasto (12·3°N)		Kumasi (11·0°N)	
Ahmedabad (13·9°N)		Guaquil (9·1°N)		Enugu (9·0°N)	
		Talara (6·6°N)	75°W	Little Legon (9·6°N)	0°
Bombay (9·8°N)		Chiclayo (4·4°N)			
Poona (8·9°N)	75°E	Chimbote (2·2°N)		Accra (9·6°N)	
Waltair (7·4°N)		Huancayo (0·6°S)			
Madras (3·3°N)		La Paz (5·0°S)			
Tiruchirapalli (1·1°N)				Bangui (5·0°N)	
Kodaikanal (0·6°N)		Paramboribo (17·0°W)	60°W	Leopoldville (3·1°S)	
Trivandrum (1·1°S)		Tucuman (15·3°S)		Tsumeb (18·3°S)	15°E
				Salisbury (19·5°S)	
Calcutta (12·2°N)	90°E				

The following significant results may be mentioned:

(i) The geomagnetic anomaly belt is confined generally within ±30° magnetic dip. The noon-time trough is more pronounced during the sunspot maximum, and lasts longer, being absent only around 0900 hours[26]. At sunspot maximum the evening 'crest' of f_0F_2 vanishes.

(ii) Stations within the anomalous equatorial belt exhibit a striking post-sunset increase in h′F[26]. This anomaly is again confined within ±30° dip. In Fig. 15 the post-sunset anomaly for Kodaikanal (dip 3·5°N) is exhibited.

(iii) The three equatorial chains do not behave identically during the IGY. It was observed (Narasinga Rao, B. C., unpublished data) that the width of the belt was larger for the Asian and African chains than for the American chain; for the former the width was around ±35°-30° in magnetic dip, and for the latter around ±25°; and the amplitude of the post-sunset increase in h′F is larger in the Asian zone than in the American zone, the corresponding values for Δh′F being about 240 and 200 km. respectively.

(iv) True height profiles for equatorial stations exhibit a sharp increase in the electron density at sunrise, the lower levels developing maximum earlier than the higher levels (Fig. 16).

(v) The equatorial sporadic E (E_s-q) in the American zone[27] is confined within a very narrow region (only about ±5°) about the geomagnetic equator[25]. This is narrower than previously supposed, but is in agreement

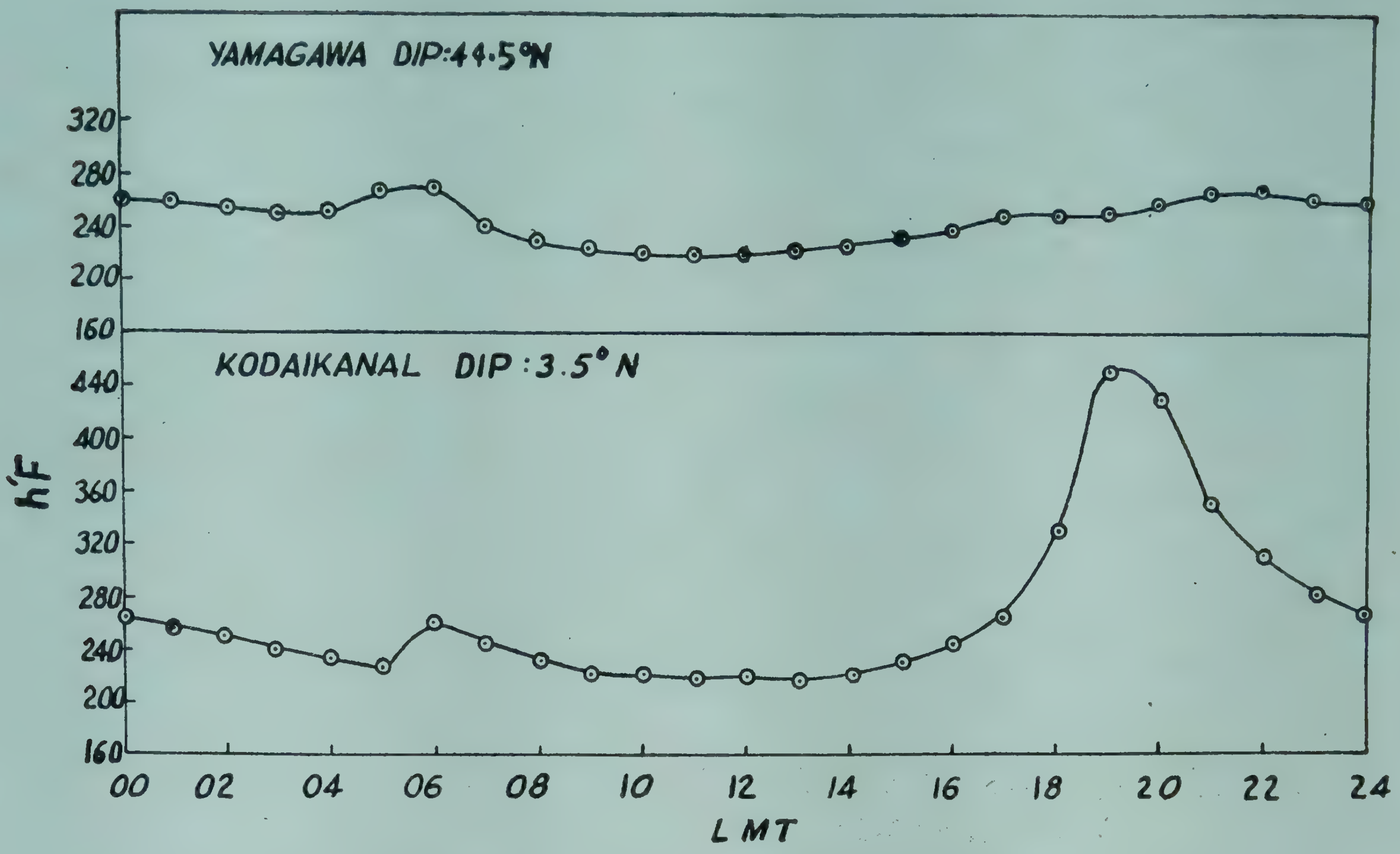

FIG. 15 — POST-SUNSET ANOMALY IN h′F AT KODAIKANAL (3·5°N)

with the width of the equatorial electrojet estimated by Forbush from experiments on the earth's magnetic field in the vicinity of the geomagnetic equator[27].

Apart from regular ionospheric soundings by ionosondes, the equatorial ionosphere has been studied by a multitude of techniques. These include measurements of ionospheric absorption and drift, the incoherent scatter experiments and VHF equatorial forward scatter. No rocket observations are available for this region. Some of the important results are outlined below:

(i) At stations near the equator the familiar inverse frequency-square law of absorption breaks down. Instead, absorption is inversely proportional to the frequency.

(ii) Analysis of some ionospheric drift data of thirteen stations by Briggs[28] shows that, in accordance with the current electrodynamical theory of ionospheric drift, the E–W component of mean drift velocity (at midnight) reverses its direction in the region of 30° magnetic latitude. At higher latitudes the drift is towards the west and below, towards the east. During midday, the directions appear to be opposite to those at midnight. The N–S component, which should vanish at the equator, appears to be appreciable at Singapore[29] and Waltair[30].

(iii) Transequatorial scatter propagation at the VHF can be consistently achieved during evening hours throughout the sunspot maximum, when special conditions prevail in the equatorial ionosphere[31,32]. Such a propagation has been reported from South America and the Far East, involving paths several thousand kilometres in length. The paths roughly bisected

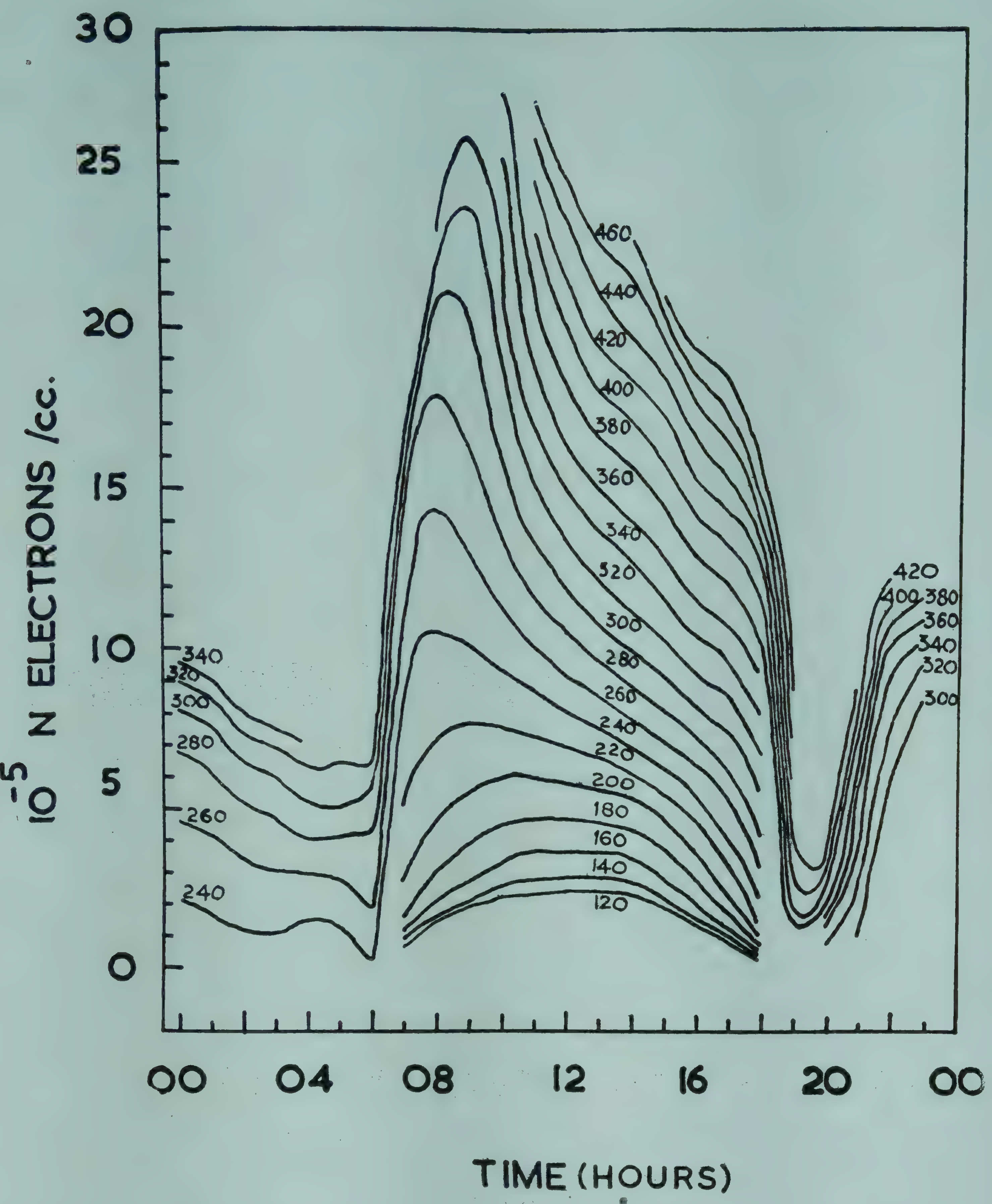

Fig. 16 — Ionization profiles over Huancayo for March 1958 as a function of local time (Numerals denote heights in km.)

the magnetic equator and their end points generally have magnetic dip angles between 20° and 60°. The frequencies have been in the neighbourhood of 50 Mc/s.

The Outer Ionosphere. The Outer Ionosphere is the region above F_2 maximum. Conventional techniques using terrestrial transmission are normally unable to explore this region. In the pre-IGY days, the exploration of the outer ionosphere had just been started by using two powerful

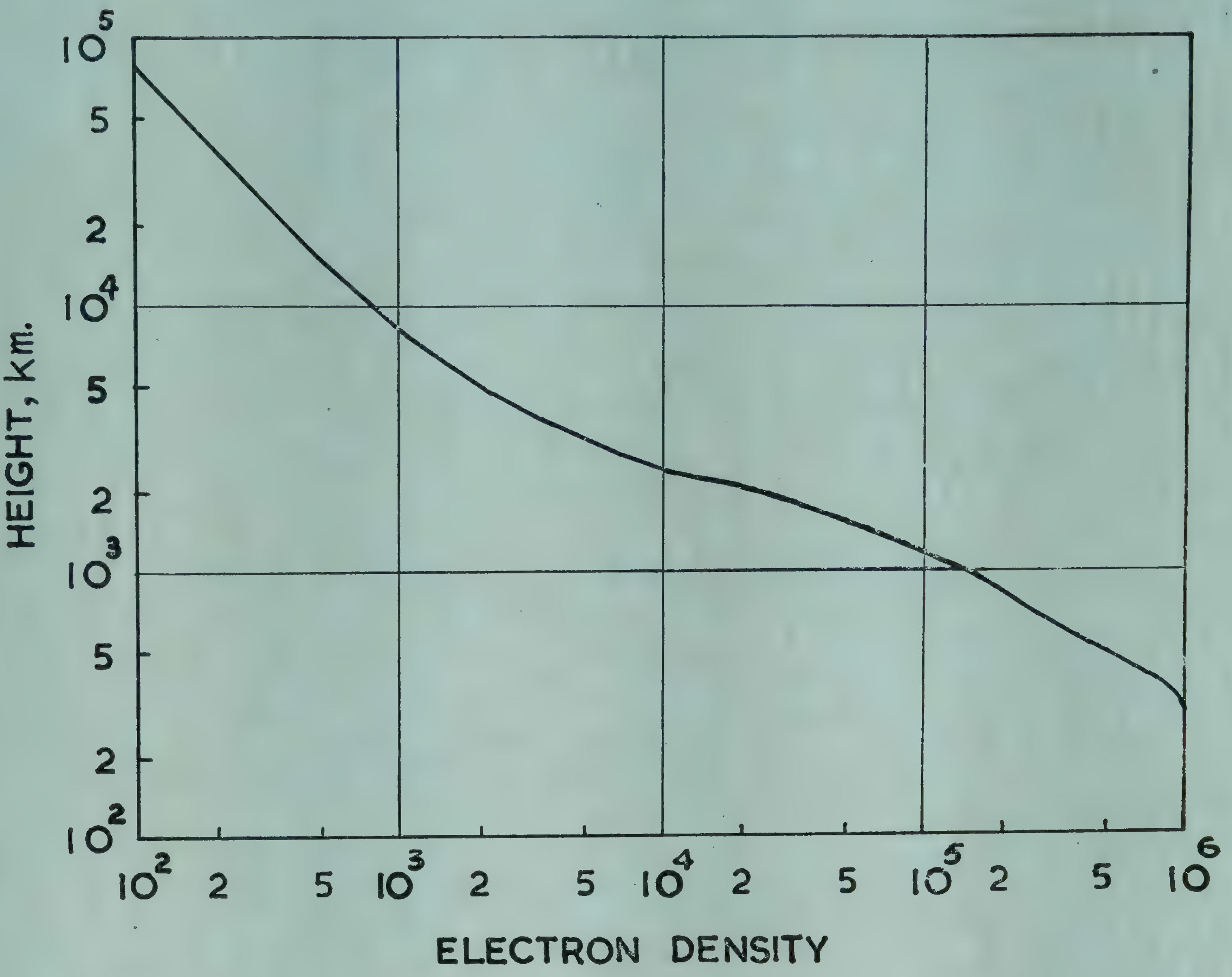

Fig. 17 — A provisional model of the ionization of the outer space drawn up to 100,000 km.

techniques, radio astronomy and whistlers. During the IGY, two more techniques, (i) Satellites[33-36] and (ii) Incoherent scatter[37] at VHF, were added and a comprehensive survey of the ionization of the outer ionosphere begun. The most important result that has emerged is that the ionization extends considerably beyond the F region maximum, and is some 10^5/cm.^{3} at 1000 km. and 10^2/cm.^{3} at 80,000 km. In Fig. 17 the approximate electron density distribution up to a height of 100,000 km. is given. The predominant ion is O^+ up to about 1000 km., above which He^+ becomes increasingly predominant. In a recent work by Bourdeau *et al.*[38] using experiments on the Explorer VII satellite (1960 *i*1), the ratio of atomic helium to oxygen atoms (He^+/O^+) is given as $1{\cdot}3 \pm 0{\cdot}3$ at an altitude of 1630 km. In contrast, the ratio is only about 10^{-2} at 600 km. (for a temperature of 1600°K.). It is also significant to note that the effective 'electronic scale height' increases from a value of about 200 km. below 1000 km. to about 3000 km. at great heights.

The F region may, therefore, be considered to terminate around 1500 km. In this portion of the F region (the 'Upper F') the ionospheric relaxation time is large, since the recombination process is essentially a radiative one with a coefficient of only 10^{-12} cm.^{3}/sec. (of the order of several weeks at

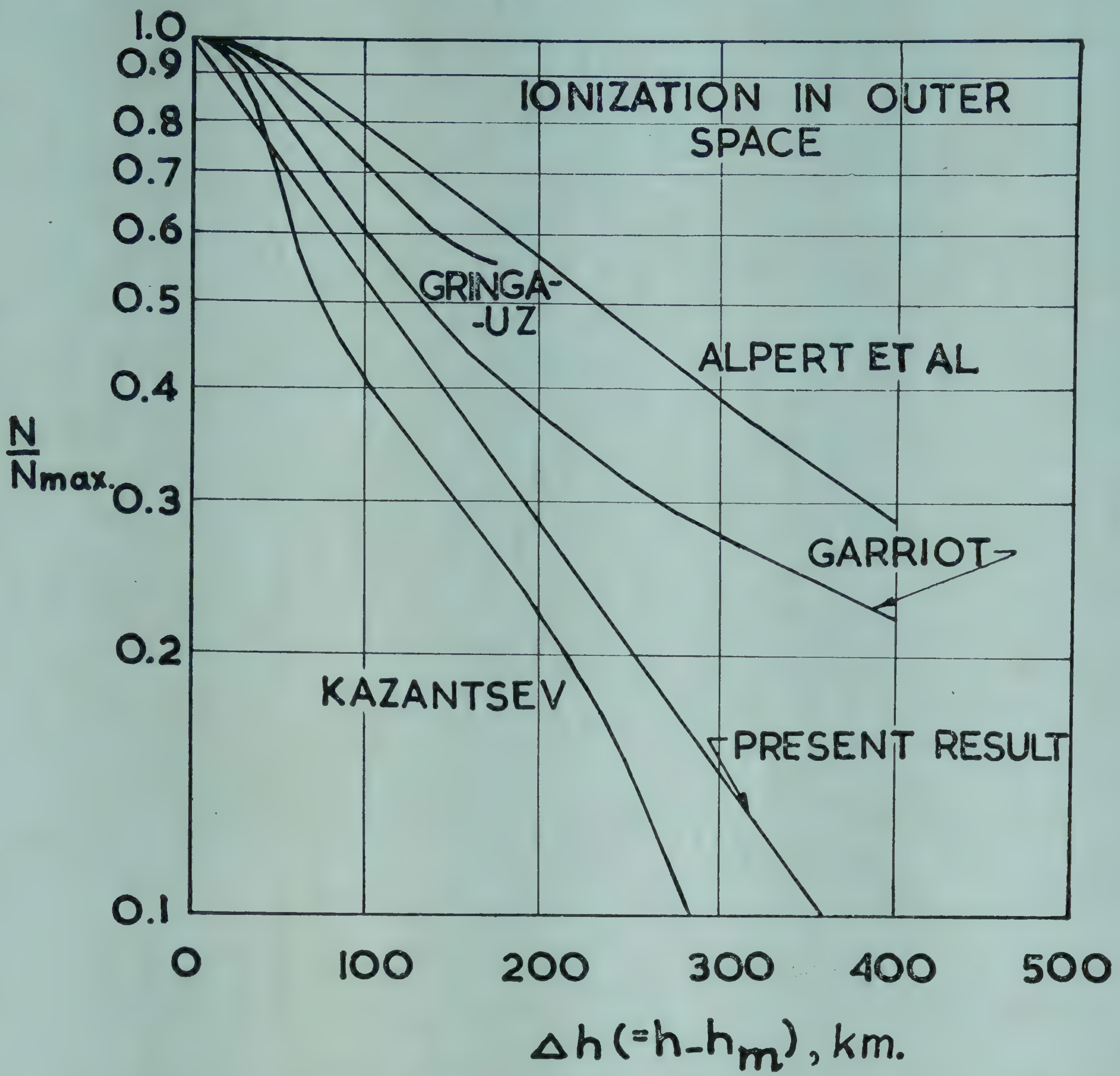

FIG. 18 — EXPERIMENTAL OBSERVATIONS ON THE IONIZATION DISTRIBUTION OF THE OUTER IONOSPHERE AT HEIGHTS IMMEDIATELY ABOVE THE F REGION MAXIMUM (AFTER SARADA AND MITRA)

1000 km.). Thus hourly variations of ionization cannot be expected, although seasonal and latitudinal variations may exist.

A host of measurements exists on the ionization of this portion of the outer ionosphere. The results are generally coherent and the different techniques (Faraday rotation, dispersive Doppler, cosmic radio noise, incoherent scatter) have given similar results. However, most of these only provide the electron content of the region and the profile can be obtained only upon an appropriate assumption about the layer shape. The incoherent scatter technique, which is one of the powerful techniques now available, however, provides local electron densities. In Figs. 18 and 19 the electron densities immediately above the F region maximum are given. Fig. 18 gives the distribution obtained by using satellite transmissions and by cosmic radio noise[39]. Fig. 19 gives some early results of the incoherent scatter technique obtained by Bowles and Cohen at Huancayo.

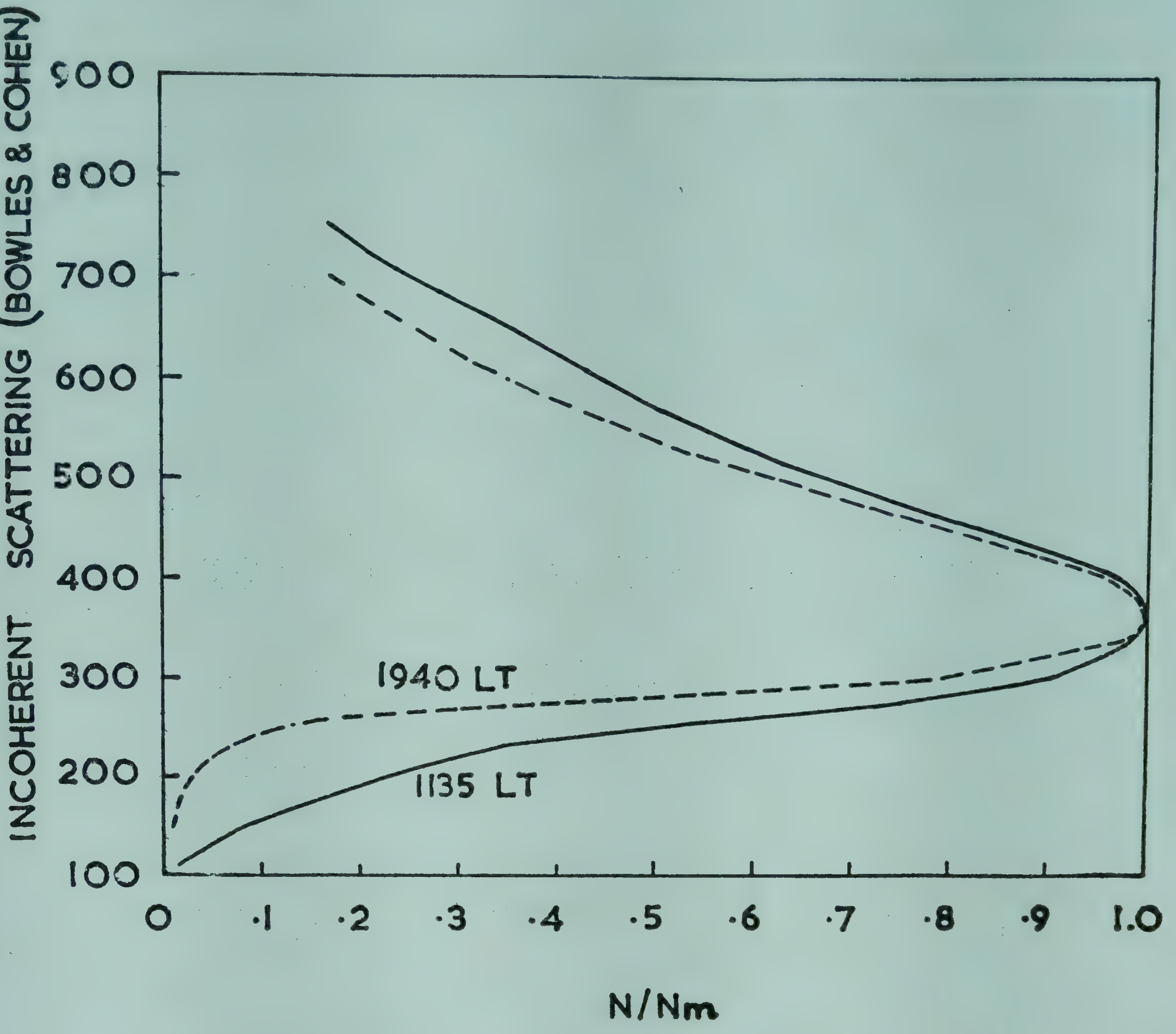

FIG. 19 — IONIZATION DISTRIBUTION IN THE OUTER IONOSPHERE OBTAINED BY BOWLES AND COHEN ON FEBRUARY 27, 1959, USING INCOHERENT SCATTER TECHNIQUE AT HUANCAYO, PERU

SOME NEW TECHNIQUES

The IGY saw wide use of some new ionospheric techniques. Of these the more important are: (i) whistlers, (ii) cosmic radio noise, and (iii) artificial perturbation of the atmosphere, as in the Argus experiment.

Whistlers. First studied extensively by Storey[40], whistlers are naturally occurring atmospherics which start above the upper limit of hearing, fall steadily in pitch at first rapidly and then more slowly at the lower frequencies. They arise from the propagation of sferics between the hemispheres along the earth's magnetic lines.

The investigations on whistlers carried out during the IGY had the following objectives: (i) to examine the conjugate point aspect of the whistler theory and the characteristics of the whistler path; and (ii) to utilize whistler data for the study of the earth's magnetic field and ionization at distances up to several earth radii.

The following are some of the more important observations on whistlers and inferences drawn from them[41]:

(i) Simultaneous observations of whistler echo trains at Alaska and at Wellington and Dunedin, New Zealand near its geomagnetic conjugate point, reported by Morgan and Allcock in 1955, have fully confirmed Storey's theory of whistler propagation.

(ii) Characteristics of multiple noise whistlers led to the hypothesis that the propagation of the individual component of whistlers takes place along discrete paths spaced in latitude. It has been suggested that the whistler energy might be guided in field-aligned columns of ionization which extended between the hemispheres and act like cylindrical waveguides.

(iii) Proton densities along the path of propagation have been deduced from low frequency behaviour of whistlers using Storey's recent method[42].

(iv) Whistler-producing discharges possess some unique properties. These have been found from simultaneous observations at Stanford and Boulder in September 1956. Whistler-producing sferics were charcaterized by a peak in the energy spectrum near 5 kc/s. They exhibited a characteristic ' sound ' which has been described by Morgan as a ' bonk '. Most of the sferics, on the other hand, peaked in the vicinity of 10 kc/s. This unusual type of sferic appeared to occur more frequently over the sea than over the land.

(v) The first man-made soundings of the outer ionosphere were made using pulses transmitted from the Navy Station NSS at Annapolis, Md, at 15·5 kc/s.[43]. Ordinary direct signals were received at all times at Cape Horn, South America. During most night-time runs an echo was heard 10–30 db. below the direct signal with an average delay of 0·7 sec. Whistlers recorded at the same time showed similar delays at 15·5 kc/s. On several occasions man-made echoes were present but no whistlers could be detected, demonstrating that when whistlers are not heard, the reason often is the absence of suitable sources.

(vi) At College and Kotzebue, a study of the nose whistlers (nose frequency = 6·4 kc/s.) indicates an apparent geomagnetic latitude of 60°, whereas the ground geomagnetic latitude is 64°. For Seattle, the nose frequency is 15 kc/s. indicating an effective geomagnetic latitude of 54° which is very close to station latitude of 53°.

(vii) Components with greater delay are relatively stronger at the higher latitudes. The dominance of one component with the same dispersion at all stations in one hemisphere is interesting. The explanation may be that there was only one good path of propagation from which all the observed whistlers came. If this is true, then the latitude of the recording station may have little relation to the latitude of the whistler path.

& Research
No. 271
7 JAN 1985
C.F.T.R.I.
ment Station

(viii) Whistler rate is higher at night than at day, presumably because of the diurnal variation of the D region absorption.

(ix) Allcock[44] estimated the electron densities in the outer ionosphere at different heights from deserved dispersion of whistlers at different geomagnetic latitudes. These electron densities fitted on exponential distribution of the type

$$N = Ne_0^{-(h-h_0)/2640}$$

for heights in the range 1000–13000 km.

Cosmic Radio Noise Measurements. The method of measurement of ionospheric absorption by cosmic radio noise, first introduced by Mitra and Shain[45] for the study of the normal ionosphere and as a method of flare patrol, has been used very widely and with great success during the IGY. One of the most remarkable achievements of this technique has been the detection of PCA events associated with low energy cosmic rays impinging on the polar atmosphere immediately after major solar flares. Since such cosmic rays are readily attenuated in the atmosphere, they are not often observed on the ground. PCA events, therefore, provide a powerful tool in the hands of the cosmic ray physicists. The method has also been used at polar latitudes to study the ionization associated with auroras.

At non-polar latitudes the method has been used: (i) to study the normal absorption of both the D and F regions at a number of locations extending from the auroral zone down to the subtropical latitudes, (ii) to detect solar flare effects (SCNA) as a part of the IGY solar patrol and to study the ionization enhancement in the D layer during solar flare, and (iii) to estimate outer ionospheric ionization. One surprising feature has been the large F region contribution in the absorption, which at frequencies around 20 Mc/s. was often greater than the D region absorption (Fig. 20). This was due to the unusually large values of f_0F_2 occurring during the IGY, which, as mentioned earlier, was a period of intense solar activity. It was also found that the F contribution increased very rapidly with increasing values of f_0F_2 (Fig. 21) with an exponent considerably greater than 2, thus indicating the importance of collisions between electrons and positive ions at these heights[46].

The D region contribution for most stations was found to behave in the usual manner: the variation with cos χ was slow, the exponent being around 1; the frequency relationship was the inverse-square law type; and the relaxation time was around 30 min. There was some indication that the cos χ exponent obtained by this technique was a little higher than that obtained by the pulse technique (around 1 and 3/4 respectively). This may have been caused by the presence of E region non-deviative absorption in the cosmic noise results.

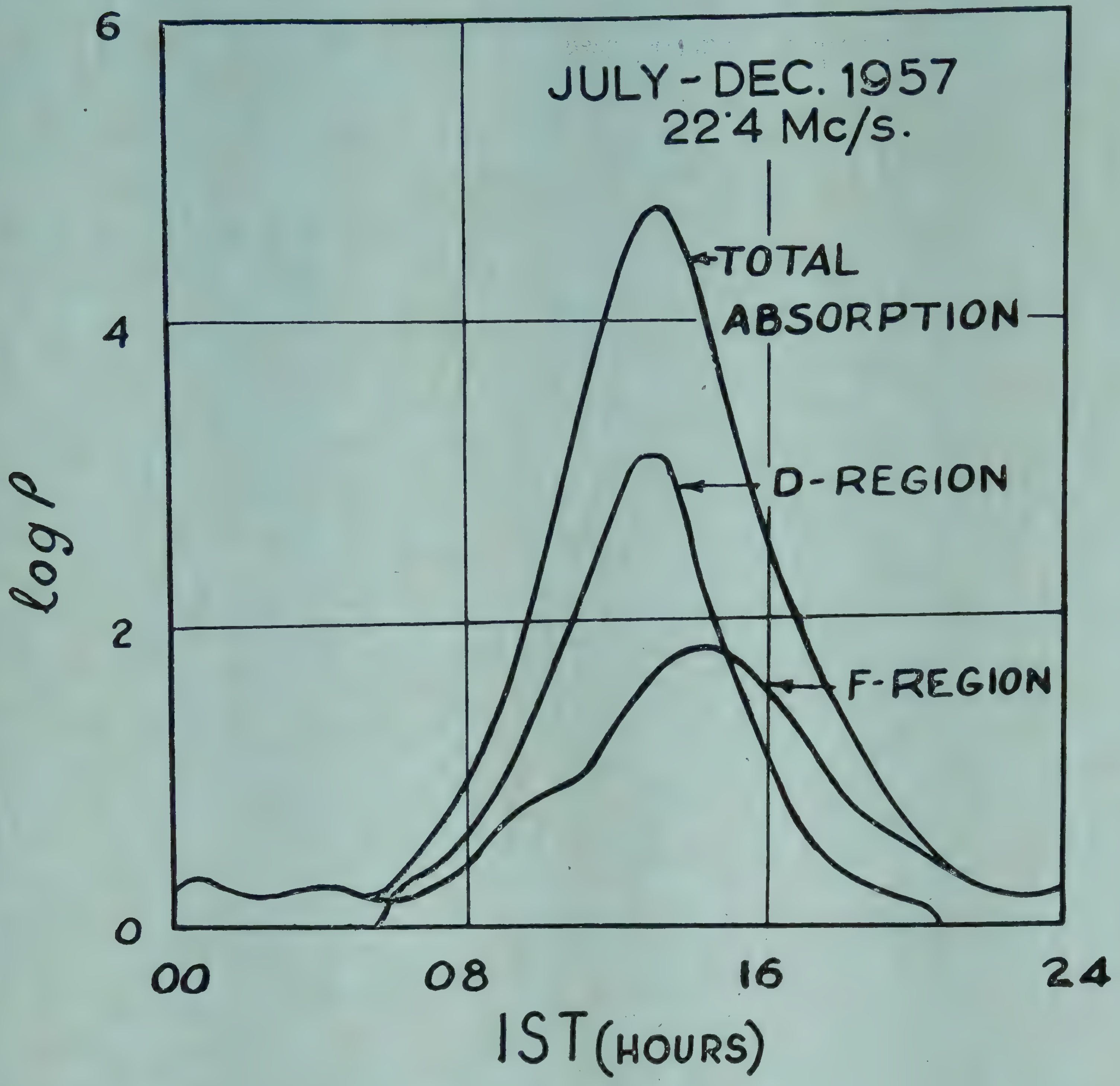

FIG. 20 — ABSORPTION CONTRIBUTIONS BY THE D AND F REGIONS OF THE IONOSPHEER AT 22·4M C/S. AT DELHI OBTAINED BY COSMIC RADIO NOISE TECHNIQUE (AFTER SARADA AND MITRA)

The cosmic radio noise measurement has proved to be a very versatile tool. In addition to the fields mentioned above, it has been used for a study of the auroral ionization in studying the characteristics of magnetic conjugate points and in the detection of high altitude nuclear detonations.

Argus Project. Another remarkable project undertaken during the IGY was the Argus project, though strictly this was not an IGY project. In this, artificial radiation belts were produced by three nuclear test explosions 300 miles above the earth on August 27 and 30, and September 6, 1958 in the South Atlantic Ocean[47]. Elaborate arrangements were made in advance to study the effects produced: the Air Force Special Weapons Centre undertook the preparation of a series of high altitude sounding rockets up to altitudes 500 miles; a variety of equipments were installed at suitable ground stations and abroad aircraft and ships and, in addition, of course, the far-flung

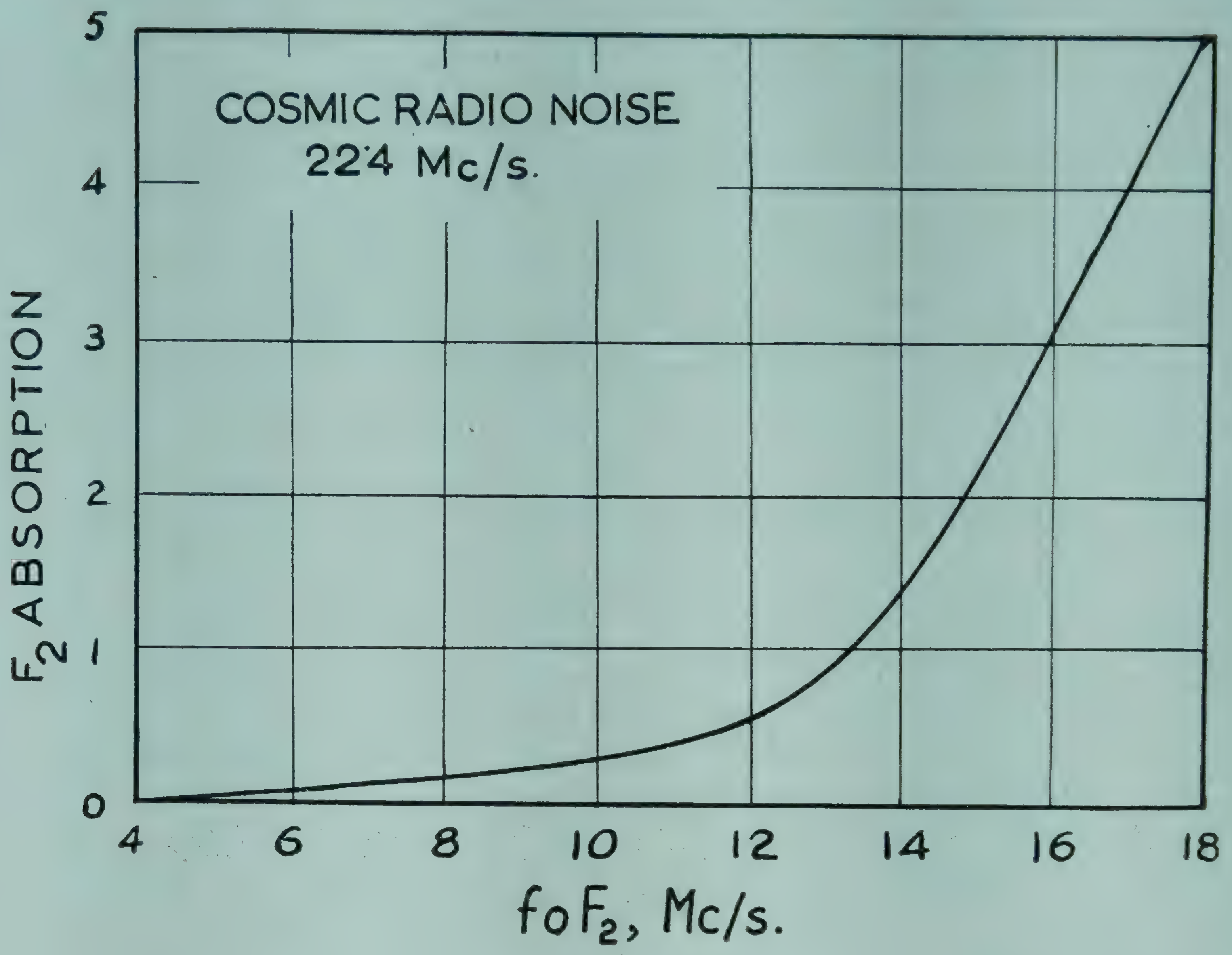

FIG. 21 — VARIATION OF F REGION ABSORPTION AT 22·4 Mc/s. AT DELHI WITH f_0F_2 (AFTER SARADA AND MITRA)

international network of the IGY was available. Explorer IV satellite was launched on July 27, 1958, one month earlier, at a steep orbit of 51° to the equator, to map first the intensity of the normal belts prior to explosion.

Following the explosions a fascinating sequence of observations was obtained. The brilliant initial flush of the explosion was followed by a fainter but persistent auroral luminescence in the atmosphere along the magnetic lines of force through the burst point. Almost simultaneously a bright auroral glow appeared at the conjugate point (near the Azores Island). A new radiation belt was produced. Its nature and intensity were mapped by Explorer IV as it criss-crossed through the man-made belt hour after hour and day after day. For the first time in history, measurements of geophysical phenomena on a world-wide scale were related to a quantitatively known cause — namely, the injection into the earth's magnetic field of a known quantity of electrons of known energies at a known position at a known time.

SOLAR FLARES AND IONOSPHERIC IONIZATION

Ionospheric Effects of Solar Flares. Immediately after the appearance of solar flares, the terrestrial ionosphere registers a number of sudden effects, conveniently described as sudden ionospheric disturbances (SID), all believed to be caused principally by a sudden enhancement of ionization in the lower ionosphere. These effects include a decrease in intensity of medium and short radio waves or an increase in intensity of LF and VLF radio waves, sudden changes in reflection height and magnetic crochets. The various effects are normally recorded as a time curve with a rapid growth and comparatively slower decay, following generally the trend of the visual flare as observed in H_α.

During the IGY the radio methods of detection of solar flares were widely used. The methods used most often were: short wave fade-out, sudden cosmic noise absorption and sudden enhancement of atmospherics. A detailed examination of many such effects by Mitra[48] has led to the following conclusions (Table 7):

(i) Short wave fade-outs appear to be principally a one-layer effect; there is no evidence of any appreciable contribution from region E.

(ii) At the level of fade-out absorption of short waves, the ionization is increased on the average by factors of 2·5, 4·5 and 7·0 for flares of class 1, class 2 and class 3 respectively. The normal quiet day level of such absorption is 90 km.; during most flares this level is unaltered and continues to be at 90 km.

(iii) At lower levels ($h < 75$ km.), the ionization enhancement is considerably larger. The sudden phase anomalies observed at 16 kc/s. indicate a drop of 2, 5·5 and 9 km. for class 1, class 2 and class 3 flares respectively. Assuming a quiet day average reflection level of 73 km. for such waves, this would require ionization enhancements of about 2·5, 14 and 140 respectively for these conditions.

(iv) At levels higher than those of SPA and SCNA, flows the fade-out current system. Its quiet day level is around 110 km., but during flares it falls down to levels of 90–100 km. The estimated ionization enhancements at the level of the fade-out current system are 0·5, 0·75 and 1·30 respectively.

(v) A comparison of SCNA's at 18·3 Mc/s. and SPA's of 16 kc/s. confirms Friedman's conclusion that the large drop in height at 16 kc/s. for major flares cannot be due entirely to L_α. Of the total excess ionization, L_α accounts for only about one-fourth for average class 2 conditions and about one-seventh for average class 3 conditions.

Origin of Flare-time Ionization. The additional ionization formed during solar flares and causing the SID's is principally located in the lower ionosphere and may be generated by L_α or X-rays of wavelengths shorter than about 10 Å. However, rocket observations over a number of years, and more recently observations in satellites have failed to indicate any measurable change in L_α intensity. On the other hand, there is now a considerable body of evidence for enhanced emission of X-rays below 10 Å.

TABLE 7 — SUMMARY OF SID OBSERVATIONS

PHENOMENA	FREQUENCY	SOURCE	SID EFFECTS			PARAMETER	RELAXATION TIME (*min.*)		REMARKS
			Class 1	Class 2	Class 3		t_0	t_f	
SWF	4 Mc/s.	Appleton-Piggot	Between 5 and 10				—	—	
	SCA: 18·3 Mc/s.	Shain-Mitra	2·5	4·5	7·0	A_f/A_0	27	30	
	SCA: 22·4 Mc/s.	Mitra-Sarada	Between 3 and 35				35	—	
Low level reflection	2 Mc/s.	Gardner	Excess ionization of about 1000/cm.^{3} at 60–75 km.; $N_f/N_0 \approx 20$			—	—	—	Effect corresponding to flare causing absorption increase by a factor of 3
SPA	16 kc/s.	Bracewell-Straker	2	5·5	9·0	Δh(km.)	23	8 (class 2) 3 (class 3)	$\Delta h'$ not known
	40–113 kc/s.	Weeks	2·5	14	140	N_f/N_0	—	—	—
	75 kc/s.	Ross		Same			16	3	$\Delta h' = 5–8$ km.
	2385 kc/s.	Findlay		2 to 4			—	—	$\Delta h' = -\Delta h$
SEA	27 kc/s.	Ellison Sachdev-Mitra		1·26			21	7	
Crochet		From McIntosh data	1·50	1·70	2·30	$\Delta H/H$			

TABLE 8 — X-RAY ENERGIES FOR AN AVERAGE STRONG FLARE

Wavelength range Å	Energy *ergs/cm.²/sec.*	Solar activity	Remarks
20–100	2	Av. of class 2 and class 1	Sunflare I expts
80–20	3×10^{-2}	do	do
2–8	10^{-2}	do	do
0·41–0·14	10^{-5}	do	Sunflare II expts

TABLE 9 — NICOLET AND AIKIN MODEL OF SOLAR X-RAY EMISSION

Nature of activity	X-ray intensity (*ergs/cm.²/sec.*)		
	2 Å	4 Å	6 Å
Completely quiet sun	10^{-8}	10^{-7}	10^{-6}
Quiet sun	10^{-7}	10^{-6}	10^{-5}
Lightly disturbed	10^{-6}	10^{-5}	10^{-4}
Disturbed	10^{-5}	10^{-4}	10^{-3}
Medium flares	10^{-4}	10^{-3}	10^{-2}
Strong flares	10^{-3}	10^{-2}	10^{-1}

The Sunflare I experiments covering 13 rocket flights during the period July 1, 1957 to September 18, 1957, and the Sunflare II experiments covering 12 flights from July 14, 1959 to September 1, 1959 provided quantitative estimates of such measurements. Both series were conducted by the U.S. Naval Research Laboratory[49]. The total X-ray flux for a class 1 flare was about 10^{-3} ergs/cm.²/sec. and about 10^{-2} ergs/cm.²/sec. for a class 2 flare. An average of several flares, mainly class 2 and 3, yielded the values given in Table 8.

Two points need special mention: First, more important than the enhancement of emission is the gradual hardening of X-rays during flares; secondly, while in general, X-ray emission has been observed in the range of 2–8 Å, still harder electro-electromagnetic radiation (with wavelenghts as low as 0·6–0·01 Å) has been observed[50].

Nicolet and Aikin[51] have proposed the model of solar X-ray emission given in Table 9.

X-rays at these wavelengths have low absorption cross-sections and are consequently able to penetrate down to 60 km. Detailed computations based either solely on X-ray emission or on a combination of L_α and X-ray emission (of which an example[48] is given in Fig. 22) indicate that the ionization enhancements are adequate to produce the observed SID effects. While this explanation is now generally accepted, it has not been satisfactorily explained why for the same flare, the SCNA and SEA (occurring at levels A and B

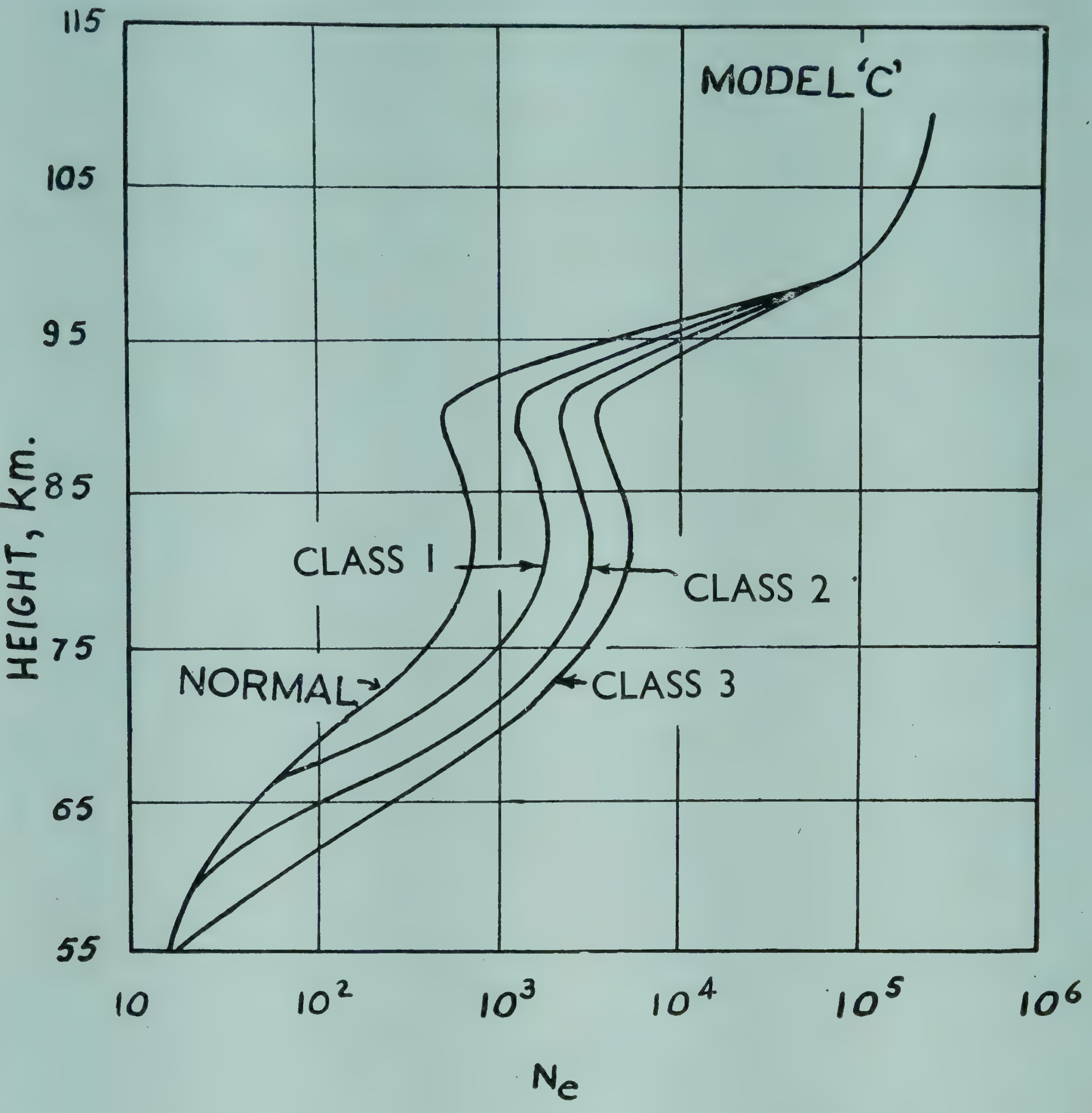

FIG. 22 — DISTRIBUTION OF FLARE IONIZATION FOR DIFFERENT TYPES OF SOLAR FLARES COMPUTED BY MITRA

respectively) differ as much as they do. It seems likely that the magnitude as well as the spectrum of the solar X-ray emission changes during the course of the flare.

PHYSICS OF THE IONOSPHERE

Only two aspects of ionospheric physics will be considered here, namely (i) origin of the ionospheric layers, and (ii) loss process in the ionosphere and the 'effective' recombination coefficient.

Origin of Ionospheric Layers. In non-polar regions the major ionizing source is the solar ultraviolet and X-rays, through a process such as

$$X + h\nu \rightarrow X^+ + e$$

For such a process the rate of electron production, q, is given by

$$q_h = \eta A(\mathrm{X},\lambda) n_h(\mathrm{X}) Q_h(\lambda)$$

where η is the ionization efficiency, $A(\mathrm{X},\lambda)$ is the absorption cross-section of the process, $n_h(\mathrm{X})$ is the particle density of the ionized constituent and $Q_h(\lambda)$ is the photon flux at any height h for the wavelength λ.

Theories regarding the origin of the ionospheric layers require that precise information should be available on (i) the photon flux Q, (ii) the particle density, and (iii) the coefficients η and A. The IGY saw great improvement in our knowledge of some of these quantities, especially of Q and n. Much of these came from information gathered by instruments flown in rockets and satellites. As a result, the origin of ionospheric layers, one of the oldest problems of ionospheric physics, can be discussed with some amount of confidence.

The suitability or otherwise of a particular process is judged mainly from the following criteria:

(i) Criterion of location

$$A_i n_{im} + \sum_k A_k n_{km} = \frac{\cos \chi (1+\beta_i)}{H_{im}}$$

(ii) Criterion of ionization

$$N_e = \sqrt{AnQ/\alpha}$$

where suffixes i and k refer to ionizing and absorbing particles respectively. An application of both the criteria and comparison with observed ionospheric characteristics indicates that the following processes are important:

Region D

(i) $\mathrm{NO} + h\nu \xrightarrow{\lambda < 1216\,\text{Å}} \mathrm{NO}^+ + e$ (main source)

(ii) Production of ionization by cosmic rays between 50 and 60 km.

(iii) $\mathrm{M} + h\nu \xrightarrow{\lambda < 10\,\text{Å}} \mathrm{M}^+ + e$ (during solar flares)

Region E

(i) $\mathrm{M} + h\nu \xrightarrow{\lambda\lambda 20-100} \mathrm{M}^+ + e$

(ii) $\mathrm{O}_2 + h\nu \xrightarrow{\lambda\lambda 800-1027} \mathrm{O}_2^+ + e$

The two processes are believed to be competitive, although the most recent feeling is that the ionization of O_2 may be the more important one[52].

Region F

It is believed that regions F_1 and F_2 have a common origin, the two layers being formed due to bifurcation occurring through the height variation of the recombination coefficient α. The ionization process is not monochromatic but occurs over a wide wavelength range of 170–900 Å, including that of the strong resonance line of HeII at 303·8 Å.

$$\mathrm{O} + h\nu \xrightarrow{\lambda\lambda 170-900} \mathrm{O}^+ + e$$

A summary of the relevant data is given in Table 10.

TABLE 10 — BASIC PHOTO-IONIZATION PARAMETERS FOR IONOSPHERIC LAYERS

REGION	PROCESS	SPECTRAL INTENSITIES AT NORMAL INCIDENCE *ergs/cm.²/sec.*	REMARKS
D	Lα (NO)	3	Intensity variable with sunspot activity
	Cosmic rays (50–60 km.)	—	Production rate given by $q(\phi) = 10^{-7} n \text{cm.}^{-3}/\text{s}$ for $\phi = 50°$
	X-rays (2–8 Å)	10^{-2}	Av. strong flare
E	X-rays (20-100 Å)	2	—
	800–1027 (O_2)	0·5	—
F	796–911 (O,O_2)	0·3	—
	400–796 (O,O_2,N_2)	0·6	—
	170–400 (Including HeII 303·8)	1·0	All contribute to F production
	[HeII 303·8]	0·3	—

Recombination Processes in the Ionosphere. The effective recombination coefficient in the ionosphere varies from a value of 10^{-6} cm.³/sec. at 70 km. to 10^{-12} cm.³/sec. at 600 km. and above, thus changing by a factor of 10^6 between the lowest and the highest ionospheric regions. No single process can be assumed to cover such a wide range of values, and several processes have been suggested to explain the ionospheric loss processes: these include the negative ion theory, dissociative recombination processes and the atom-ion interchange process.

While the loss processes are different at different ionospheric levels, it is nevertheless possible to derive one single relationship for the entire ionosphere. This is given by

$$\alpha = \alpha_e + \lambda\alpha_i + \frac{k\alpha_D n(YZ)}{kn(YZ) + \alpha_D N}$$

where α_e is the coefficient of radiative recombination, λ the negative ion to electron ratio, k the coefficient for atom-ion interchange, and $n(YZ)$ is the particle concentration of the molecule YZ involved in the atom-ion interchange process. Mitra[53] has given an empirical relationship, based on an extensive analysis of recombination coefficient values for the various ionospheric regions. This is given by

$$\alpha \simeq 2\times10^{-35} n^2(O_2) + 3\times10^{-20} n(O) + \frac{2\times10^{-19} n(O_2)}{2\times10^{-11} n(O_2) + 1\times10^{-8} N} + 1\times10^{-12} \text{cm.}^3/\text{sec.}$$

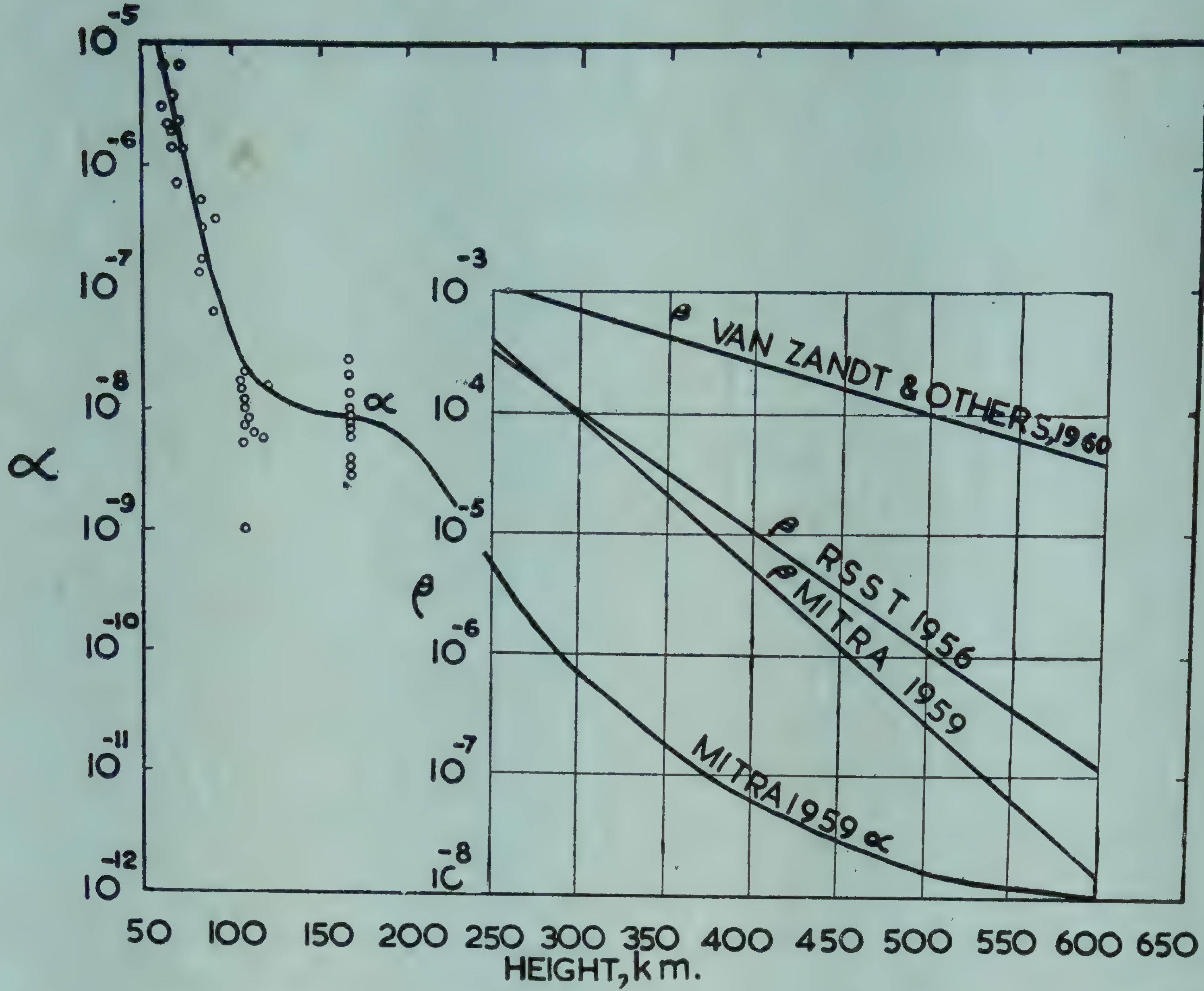

FIG. 23 — AN EMPIRICAL DISTRIBUTION OF THE EFFECTIVE RECOMBINATION COEFFICIENT NEAR NOON FOR HEIGHTS 50–600 KM. GIVEN BY A. P. MITRA

This reduces to the following simple expressions in the different regions:

Region D

$$\alpha \simeq 2\times10^{-35}n^2(O_2)+3\times10^{-20}n(O)+1\times10^{-8}$$

Region E

$$\alpha = 1\times10^{-8}$$

Region F

$$\alpha \simeq \frac{2\times10^{-19}n(O_2)}{2\times10^{-11}n(O_2)+1\times10^{-8}N}$$

or

$$\beta = 2\times10^{-11}n(O_2) \quad \text{(For h > 250 km.)}$$

Outer Ionosphere

$$\alpha \simeq 1\times10^{-12}$$

At heights between 250 and 400 km., the loss process simulates an attachment process, with an effective coefficient given by $\beta(=\alpha N)$.

In Fig. 23 values of α and β derived by Mitra are indicated.

References

1. Dodson, H. W. & Hedeman, E. R., *J. geophys. Res.*, **65** (1960), 123.
2. Bartels, K., *Symposium on the July 1959 Events and Associated Phenomena, IUGG Monograph* No. 7, 1960.
3. Sterne, T. E., *Smithsonian Astrophysical Observatory Spec. Rep.* No. 11, 1958.
4. Schilling, G. F. & Sterne, T. E., *J. geophys. Res.*, **64** (1958), 1.
5. Krassovsky, V. I., *Proc. Inst. Radio Engrs, N.Y.*, **47** (1959).
6. Groves, G. V., *Nature, Lond.*, **183** (1959), 179.
7. Schilling, G. R. & Whitney, C. A., *Smithsonian Astrophysical Observatory Spec. Rep.* No. 18 (1958), 13.
8. Martin, H. A., Neveling, W., Priester, W. & Roemer, M., *Space Research* Vol. II (North Holland Publishing Co., Amsterdam), 1961.
9. Kallman, H. K., *J. geophys. Res.*, **64** (1959), 615.
10. Mathur, S. B. & Mitra, A. P., *J. sci. industr. Res.*, **19A** (1960), 311.
11. Hulbert, E. O., *Advances in the Physics of the Upper Air Since 1950, Naval Research Laboratory, Washington, Rep.* No. 4600, 1955.
12. Kallman-Bijl, H., Boyd, R. L. F., Lagow, H., Poloskov, S. M. & Priester, W., *CIRA* 1961: *COSPAR International Reference Atmosphere,* 1961 (North Holland Publishing Co., Amsterdam), 1961.
13. Jacchia, L. G. & Briggs, R. E., *Smithsonian Astrophysical Observatory Spec. Rep.* No. 18, 1958.
14. Nicolet, M., *Physics of the Upper Atmosphere,* Ed. J. A. Ratcliffe (Academic Press, New York), 1960, 17.
15. Jastrow, R. & Bryant, R., *J. geophys. Res.*, **65** (1960), 3512.
16. Byram, E. T., Chubb, T. A. & Friedman, H., *Phys. Rev.*, **98** (1955), 1594.
17. Kupperian, J. E. (Jr), Byram, E. T., Friedman, H. & Unzicker, A., *Annals of the IGY,* Vol. XII, Part I (Pergamon Press, London), 1960, 440.
18. Nicolet, M., *Scientific Rep.* No. 102, *Ionosphere Research Laboratory, Pennsylvania State University,* 1958.
19. Townsend, J. W. (Jr), Johnson, C. Y., Holmes, J. C. & Meadows, E. G., *Annals of the IGY,* Vol. XII, Part I, 1960, 431.
20. Poloskov, S. M., *Space Research,* Ed. Kallman-Bijl (North Holland Publishing Co., Amsterdam), 1960, 95.
21. Little, C. G. & Leinpach, H., *Proc. Inst. Radio Engrs, N.Y.*, **46** (1958), 334.
22. Bailey, D. K., *J. geophys. Res.*, **12** (1957), 431.
23. Reid, G. C. & Leinbach, H., *J. geophys. Res.*, **64** (1959), 1801.
24. Seddon, J. C. & Jackson, J. E., *IGY Rocket Rep. Ser.* No. 1, *IGY World Data Centre A* (National Academy of Sciences, Washington), 1958, 149.
25. Gates, David, M., *J. Res. nat. Bur. Stand.*, **63D** (1959), 1.
26. Appleton, E. V., *Some Ionospheric Results Obtained During the International Geophysical Year,* Ed. W. J. G. Beynon (Elsevier Publishing Co., Amsterdam), 1960, 3.
27. Odishaw, H., *Science,* **128** (1958), 1599.
28. Briggs, B. H., *Some Ionospheric Results Obtained During the International Geophysical Year,* Ed. W. J. G. Beynon (Elsevier Publishing Co., Amsterdam), 1960, 297.
29. Purslow, B. W., *Nature, Lond.*, **181** (1958), 35.
30. Rao, B. R. & Rao, E. B., *J. atmos. terr. Phys.*, **14** (1959), 94.
31. *IGY Bull.* No. 40 (National Academy of Sciences, Washington), 1960, 9.
32. Southworth, M. P., *J. geophys. Res.*, **65** (1960), 601.
33. Garriot, O. K., *J. geophys. Res.*, **65** (1960), 1139.
34. Ross, W. J., *J. geophys. Res.*, **65** (1960), 2607.
35. Nisbet, J. S., *J. geophys. Res.*, **65** (1960), 2597.
36. Alpert, Dobriakova, Chudesenko & Shapero, *Dokl. Akad. Nauk. S.S.S.R.*, **120** (1958).
37. Little, C. G. & Lawrence, R. S., *Space Research,* Ed. Kallman-Bijl (North Holland Publishing Co., Amsterdam), 1960, 340.
38. Bowles, K. L., *J. Res. nat. Bur. Stand.*, **65D** (1961), 1.
39. Mitra, A. P. & Sarada, K. A., *J. atmos. terr. Phys.*, **23** (1962), 347.
40. Storey, L. R. O., *Phill. Trans.*, **246A** (1953), 113.
41. Heliwell, R. & Morgan, M. G., *Proc. Inst. Radio Engrs, N.Y.*, **47** (1959), 200.
42. Storey, L. R. O., *Canad. J. Phys.*, **34** (1956), 1153.
43. Helliwell, R. & Gehrels, E., *Proc. Inst. Radio Engrs, N.Y.*, **46** (1958), 785.
44. Allock, G., *J. atmos. terr. Phys.*, **14** (1959), 185.
45. Mitra, A. P. & Shain, C. A., *J. atmos. terr. Phys.*, **4** (1953), 204.

46. Ramanathan, K. R., Bhonsle, R. V. & Degaonkar, S. S., *J. geophys. Res.*, **66** (1961), 2763.
47. Peterson, All[illegible] M., *J. geophys. Res.*, **64** (1959), 933.
48. Mitra, A. P., [illegible]*ific Rep*. No. 112, *Ionosphere Research Laboratory, Pennsylvania State Univer*[illegible], Oct. 15, 1958.
49. Chubb, T. A., [illegible]riedman, H. & Kreplin, R.W., *Space Research*, Vol. I, Ed. Kallman-Bijl (North Holland Publishing Co., Amsterdam), 1960, 695.
50. Peterson, L. E. & Winckler, J. A., *J. geophy. Res.*, **64** (1960), 697.
51. Nicolet, M. & Aikin, A. C., *J. geophys. Res.*, **65** (1960), 1469.
52. Watanabe, K. & Hinteregger, H. E., *J. geophys. Res.*, **67** (1962), 999.
53. Mitra, A. P., *J. geophys. Res.*, **64** (1959), 733.

Ionospheric observations at Tiruchirapalli

S. RANGASWAMY
C. S. R. RAO

Research Department, All India Radio
New Delhi

Some of the characteristics of the F_2 layer of the ionosphere as revealed by the data collected during IGY and IGC observations at Tiruchirapalli are presented.

The diurnal variations of the critical frequency of the F_2 layer are typical of an equatorial station, the midday 'bite-out' effect being prominent in all three seasons. Very high values of height of maximum ionization, hpF_2 (400-600 km.) have been recorded in day-time. One peculiar feature of the height variations has been a sudden increase just after sunset. Such an effect appears to be common to equatorial stations only. An attempt is made to explain this effect.

All India Radio established an ionospheric station at Tiruchirapalli (10°49′N: 78°42′E, geomag. lat. 01°05′N) in 1944 and regular measurements of ionospheric characteristics have been in progress ever since. The data collected have also been regularly published. During the IGY and IGC, the station took part in the regular programme of observations. The present paper deals with an analysis of some of the characteristics of the ionosphere as revealed from the data collected during 1957–58.

The height of maximum ionization of F_2 layer has been taken as the height corresponding to the virtual height measured at a frequency equal to 0·834 times the critical frequency. The monthly mean values of the data have been averaged to give the seasonal values for the three different seasons — summer, winter and equinox — in the usual way.

Critical Frequency. Fig. 1 shows the diurnal variation of critical frequency for the three seasons. The general characteristics of an equatorial station are clearly evident. High value of critical frequency is reached in

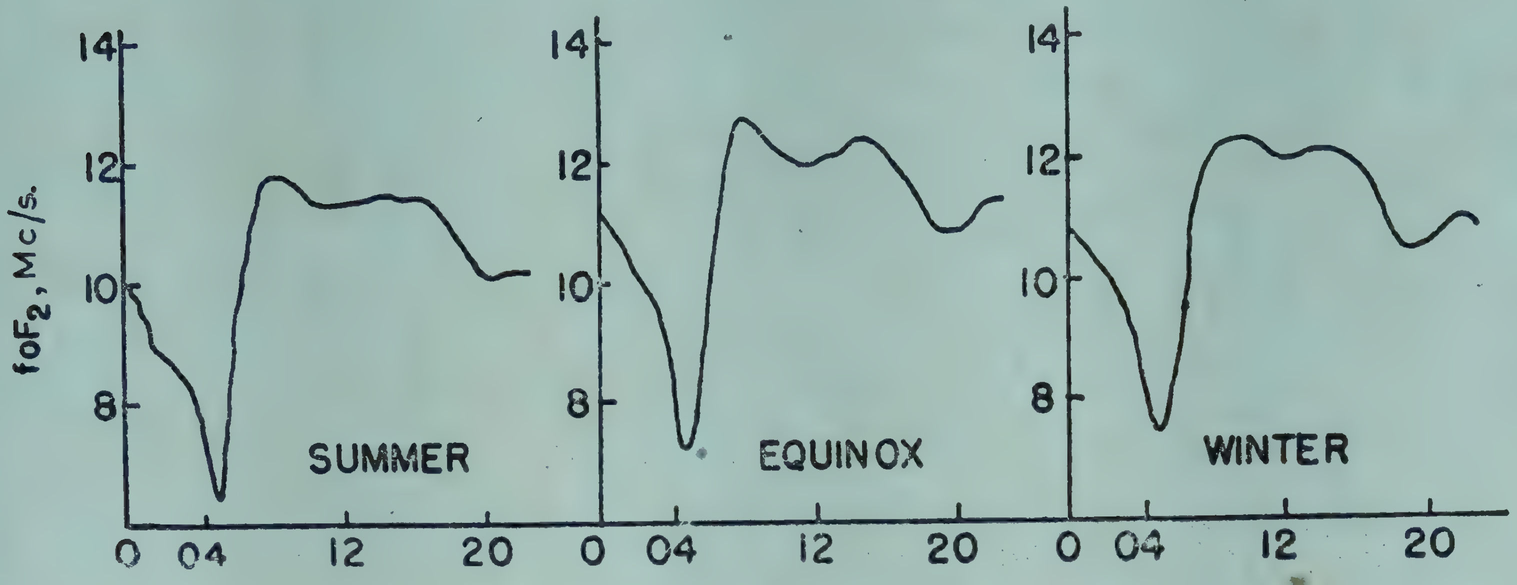

Fig. 1 — Diurnal variation of the critical frequency for the summer (1957), equinox (1957) and winter (1957–58) months at Tiruchirapalli

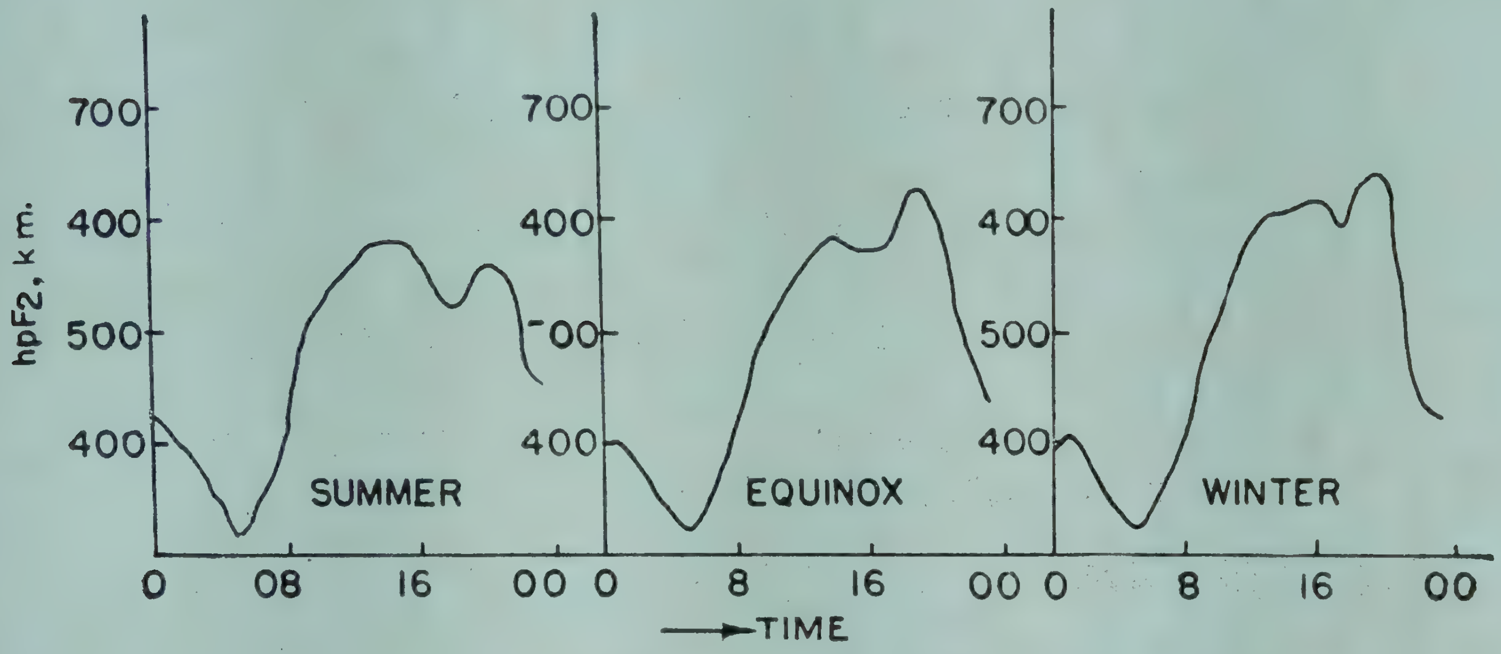

Fig. 2 — Diurnal variation of hpF$_2$ for the summer (1957), equinox (1957) and winter (1957–58) months at Tiruchirapalli

equinox, while summer values are the lowest. There is a sudden pre-sunrise fall in the critical frequency. This is followed by a rapid rise after sunrise. High values of critical frequency are maintained throughout the day with 'bite-out' effect at noon. The midday 'bite-out' effect is shown in all seasons, maximum being in equinox. A slight fall of critical frequency of the order of 2 Mc/s. occurs between sunset and about 2000 hours. Thereafter, almost a constant value is maintained till midnight. There is, however, a tendency for the critical frequency to rise slightly near midnight. This increase appears to be due to a contraction of the layer. This contraction may be compared with the expansion by the same amount near the maximum of critical frequency[1] and may be of tidal origin[2]. After midnight, there is a sharp fall in critical frequency; the lowest value is reached before sunrise.

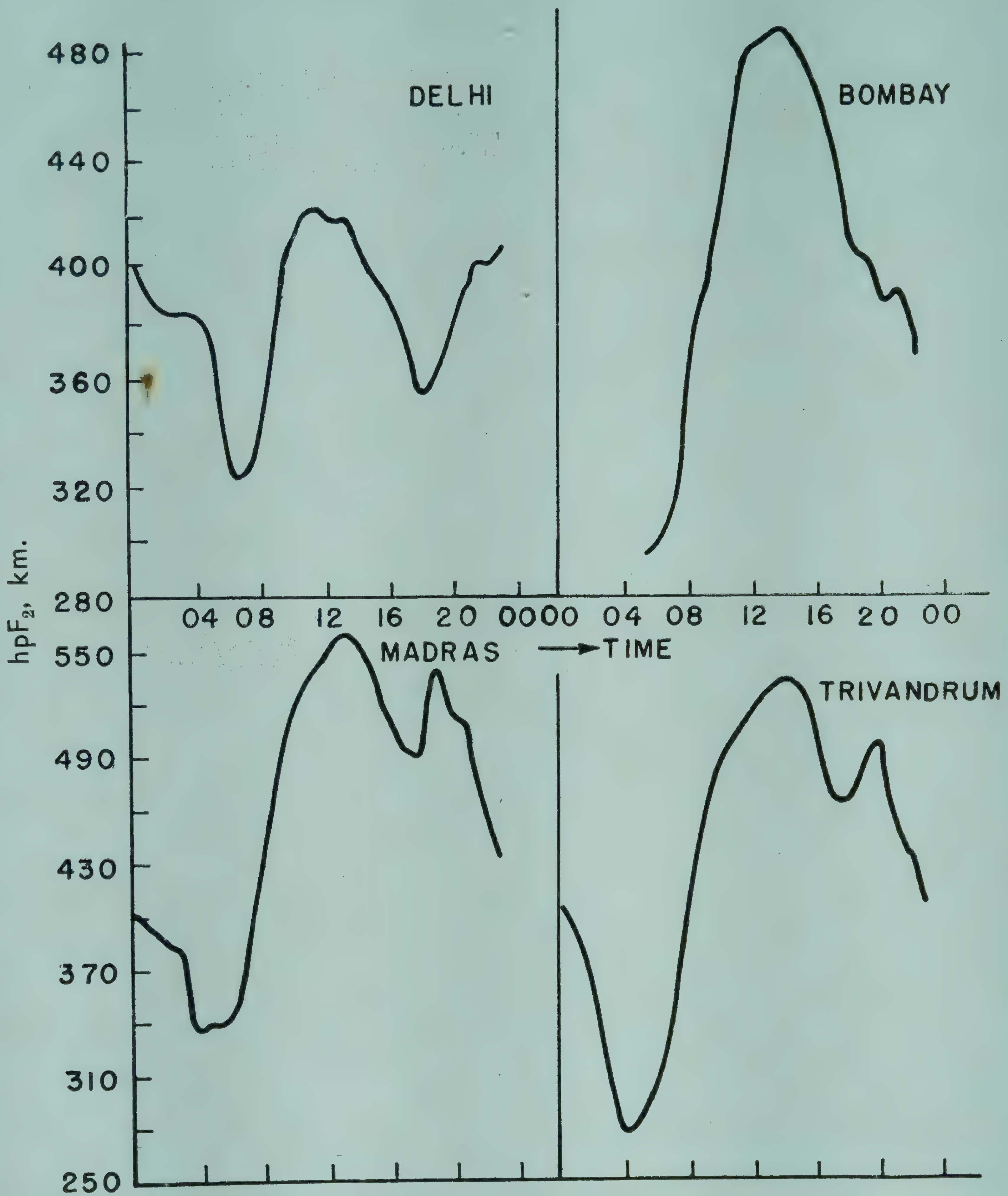

FIG. 3 — DIURNAL VARIATION OF hpF_2 FOR SUMMER MONTHS AT TRIVANDRUM, MADRAS, BOMBAY AND DELHI

Height of Maximum Ionization. Fig. 2 shows the variation of the height of maximum ionization, hpF_2, for the three seasons. Highest value of hpF_2 is reached in winter and the lowest in summer. Very high values of the order of 500–600 km. have been recorded in day-time. This is again another characteristic of an equatorial station, as can be observed from the data from Kodaikanal and Singapore. One particular feature of the

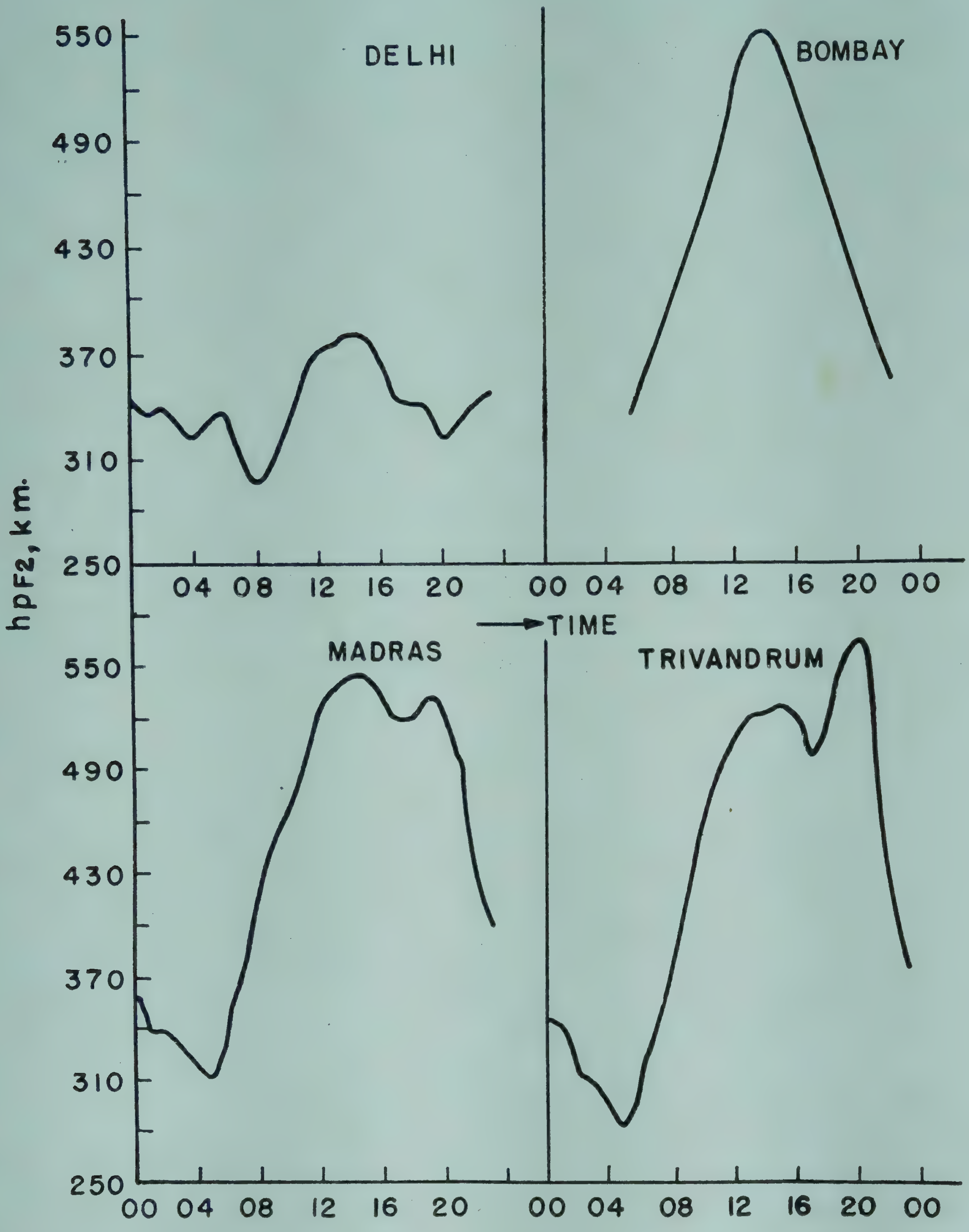

Fig. 4 — Diurnal variation of hpF_2 for winter months at Trivandrum, Madras, Bombay and Delhi

diurnal variation is the sudden rise and fall of the height near sunset. This is dealt with in detail in the following section.

Sunset Effect. As the diurnal variation of the height at Tiruchirapalli is followed, it is observed that the height gradually rises from a low value at sunrise to a very high value in day-time reaching a maximum at about

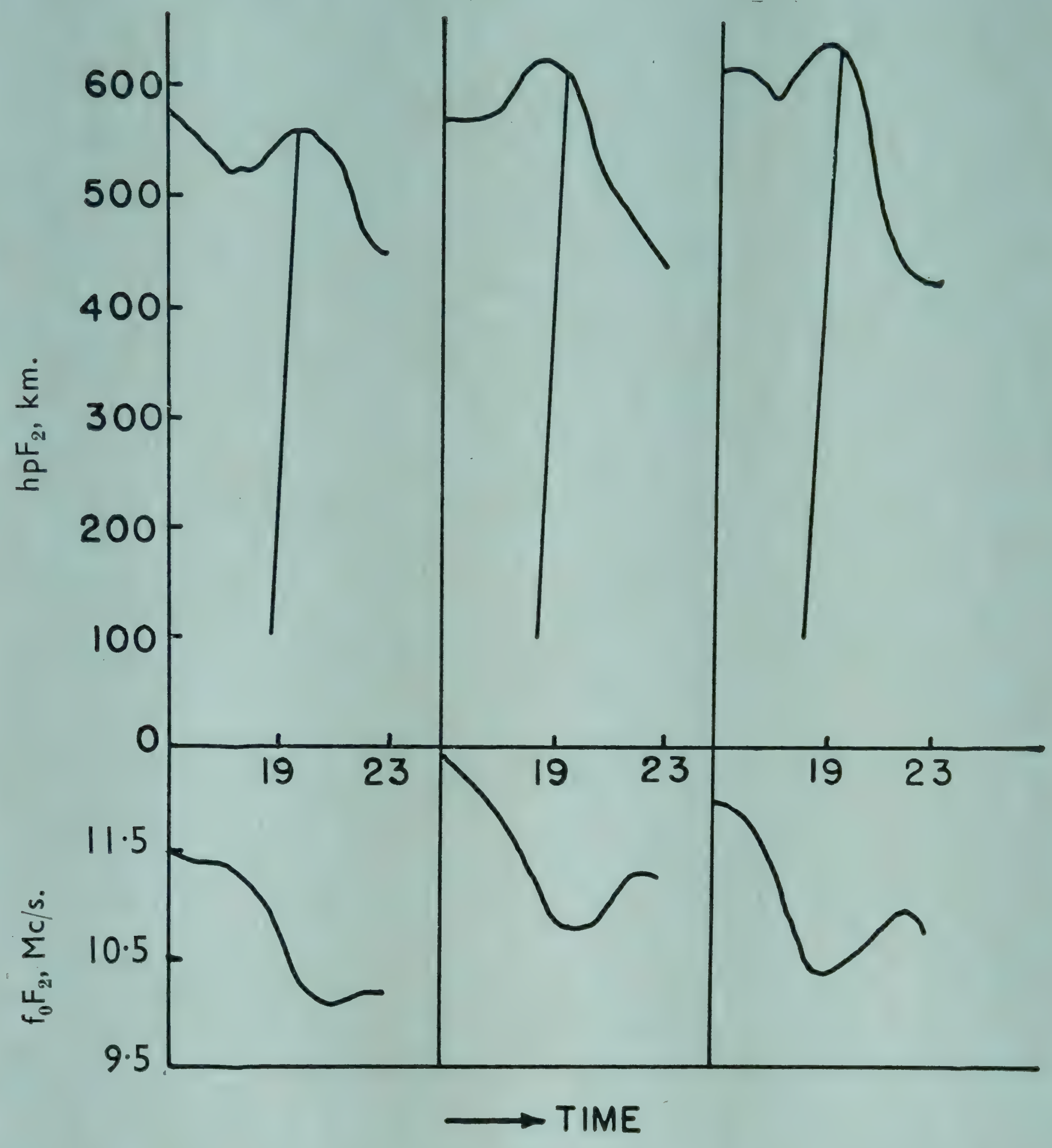

Fig. 5 — Illustrating the 'sunset' effect as observed at Tiruchirapalli

1400 hours. Thereafter, a gradual fall is noted up to about 1600 hours (depending on the season). At this time, there is again a sudden rise of about 50–75 km. followed by a rapid fall in height. Such a type of variation occurs in all the three seasons as shown in Fig. 2.

That such a type of phenomenon appears to be common to equatorial latitudes is shown in Figs. 3 and 4. In these figures, the diurnal variation of hpF$_2$ for Delhi (geomag. lat. 19°11′N), Bombay (geomag. lat. 10°00′N), Madras (geomag. lat. 03°05′N) and Trivandrum (geomag. lat. 00°54′S) are shown for the summer and winter of 1956–57. It may be observed from these figures that while the effect is prominent at Trivandrum and Madras, it is absent at Bombay and Delhi.

TABLE 1 — SUNSET TIME AT DIFFERENT HEIGHTS AND AT DIFFERENT SEASONS

HEIGHT *km.*	TIME OF SUNSET, *hr*			
	July 1	Oct. 1	Dec. 1	Mar. 31
100	1904	1852	1827	1843
200	1923	1909	1845	1900
300	1937	1921	1858	1912
400	1949	1932	1909	1923
500	2000	1941	1919	1932
600	2010	1949	1927	1940

In regard to the variation observed at Tiruchirapalli, it may be seen from Fig. 5 that while the height increases during the post-sunset period, there is a corresponding fall in f_0F_2 during the same period. After about 2000 hours, when f_0F_2 values do not vary much, as discussed previously, the height values again show a rapid fall. Taking into account the sunset time at the ground and at different levels in the ionosphere, it may be seen that the time at which the height values start increasing or the f_0F_2 values start decreasing in the afternoon corresponds to the ground sunset time and the time at which the height values start falling or the f_0F_2 values stay without much variation correspond to the ionospheric sunset time. Such an effect has been observed by Osborne[3] for the h′F values at Singapore. Sunset time at different heights over the earth's surface and for different months are shown in Table 1.

These effects may be explained tentatively as follows.

The time of ionospheric sunset is later than the time of ground sunset. During this period, the ionizing radiation sweeps upwards from a horizontal position. So far as the ionosphere is concerned, this would mean that the source of ionization is removed from bottom upwards. This leads to a decay of ionization at lower levels and consequent erosion of the undersurface. Thus, there is an increase in h′F. The effect of removing the ionizing source from bottom upwards, together with a gradient in the recombination coefficient would also lead to an increase in hpF_2.

At equatorial latitudes the drift is upwards in the evening and night hours up to midnight and this would lead to a decrease in the hpF_2 values[2]. This decrease is, however, temporarily reversed during the period of ground and ionospheric sunsets due to the sunset effect described above.

Sporadic E. Observations on sporadic E which were started in January 1958 show that the E_s layer is present on all days during day-time. This has been observed in other equatorial stations. The height of the layer

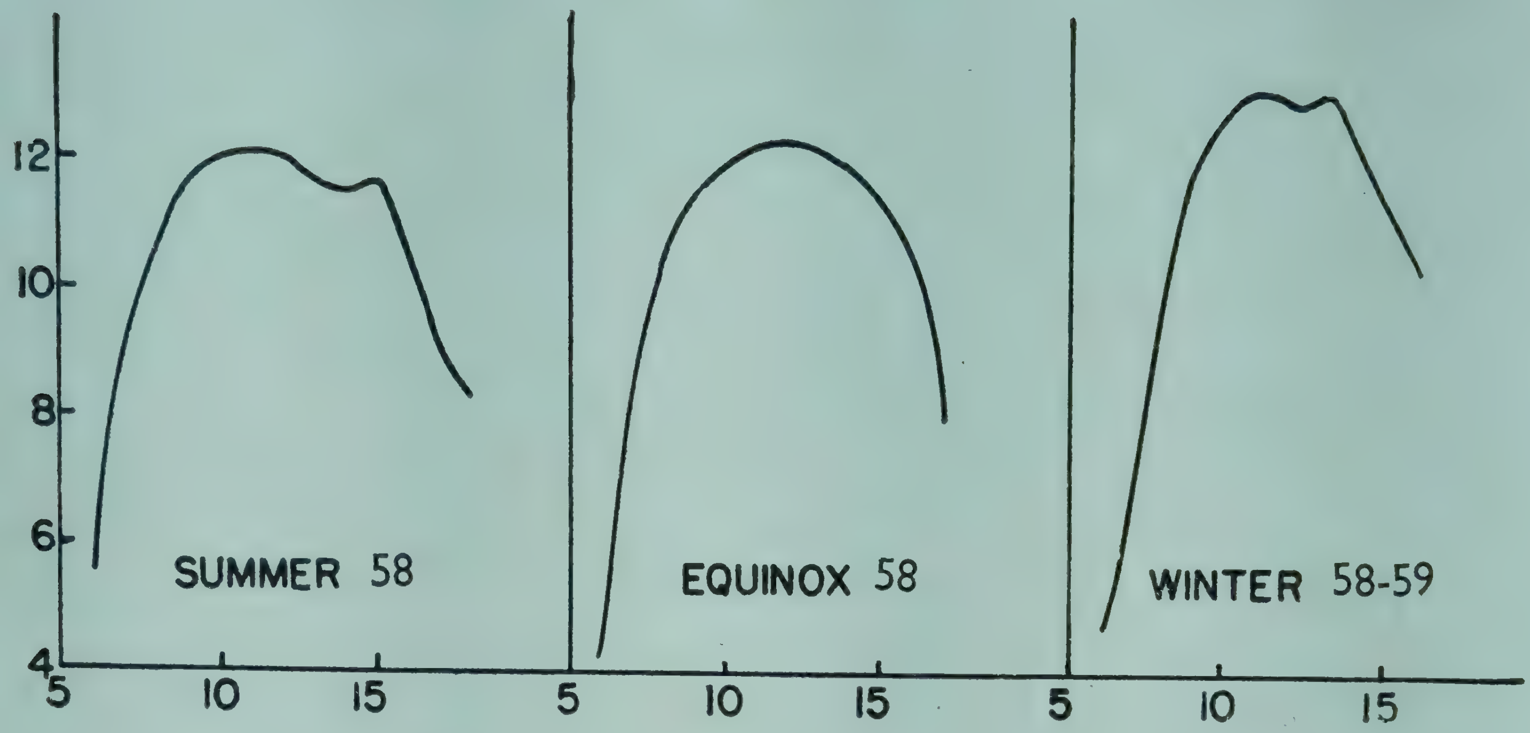

FIG. 6 — DIURNAL VARIATION OF fEs DURING 1958 AT TIRUCHIRAPALLI

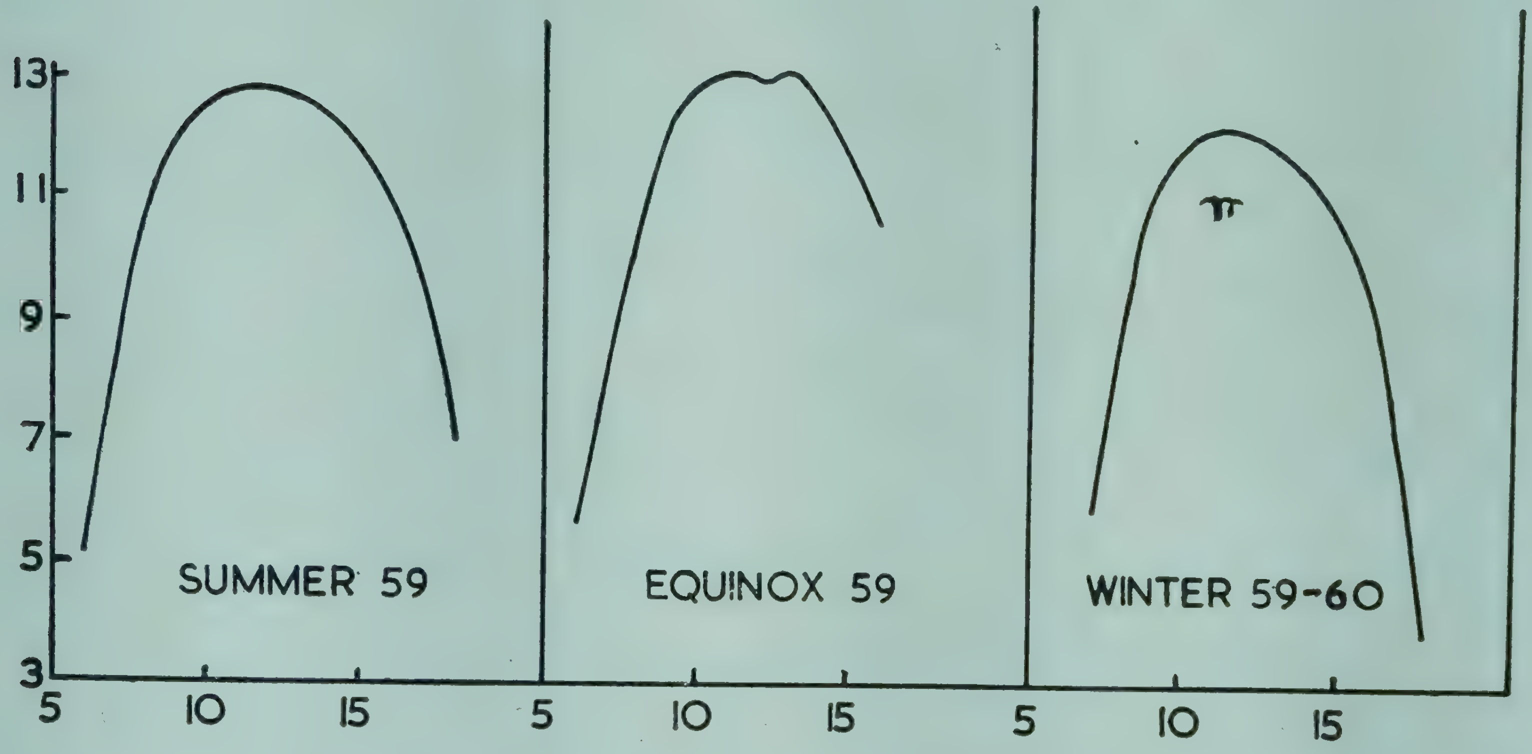

FIG. 7 — DIURNAL VARIATION OF fEs DURING 1959 AT TIRUCHIRAPALLI

varies between 80 and 100 km. E_s reflection is quite intense in day-time and sometimes blankets the higher layers.

E_s appears at about sunrise time, though on some days it is delayed by an hour or so and fE_s is low. Thereafter, this frequency rises steeply till the maximum value is reached just before noon. The value falls again till about sunset time when E_s disappears. E_s has been observed in night-time occasionally. There does not seem to be any well-defined seasonal variation as observed in Figs. 6 and 7.

The frequency of disappearance for E_s has been observed at Tiruchirapalli to be as high as 18 Mc/s. E_s echoes sometimes are found to disappear suddenly and reappear after a period of half an hour or so. This has been reported for other equatorial stations like Huancayo[4], Kodaikanal and Trivandrum.

During a Dellinger fade-out it has often been observed that returns from F layer were first to appear although both E_s and F were present before the fade-out occurred.

ACKNOWLEDGEMENT

Thanks are due to Shri Y. N. G. Rao, Station Engineer, All India Radio, Tiruchirapalli, and the IGY staff at the station for supplying the data.

REFERENCES

1. APPLETON, E. V., *J. atmos. terr. Phys.*, **5** (1954), 348.
2. MARTYN, D. F., *Proc. roy. Soc.*, **194A** (1948), 445.
3. OSBORNE, B. W., *J. atmos. terr. Phys.*, **2** (1951), 66.
4. MATSUSHITA, S., *J. Geomag. Geoelect.*, **7** (1955), 91.

Ionosphere over Trivandrum: Part II — Ionospheric observations during 1957-59

CH. SATYANARAYANMURTHY

Trivandrum Ionospheric Station
Research Department, All India Radio
New Delhi

Data collected during the years 1957-59, in connection with India's participation in the observations during IGY and IGC, have been analysed. The diurnal and seasonal variations of the critical frequency of F_2 layer, which show the typical characteristics of an equatorial station, have been studied in detail. Characteristics of the sporadic E layer are described. Diurnal and seasonal variation of the height of maximum ionization of F_2 layer and observations regarding spread F are recorded. Very high values of the heights have been observed. The data have also been compared with those observed at Kodaikanal and Madras.

An ionospheric station was established at Trivandrum towards the end of 1956 and regular measurements of the ionospheric characteristics are in progress since January 1957. The aspects of the F_2 layer dealing with the total electron content, temperature and recombination coefficient have been dealt with in Part I[1]. In this paper, the observations during 1957–59 of the F_2 layer regarding the critical frequency and height of maximum ionization, sporadic E and occurrence of spread echoes are reviewed.

Critical Frequency Variations (f_0F_2). The diurnal variation of f_0F_2 is generally represented by a double humped curve, which is a characteristic of the equatorial station. Fig. 1 shows the variations for the three different seasons averaged for the years 1957, 1958 and 1959.

After the early morning dip which occurs always around 0530 hours, there is a steep rise and the forenoon maximum is reached at 0900 hours. This is followed by a dip around noon and an afternoon maximum at about 1600 hours. After 1600 hours there is a slight fall (by about 2·5 Mc/s.)

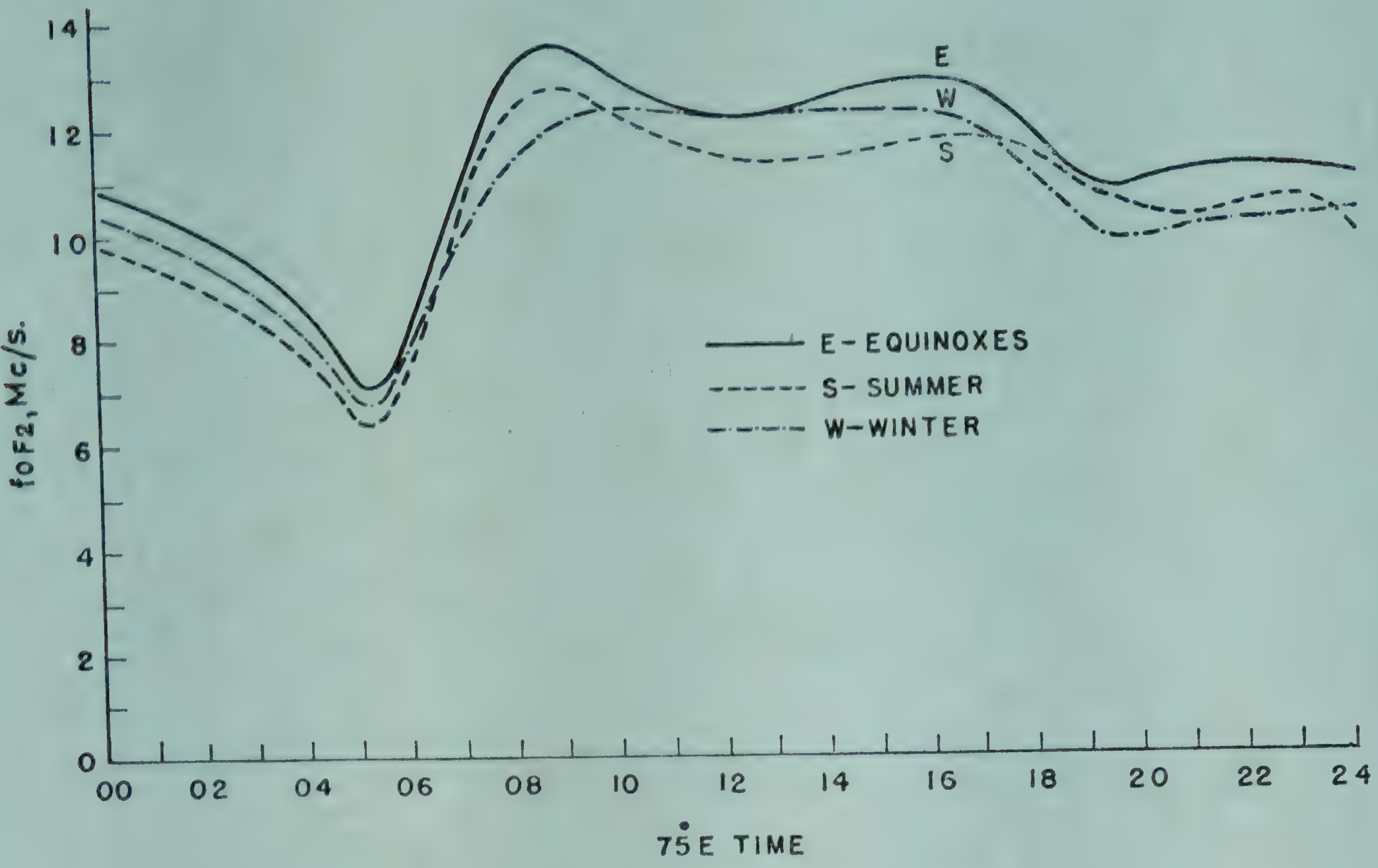

FIG. 1 — SEASONAL VARIATION OF f_0F_2 FOR 1957–59

up to about 1930 hours, after which the f_0F_2 values remain almost stationary up to midnight. After that there is a gradual fall, the lowest values being reached at about 0530 hours. The observations for the different seasons are described below.

Equinox Months. The f_0F_2 values are the highest for the year. The forenoon maximum occurs at 0900 hours. The dip in f_0F_2 values occurs at or just before noon and the afternoon maximum at about 1600 hours. Observations during the month of March show that the diurnal variation is an exact double humped curve, with two maxima not only centred around noon but exactly equal, while the forenoon maximum is comparatively higher than the afternoon maximum for equinox as a whole, the two maxima being exactly equal in March for all the three years considered.

Summer Months. The 'bite-out' effect is observed in summer. The critical frequencies are lower than those in the other two seasons. The midday dip appears just after the noon and the afternoon maximum occurs a little later than in equinox. From August onwards, as the equinox is approached, the values of f_0F_2 during day again increase and the time of afternoon maximum also shifts.

Winter Months. The 'bite-out' effect is not very prominent in winter due to the absence of the afternoon maximum. The day-time values are lower than the corresponding ones in equinox and the night-time values are the lowest for all the three seasons.

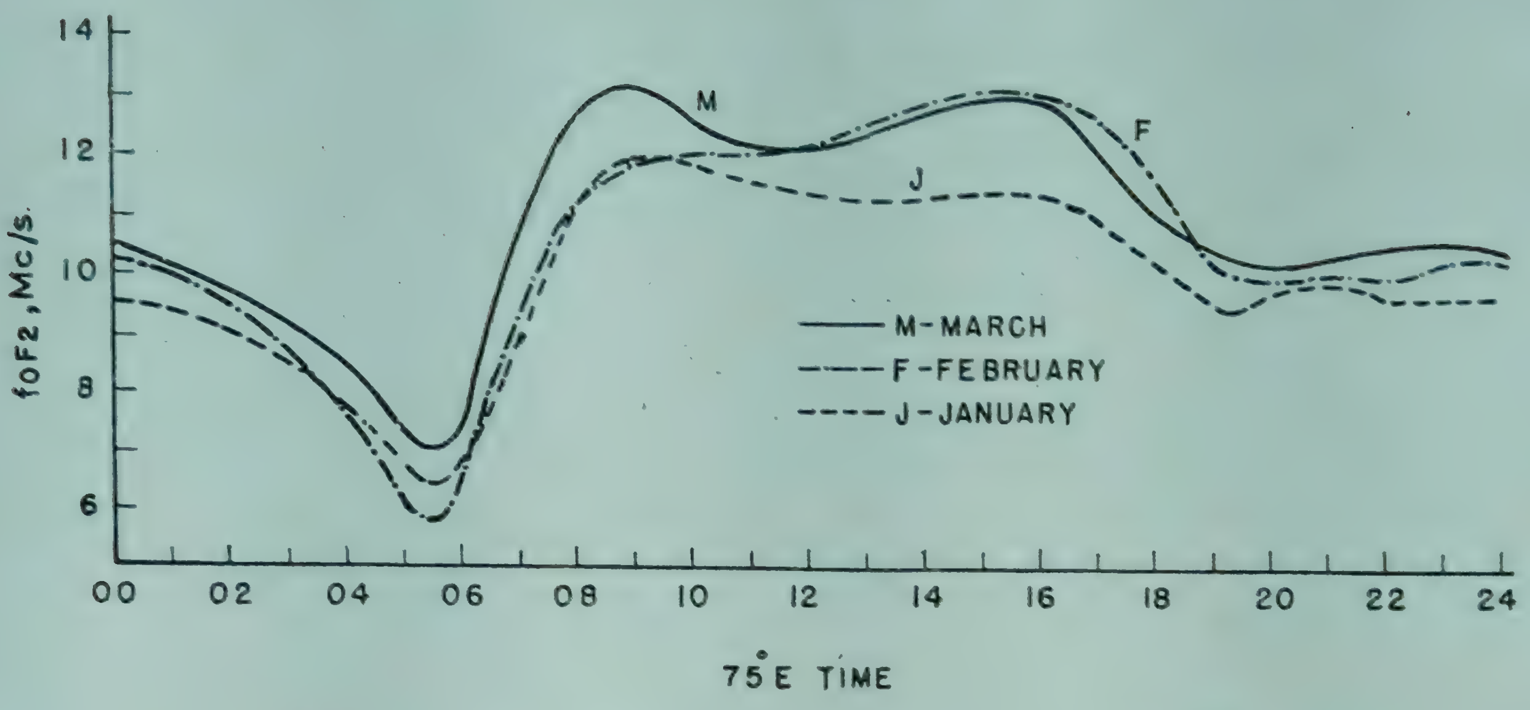

FIG. 2 — DIURNAL VARIATION OF f_0F_2 FOR 1957–59

The observations for the month of February are quite interesting. While the forenoon maximum corresponds to that of January, which is a typical winter month, the afternoon maximum corresponds to that of March. This is clearly shown in Fig. 2. Thus the month of February may be considered as a transition month, the conditions changing from those of winter to those of summer.

Comparison with the Data from Kodaikanal. A comparison of the diurnal variation of f_0F_2 at Trivandrum for different seasons is shown in Fig. 3. It may be seen from the curves in the figure that diurnal and seasonal variations for both the places are similar in almost all the three respects which have been considered just before. However, the values for Trivandrum are slightly higher for most part of the day in all seasons.

Height of Maximum Ionization (hpF_2). The height of maximum ionization corresponds to that value which is measured at a frequency equal to 0·834 times the critical frequency of the F_2 layer. The variations for all the three seasons for the years 1957–59 are shown in Fig. 4. Due to the presence of spread echoes in the night hours, an accurate analysis of the hpF_2 variation for those hours has not been possible.

The diurnal variation of hpF_2 is generally the same throughout the year. Lowest value of hpF_2 occurs at about 0500 hours (corresponding to the f_0F_2 minimum). This is followed by a steady increase, the maximum value being reached at about 1400–1500 hours. After this, there is a slow decrease till about the sunset time, when there is again a slight increase for about an hour or so. A general decrease in the values occurs thereafter till the minimum is reached. The maximum values of virtual heights are reached during winter day-time.

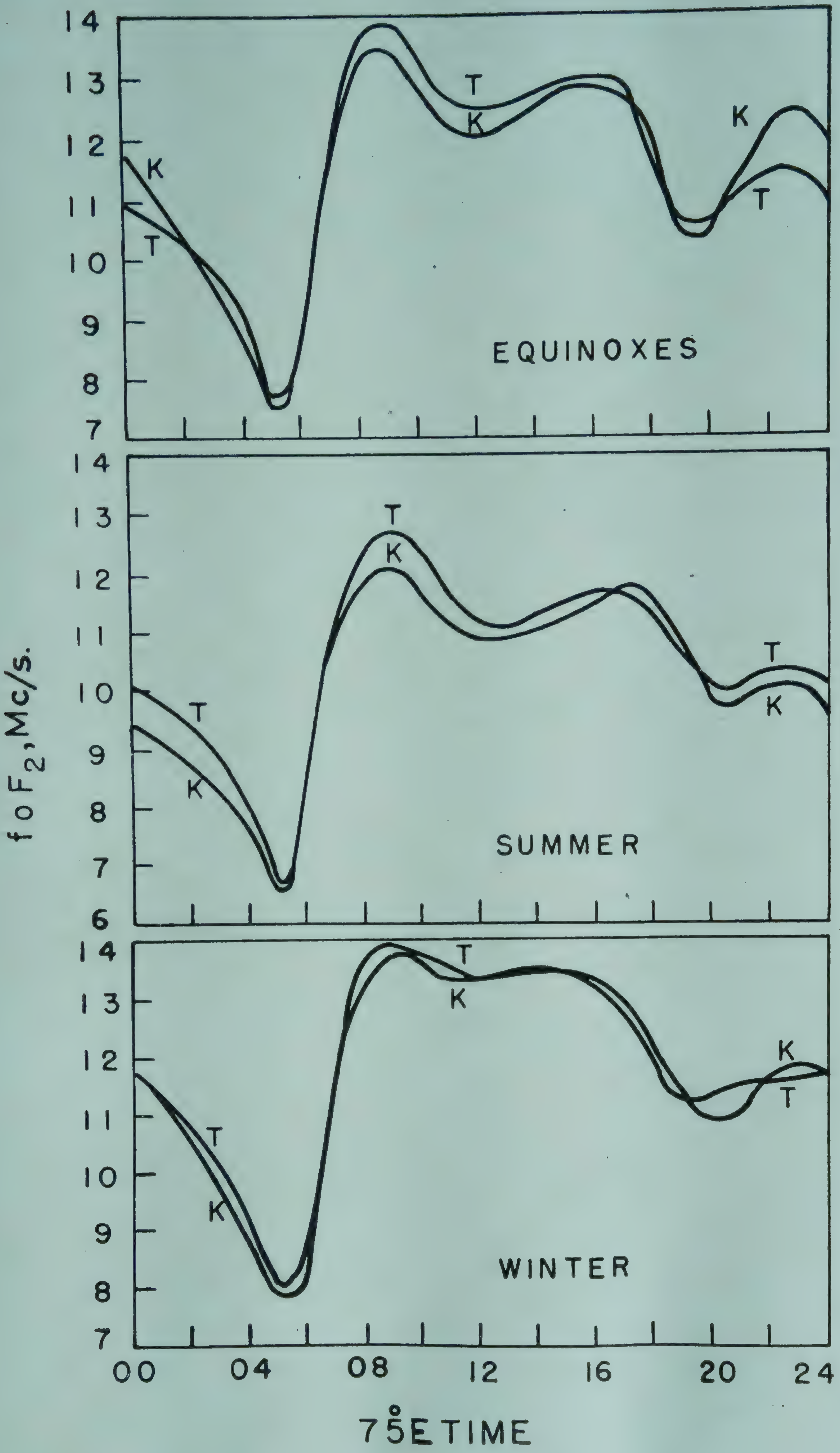

FIG. 3 — SEASONAL VARIATION OF f_0F_2 FOR TRIVANDRUM (T) AND KODAIKANAL (K)

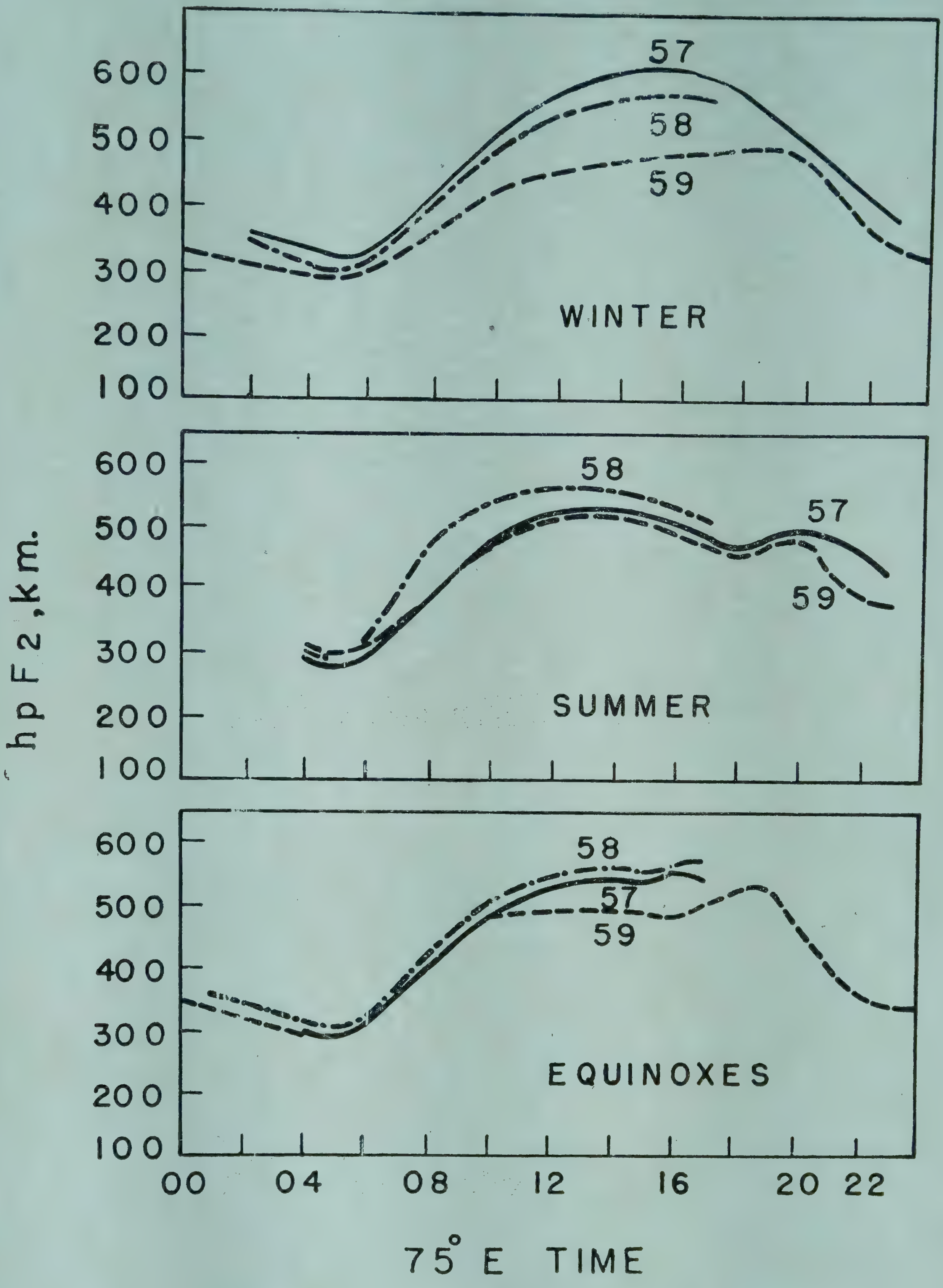

Fig. 4 — Diurnal variation of hpF_2 for 1957, 1958 and 1959

Sporadic E Observations. A regular feature of ionospheric observations at Trivandrum is the presence of sporadic E reflections throughout most of the daylight hours. The diurnal variation of fE_s is very regular and symmetric about noon. Reflections are first noticed within an hour of the

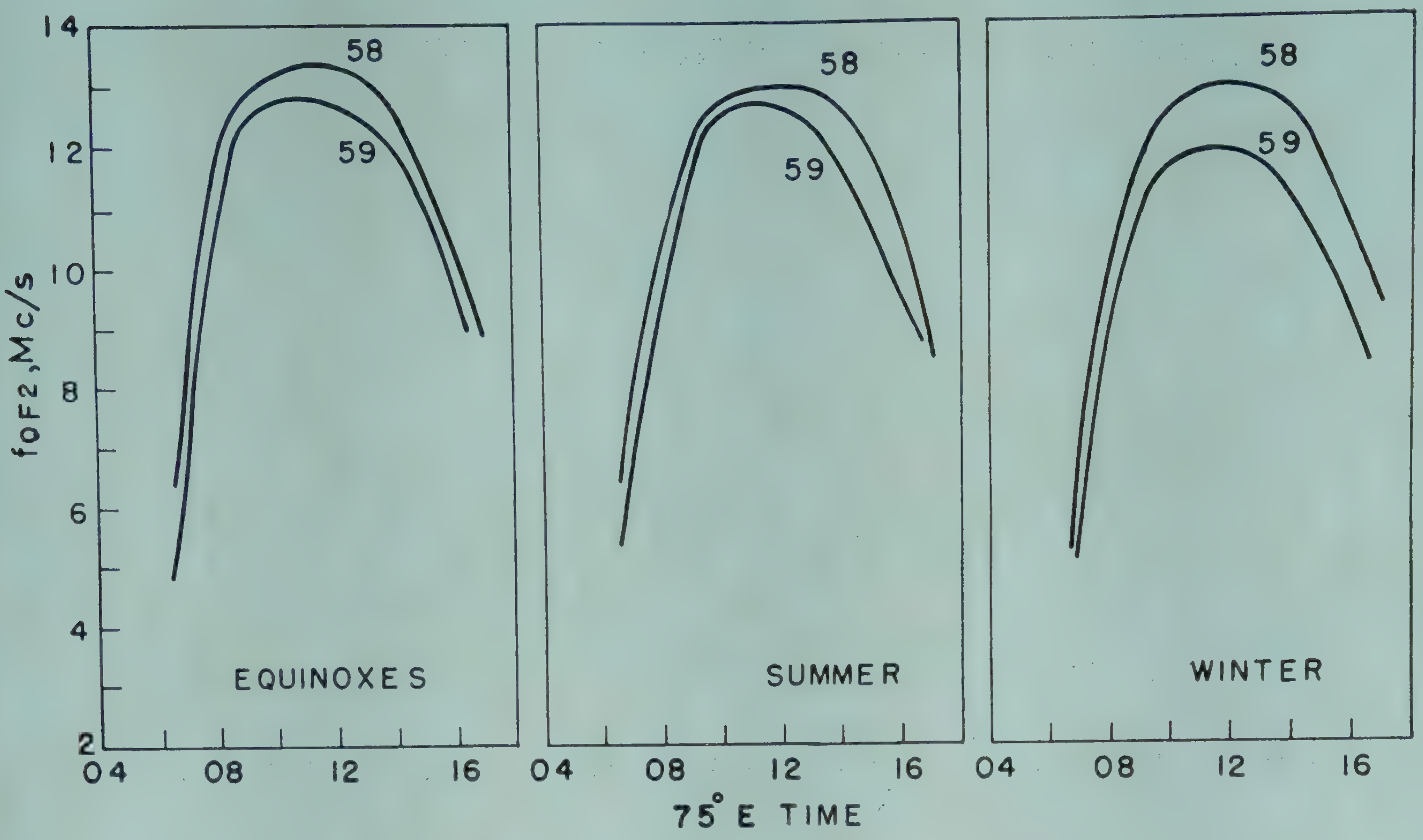

Fig. 5 — Diurnal variation of fEs for 1958 and 1959

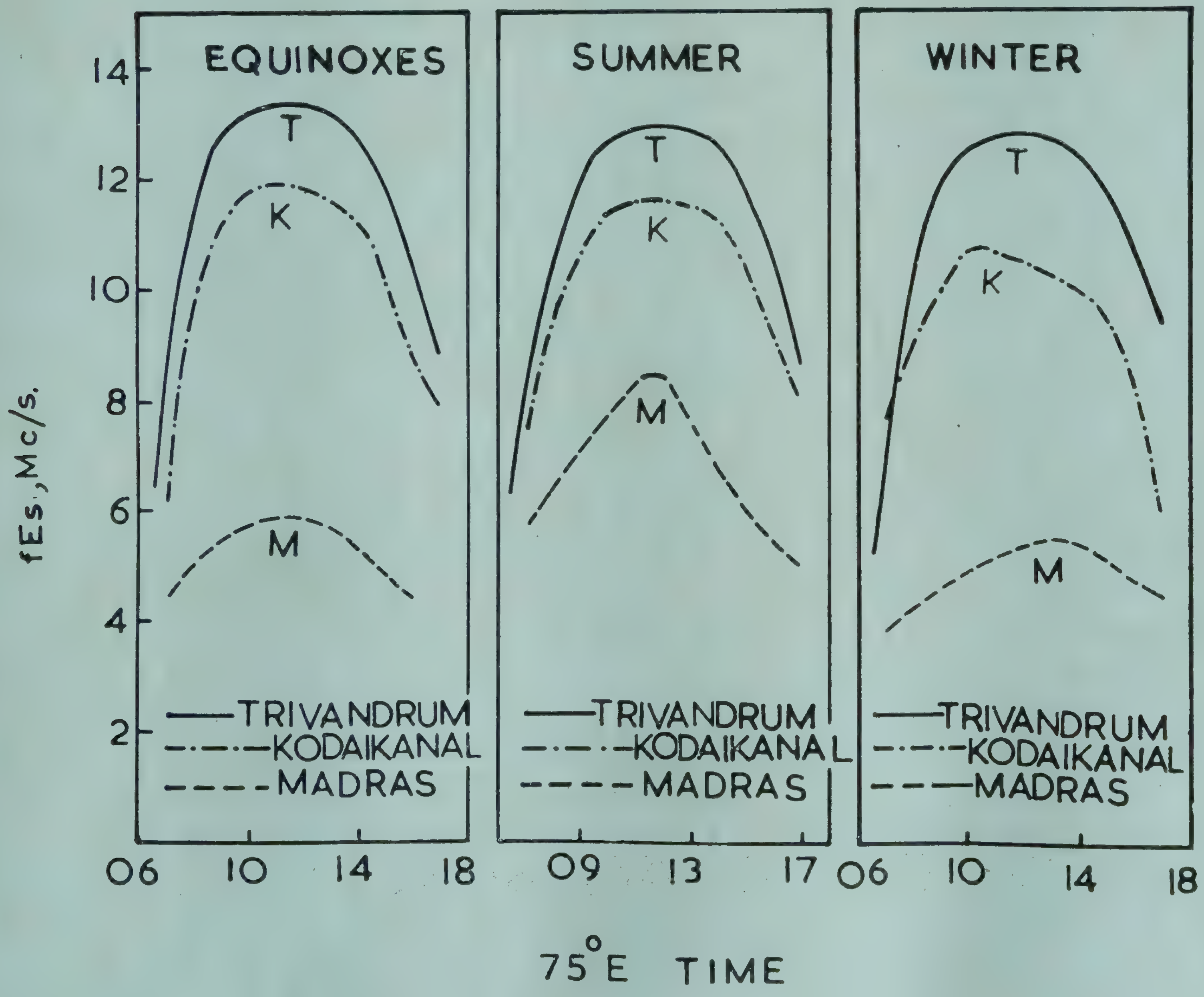

Fig. 6 — Diurnal variation of fEs for 1958

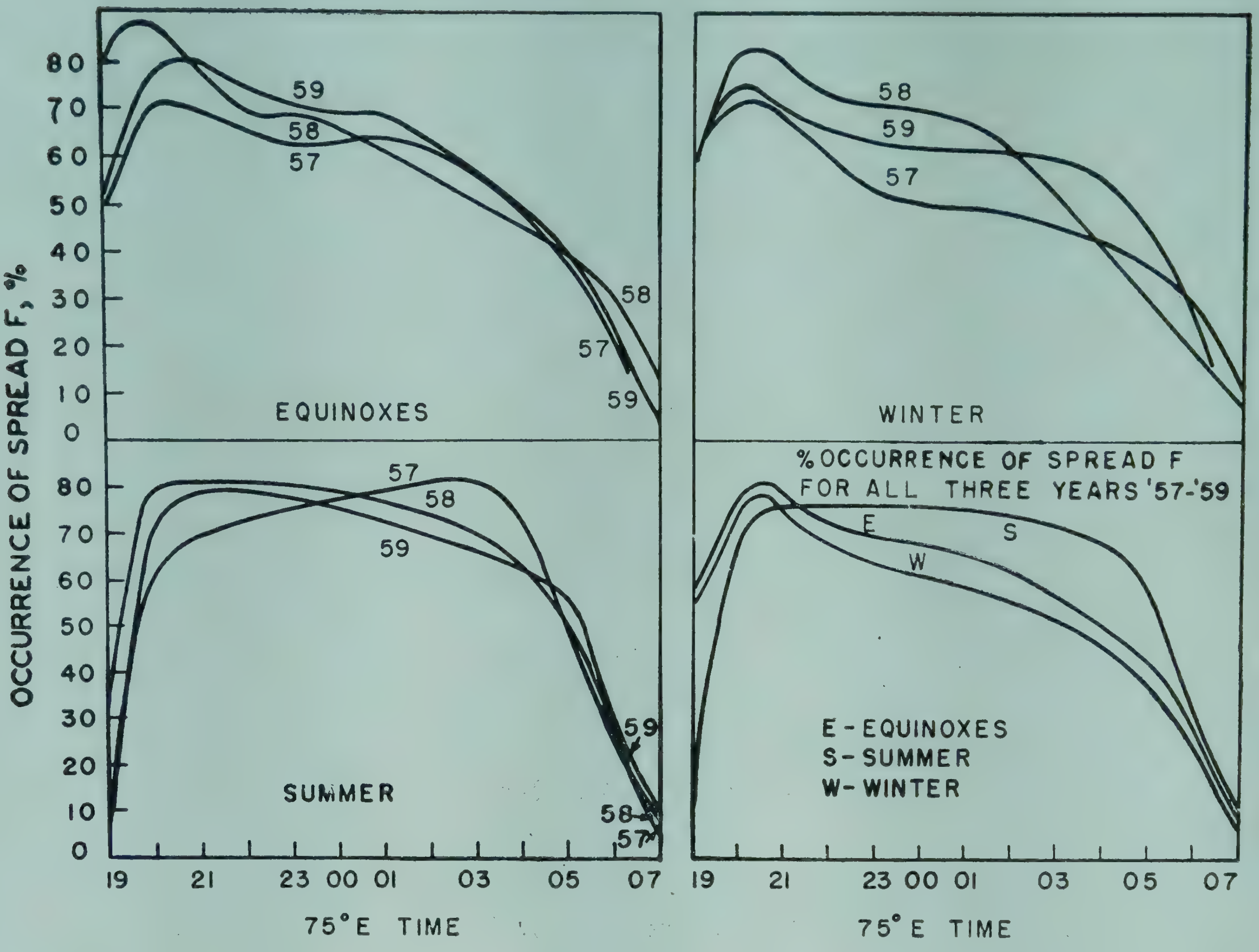

FIG. 7 — SEASONAL VARIATION OF PER CENT OCCURRENCE OF SPREAD F AT TRIVANDRUM (1957–59) AND PER CENT OCCURRENCE OF SPREAD F FOR ALL THREE YEARS (1957–59)

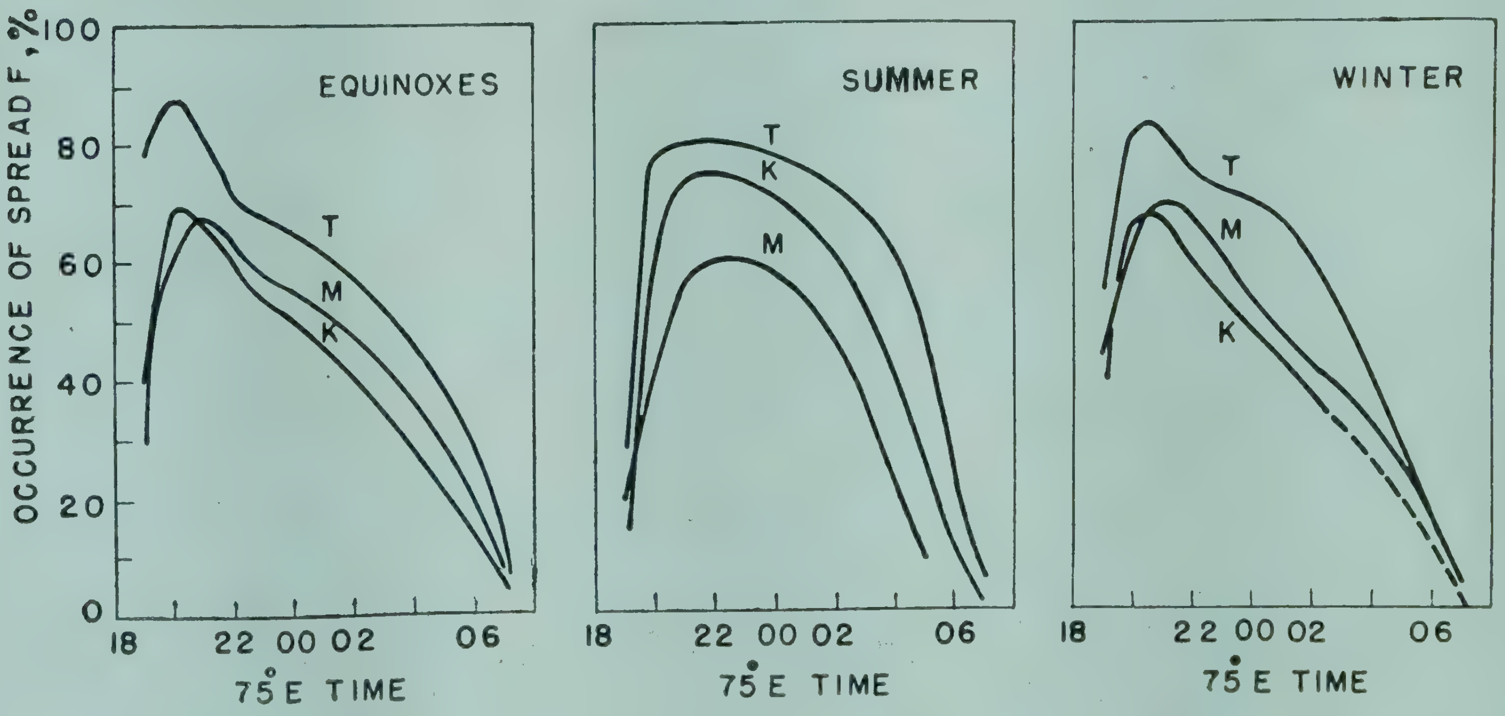

FIG. 8 — PER CENT OCCURRENCE OF SPREAD F AT TRIVANDRUM (T), KODAIKANAL (K) AND MADRAS (M) FOR 1958

sunrise and fE_s increases till the maximum values are reached near about 1000–1400 hours. There is only slight variation in fE_s between 1000 and 1400 hours. Between 1400 and 1700 hours, there is a rapid decrease in the fE_s after which the fE_s reflections cease to appear.

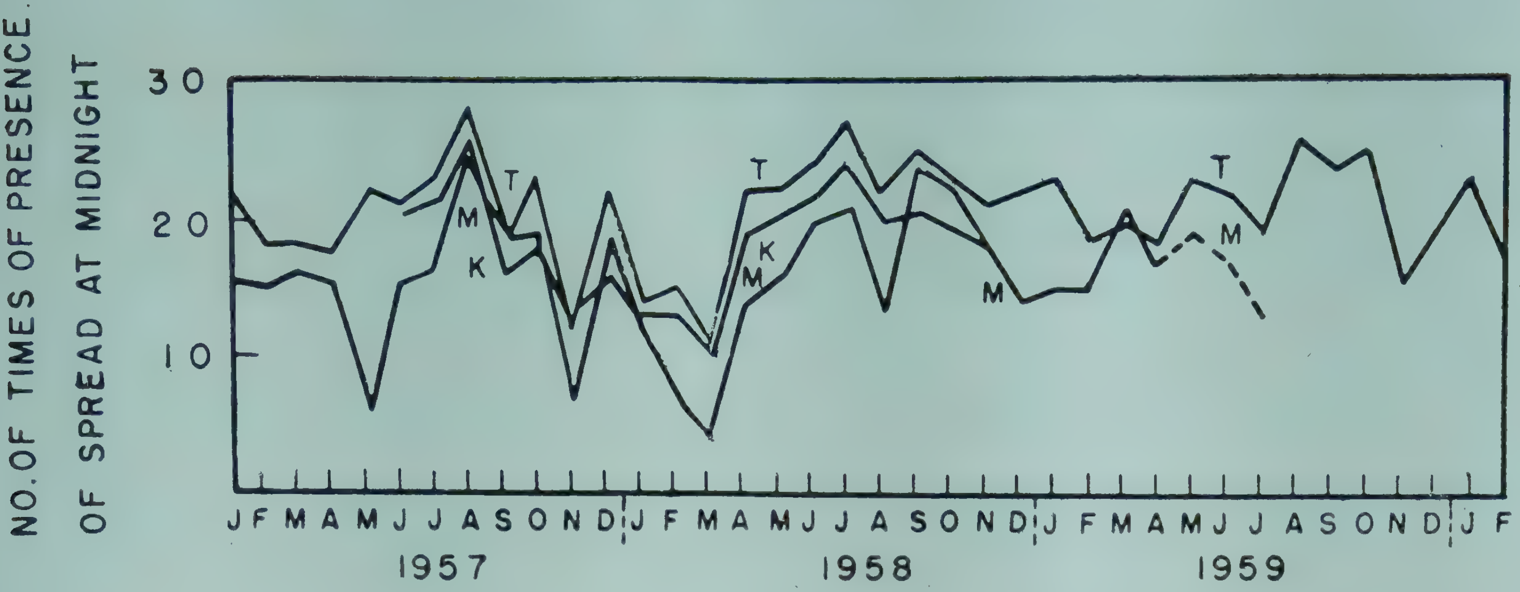

FIG. 9 — MONTHLY VARIATION OF SPREAD F DURING 1957–59

Mean fE_s values for the three seasons for the years 1958 and 1959 are shown in Fig. 5. It may be observed that the value of fE_s at any time of the day is highest during the equinox. Summer values are generally greater than winter values. When compared with the f_0F_2 variations, it may be seen that both reach maximum values in equinox; but while the f_0F_2 values are greater in winter than in summer, the converse is the case with fE_s values. Also around noon-time the fE_s values are always greater than the f_0F_2 values throughout the year except during magnetically disturbed days when f_0F_2 values are enhanced.

The fE_s observations at Trivandrum and those at Kodaikanal and Madras are compared in Fig. 6. The diurnal variations at Kodaikanal and Trivandrum are similar, but the magnitude at the latter place is greater than that at the former place. The fE_s values at Madras are much smaller than those at either Trivandrum or Kodaikanal.

Other features of sporadic E echoes are: (i) The echoes are always spread; (ii) the echoes disappear completely during radio fade-outs; on many occasions the echoes from E_s cease to appear a little earlier than the F_2 layer echoes and reappear after the echoes from F_2 layer start appearing on the lowest frequencies and the normal fE_s values are reached only some time after the conditions have become normal; and (iii) even under normal conditions, the E_s echoes suddenly disappear for some time and appear again after a lapse of about $\frac{1}{2}$–2 hr.

Observations on Spread F. Another characteristic of the observations at Trivandrum is the presence of spread F echoes during nights. They are observed almost throughout the year. They start appearing after about 1900 hours and remain till morning at times and at other times disappear during the course of the night.

The percentage occurrence of spread echoes for the different seasons are shown in Fig. 7 and a comparison with the data for Kodaikanal and Madras for 1958 is shown in Fig. 8. The percentage is greatest for Trivandrum and smallest for Madras.

The percentage occurrence of spread F at midnight for all the months for the three years is shown in Fig. 9. Maximum occurrence is in summer. The similarity in curves for Trivandrum and Kodaikanal are striking.

A detailed study of the spread echoes is being made separately.

REFERENCE

1. RAO, C. S. R. & RANGANATHAN, T. N., *J. Instn Telecomm. Engrs*, **6** (1960), 161.

Determination of loss coefficient in F region from true height profiles over Delhi

K. K. MAHAJAN
A. P. MITRA

National Physical Laboratory
New Delhi

An examination of the true height ionization profiles over Delhi obtained from ionograms taken by a C-4 ionospheric recorder during the IGY and IGC shows that the attachment coefficient β, in the F region, for heights between 260 and 380 km. follows approximately the empirical relationship:

$$\beta = 6\times10^{-5} \text{ exp.} \left[\frac{300-h \text{ (km.)}}{100}\right] \Big/ \text{sec.}$$

Though there is a large variation of β from day to day and from season to season, the apparent scale height remains approximately constant. There is some evidence indicating that the loss coefficient reduces slightly during a disturbed day

A number of attempts[1–4] have been made in the past to determine the loss rates for different heights in the F region of the ionosphere, but the results have not been quite satisfactory due to the uncertainty of the assignments of heights for such determinations, since such heights were obtained from values of hpF_2, the equivalent height for $0{\cdot}84\ f_c$. In recent years, however, true height profiles have been very successfully applied by Ratcliffe and others[5], who found the loss coefficient to be of the attachment type for height ranges 250–350 km. following the relationship

$$\beta = 10^{-4} \text{ exp.} \left[\frac{300-h \text{ (km.)}}{50}\right] \Big/ \text{sec.} \qquad (1)$$

Following this work, the loss coefficient for the F region has been estimated from the true height profiles by a few more authors[6,7]. Van Zandt and others have analysed F_2 region electron density data from the eclipse of

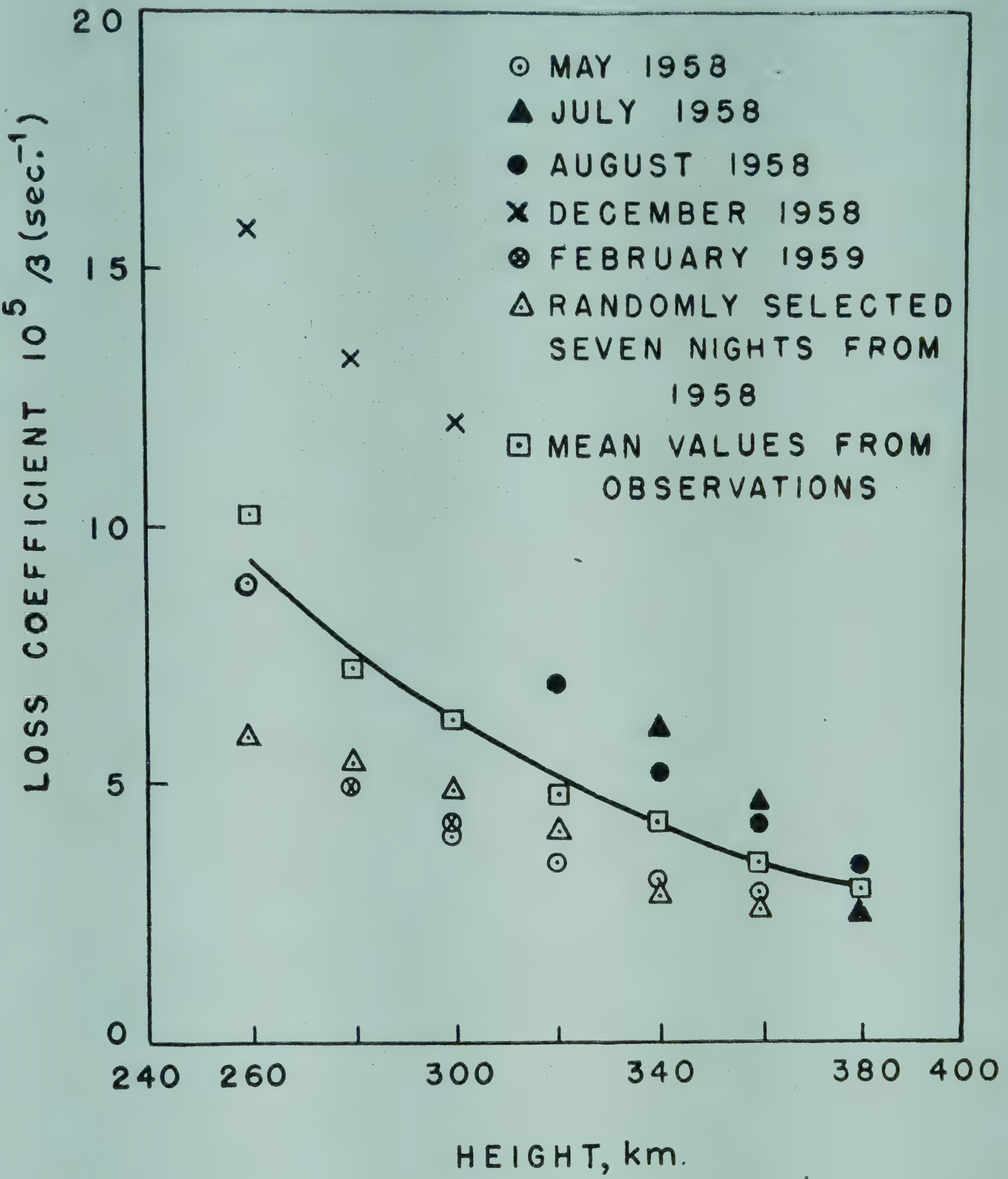

Fig. 1 — Loss coefficient β determined from night-time observations at Delhi for International Quiet Days

October 12, 1958 at Danger Islands and have found substantially higher values of β. They found that for heights from 290 to 400 km., the loss coefficient varies as

$$\beta = 6{\cdot}8\times10^{-4}\ \text{exp.}\left[\frac{300-h\ (\text{km.})}{103}\right]\Big/\text{sec.} \qquad (2)$$

During the IGY and IGC that followed, the National Physical Laboratory, New Delhi, has been running a C-4 automatic ionospheric recorder obtained through a grant of the Technical Cooperation Mission. After the end of the IGY, a programme was undertaken to reduce the ionograms for specially

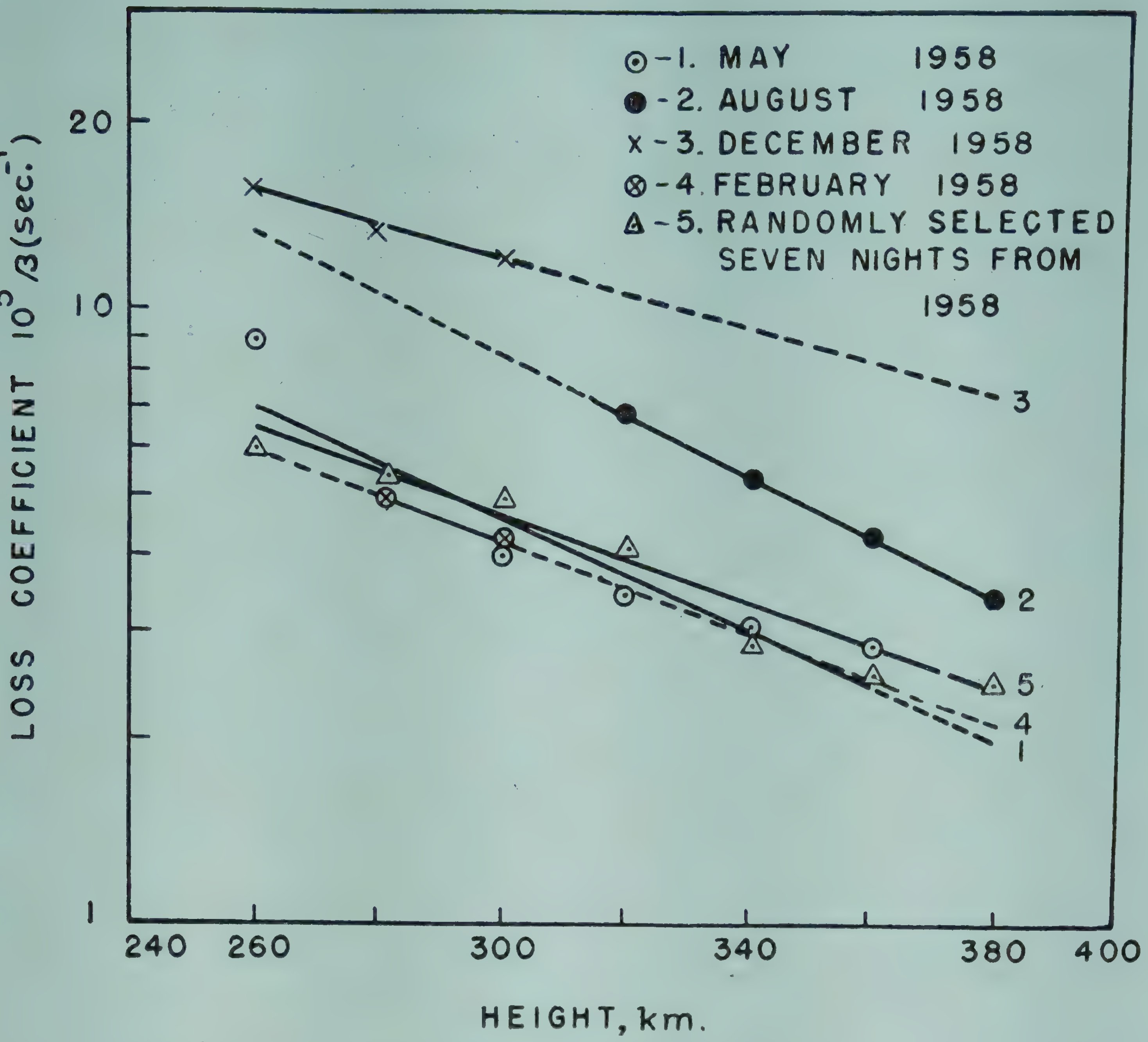

FIG. 2 — DISTRIBUTION OF LOSS COEFFICIENT FOR DIFFERENT HEIGHTS AT DELHI FOR DIFFERENT GROUPS OF DAYS

selected days, using the Schmerling-Ventrice manual method. This reduction programme is not complete. However, a large number of reductions has been effected, and the resultant ionization profiles have been examined in several ways. One area of study has been to use these profiles for the determination of loss coefficient for F region heights.

In this paper the preliminary results of this study are presented. It has been found that in the F region over Delhi, between the height 260 and 380 km., the average attachment coefficient is given by

$$\beta = 6 \times 10^{-5} \exp.\left[\frac{300-h \text{ (km.)}}{100}\right] \Big/ \text{sec}, \qquad (3)$$

METHOD OF ANALYSIS AND RESULTS

The analysis of data is based on the familiar night-time equation

$$\frac{dN}{dt} = -\beta N \qquad (4)$$

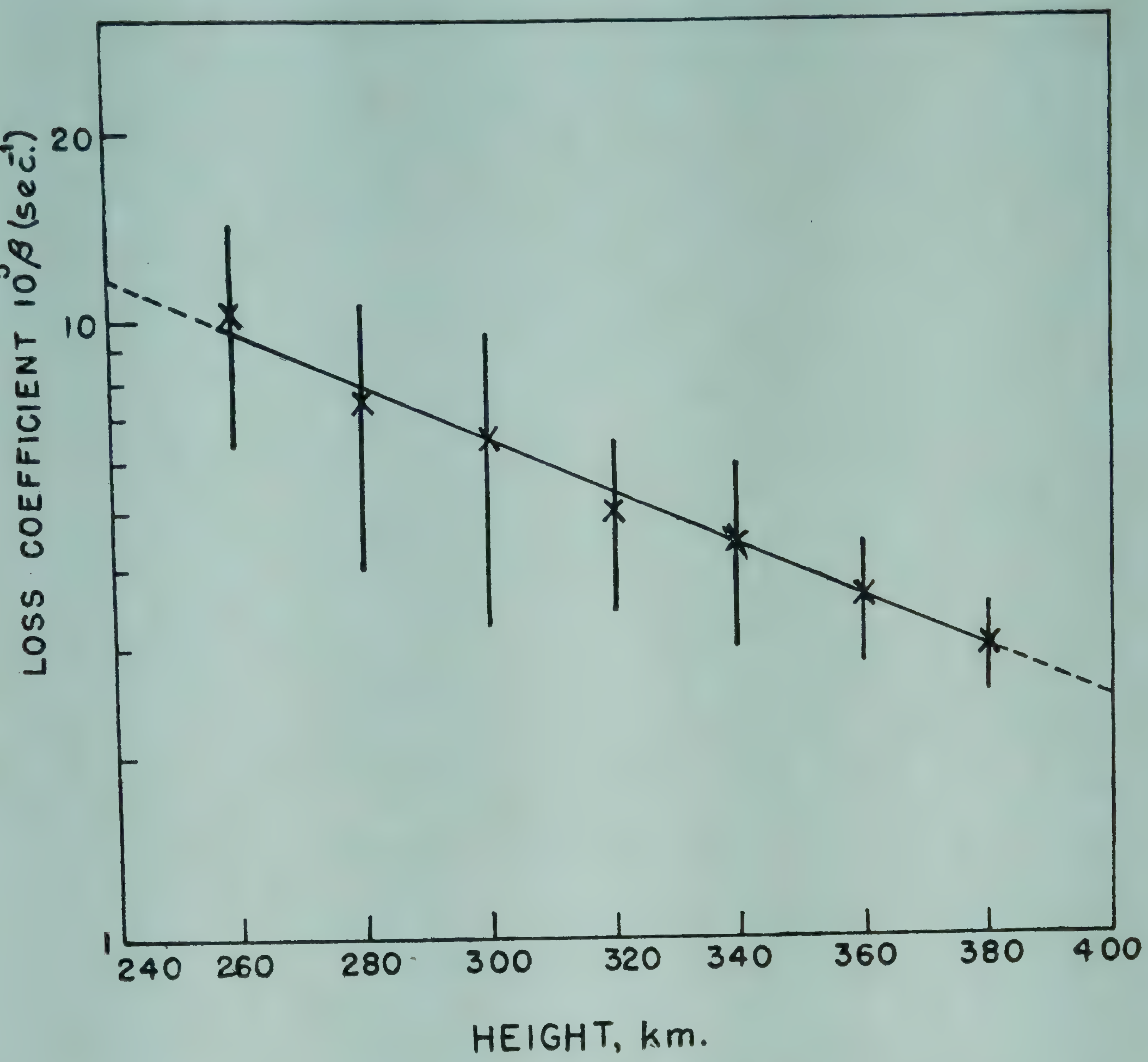

FIG. 3 — MEAN DISTRIBUTION OF THE ATTACHMENT COEFFICIENT FOR F REGION AT DELHI (CROSSES REPRESENT MEAN VALUES FOR ANY ONE HEIGHT, AND BARS REPRESENT THE STANDARD DEVIATION FROM THE MEAN)

where dN/dt is the rate of change of electron density, β the attachment coefficient and N the electron density. The above equation gives a solution of the form

$$N = N_0 e^{-\beta t} \tag{5}$$

N(t) curves for various fixed heights can be used to get the value of β.

Determination of the loss coefficient by such techniques are made uncertain because of the presence of perturbation from dynamical forces. There is no method known for eliminating such effects completely, but attempts have been made in the past to minimize these effects in various ways. In the case studied by the authors, such effects were sought to be reduced by restricting the analysis to intervals for which there was a gradual decrease of electron density.

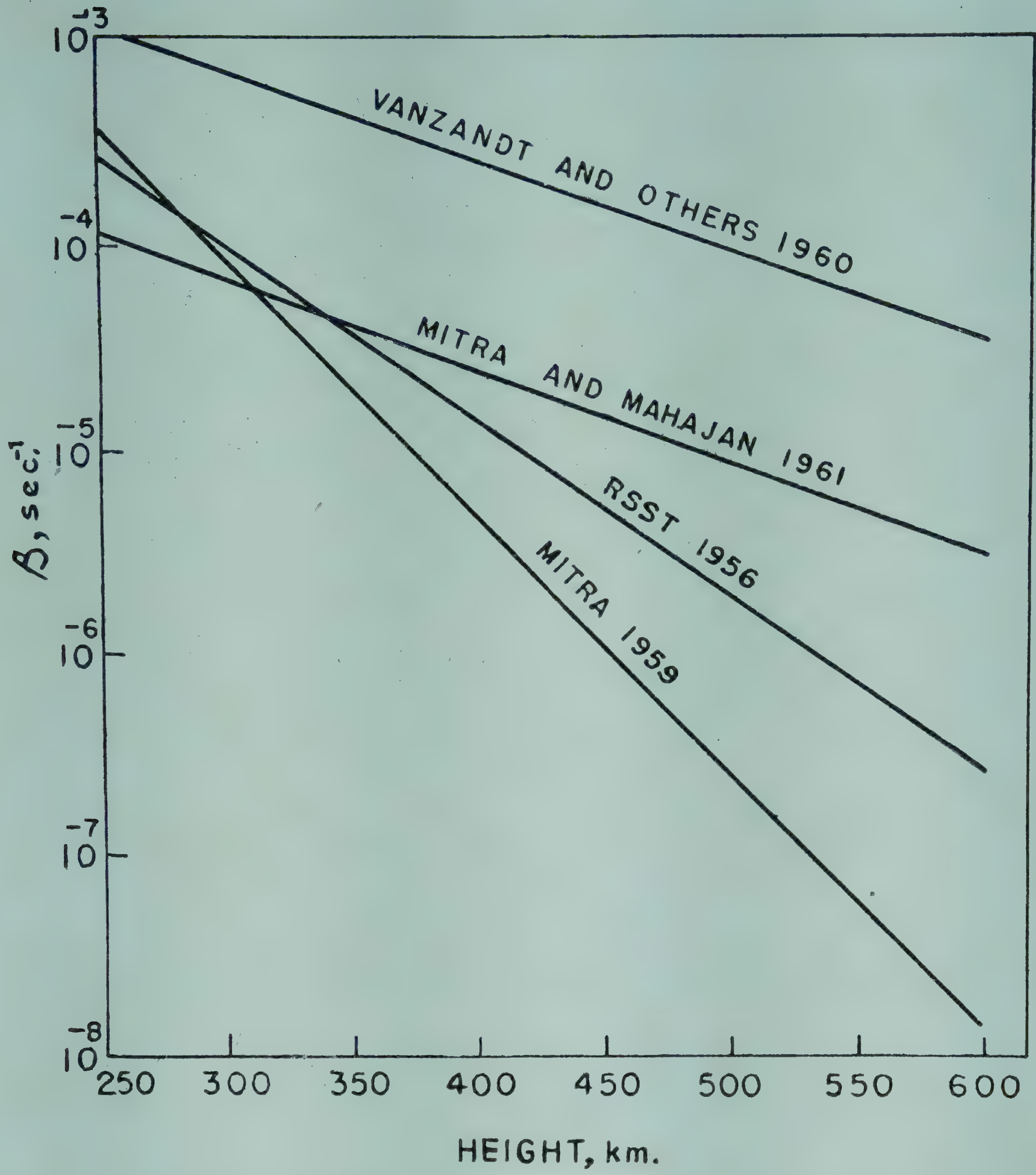

FIG. 4 — COMPARISON OF F REGION ATTACHMENT COEFFICIENT FOR DELHI WITH VALUES OBTAINED BY OTHER WORKERS

In determining β, International Quiet Days during the months of May, July, August and December in 1958 and February in 1959 have been selected. Some International Disturbed Days have also been analysed.

Fig. 1 shows the values of β against heights for the different groups of International Quiet Days. A smooth curve has been drawn through the average values at different fixed heights. Fig. 2 shows log β against height for the different groups of days. The variation is quite linear for the heights from 260 to 380 km. It can also be seen that the different groups of days show approximately parallel lines.

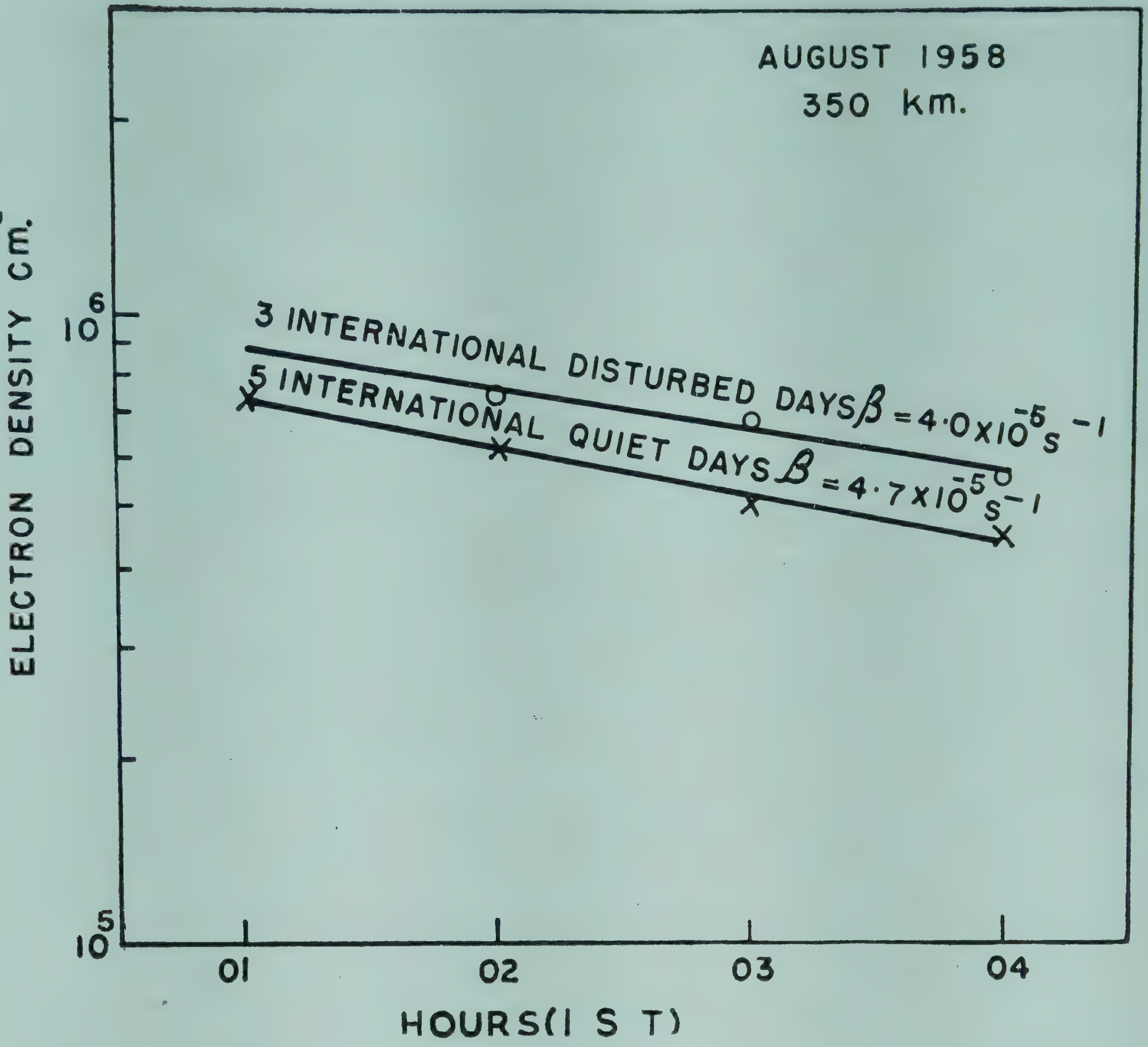

FIG. 5 — COMPARISON OF LOSS COEFFICIENT FOR DISTURBED AND QUIET DAYS AT DELHI

The average values of β are plotted against height in Fig. 3. The standard deviations from the points are represented by bars to show the possible range of variation of β for any particular height. In the range 260–380 km. the mean values fall almost on a straight line. The average loss coefficient for the heights 260–380 km. is found to follow the following approximate relationship

$$\beta = 6\times10^{-5}\ \text{exp.}\left[\frac{300-h\ \text{(km.)}}{100}\right]\Big/\text{sec.} \tag{6}$$

From the above analysis it appears that the loss coefficient decreases with an approximately constant scale height of about 100 km. If the logarithmic decrements of β in Equation (3) are considered as the scale heights of N_2, O_2 or NO, they show a temperature of more than 3000°K. in these heights. This temperature is indeed about double the value normally associated with these heights. These results are compared with the β-distribution of Ratcliffe *et al.*[5], Van Zandt *et al.*[6] and Mitra[8] (Fig. 4).

The attachment coefficient seems to be different on different groups of days. Thus, at 300 km., for example, the range is 4×10^{-5}/sec. to 12×10^{-5}/sec. Such variations may arise from changes of temperature from day to day or season to season or from electrodynamical drifts and diffusion, which are quite predominant at these levels.

It has also been found that the value of loss coefficient decreases slightly on a disturbed day. Fig. 5 shows a comparison of loss coefficient on disturbed and quiet days of August 1958 at 350 km.

ACKNOWLEDGEMENT

The authors are grateful to Sarvashri A. M. Arora and A. R. S. Vashist for their assistance in reduction of ionograms.

REFERENCES

1. APPLETON, E. V., *Proc. roy. Soc.*, **162A** (1937), 451.
2. SEATON, S. L., *J. Met.*, **4** (1947), 197.
3. BARAL, S. S. & MITRA, A. P., *J. atmos. terr. Phys.*, **6** (1950), 95.
4. MITRA, A. P., *J. atmos. terr. Phys.*, **1** (1951), 286.
5. RATCLIFFE, J. A. *et al.*, *Phil. Trans.*, **248A** (1956), 621.
6. VAN ZANDT, T. E., NORTAN, R. B. & STONEHOCKER, G. H., *J. geophys. Res.*, **65** (1960), 2003.
7. BANDOPADHYAY, P., *J. atmos. terr. Phys.*, **18** (1960), 132.
8. MITRA, A. P., *J. geophys. Res.*, **64** (1959), 733.

A note on changes of maximum of ionization of F_1 layer associated with sunspot activity

C. S. G. K. SETTY
I. R. KAMAL

Department of Physics, Delhi University
Delhi

Ratcliffe, Schmerling, Setty and Thomas[1] have shown that there exists a simple relationship between the F_1 layer maximum of ionization and the monthly average relative Zürich sunspot number. The relation between the critical frequency and the maximum production rate for the vertical sun, q_0, is given by the standard equation

$$\begin{aligned} N_m &= (1{\cdot}24\times 10^4)(f_0F_1)^2 \text{ electrons/cm.}^3 \\ &= \sqrt{\{(q_0 \cos \chi)/\alpha\}} \qquad (1) \end{aligned}$$

where the symbols have the usual meaning and f_0F_1 is in Mc/s. The magnitudes of q_0 deduced from Equation (1) with $\alpha = 5\times 10^{-9}$ cm.^{3}/sec., from the published data for Slough, together with averages of world-wide data plotted against mean sunspot number $\bar{R}$ are shown in Fig. 1. It can be seen from the figure that the relation between q_0 and $\bar{R}$ is linear up to $\bar{R} = 140$ and is represented by the equation

$$q_0 = 280(1+1{\cdot}4\times 10^{-2}\bar{R}) \text{ cm.}^{-3}\text{/sec.} \qquad (2)$$

Beyond this value there may be departure from the linear relationship. It could not be decided whether the departure was real or not as the number of sunspots observed until recently did not go beyond 160. As the observed sunspots in the current sunspot maximum epoch has reached over 200, it is of interest to inquire whether the linear relation really breaks down above a certain critical sunspot number.

Fig. 2 shows a plot of q_0 versus $(\bar{R})$ calculated from Equation (1) for the stations Ahmedabad and Haringhata (Calcutta), the data being taken from

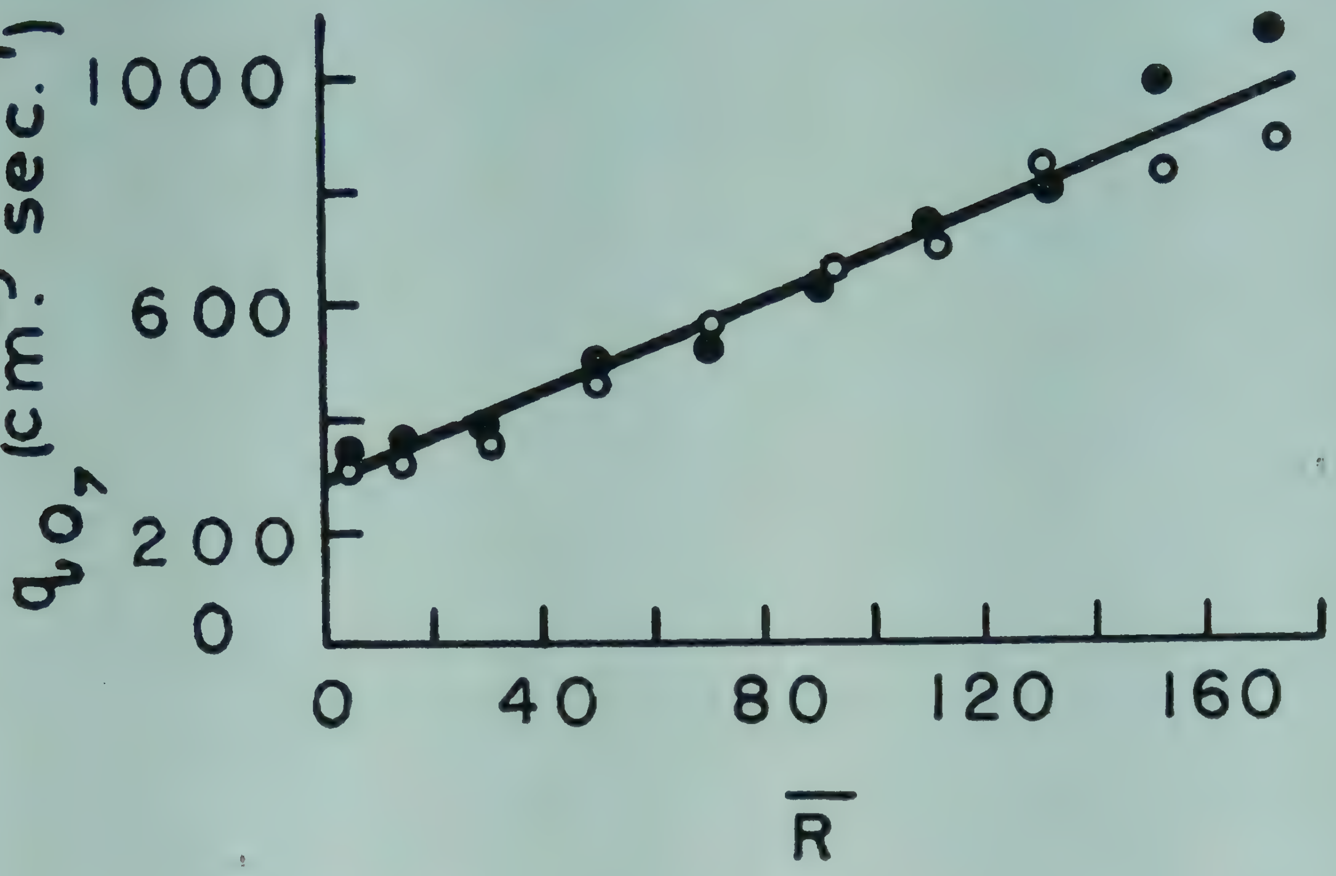

FIG. 1 — RELATION BETWEEN THE MEAN SUNSPOT NUMBER AND MAXIMUM ELECTRON PRODUCTION RATE

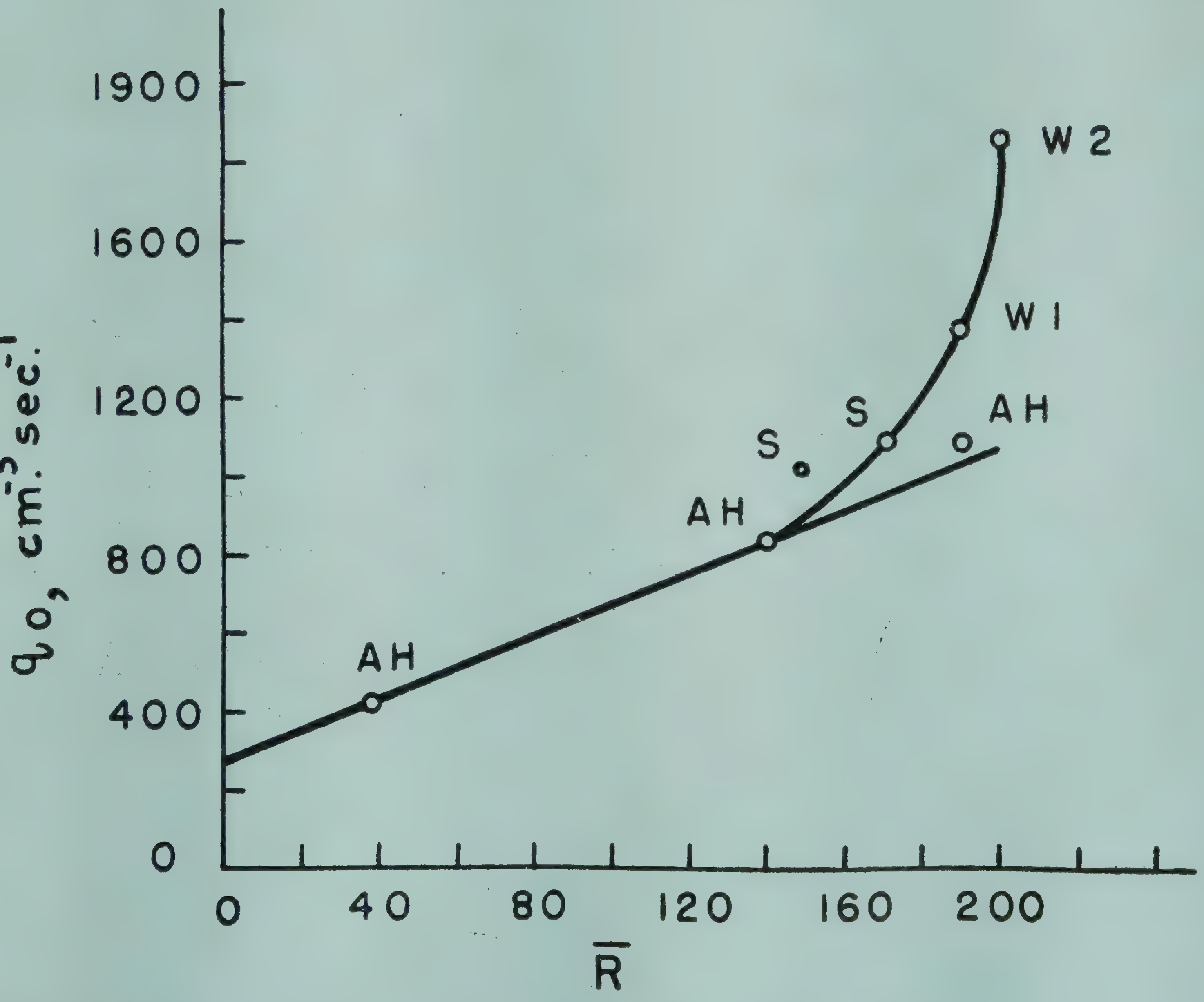

FIG. 2 — VARIATION OF q_0 WITH $\overline{R}$ AT AHMEDABAD-HARINGHATA (AH) AND OTHER STATIONS

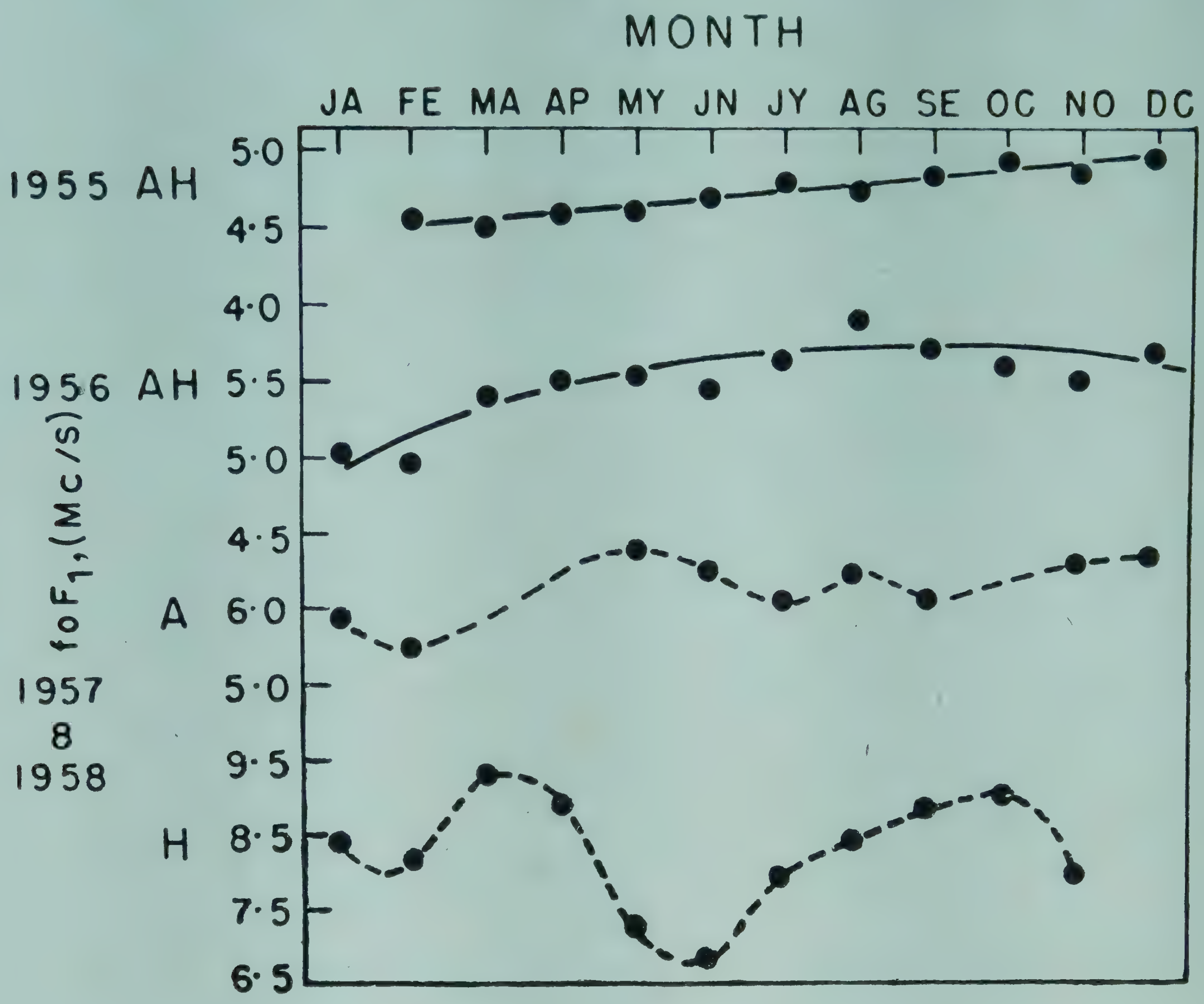

FIG. 3 — VARIATION OF f_0F_2 WITH MONTH AT AHMEDABAD (A) AND HARINGHATA (H) DURING 1955–58

the Radio Research Committee *Ionosphere Data* books, and for other stations from the CRPL *Ionospheric Data* books. It is apparent from Fig. 2 that the departure is quite marked for $\bar{R}>140$.

In view of the result just mentioned, it is of interest to inquire whether there is a change in the basic behaviour of the F_1 layer during the period of very high solar activity.

Fig. 3 shows the plots of monthly mean noon critical frequency of the F_1 layer at Ahmedabad and Haringhata near 23°N latitude, plotted against months of the years 1955–58. During the years 1955–56 the behaviour of f_0F_1 may be said to be normal. The value is not expected to show a simple $\cos^n\chi$ variation as the monthly mean Zürich sunspot number increases progressively with the month of the year. However, its behaviour in the years 1957–58 is quite unexpected. The sunspot number is nearly constant throughout the two years and a simple $\cos^n\chi$ variation is to be expected on the basis of the standard theory. This is an anomaly exhibited by the F_1 layer only during the highest solar activity.

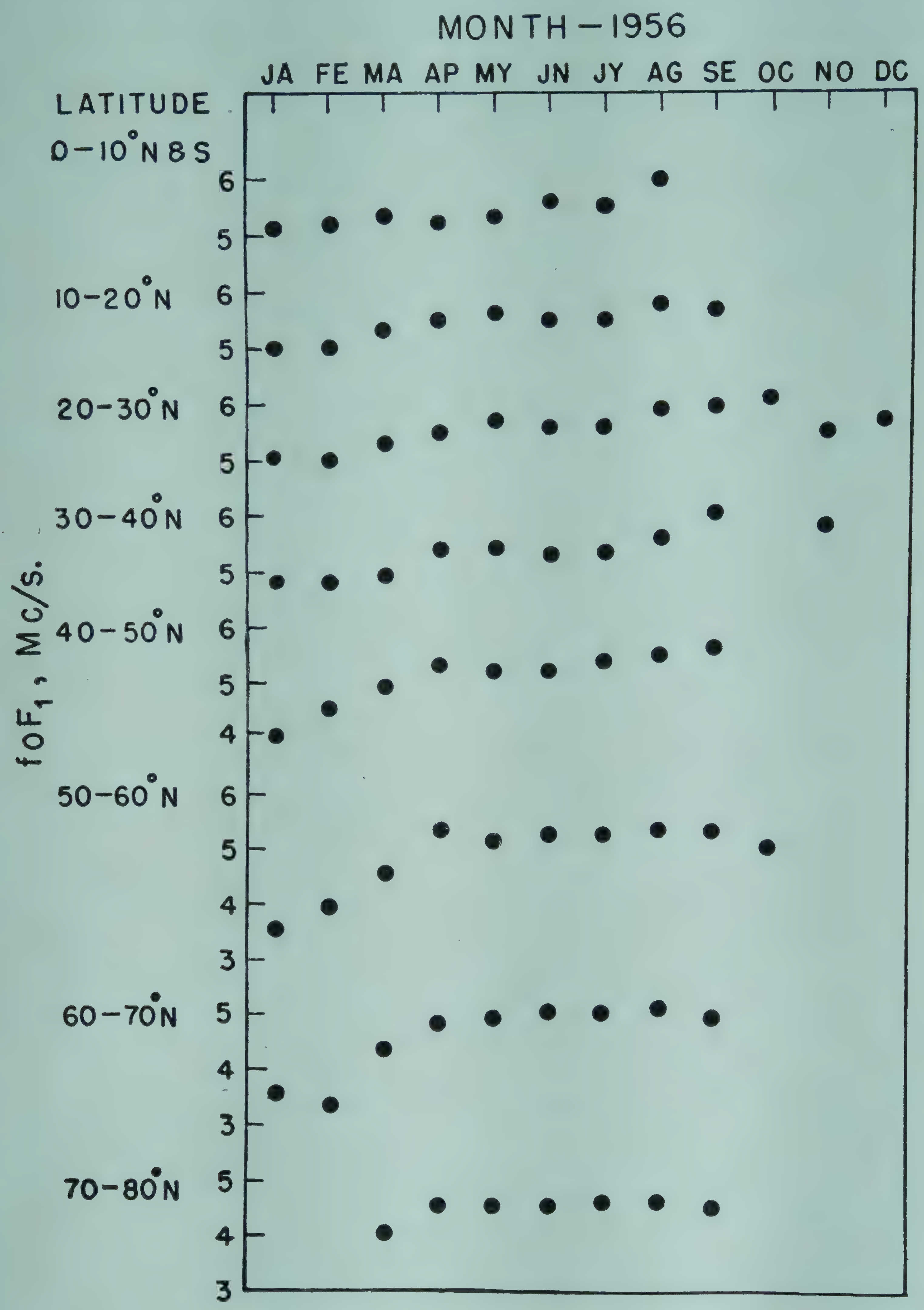

Fig. 4 — Variation of f_0F_1 with month at different latitudes during 1956

Figs. 4 and 5 show variations of the critical frequency with month during the years 1956 and 1957–58 respectively when the solar activity was

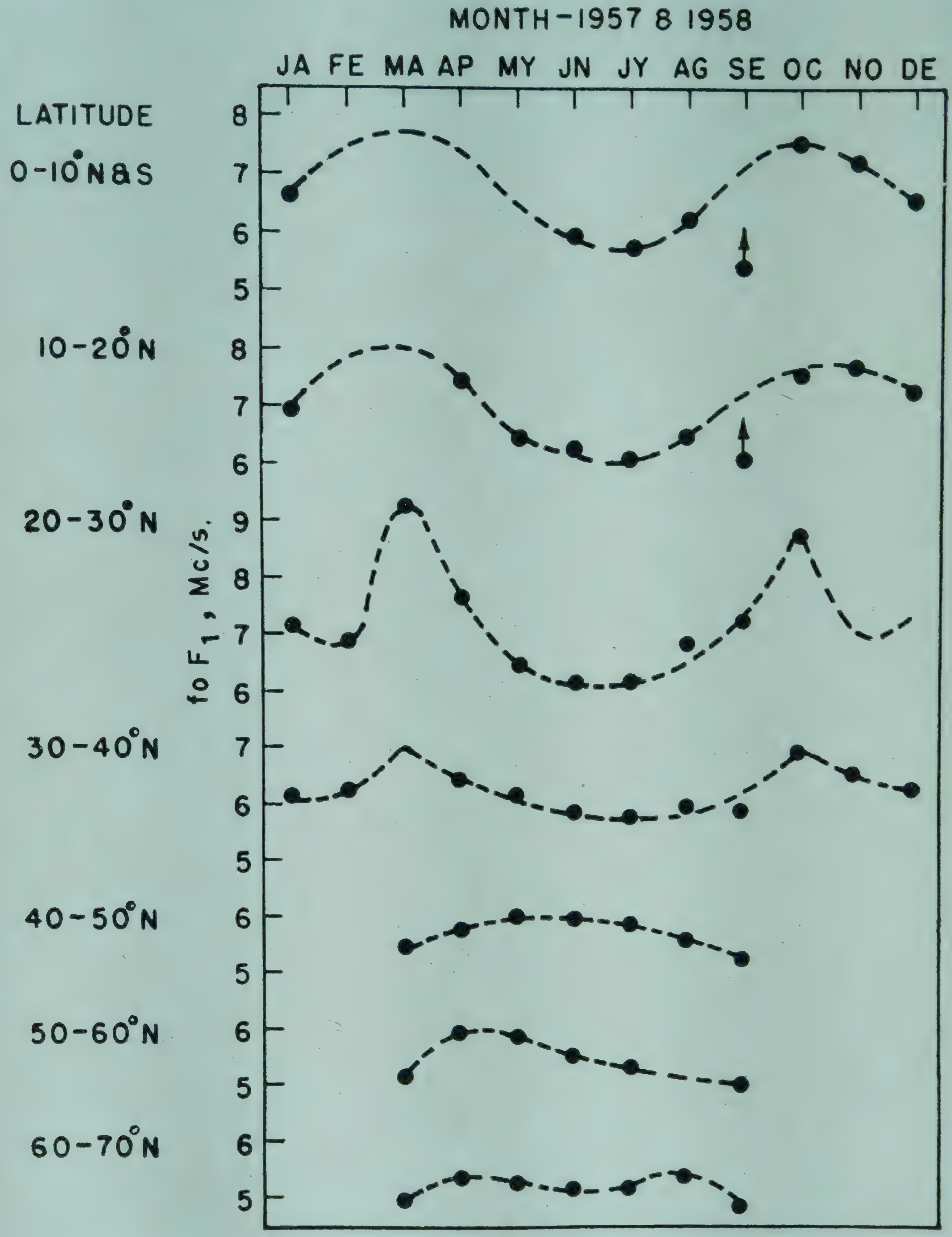

FIG. 5 — VARIATION OF f_0F_1 WITH MONTH AT DIFFERENT LATITUDES DURING 1957–58

moderately high and very high respectively. It is apparent from the figures that the behaviour of the layer is normal during the year 1956, whereas it departs considerably from it in the years 1957–58, when the solar activity was very high.

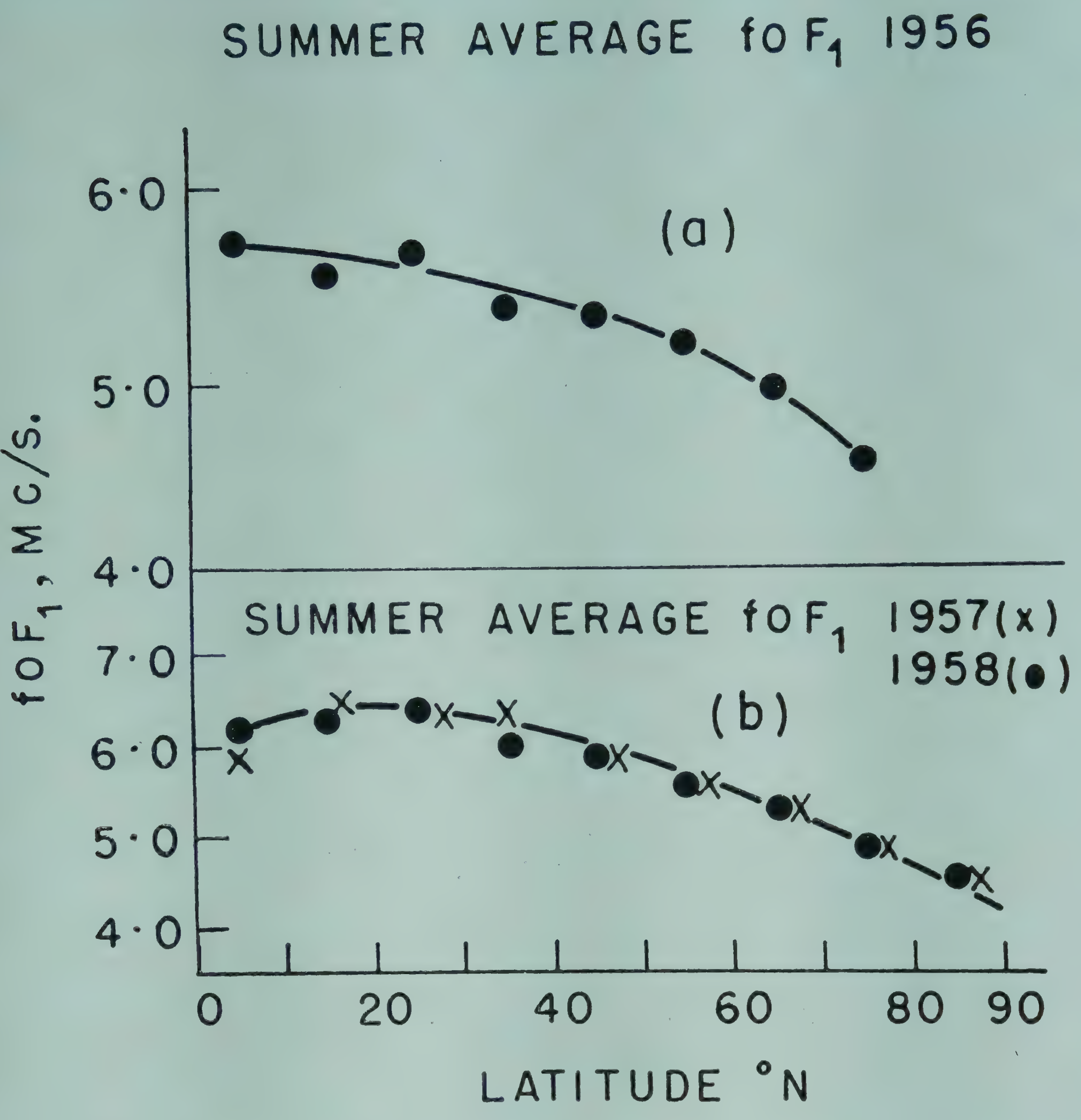

FIG. 6 — VARIATION OF f_0F_1 WITH LATITUDE DURING (a) 1956 AND (b) 1957–58

Fig. 6 (a, b) shows the plots of monthly mean noon critical frequency of the layer plotted against geographic latitude for several stations for the years 1956 and 1957–58. From Fig. 6(a) it can be seen that f_0F_1 increases progressively towards the equator. This is the normal F_1 layer behaviour. However, in Fig. 6(b) it is seen that f_0F_1 goes through a minimum at the equator. This phenomenon is similar to that of the F_2 layer which is usually referred to as the equatorial 'bite-out'.

In conclusion, the F_1 layer which behaves normally, in accordance to the simple standard theory, under moderate sunspot activity departs from it considerably during very high solar activity. Its variation with the season is anomalous and it exhibits the phenomenon of the equatorial ‘ bite out ’.

REFERENCE

1. RATCLIFFE, J. A. *et al.*, *Phil. Trans.*, **248A** (1956), 621.

* * *

Ionosphere over Trivandrum: Part I — Total Electron Content in the Ionosphere. C. S. R. RAO & T. N. RANGANATHAN, Research Department, All India Radio, New Delhi [*J. Instn Telecomm. Engrs*, **6** (1960), 161].

Some of the characteristics of the F_2 region of the ionosphere over Trivandrum have been studied. The data obtained during 1957 have been utilized for studying the total electron content of the F_2 region, calculation of the recombination coefficient and the temperature of the F_2 region. The total electron content in a vertical column of unit cross-section below the level of maximum ionization has been studied for different times of the day and for summer, equinox and winter seasons of the year. Analysis of the data indicates that the diurnal variation of the total electron content is smoother than that of the electron density. The ‘ bite-out ’ effect observed in the variation of electron density is completely removed when the variation of electron content is considered. The recombination coefficient has been calculated for different seasons from a consideration of the rate of variation of the total electron content at times equally spaced out on either side of the local noon. The values obtained are comparable with those obtained by other workers. The temperature of the F_2 region varies from about 800° to 1800°K. at different times of the day. The existence of such high temperatures at the F_2 region has been confirmed from recent rocket and satellite explorations. (*Abstract*)

Ionosphere over Trivandrum: Part III — Profiles and Electron Distribution in the Ionosphere. C. S. R. RAO & S. C. BOSE, Research Department, All India Radio, New Delhi [*J. Instn Telecomm. Engrs*, **7** (1961), 181].

Using h′-f records taken from April 1959 and coefficients given by Schmerling and Ventrice, a preliminary study of the electron distribution in the ionosphere has been made. Analysis has been made for a few selected quiet days during the months of June, September and December in 1959 and March in 1960 which are taken as representative of the different seasons of the year. The N(t) curves at fixed heights have been drawn for the different months. Comparison of the diurnal variation of hpF_2 (height measured at a frequency equal to 0·834 times the critical frequency of F_2 layer assuming a parabolic structure) with $h_{max.}F_2$ indicates that, while during the nights the curves nearly coincide, during day-time almost a constant difference is maintained between the hpF_2 and the corresponding $h_{max.}F_2$ values. Curves for sub-peak electron content of the ionosphere have also been drawn and compared with the corresponding maximum electron density curves. The midday ‘ bite-out ’ effect is removed to a considerable extent when one considers the sub-peak electron content curves instead of the maximum electron density ones. (*Abstract*)

A new ionospheric drift recorder

B. RAMACHANDRA RAO
R. RAGHAVA RAO

Ionospheric Research Laboratories
Andhra University, Waltair

Details of a new direct reading ionospheric drift recorder using the spaced receiver method are presented. The recorder enables the determination of average time delay between fading signals from any pair of closely spaced aerials by a magnetic tape delay circuit. The method is rapid, reliable and accurate.

In recent times the spaced receiver method of Mitra[1] has been extensively used for measurement of horizontal drifts in the ionosphere. This method records the amplitude variations of radio waves singly reflected from the ionosphere at three closely spaced points on the ground, the separation being of the order of one wavelength. The method utilizes the time difference between similar fades in the three spaced receiver fading records to calculate the drift speed and direction. For recording these time differences, Mitra used three single beam oscillographs so aligned with mirror arrangement as to enable recording in a single camera. Rao *et al.*[2] used triple beam oscillograph with independent controls for the three beams. Though the procedure for calculating the drift velocity from the fading records is simple, the major drawbacks of these methods of recording are: (i) they involve time-consuming analysis of drift records to obtain the time differences, and (ii) the use of the expensive photographic recording film. Phillips[3] developed a recorder by which the time displacements are directly recorded instead of laboriously deducing them from the signal fading pattern records. This is achieved by charging a condenser during the interval of two successive minima of any two pairs of signals, and recorded on a pen recorder the voltages developed, when the condenser is discharged through a known resistance. These spikes on the record are taken as proportional to the time differences between minima. The sense of time difference is also obtained in this recorder. A series of fast relays are used to effect all these operations. Though this method is decidedly an improvement over the photographic recording method, considerable time is required to measure the time delays from the spikes in the recorder and to obtain average time displacements. A method based on a new principle has been developed by the authors[4]; in this method the average time displacement between any two fading patterns can directly be measured without recourse to measuring time displacements between individual maxima or minima. Details of the new method are presented in this paper.

Principle of the Method. For the ideal case when the fading signals from two spaced aerials are exactly identical in amplitudes, the difference signal between them will be zero if there is no time difference. But the fading curves of signals from any two closely spaced aerials generally show a certain amount of dissimilarity and also the time difference between any two maxima or minima will seldom be zero. Hence, the difference signal will be an irregular alternating waveform whose r.m.s. amplitude will be a minimum when the average time difference between the two signal patterns is zero and increases as the time difference increases.

The present method is based on the principle of artificially introducing time delay in one of the pairs of the fading signals such that the average time difference is zero and the difference signal is minimum. The variable time delay is introduced by a magnetic tape recording circuit with an endless tape and a manually variable record-reproducing head. The block diagram of the entire experimental set-up is shown in Fig. 1. Signals from aerials A_2 and A_1 or A_3 are fed into two identical receivers and a SPDT switch S_1 permits the use of one of the aerials A_1 or A_3 at a time. The signals from the pair of aerials A_2 and A_1 or A_2 and A_3 can be fed into two gated integrators I and II through two receivers. These integrators serve the purpose of isolating the required ionospheric pulsed signals from the ground pulses and the unwanted signals from other layers. These isolated pulsed signals are also smoothed out by integrating circuits having a sufficiently high time constant of the order of 0·1 sec. to make the output of the integrator a fluctuating d.c. voltage which follows truly the variations of the input signal. This output from the gated integrator I is fed into a frequency modulator which generates square waves whose frequency varies from 9·8 to 4·2 kc/s. as the input signal varies by 24 V. from minimum to maximum. The frequency-modulated signals from this unit are fed into a magnetic recording head which is in contact with a continuous magnetic tape loop driven at a speed of 7·5 in./sec. The signals recorded on the tape are received by a reproducing head whose position can be continuously varied so that a known time delay is introduced on the signal impressed on the tape. The signal picked up by the reproducing head is fed into an amplifier and demodulator whose output is an exact replica of the original signal with a time delay. The output voltages from the demodulator and the gated integrator II are adjusted to be of equal amplitude and are fed to the two grids

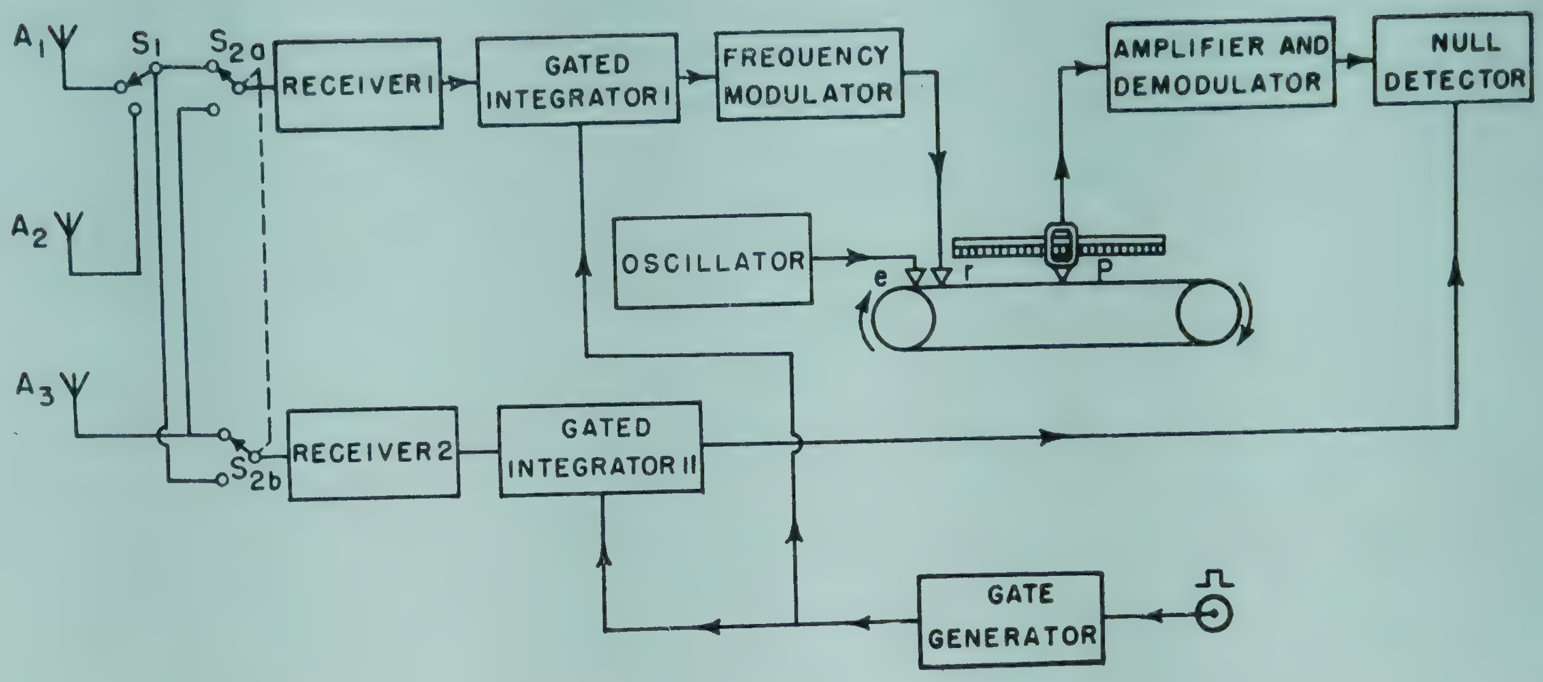

FIG. 1 — SCHEMATIC DIAGRAM OF IONOSPHERIC DRIFT RECORDER

of a double triode balanced cathode follower amplifier and detector. The deflection in the galvanometer of the detector reaches a minimum when the average time difference between the two signals is nullified by introducing the same time delay artificially in one of the signals for which maxima or minima occur earlier than the other on the average, so as to make the net average time difference zero. The DPDT switch S_2 enables the aerials connected to the integrators through receivers to be interchanged so as to see that the signal in which maxima or minima occur earlier passes through the tape delay circuit. Only in one of the positions of DPDT switch S_2 the galvanometer shows a minimum deflection at a particular position of the reproduce head from which the time delay introduced by the magnetic tape recording circuit can be easily calculated knowing the tape speed and record reproduce head distance. After determining the average time delay T_x between fading patterns of aerials A_2 and A_1 and noting the sense of direction, aerial A_1 is replaced by aerial A_3 by using SPDT switch S_1 and following the same procedure, the time delay T_y between the signals of A_2 and A_3 can be estimated. Thus, T_x and T_y are determined alternately about ten times and average values of T_x and T_y are obtained from which the velocity of the drift is calculated by the usual relations. The details of the various electronic units employed in the recorder are given below.

Gate Generator. The gate generator is of conventional type. This unit generates a negative rectangular pulse of variable width which can be delayed by the required amount with respect to the transmitted pulse. By applying this negative pulse to the input of the gating circuit shown in Fig. 2 and by adjusting its time delay it is possible to select any one of the reflected echoes from the ionosphere. The gate generator is triggered by the same positive pulse which triggers the transmitter.

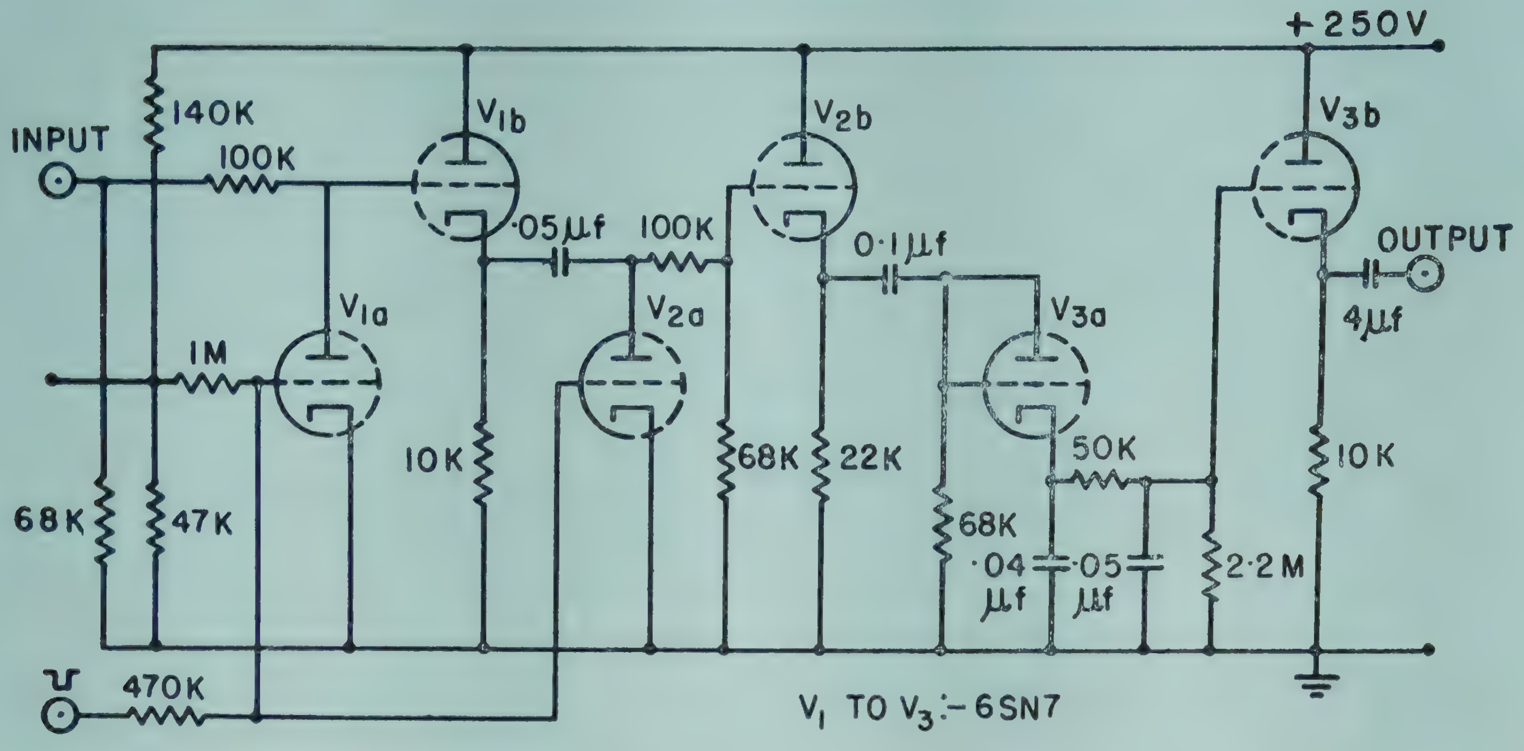

FIG. 2 — CIRCUIT DIAGRAM OF THE GATED INTEGRATOR

Gated Integrator. The circuit diagram of the gated integrator is given in Fig. 2. By adjusting the delay as well as the width of the negative gate pulse, which is applied at the grids of V_{1a} and V_{2a}, the desired echo can be isolated and passed on to further stages. All other signal voltages including the ground signal and noise voltages are suppressed by the by-passing action of V_{1a} and V_{2a}. The valve V_{1b} is connected as a cathode follower. V_{2a} is an identical gating stage as V_{1a} to obtain better rejection of unwanted signals. The output from the cathode of V_{2b} is applied to the integrator consisting of V_{3a} and the associated circuit in its cathode. The 0·04 Mfd capacitor can be fully charged in one pulse duration. Though the charging and discharging time constants of RC network are markedly different, the discharge time constant is small enough to make the output d.c. voltage of the integrator follow accurately the fading of the pulsed signal. The output of the gated integrator I is taken through an amplifier whose plate voltage is adjusted to give the required voltage for coupling to the frequency modulator stage described below.

Frequency Modulator. The circuit diagram of frequency modulator is shown in Fig. 3. The first two stages V_{1b} and V_{2a} constitute a symmetrical free-running multivibrator. If the grids were returned directly to cathodes the frequency of the multivibrator would be approximately 3 kc/s. But if the grids were driven 30 V. more positive than the cathodes which are kept at +75 V., the free-running frequency increases to 10 kc/s. For the present purpose, 7 kc/s. is chosen as the centre frequency and the grid bias required for this frequency is +17 V. If a signal of 12 V. peak value is applied, the frequency is found to vary from 9·8 to 4·2 kc/s. corresponding to the positive and negative peaks of the signal. This causes a ±40 per cent peak deviation of the centre frequency. The integrated signal output

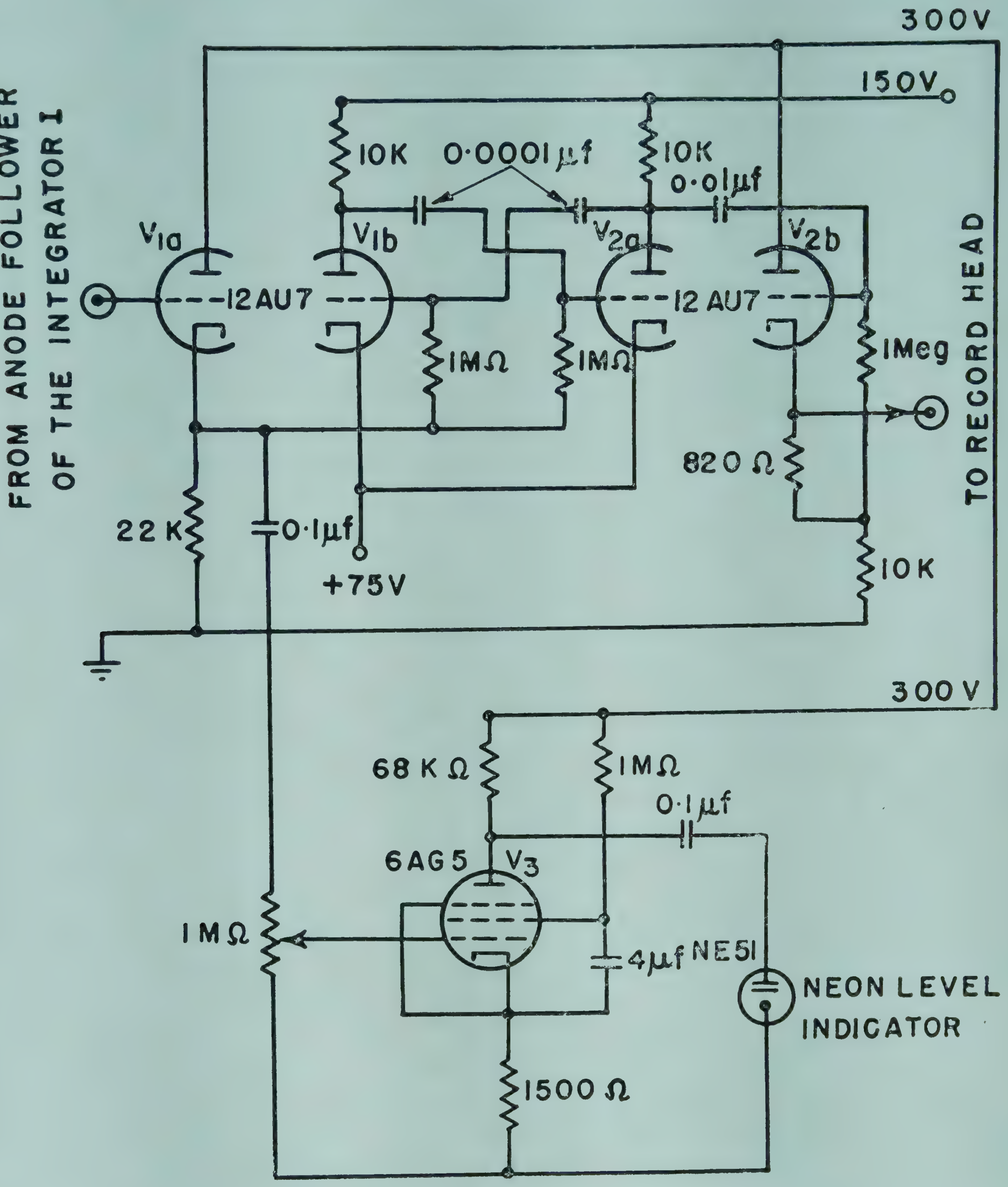
300V
150V
10K
0·0001µf
10K
0·01µf
V1a
V1b
V2a
V2b
12AU7
12 AU7
FROM ANODE FOLLOWER OF THE INTEGRATOR I
TO RECORD HEAD
1MΩ
1MΩ
1Meg
820 Ω
22 K
0·1µf
+75V
10K
300 V
68 K Ω
1MΩ
0·1µf
6AG5
V3
1MΩ
4µf
NE51
NEON LEVEL INDICATOR
1500 Ω

Fig. 3 — Circuit diagram of the frequency modulator

whose amplitude lies between 0 and 24 V. positive is applied to the frequency modulator in the following manner. The gated integrator I circuit is a modified form of the integrator shown in Fig. 2, in which the last cathode follower stage is replaced by a resistance coupled amplifier whose plate voltage is adjusted to be 92 V. when the integrated signal applied is half the maximum value. This voltage applied to the frequency modulator through the cathode follower stage V_{1a} in Fig. 3 keeps the grids of the multivibrator at 17 V. more positive than the cathodes. When the signal is undergoing maximum fluctuation the voltage output of the cathode follower V_{1a} varies in the range 80–104 V. As these variations are fed to the grids of the symmetrical multivibrator, the multivibrator frequency undergoes 40 per cent peak deviation. The neon level indicator is provided in the amplifier stage V_3 to flash whenever the modulating signal voltage reaches the 40 per cent peak deviation level of the multivibrator frequency. The output of the multivibrator is fed to the record head through the cathode follower stage V_{2b}.

Tape Transport System. The tape transport is used to introduce the time delay in the entire fading pattern of one of the two aerials for which the fading pattern is ahead in time with respect to the other. The usual average time displacements are in general found to be in the range 0–1·5 sec. At times when there is long period fading, the time displacement between any two fading patterns may exceed 2 sec. depending on the direction and magnitude of drift velocity.

The average time displacements within 2·2 sec. can be measured by adopting tape transport system shown in Fig. 1. An endless loop of magnetic tape of length 44 in. and width $\frac{1}{4}$ in. is wound round two aluminium pulleys (diam., 2·386 in.), one of which is driven by a synchronous motor at the rate of 1 r.p.s. giving a tape speed of 7·5 in./sec. The output signal from the frequency modulator is fed to the recording magnetic head 'r' which is fixed close to the left side pulley on the front panel of the tape transport system such that the tape is in contact with the head. The tape is transported in the clockwise direction. The reproducing head 'p' is mounted on a sliding carriage moving on a horizontal rectangular guide provided with a linear scale. The minimum time displacement that can be measured is 0·07 sec. and is limited to this value by the minimum separation of 0·55 in. between the record and reproduce heads when they are adjacent. There is a length of 16·5 in. available on the loop for the movement of reproducing head to produce any time delay in the range 0·07–2·2 sec. An erase head 'e' is mounted just before the recording head and is fed from a conventional oscillator working on a frequency of 45 kc/s.

Frequency Demodulator and Detector. The output of reproduce head is amplified by a series of amplifier-clipper pairs and demodulated the circuit of which was the same as adopted by Guttwein and Leslie[5]. The demodulated signal is amplified by a d.c. amplifier followed by a cathode follower. The output signal thus obtained is a delayed signal, the delay being variable and is applied to the grid of V_a of a double triode balanced cathode follower amplifier null detector, shown in Fig. 4. The undelayed signal from the integrator II is applied to the grid of V_b and both the amplitudes are adjusted to be equal. The alternating voltage across the two cathodes which depends on the time delay between the input signals is rectified by a bridge rectifier using IN34 crystal diodes and the detected current

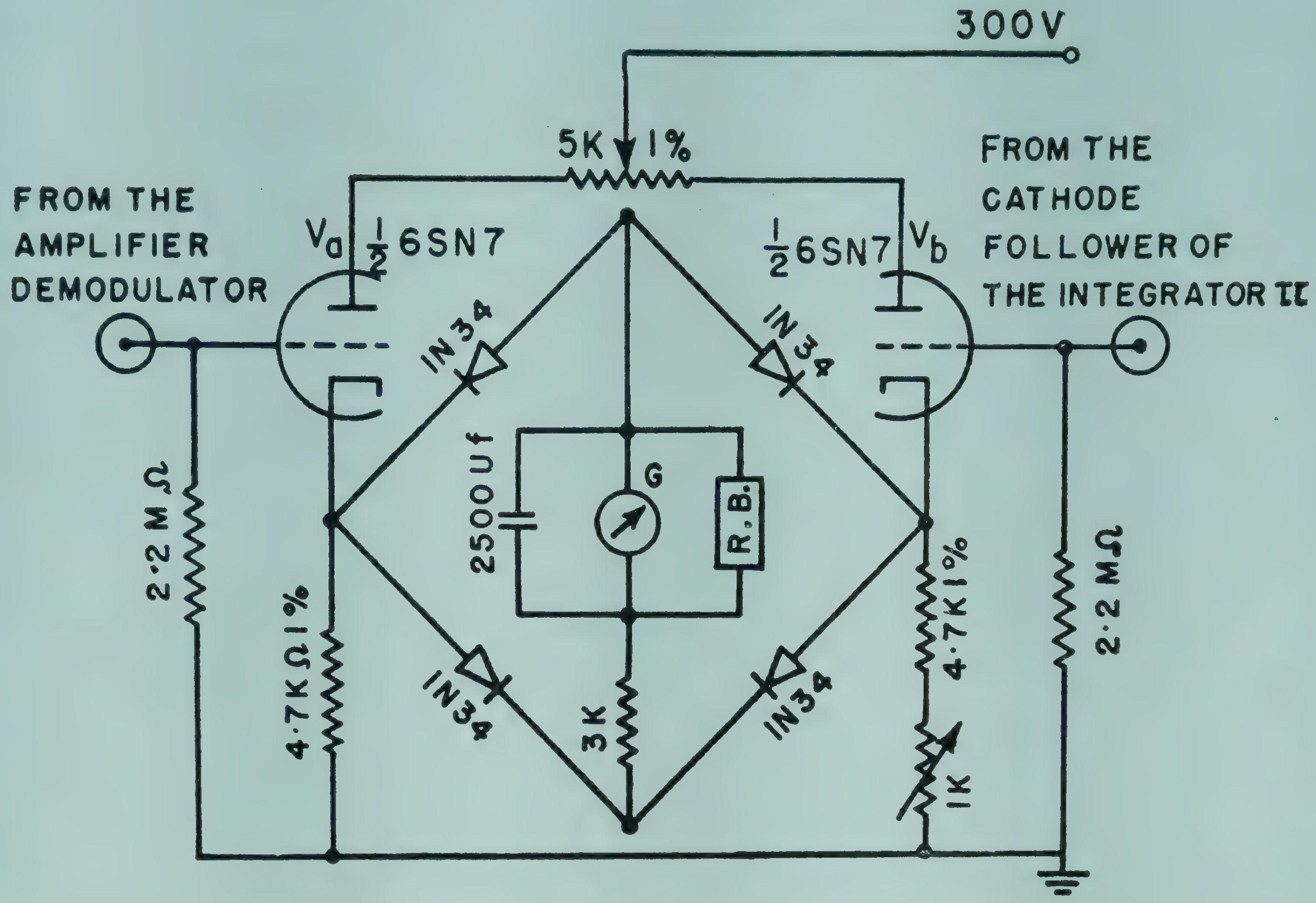

Fig. 4 — Circuit diagram of the null detector

is measured by a galvanometer with a shunt resistance box to vary its sensitivity. A series resistance of 3 KΩ is introduced to limit the current and to enable effective filtering action by the 2500 Mfd condenser across the output terminals. The anode potentiometer 5 KΩ and cathode potentiometer 1 KΩ are adjusted to give null deflection in galvanometer without signals and also when same signal is applied to both grids. By adjusting the delay of the signal from the appropriate receiver which is ahead of the other such that the average time delay is zero, the galvanometer deflection is reduced to a minimum. The scale of the reproducing head can be calibrated in apparent velocities, so that the reading of the index mark directly gives V_x' and V_y' the apparent velocity components of drift in the E–W and N–S directions. For obtaining accurate values, a few measurements should be made alternately using the two pairs of aerials.

To check the reliability of the performance of the integrator and the demodulator circuits, photographs of the gated signal output from the receiver, output of gated integrator I and demodulator without introducing any delay are taken by applying these signals to the Y plates of the triple beam oscillograph and one such photograph is shown in Fig. 5. The signal shown in the middle trace of the figure is 180° out of phase with respect to the signal output from the receiver on account of single stage resistance coupled amplifier at the end of gated integrator I. This phase difference is compensated again by another resistance coupled amplifier at the output of the demodulator with the result the signal from this unit is exactly in phase with the

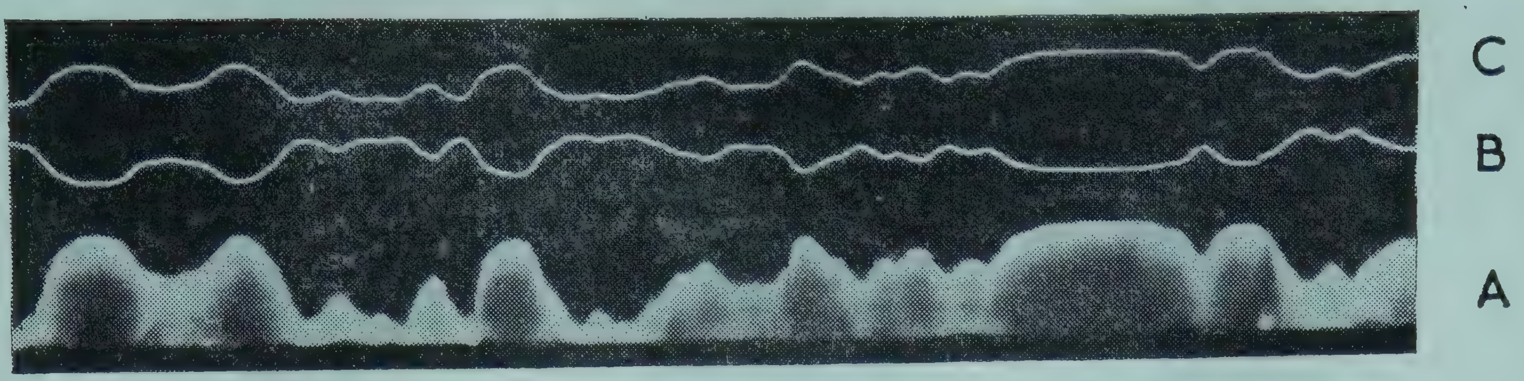

Fig. 5 — Gated signal output from the receiver, output of gated integrator I and demodulator

original signal from the receiver. Thus the input integrated signals fed to the final amplifier detector unit are true replicas of the original signals without any distortion or phase delay other than the delay introduced by the magnetic tape system.

Conclusions

An interesting feature of the present method is that the recording of the time displacements does not utilize particular points like maxima or minima but uses the entire fading curve. Thus a certain amount of averaging of the individual time displacements is automatically affected in the recorder on account of the large time constant of the detector circuit. The detecting meter does not respond to the quick individual variations of the time displacements between small portions of the fading record.

The major advantage of this method is the extremely simple manner of obtaining the average time displacements between the three spaced receiver fading signals over a small interval of time without having recourse to taking any fading records as in Mitra's method or Phillips' records and analysing them.

The accuracy of setting of the delay controls for minimum is generally not very high, but when a few observations are taken and averaged, the overall accuracy of the final result is considerably improved.

Although the recorder has the limitation that the lower limit for the time delay is 0·07 sec., it may be safely assumed that the velocity components corresponding to time delays less than 0·07 sec. are negligibly small.

References

1. Mitra, S. N., *Proc. Instn elect. Engrs,* **96** (1949), Pt III, 441.
2. Rao, B. R., Rao, M. S. & Murty, D. S. N., *J. sci. industr. Res.,* **15A** (1956), 75.
3. Phillips, G. J., *J. atmos. terr. Phys.,* **6** (1955), 124.
4. Ramachandra Rao, B. & Raghava Rao, R., *J. atmos. terr. Phys.,* **21** (1961), 208.
5. Guttwein, G. K. & Leslie (Jr), J. M., *Electronics,* **27**(2) (1954), 154.

Height variation of anisotropy and drift of irregularities in the ionosphere

B. RAMACHANDRA RAO
K. V. V. RAMANA

Ionospheric Research Laboratory
Andhra University, Waltair

The results of a study of the variation of steady and random horizontal drift velocity of the irregularities in the ionosphere at Waltair with height together with a study of the height variation of the constants of the correlation ellipse are presented. The steady horizontal drift speed at first decreases with height and then rises suddenly. The drift speed, axial ratio and the random change factor reach a maximum in the height range 250-300 km. It is suggested that this region is the seat of spread F and radio star scintillations.

Several investigators have studied the variation of horizontal drift velocity with height in the E and F regions of the ionosphere. Utilizing the meteor method for the determination of horizontal drifts, Greenhow[1] and Elford and Robertson[2] obtained 2·5 and 3·6 m. sec.^{-1} km.^{-1} respectively as height gradients of drift speed in the E region. The gradient of the drift speed in the F region is always lower than that obtained for the E region.

In analysing the drift records obtained by Mitra's[3] spaced receiver technique, most investigators have used the simple, similar fades method. In the following investigation the authors have made an attempt to study the variation of drift speed in the ionosphere by analysing the fading records by using Phillips and Spencer's correlation method[4]. The method has been applied for analysing the drift records to get the data of random drift speed along the direction of steady drift as well as the constants of the anisotropy ellipse.

EXPERIMENTAL PROGRAMME

The experimental technique adopted in this investigation is the conventional spaced receiver technique described by Mitra[3]. Records were obtained at three points on the ground which form a right-angled isosceles triangle. For 2·5 Mc/s. reflections the aerials used were tuned dipoles. For the higher frequency reflections, loop aerials were used to obtain the fading records. The spacing of the east and north dipoles from the central dipole was 108 m., while the corresponding distance was 30 m. in the case of loop aerials. Twenty-eight fading records taken during morning hours corresponding to six days of observation were analysed by the Phillips and Spencer's method. Each set of records corresponding to different heights in the ionosphere for a particular day were taken in a period of 15–20 min., with the assumption that the drift parameters do not change appreciably during the interval. Since all the records on all frequencies could not be taken simultaneously, they were taken one after another in quick succession. It was assumed, following the work of Jones[5], that the drifts corresponded to the levels of reflection where the fading was expected to be superposed on the signal as shown by Booker[6]. With a view to obtaining the true height of reflection, h′-f record was taken manually after each set of observations on all the six days and the method of Schmerling[7] was utilized to deduce the true heights.

RESULTS AND DISCUSSION

The data of steady drift speed (v), the drift direction in degrees E of N (δ), the random drift speed along the direction of the steady drift (V_c), the axial ratio of the anisotropy ellipse (r), the orientation of the major axis of the anisotropy ellipse with respect to the north measured clockwise (ν) and the random change factor ($V_c/2v$) were derived by the application of

TABLE 1 — HEIGHT VARIATION OF DRIFT AND ANISOTROPY PARAMETERS

HEIGHT *km.*	$v(=V/2)$ *m./sec.*	δ *deg. E of N*	AXIAL RATIO	ν *deg. E of N*	$V_c/2v$
105	111	232	2·6	131	1·4
159	85	202	1·9	145	1·7
163	71	290	1·8	163	0·7
192	18	236	4·8	11	1·1
203	38	224	1·9	113	0·6
235	32	232	2·1	174	1·3
252	8	85	2·0	58	5·2
278	228	103	6·0	99	—
286	140	200	5·5	76	3·7
310	18	75	3·4	71	0·8
328	57	304	2·7	132	1·5
342	165	115	6·2	107	1·4
363	124	212	2·1	45	1·4

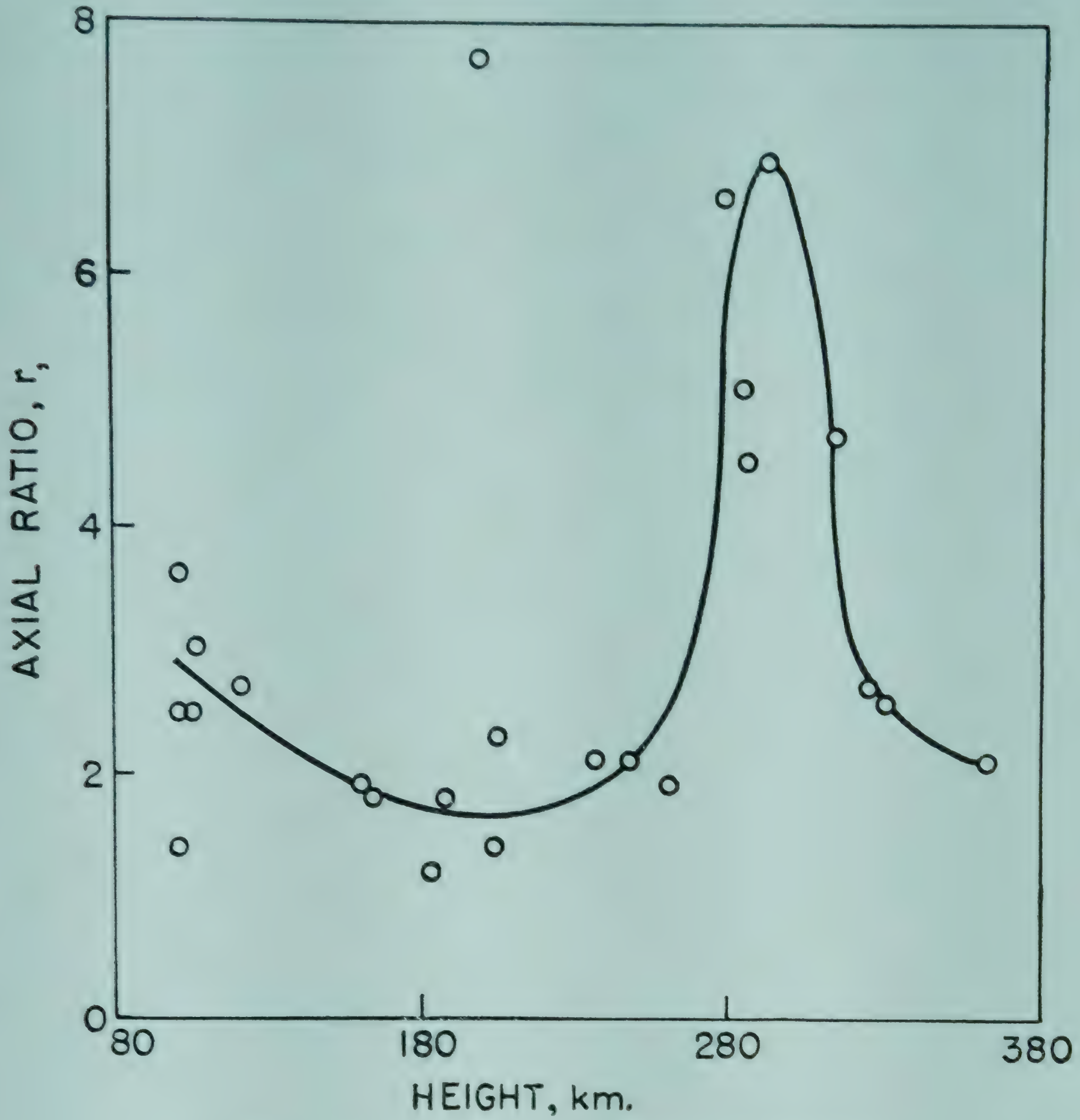

Fig. 1 — Variation of axial ratio with height

Phillips and Spencer's method of analysis to the twenty-eight records taken on six days during 0800–1130 hours IST. The data were arranged corresponding to groups of height 101–120, 121–140, 141–160, etc., and averages were obtained of each parameter pertaining to each range of heights. The data along with the average of each group of heights are presented in Table 1. A study of the drift speed data given in Table 1 shows that the drift speed at first decreases with height in general, and suddenly shoots up at the height of about 280 km. and then fluctuates. The height gradient of drift speed comes out roughly as $-0{\cdot}7$ m. sec.$^{-1}$ km.$^{-1}$ in the height range 100–250 km. This phenomenon of decrease of drift speed at the F_1 region heights has also been noticed by Yerg[8] and Manring *et al.*[9]. It is interesting to note that Yerg, by utilizing his own correlation method, could also obtain similar results. No systematic variation can be

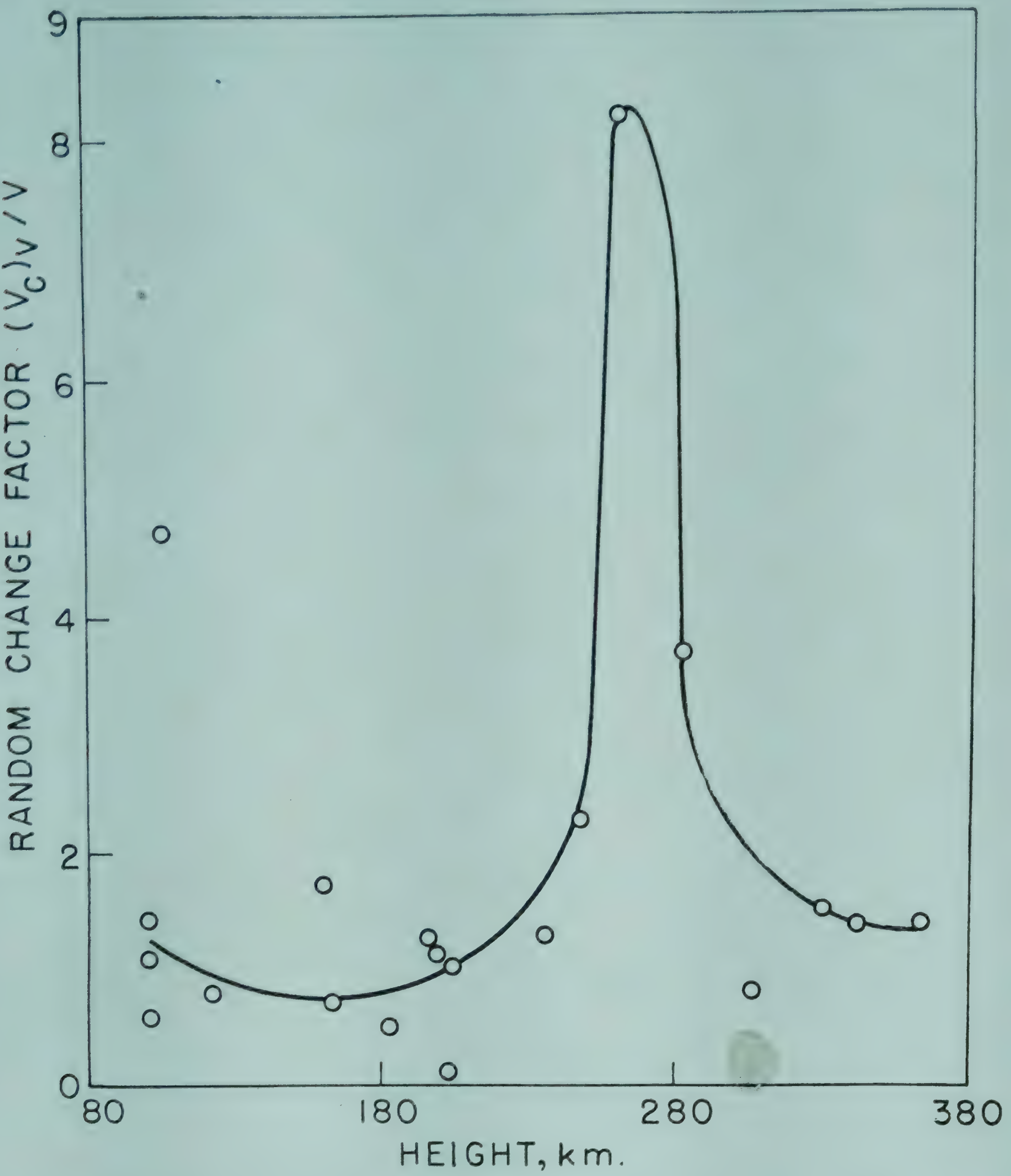

FIG. 2 — VARIATION OF THE RANDOM CHANGE FACTOR WITH HEIGHT

noticed with regard to the data of drift direction from a study of Table 1. But, results on individual days showed a nearly systematic increase or decrease of δ with height on at least five of the six days of observation. The gradient of drift direction was higher in the F region heights.

From the data of the axial ratios presented in the table, it can be seen that r takes high values in the height range 270–290 km., although there are instances of a high value for r at the heights of about 163 and 342 km. This feature can be seen strikingly from a study of Fig. 1 which shows a plot of axial ratio versus height for the individual observations. A smooth curve is drawn which passes through most of the observations. It is clearly seen from this figure that r decreases with height, at first, slowly from about 100 to 190 km., then rapidly rises, reaching a maximum value of about seven at a height of about 290 km. Above this height, it decreases rapidly.

From the data of $V_c/2v$ presented in the table, it is apparent that it takes high values in the height range 250–290 km. Fig. 2 presents a plot of $V_c/2v$ variation with height. In this case also a smooth curve is drawn passing through as many observations as possible. This plot of $V_c/2v$ is nearly similar to the one in Fig. 1 except that the peak occurs at about 270 km. instead of at 290 km. It is also interesting to note here that the steady drift velocity is also the highest in these regions. Thus it appears from this study that in the region 250–300 km. the irregularities are highly anisotropic and that large random changes are present in the irregularities. It may be of interest, here, to quote Yerg who concluded that 'large random changes are highly anisotropic and tend to change the correlation ellipse to be oriented along the earth's magnetic field'. The latter observation of Yerg, namely that the correlation ellipse is oriented along the earth's magnetic field when large random changes are present, is not supported by the present investigation. On the other hand, a study of Table 1 shows that in these regions the tendency of the correlation ellipse is to orient itself nearly along the E–W direction.

From considerations of turbulence in the ionosphere, Booker[10] suggested that the radio star scintillations cannot be explained in terms of turbulence at a height of 400 km., but that reasonable results can be obtained if the level is assumed to be somewhere between 200 and 300 km. From the present investigation it can be concluded that highly anisotropic irregularities with large random motions do occur in the height range 250–300 km. Thus, it is quite likely that this height range is the seat of radio star scintillation and spread F. However, it may be pointed out that the investigations were conducted only during day-time. The observations of intense spread F echoes in the range 200–300 km. at this station also seem to lend support to this view.

References

1. Greenhow, J. S., *Phil. Mag.*, **45** (1954), 471.
2. Elford, W. G. & Robertson, D. S., *J. atmos. terr. Phys.*, **4** (1953), 271.
3. Mitra, S. N., *Proc. Instn elect. Engrs*, **96** (1949), Pt III, 441.
4. Phillips, G. J. & Spencer, M., *Proc. phys. Soc. Lond.*, **68** (1955), 481.
5. Jones, I. L., *J. atmos. terr. Phys.*, **12** (1958), 68.
6. Booker, H. G., *J. atmos. terr. Phys.*, **7** (1955), 343.
7. Schmerling, E. R., *J. atmos. terr. Phys.*, **12** (1958), 8.
8. Yerg, D. G., *J. atmos. terr. Phys.*, **8** (1956), 247.
9. Manring, E. *et al.*, *J. geophys. Res.*, **64** (1959), 587.
10. Booker, H. G., *Polar Atmosphere Symposium*, Pt II, Ionos. Sec., P52 (1957).

Effects of moving anisometric irregularities in F region of ionosphere

R. N. SINGH

Physics Department
Banaras Hindu University
Varanasi

The method of similar fades used to calculate the drift velocity and direction from the three spaced receiver records is based on the assumption that the moving irregularities are statistically isometric, the irregularities possessing circular symmetry in the two-dimensional figure and spherical symmetry in the three-dimensional figure.

In the case of moving irregularities, this assumption is far from valid and the isometric irregularities are changed into an anisometric ones having elliptical and ellipsoidal symmetries in the two and three dimensions. The error that arises if isometric assumption is not valid has been considered in the present paper. The axial ratio and the orientation of the characteristic ellipse in the F region has been evaluated from three spaced receiver fading records taken at Banaras (30°20′N : 78°3′E) during night (1800-0600 hours IST). The actual velocity and the direction of the drift have been determined. The mean error in the direction has been found to be 26° and the greatest error to be 67°. The mean value of the apparent to actual velocity has been found to be 0·79. The results are illustrated with the help of histograms.

The fading of the radio signals reflected from the ionosphere is characteristic of the moving irregularities in the ionospheric layer. For theoretical purposes the ionospheric layers are assumed to be plane, horizontally stratified and having parabolic electron density profile. However, electron density discontinuities do exist as undulations in the lower boundary of the ionospheric layer or in the form of ion clouds or patches of increased ionization due to meteoric showers, solar flares, magnetic storms, atoms and molecules in thermal agitation, etc., or due to variations in the atmospheric current systems. Such electron density discontinuities or irregularities in the ionosphere are found to drift with finite velocity in certain directions.

The three spaced receiver method of Mitra[1] as modified by Singh and Khastgir[2] has been used. These fading patterns have been analysed to determine the velocity and direction of the ionospheric drift either by method of similar fades or by the method of cross-correlation analysis. The main simplifying assumption underlying the methods is that the irregularities are statistically isometric, i.e. the separation of the two points for which the amplitudes have a given fixed correlation is independent of direction or, in other words, irregularities possess circular symmetry. This assumption may, however, be valid in the idealized case of stationary ionospheric layer containing electrons and ions having equal diffusion coefficients along, and perpendicular to, the magnetic lines of force, but in practice this assumption is not valid and the irregularities set themselves stretched along a certain direction and become anisometric. In other words, the circular symmetry pattern, when stretched in a certain direction, gives rise to a characteristic elliptic pattern. The error due to the anisometric irregularities may be quite serious. In the present paper the velocity and the direction of the anisometric ionospheric irregularities have been determined by the method of analysis developed by Phillips and Spencer[3]. The axial ratio and the orientation of the characteristic ellipse have been calculated, and with the help of these parameters, the true magnitude and direction of the ionospheric drift have been determined. The results are shown with the help of various histograms.

THEORETICAL CONSIDERATIONS

Practical Determination of the Parameters of the Characteristic Ellipse. In the practical case of moving irregularities, the assumption of isometric irregularities does not hold good and irregularities change themselves in form and may finally possess some geometrical configuration. Let the distorted form be represented by a characteristic ellipse. Analysis of the three spaced receiver fading records gives the parameters of the characteristic ellipse.

Consider the analysis of the fading patterns for the points R_1, R_2 and R_3 at the corner of an isosceles right-angled triangle of sides $R_1R_2 = R_1R_3 = a$. We proceed thus:

(i) From one of the three fading patterns, the complete temporal auto-correllogram was drawn. (Since the auto-correlation function is the same for all the three points on the ground, only one fading curve need be drawn.)

(ii) The cross-correlation functions for $\tau = 0$ corresponding to the fading patterns at (R_1, R_2), (R_1, R_3) and (R_2, R_3) were determined. Each of these would be called the zero-time cross-correlation function.

(iii) From the temporal auto-correllogram, the values of τ, viz. τ_{12}, τ_{13} and τ_{23}, corresponding to three values of the zero-time cross-correlation function were found.

(iv) The axial ratio r, and the orientation ψ of the major axis of characteristic ellipse were evaluated from Equation (1).

$$r^2 = \frac{R+(P^2+Q^2)^{1/2}}{R-(P^2+Q^2)^{1/2}} \quad \text{and} \quad \tan 2\psi = \frac{P}{Q} \tag{1}$$

where $P = \tau_{12}^2+\tau_{13}^2-\tau_{23}^2$; $Q = \tau_{12}^2-\tau_{13}^2$ and $R = \tau_{12}^2+\tau_{13}^2$

The orientation of the major axis of the characteristic ellipse is measured clockwise from the north, which is taken as reference direction, and the ambiguity of the direction in the range $0° \leqslant \psi° \leqslant 180°$ is resolved by taking the value of $\cos 2\psi$ which has the same sign as Q.

Expressions for the True Velocity and the True Direction of the Ionospheric Drift. If the amplitude patterns received at the three spaced points are produced due to the movement of isotropic irregularities, the velocity V and the direction of the drift ϕ, measured clockwise from the north, which is taken as the reference direction, are given by Equation (2).

$$\frac{1}{4V^2} = \frac{1}{V_x^2} + \frac{1}{V_y^2} \quad \text{and} \quad \tan \phi = \frac{V_y}{V_x} \tag{2}$$

where V_x and V_y are the components of drift velocity along the E–W and N–S directions.

If these equations are used when the assumption of isometric irregularities is not justified, the values of the velocity and the direction are only apparent and may be denoted by V_a and ϕ_a respectively. The complete solution of the problem, when the irregularities are anisometric and change in their details as they move, has been given by Phillips and Spencer[3]. The results obtained by them are given by Equations (3) and (4).

$$\tan(\phi-\phi_a) = \frac{(r^2-1)\tan(\phi_a-\psi)}{1+r^2\tan^2(\phi_a-\psi)} \tag{3}$$

and

$$\frac{V_a}{V'} = \cos(\phi-\phi_a) \tag{4}$$

Here, r and ψ are the axial ratio and the orientation of the characteristic ellipse respectively and ϕ is the angle which V' makes with the north,

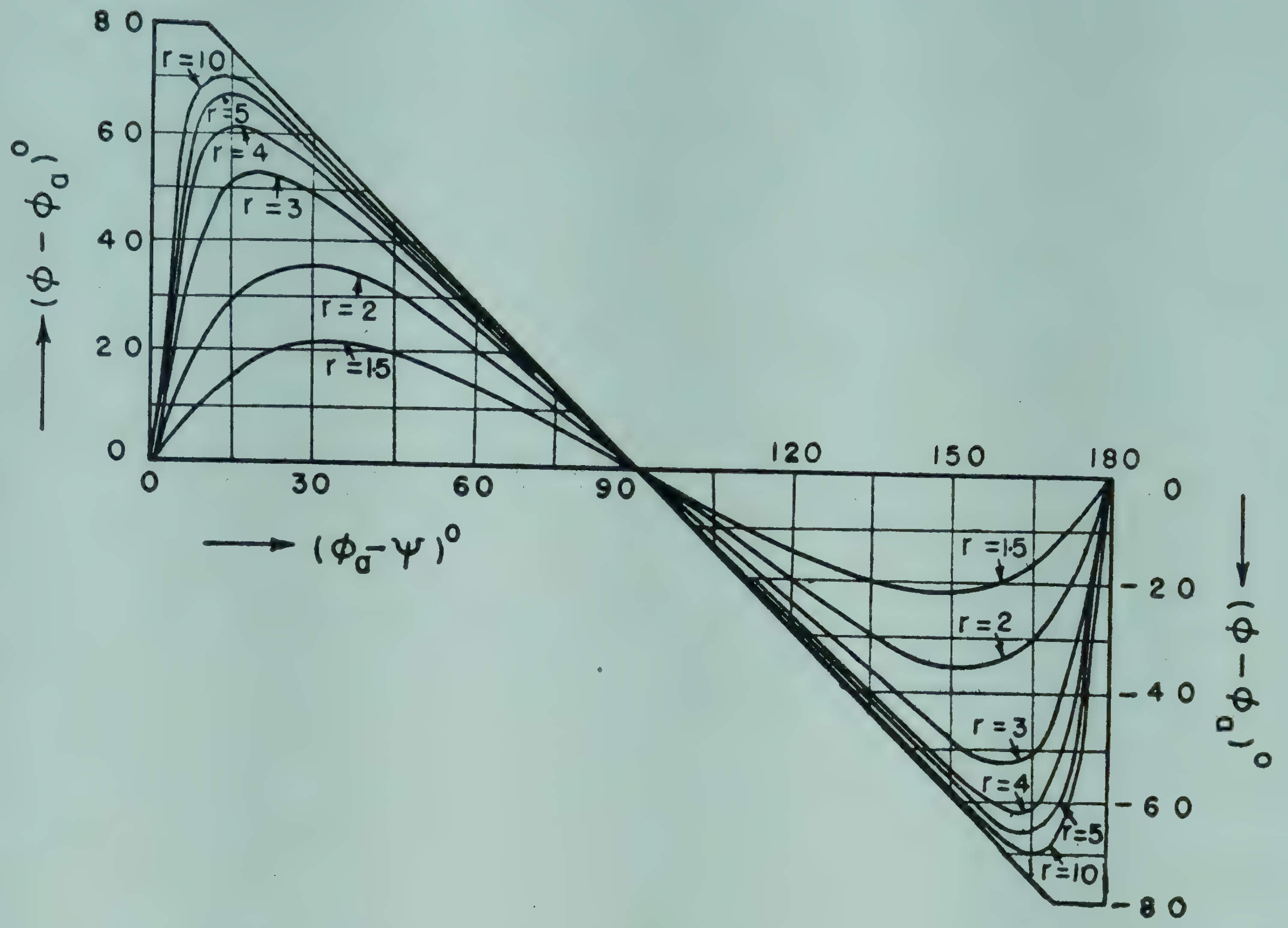

Fig. 1 — Theoretical relation between ($\phi-\phi_a$) and ($\phi_a-\psi$) for different axial ratios

i.e. with the R_1-R_3 direction and V' is related to the true velocity by Equation (5).

$$V' = \frac{(V'_c)_v^2}{V} \tag{5}$$

where

$$(V'_c)_v^2 = \frac{1+(r^2-1)\ \cos^2\ \psi}{1+(r^2-1)\ \cos^2\ (\phi-\psi)}\ (V'_c)_{13}^2$$

$(V'_c)_{13} = a/\tau_{13}$ and τ_{13} is the value of τ corresponding to the zero-time cross-correlation function for (R_1R_3). Briggs, Phillips and Shinn[4] called V'_c the fading velocity.

As we are principally concerned with the errors in velocity and direction of the ionospheric drift due to the anisometry of the moving irregularities, V' may be taken as equivalent to the true velocity V, when it is possible to neglect the changes in certain details of amplitude variation patterns.

The difference ($\phi-\phi_a$) between the true and the apparent directions of drift is related to the angle ($\phi_a-\psi$) between the apparent direction and the major axis of the characteristic ellipse as shown in Fig. 1. These curves have been drawn from the theoretical relation given in Equations (3) and (4) for the

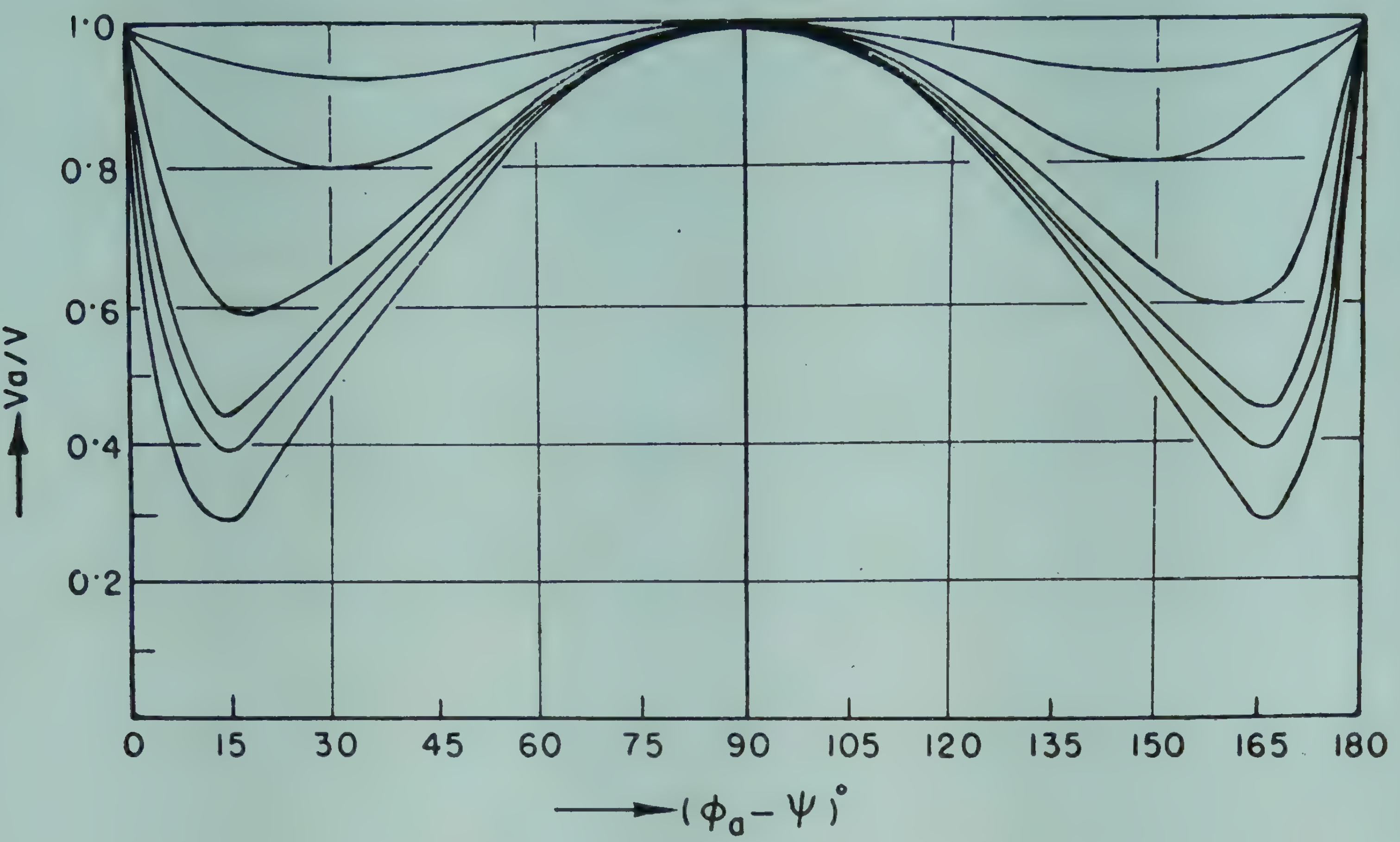

Fig. 2 — Theoretical relation between the ratio (V_a/V') and the angle ($\phi_a - \psi$)

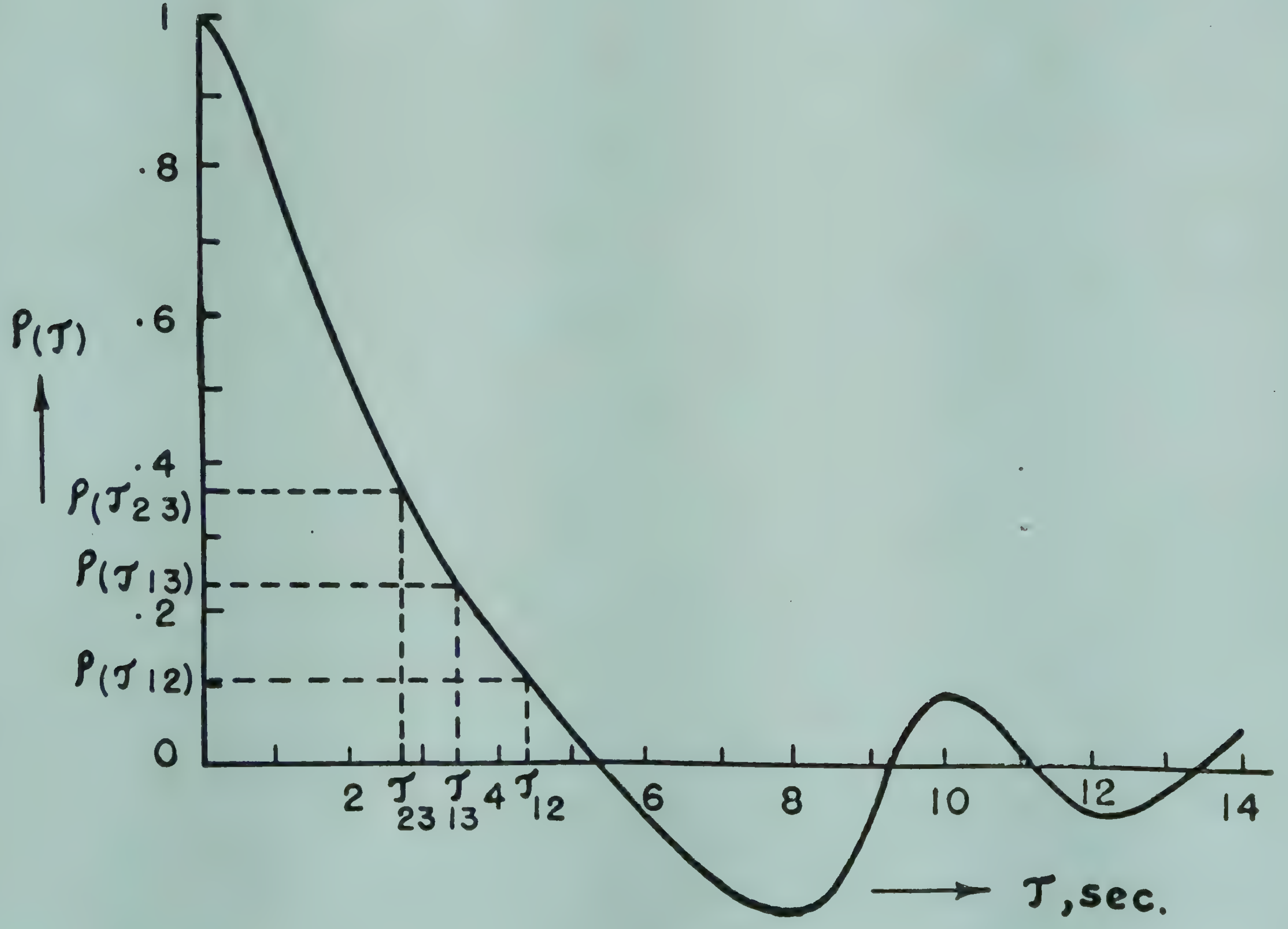

Fig. 3 — Auto-correlogram showing values of τ_{12}, τ_{13} and τ_{23} corresponding to three values of zero-time cross-correlation function for fading record taken on March 19, 1958 at 2200 hours IST

TABLE 1 — RESULTS OF AN ILLUSTRATIVE ANALYSIS

Auto-correlation function		Zero-time cross-correlation function $\rho_R(a, 0)$ for $\tau = 0$	
τ *sec.*	$\rho_R(\tau)$	Pair of records	Zero-time cross-correlation function $\rho_R(a, 0)$
0	1·0	R_1R_2	0·11
2	0·42	R_1R_3	0·25
4	0·15	R_2R_3	0·37
6	−0·05		
8	−0·22		
10	+0·12		
12	−0·07		
14	+0·052		

TABLE 2 — PARAMETERS OF THE CHARACTERISTIC ELLIPSE

Pairs of records	τ *sec.*	Axial ratio (r)	Orientation	$(V_c')_{13}$
R_1R_2	$\tau_{12} = 4{\cdot}2$	2·8	37°27′	30
R_1R_3	$\tau_{13} = 3{\cdot}4$			
R_2R_3	$\tau_{23} = 2{\cdot}6$			

TABLE 3 — VELOCITY AND DIRECTION OF THE IONOSPHERIC DRIFT

Particulars	Magnitude
Apparent velocity, (V_a)	110 m./sec.
Apparent direction, (ϕ_a)	110°
True velocity component, (V')	115 m./sec.
True direction of V', (ϕ)	125°
Ratio of apparent to true velocity, (V_a/V')	0·96

different values of the axial ratio, r. The relation between the ratio V_a/V' and the angle $(\phi_a - \psi)$ is shown in Fig. 2. It is evident from these curves that there is no error in the magnitude of the velocity or in the direction of the drift when $(\phi_a - \psi) = 0°$, 90° or 180°, i.e. when the characteristic ellipse moves having its major or minor axis directed along the true direction of drift.

Analysis of Three Spaced Receiver Fading Records for Determination of True Velocity and True Direction of Ionospheric Drift. The temporal auto-correlation function for one of the fading patterns has been evaluated for different values of τ and the auto-correllogram drawn as shown in Fig. 3. The zero-time cross-correlation functions corresponding to pairs

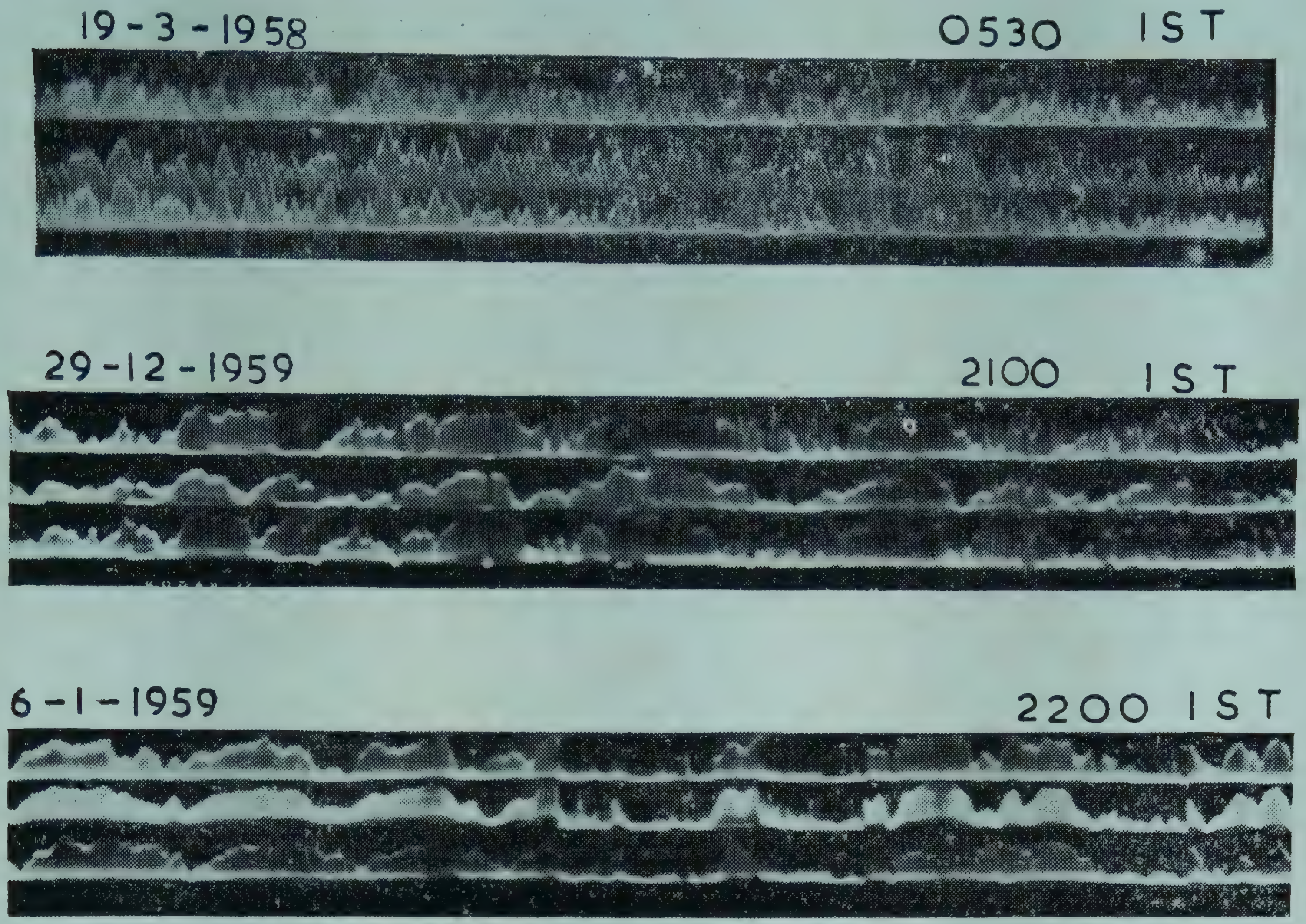

Fig. 4 — Typical three spaced receiver fading records produced due to the movement of anisometric irregularity in the reflecting layer

of fading patterns are also determined. The results of an illustrative analysis are given in Table 1.

The three values of τ, viz. τ_{12}, τ_{13} and τ_{23}, corresponding to three zero-time cross-correlation functions for pairs of fading records at R_1R_2, R_1R_3 and R_2R_3 have been obtained from the temporal auto-correllogram shown in Fig. 3. These three values have been used to determine the axial ratio and the orientation of the characteristic ellipse using Equation (1). The values are given in Table 2.

The parameters of the characteristic ellipse obtained above have been used to calculate the true direction and the magnitude of the velocity using Equations (3) and (4). The results obtained are given in Table 3.

Experimental Results

A scrutiny of the three spaced receiver fading records shows considerable variation in the individual time displacement between the two pairs of records along the N–S and E–W directions. Such a variation in the time displacement of the maxima was attributed by Ratcliffe[5] to the different forms and orientations of the line of maximum amplitude of a moving ionospheric irregularity. Assuming such irregularities to be anisometric and having elliptic symmetry in the two-dimensional plane, some three

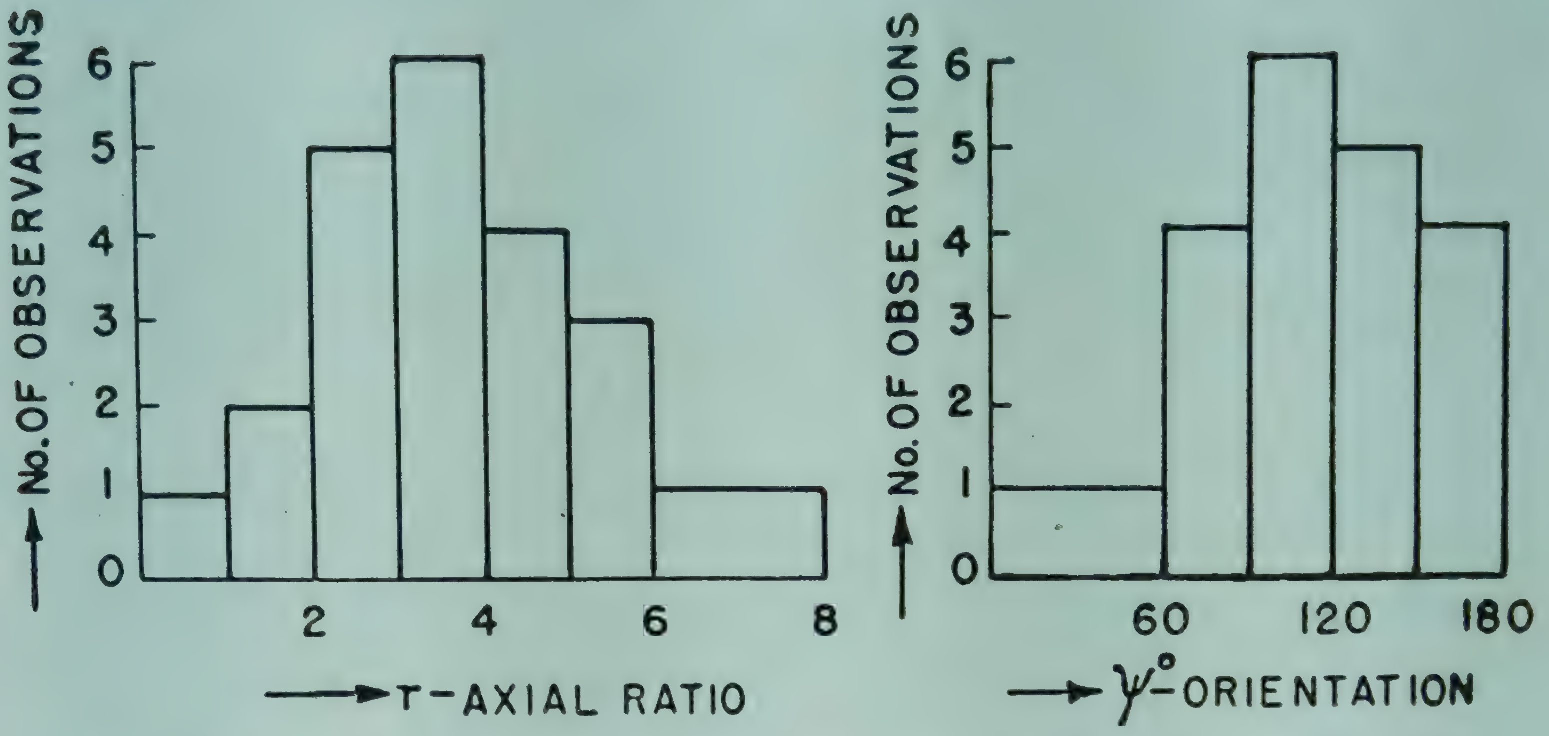

FIG. 5 — HISTOGRAMS SHOWING THE AXIAL RATIO AND ORIENTATIONS OF THE 'CHARACTERISTICS ELLIPSE'

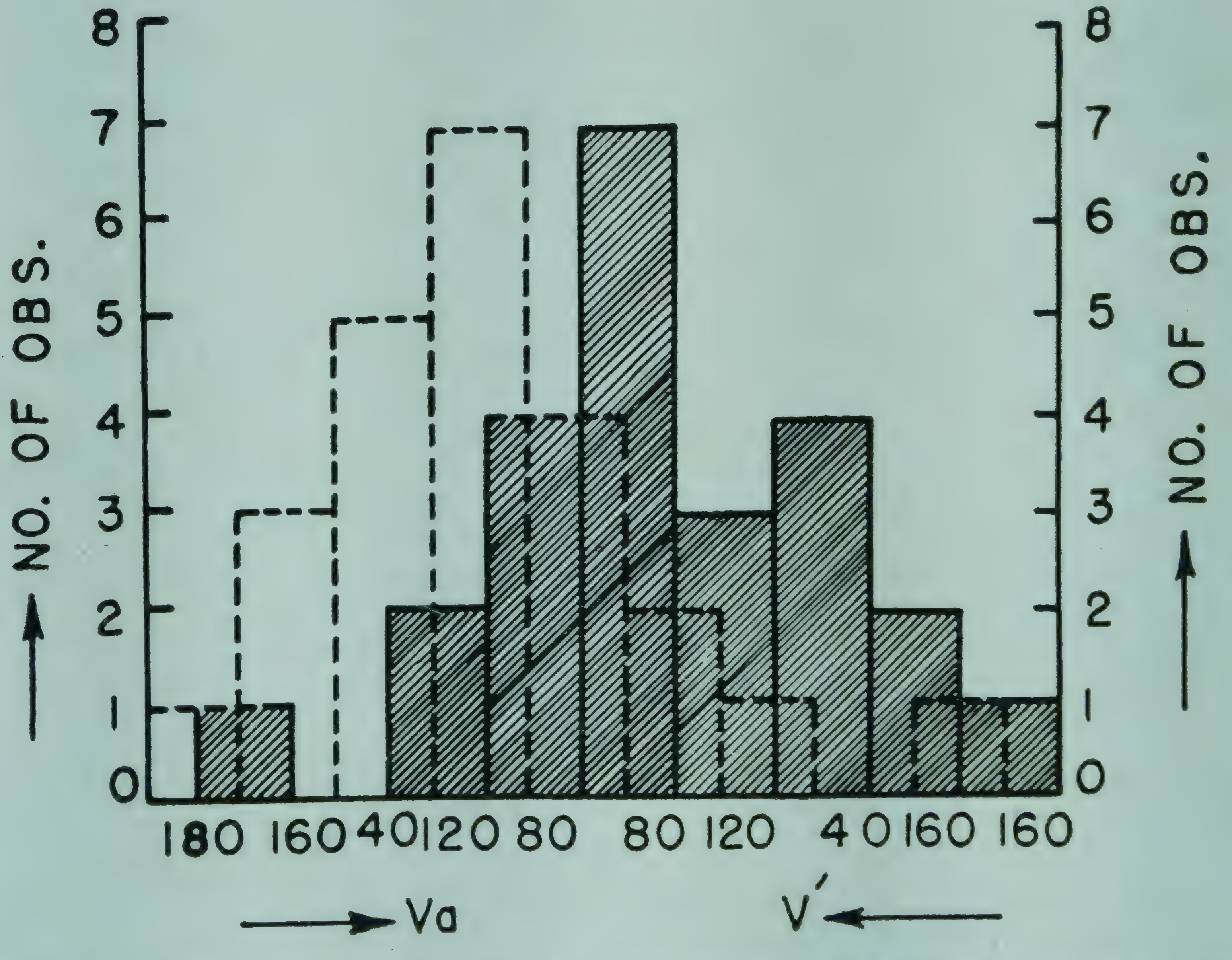

FIG. 6 — DOTTED HISTOGRAM SHOWING DISTRIBUTION OF APPARENT VELOCITY (V_a) AND SHADED HISTOGRAM SHOWING DISTRIBUTION OF ACTUAL VELOCITY (V')

spaced receiver fading patterns, which were considered to be produced as a result of the movement of an anisometric irregularity as shown in Fig. 4 were analysed. The method of Phillips and Spencer[3] as illustrated

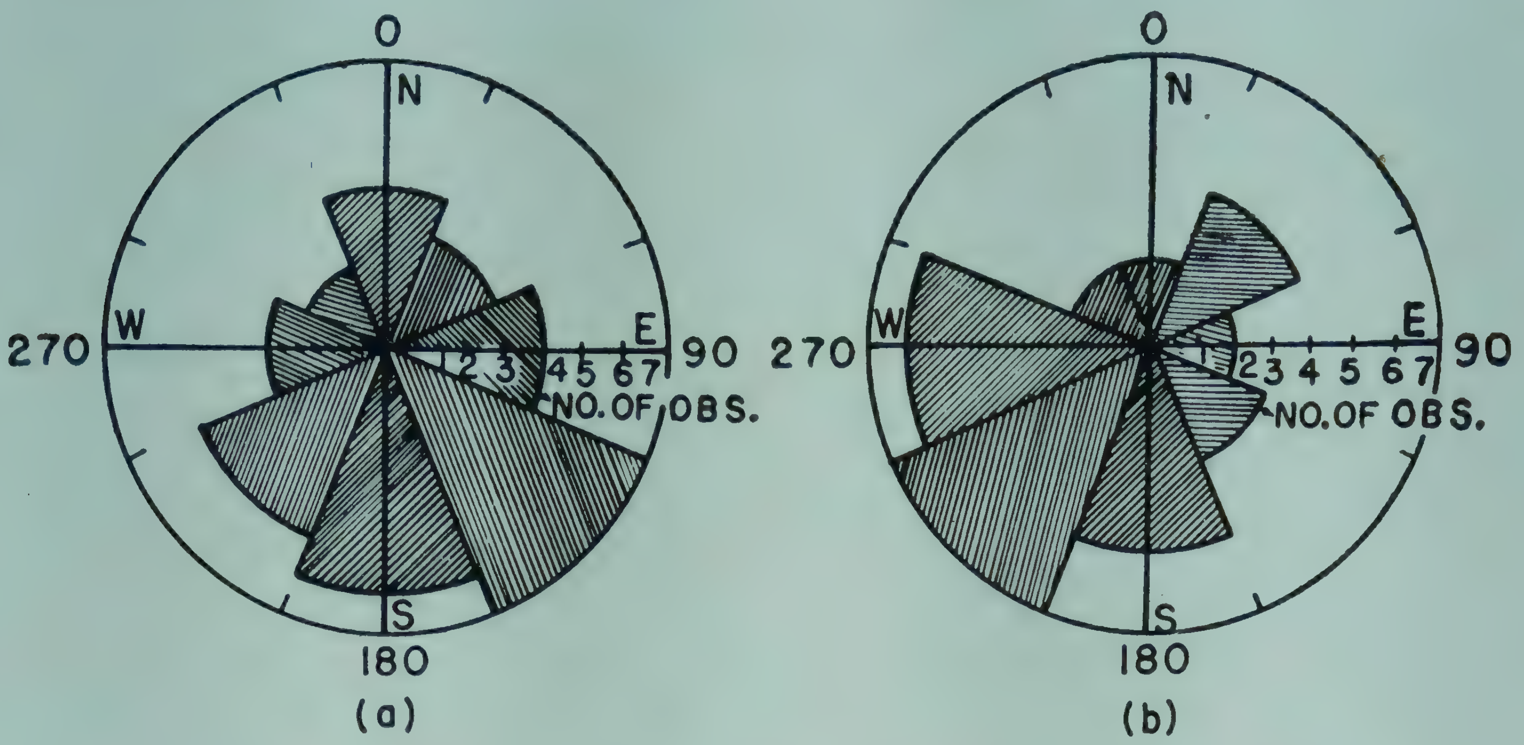

FIG. 7 — (a) POLAR HISTOGRAM SHOWING DISTRIBUTION OF APPARENT DIRECTION (ϕa); (b) POLAR HISTOGRAM SHOWING DISTRIBUTION OF ACTUAL DIRECTION (ϕ)

in the present paper has been adopted. The parameters of the characteristic ellipse for the different amplitude patterns have been evaluated and are shown with the help of histograms in Fig. 5. Using these parameters the characteristic ellipse, the true velocity and the true direction of the ionospheric drift have been calculated. The results are illustrated with the help of histograms shown in Fig. 6, and polar diagram shown in Fig. 7. In the histograms shown in Fig. 6, the dotted histogram is for the apparent velocity of the drift and the shaded histogram for the corrected true velocity. It is evident that the corrected velocity is more than the apparent velocity in many cases. The most probable value of V_a is found to be 70 m./sec. and that of V' is found to be 90 m./sec. The polar diagrams for the distribution of the apparent and the true direction of the drift are shown separately in Fig. 7 (a) and (b). The apparent direction of the drift is concentrated within second quadrant, i.e. $\pi/2$ and π, whereas the corrected true direction lies within the third quadrant, i.e. within π and $3\pi/2$. The greatest error in the direction has been found to be 67° and the mean error to be 26°. The mean value of V_a/V' has been found to be 0·79. Sometimes the error in the direction has been found to be large. Ignoring these large values, the mean error has been 1·7 times more than the mean error obtained by Phillips and Spencer for the E layer.

DISCUSSION AND CONCLUSIONS

The results obtained for the F layer employing a frequency of 3·8–4·2 Mc/s. were found to be different from those reported by Phillips and Spencer. It may be noted that the results obtained by Phillips and

Spencer were based only on the analysis of three records. The values of the parameters of the characteristic ellipse obtained by us for the irregularities in the F region are found to be more than those reported by Phillips and Spencer for the E layer. This is explicable, because the pressure in the F region is very low and diffusion coefficient very high as compared to the E layer, so that the axial ratio and the angle of orientation are expected to be more for the F layer than for the E layer.

In the idealized case of stationary ionosphere, the irregularities in the electron density produced by the different agencies may be isometric, but the diffusion of electrons takes place to equalize the electron density in the layer. The effective diffusion coefficient along, and perpendicular to, the earth's magnetic lines of force are in the ratio of corresponding mobilities. The ratio is equal to $(\nu^2+w^2)/\nu^2$, where ν and w are the relevant electron collisional frequency and the angular gyrofrequency. The diffusion is governed by the frequency of collisions of the ions with neutral particles or other ions, because electrons cannot diffuse without them and the collisions of electrons with ions do not appreciably deflect the ions.

The value of the electron collisional frequency in the F region over Varanasi during the night hours has been found to be 4×10^3/sec. by Murty *et al.*[6]. The gyrofrequency of the ions and electrons is very high and the ratio of the diffusion coefficients along, and perpendicular to, the magnetic lines of force comes out to be much more than 200. This large ratio shows that even if an irregularity starts with circular symmetry, it subsequently diffuses out into one which is extended along the earth's magnetic lines of force. The ratio of the diffusion coefficients in the F region was found by Spencer[7] to be 200, which suggests that the isometric irregularities formed by the different sources in the region, change into anisometric irregularities in a few minutes' time.

An irregularity in a layer can move in any direction which is mainly governed by the ionospheric conditions. When they move in a certain direction with some velocity the whole pattern is elongated in the direction of the movement. The pattern which is originally extended along the magnetic lines of force might drift along the movement of the layer with suitable orientation of their axes from the reference direction. The irregularities in such cases might set themselves along a direction which is the resultant of the direction of high diffusion coefficient N–S and the true direction of the movement. The error in the magnitude and the direction, however, becomes negligible when the drift is mainly directed towards or perpendicular to the N–S direction. The parameters of the characteristic ellipse obtained here are in contrast with the result obtained by Spencer in the F region at a height of about 400 km. (above the normal reflection layer). He found that the amplitude patterns on the ground were highly anisometric, the axial ratio of the characteristic ellipse being always greater than five. Such a striking difference in the result appears to be due to some fundamental difference in the mode of propagation of radio waves. However, the parameters would definitely be smaller at lower heights and would probably increase exponentially with the increase in height. The results reported in this paper refer to the reflection height of 250 km. which is intermediate between the working level of Phillips and Spencer[3] and that of Spencer[7]. These results seem, therefore, plausible and comparable with those of Phillips and Spencer but the striking difference from the results of Spencer should be accounted for.

ACKNOWLEDGEMENT

The author is grateful to Prof. S. R. Khastgir for his keen interest and valuable suggestions during this investigation.

REFERENCES

1. MITRA, S. N., *Proc. Instn elect. Engrs*, **96** (1949), Pt III, 441.
2. SINGH, R. N. & KHASTGIR, S. R., *J. atmos. terr. Phys.*, **16** (1959), 376.
3. PHILLIPS, G. J. & SPENCER, M., *Proc. phys. Soc. Lond.*, **68B** (1955), 481.
4. BRIGGS, B. H., PHILLIPS, G. J. & SHINN, D. H., *Proc. phys. Soc. Lond.*, **63B** (1950), 106.
5. RATCLIFFE, J. A., *J. atmos. terr. Phys.*, **5** (1954), 173.
6. MURTY, Y. S. N., SINGH, R. N. & KHASTGIR, S. R., *J. sci. industr. Res.*, **18A** (1959), 507.
7. SPENCER, M., *Proc. phys. Soc. Lond.*, **68B** (1955), 493.

* * *

Horizontal Drift in the Ionosphere over Delhi. S. N. MITRA, K. K. VIJ & P. DASGUPTA, Research Department, All India Radio, New Delhi [*J. atmos. terr. Phys.*, **19** (1960), 172].

Some results obtained at Delhi on the measurements of ionospheric drift by the spaced receiver technique are described. Most probable velocities on reflections from F layer in different seasons have been evaluated and presented in the form of histograms. The diurnal variations of the magnitude and the direction of the drift velocity have been plotted graphically. Harmonic analysis of the E–W and N–S components of the drift velocity has been made. No predominant periodicity in any of the components has been observed. An interesting observation is that the most probable direction of the drift velocity is towards the south and northward component is almost completely inhibited. During magnetic storms, however, the northward component increases and its variation appears to be well correlated with the variation of K index.

The most probable value of the resultant drift velocity on reflections from the F layer is 85 m./sec. Velocities less than 30 m./sec. and greater than 160 m./sec. have not usually been observed. The most frequent value of the E–W and N–S components is 65 m./sec. The most probable velocity is higher in equinox and winter than in summer. (*Abstract*)

Study of Horizontal Drifts in the E Region at Waltair. R. RAGHAVA RAO & B. RAMACHANDRA RAO, Ionosphere Research Laboratory, Andhra University, Waltair [*J. atmos. terr. Phys.*, **22** (1961), 81].

Results of analysis of drift data for the E region taken at Waltair over a period of two years are presented. The main features of diurnal and seasonal variation of drifts in the E region at this low latitude station are compared with earlier results from high latitude stations. The 24-hourly drift vector is predominant in all seasons. This shows clockwise rotation in all seasons except summer. The 12-hourly drift vector is invariably smaller than the 24-hourly drift vector and shows clockwise sense of rotation in all seasons. The steady component is generally directed towards SSE. The polar plots of 24-hourly and 12-hourly drift vectors show highly elliptical forms, the major axes being oriented nearly along E–W and N–S respectively. The results are compared with the winds deduced for E region levels from S_q variations. (*Abstract*)

Simultaneous Study of Drifts at Different Levels in the Ionosphere by Spaced Receiver Method. E. BHAGIRATHA RAO & B. RAMACHANDRA RAO, Ionosphere Research Laboratory, Andhra University, Waltair.

Results of simultaneous study of drifts in different regions of the ionosphere measured at Waltair over a period of two years are presented. F_2 drift speeds are generally higher than F_1 drift speeds measured simultaneously. On a few occasions when f_0F_1 was high, F_2 drift velocities are found to have been affected by drifts prevailing in F_1 at that time. F_2 drift measurements have been found to be affected by drifts in E_s region when F_2 region operating frequency is sufficiently above to fE_s. F_2 region drift gradients have also been estimated by a simultaneous study on two frequencies and drift gradients less than 1 m./sec. per km. have been obtained. (*Abstract*)

Statistical Analysis of Fading of a Single Downcoming Wave. P. Dasgupta & K. K. Vij, Research Department, All India Radio, New Delhi [*J. atmos. terr. Phys.*, **18** (1960), 265].

Fading of a single wave reflected (vertically) from the F region of the ionosphere has been statistically analysed. The amplitude distribution of these fading records which are random have been found to be Rayleigh, Gaussian or log-normal by other workers. But the present analysis shows that the amplitude distribution is Rayleigh only in the case of rapid fading, whereas for slow and quasi-periodic fading it represents what can be termed as an M type. The distribution of successive differences in the amplitudes has also been studied; for a Rayleigh amplitude distribution the time analysis gives rise to a Type VII distribution of Pearson as originally pointed out by Mitra, while in the case of M type amplitude distribution it becomes Gaussian. Following Mitra's analysis, the r.m.s. value of the random velocity, v_0 of the ionospheric irregularities has been calculated from the time analysis. The value of v_0 has also been calculated from the auto-correlation coefficient of the amplitude R, following Booker *et al.* The two values of v_0 thus obtained are found to agree well. (*Abstract*)

Results of cosmic noise observations at Delhi on 22.4 Mc/s.

K. A. SARADA
A. P. MITRA

National Physical Laboratory
New Delhi

Some of the results of ionospheric absorption measurements at Delhi using cosmic radio noise at a frequency of 22·4 Mc/s. and using essentially the method of Mitra and Shain with certain improvements in the development of the sidereal time curve are reported.

The normal day-time absorption is considerably higher than that observed by Mitra and Shain, the average noon-time value for the months July-December 1957 being about 5 db. Of the total absorption, a substantial portion comes from region F_2, this contribution is dependent principally on, and increases very rapidly with, f_0F_2. The remaining absorption is principally from region D. The comparison of the noon-time D region absorption with observations made by A.I.R. and at Ahmedabad with terrestrial techniques shows that $(f+f_L)^{-2}$ law is obeyed.

Even on normal days the night-time absorption, for the same values of f_0F_2 are greater than the day-time absorption; the value is greater still during those nights in which spread F echoes have been observed.

The use of cosmic radio noise for the study of ionospheric absorption was introduced by Mitra and Shain[1] in Australia at a frequency of 18·3 Mc/s. Since then such studies have been carried out at several places, and have formed part of the IGY programme of several countries.

From such measurements, three different types of ionospheric absorption studies have been made. First, the measurements have been used to study the regular day and night absorption arising from the various ionospheric layers. It has been shown that the regions D and F of the ionosphere play the most important role in the absorption of extraterrestrial signal, the F region contribution increasing in severity as the critical frequency of the layer increases[1].

Secondly, such measurements provide a very reliable tool for studying the ionospheric effects of solar flares. A detailed account of such studies first given by Shain and Mitra[2] showed that the effects, known as SCNA, are well correlated with solar flares.

Thirdly, the measurements at high latitudes have been used to study auroral ionization. At these latitudes an additional source of absorption arises from ionization associated with corpuscular bombardment of the earth's upper atmosphere. In extreme cases, this absorption may be so severe as to cause a polar blackout, during which ionospherically propagated HF signals are rendered so weak as to be unusable.

As a part of Indian programme for the IGY, measurement of cosmic radio noise was undertaken[3] at the National Physical Laboratory (NPL), Delhi (28°38′N : 77°13′E), at a frequency of 22·4 Mc/s. The measurements continued for the greater part of 1957. Later, because of the severity of interfering noise at the NPL, new measurements were undertaken at Mussoorie (Landour Cantonment) at a frequency of 30 Mc/s., and were continued from the beginning of 1958 to the middle of 1959. This work had the following objectives:

(i) To obtain as complete a picture as possible of the ionospheric absorption occurring in a tropical station for which absorption data are generally inadequate. It was a matter of particular advantage that the A.I.R. at Delhi had, for some time, been making absorption measurements using a pulse technique and had planned to continue such observations. Simultaneous measurements of absorption at the same place by both extraterrestrial and terrestrial techniques, and using widely different frequencies, were expected to provide information of interest.

(ii) Secondly, it was intended to examine the efficacy of the SCNA as a tool for continuous radio flare patrol. The period of observation coincided with solar activity of an unprecedented magnitude, and it was expected that intense solar flares would occur in great numbers.

(iii) Thirdly, it was hoped that the cosmic noise data would yield information of value for understanding some of the physical properties of the ionized regions.

In the following sections a detailed account is given of some of the observational results on the ionospheric absorption of cosmic radio noise at 22·4 Mc/s. at Delhi, analysis of such observations, and their implications in the study of ionospheric physics.

EQUIPMENT AND METHOD OF ANALYSIS

The cosmic radio noise observations reported here were made by an equipment designed, built and installed in the NPL premises in 1956, as part of the Indian programme for IGY. The aerial, which consisted of 4 dipoles, provided with corner reflectors, had beam-widths of ±18° and ±24° in the N–S and E–W directions. Details of other equipment have been reported previously[3].

Measurements of ionospheric absorption from observations of cosmic noise requires a previous knowledge of the sidereal time variation of the unattenuated cosmic noise power received at that frequency. This curve, often referred to as ‘ quiet-day curve ’, was derived by Mitra and Shain[1] by using observations extending for a period of about one year and using records for specially selected intervals for which the ionospheric effect could be assumed to be minimum (e.g. around 0004 hours local time). The value of ionospheric absorption under any condition was then calculated by comparing the observed intensity P with the unattenuated intensity P_0 for the sidereal time of the observation.

In building up the sidereal time curve the night-time records for the period 2100–0600 hours, restricting them to days for which values of f_0F_2 were lower than usual (and especially days in which spread F was absent) have been used. The sidereal time curves were drawn following the current practice, from the envelopes of all night-time values, and also from the mean values at all sidereal hours (curves B and A in Fig. 1 respectively). These have, however, been supplemented with a new technique of analysis. It has been found that values of cosmic noise power, when normalized with respect to the average night-time value, has substantially the same kind of variation with solar time for different solar hours. An example is given in Fig. 2. Use of this result has yielded the curve C in Fig. 1.

NORMAL ABSORPTION

Total Absorption. The total ionospheric absorption suffered by the cosmic radio noise has been computed, every half-hour, from interference-free records for the period July-December 1957. Special care has been taken to select days for which station or man-made interferences were negligible, and a continuous set of observations was available. Doubtful records were strictly rejected, resulting in the rejection of about 8–10 days' records every month.

The resulting absorption values are averaged, hour by hour, for each month and are grouped separately for northern solstice months (J), equinoxial months (E) and southern solstice months (D). Diurnal variation of absorption for these periods and for the entire average is shown in Fig. 3 (a, b, c and d).

The following features may be noted:

(i) The day-time absorption for Delhi during 1957 at 22·4 Mc/s. was appreciable, and was considerably larger than the Hornsby values, even though

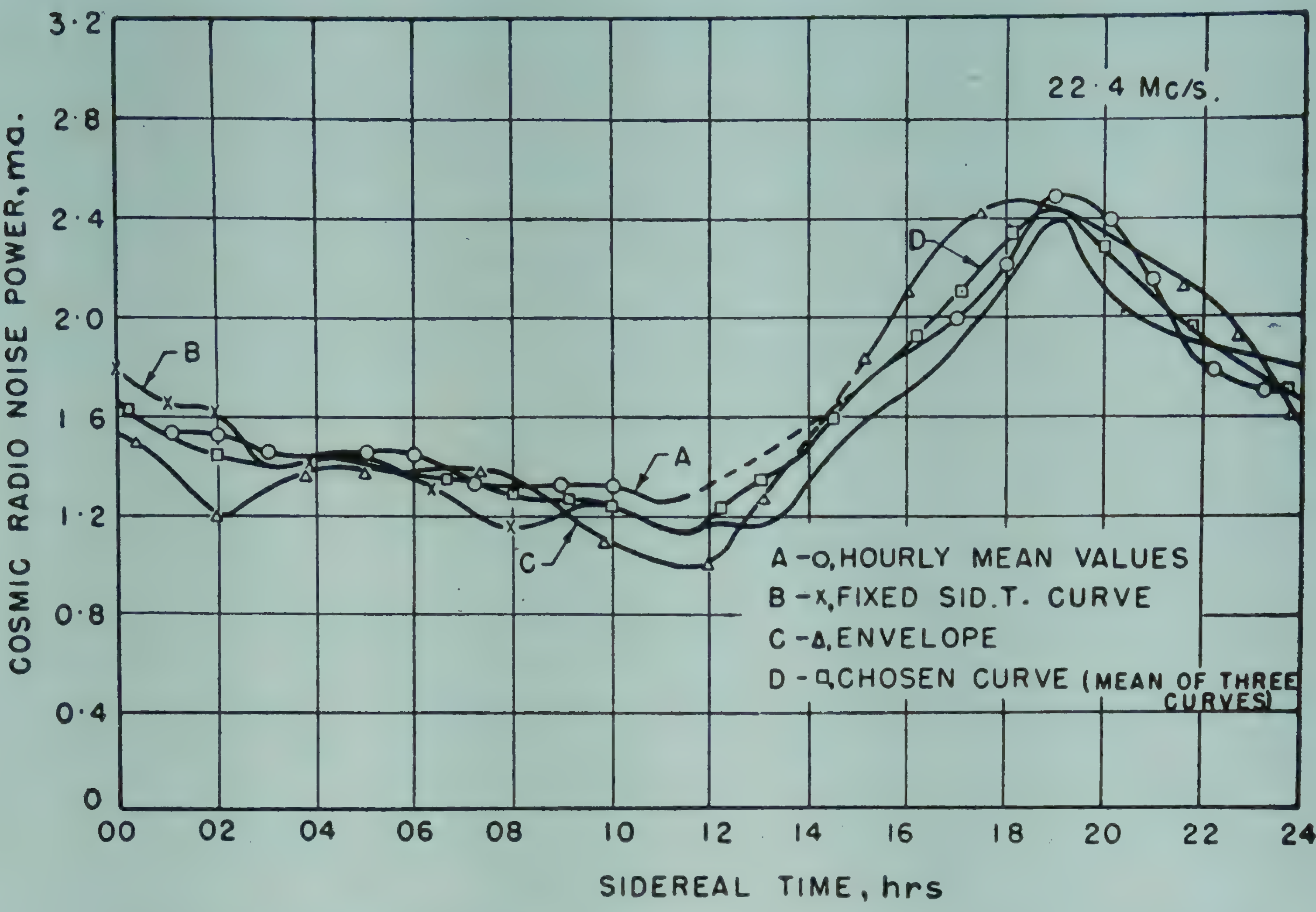

FIG. 1 — VARIATION OF UNATTENUATED COSMIC RADIO NOISE POWER WITH SIDEREAL TIME FOR DIFFERENT METHODS

the latter were obtained at a lower frequency (18·3 Mc/s.). Near noon the average absorption exceeded 4 db. for all the seasons, and it was not unusual to encounter individual values exceeding 6 db. on days otherwise normal. Similarly, large values have also been obtained at Ahmedabad[4].

(ii) As in the Hornsby observations, absorption during winter months was larger than during summer months. Noon-time values for the summer, equinox and winter months were 4·2, 4·8 and 5·3 db. respectively.

Region F Absorption. The total absorption measured is the sum total of the contributions from the ionospheric regions D, E, E_s, F_1 and F_2 (including the region above F_2 maximum). Of these, the contributions from regions D and F_2 are expected to be the most important.

The F region contribution depends principally on the value of f_0F_2 (Fig. 4). For $f_0F_2 < 6$ Mc/s., the contribution is not measurable with the present equipment. With increasing values of f_0F_2, the contribution becomes progressively larger.

It is possible to separate the actual magnitudes of the F_2 region contribution following a procedure originally introduced by Mitra and Shain[1]. Such a separation yields the F region absorption curve as given in Fig. 5.

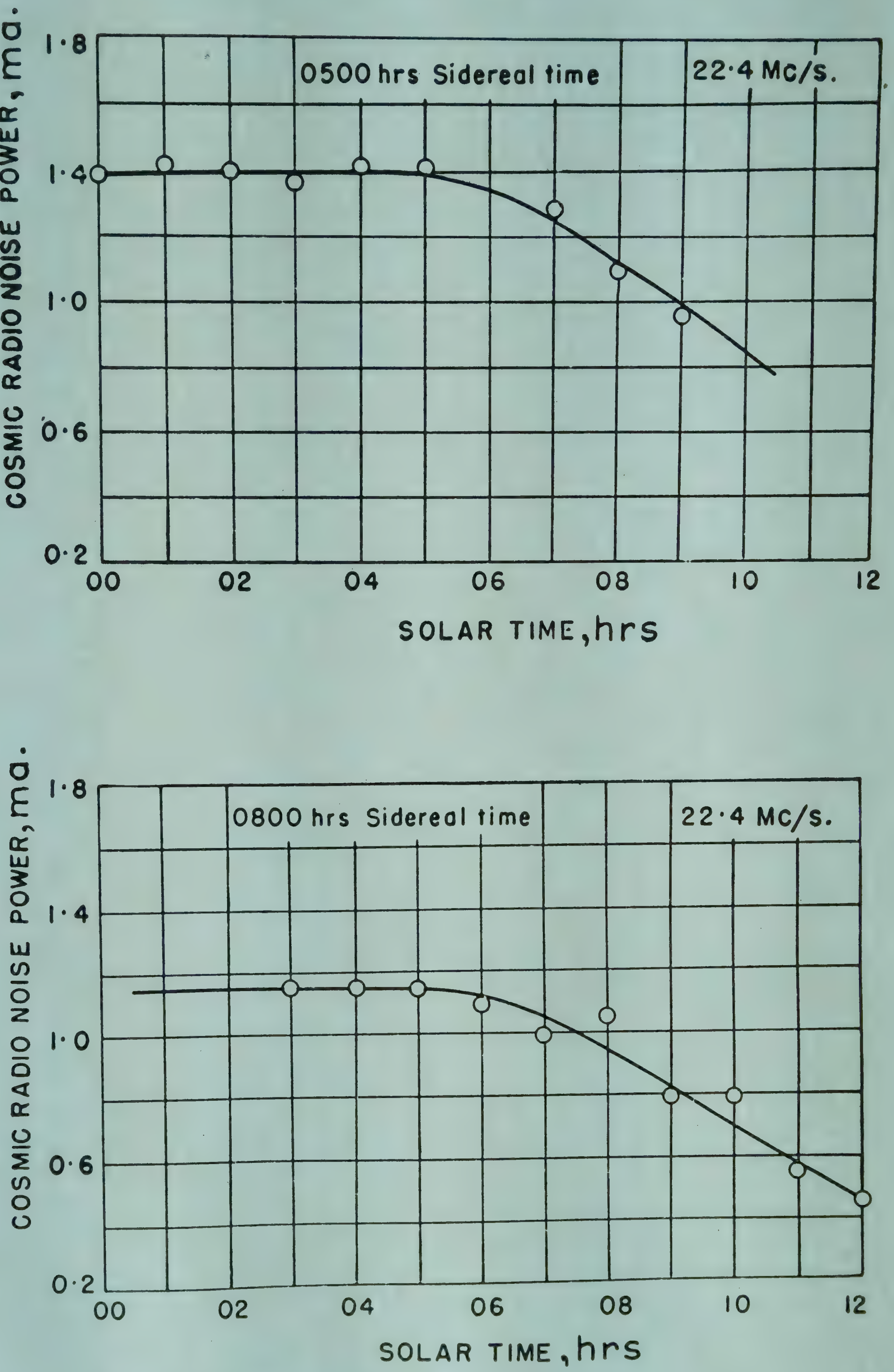

Fig. 2 — Variation of cosmic noise power with solar time for fixed sidereal hours

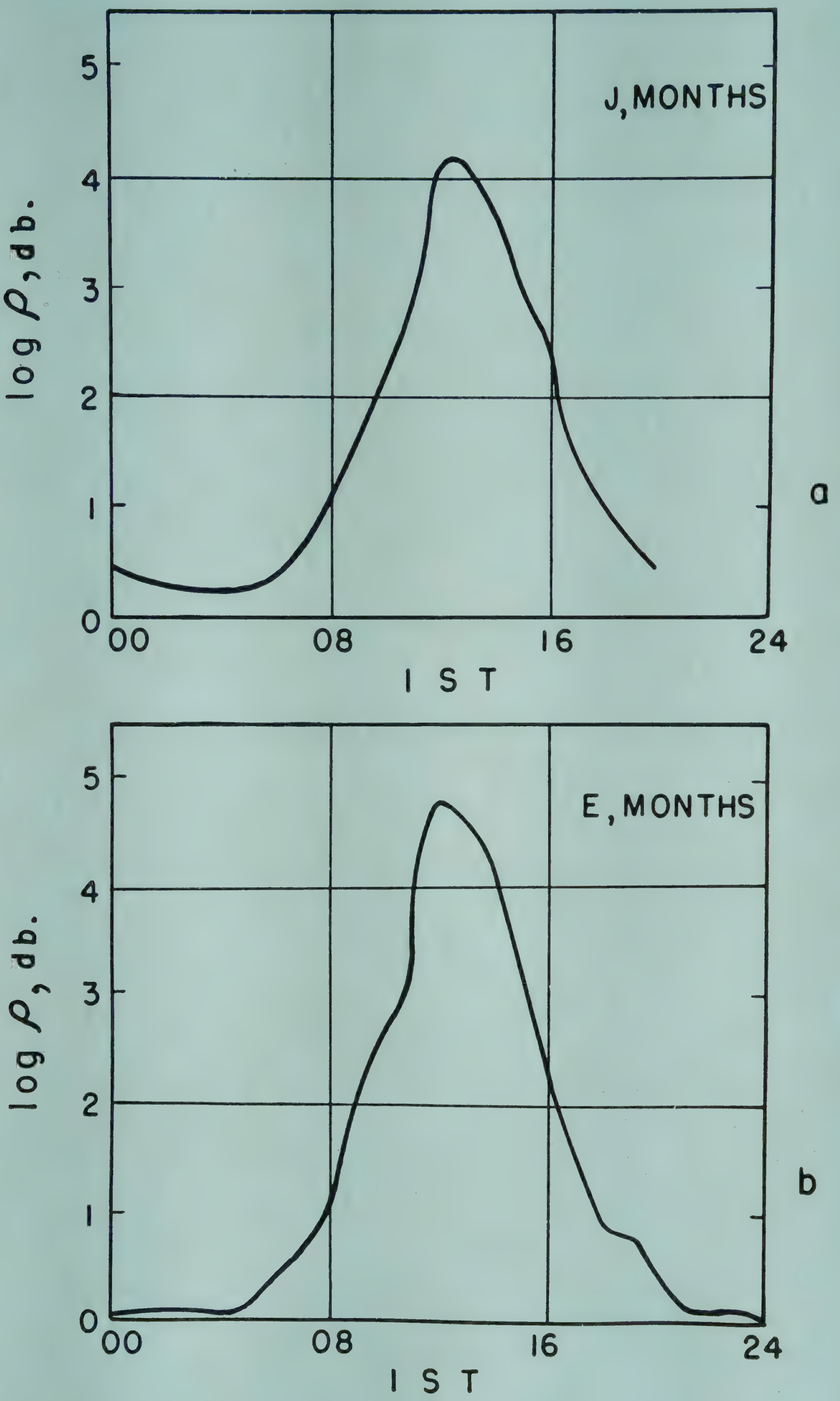

FIG. 3 — (a) DIURNAL VARIATION OF ABSORPTION FOR NORTHERN SOLSTICE MONTHS; (b) DIURNAL VARIATION OF ABSORPTION FOR EQUINOXIAL MONTHS

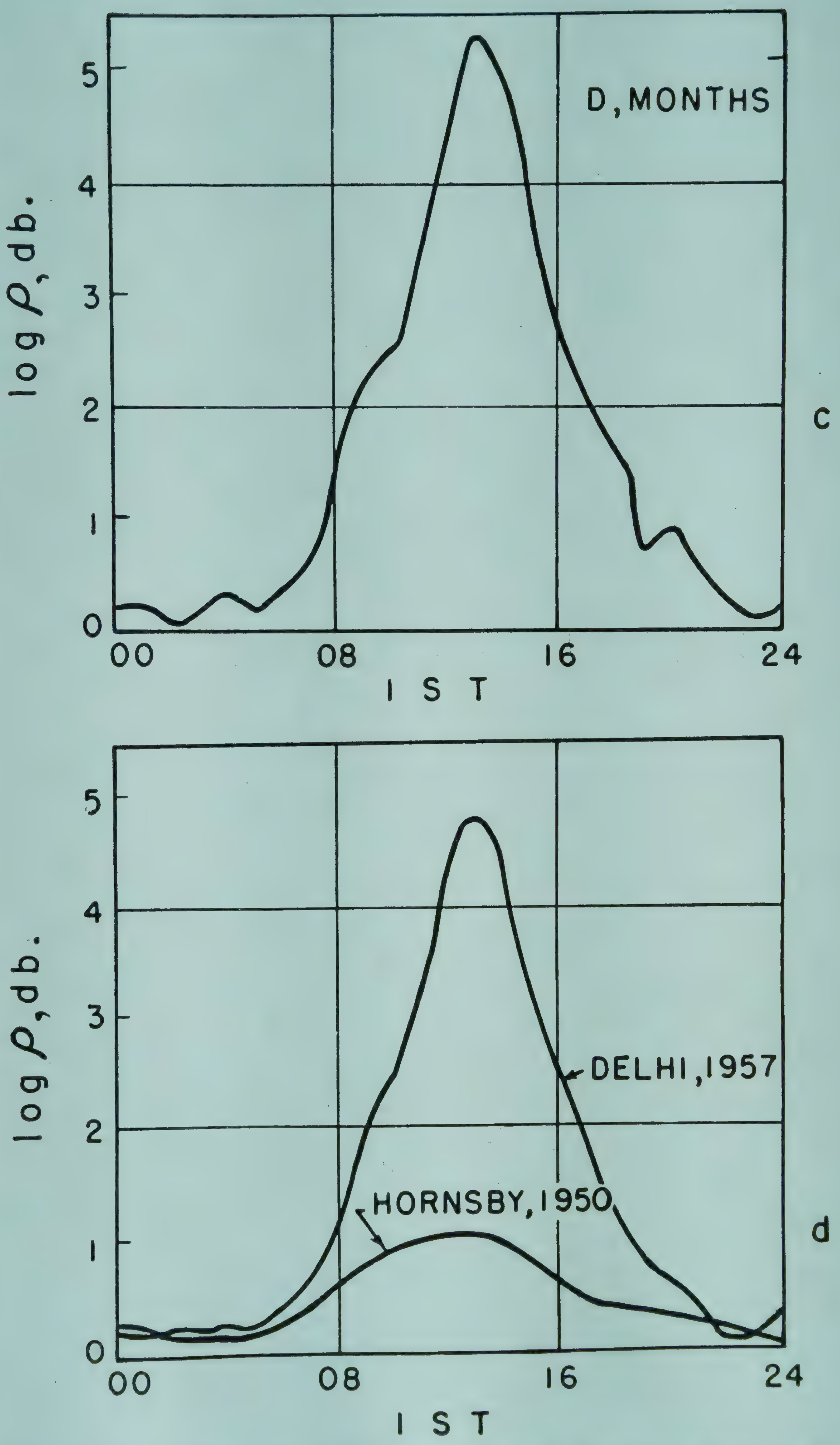

Fig. 3 — (c) Diurnal variation of absorption for southern solstice months; (d) diurnal variation of absorption for Delhi and Hornsby

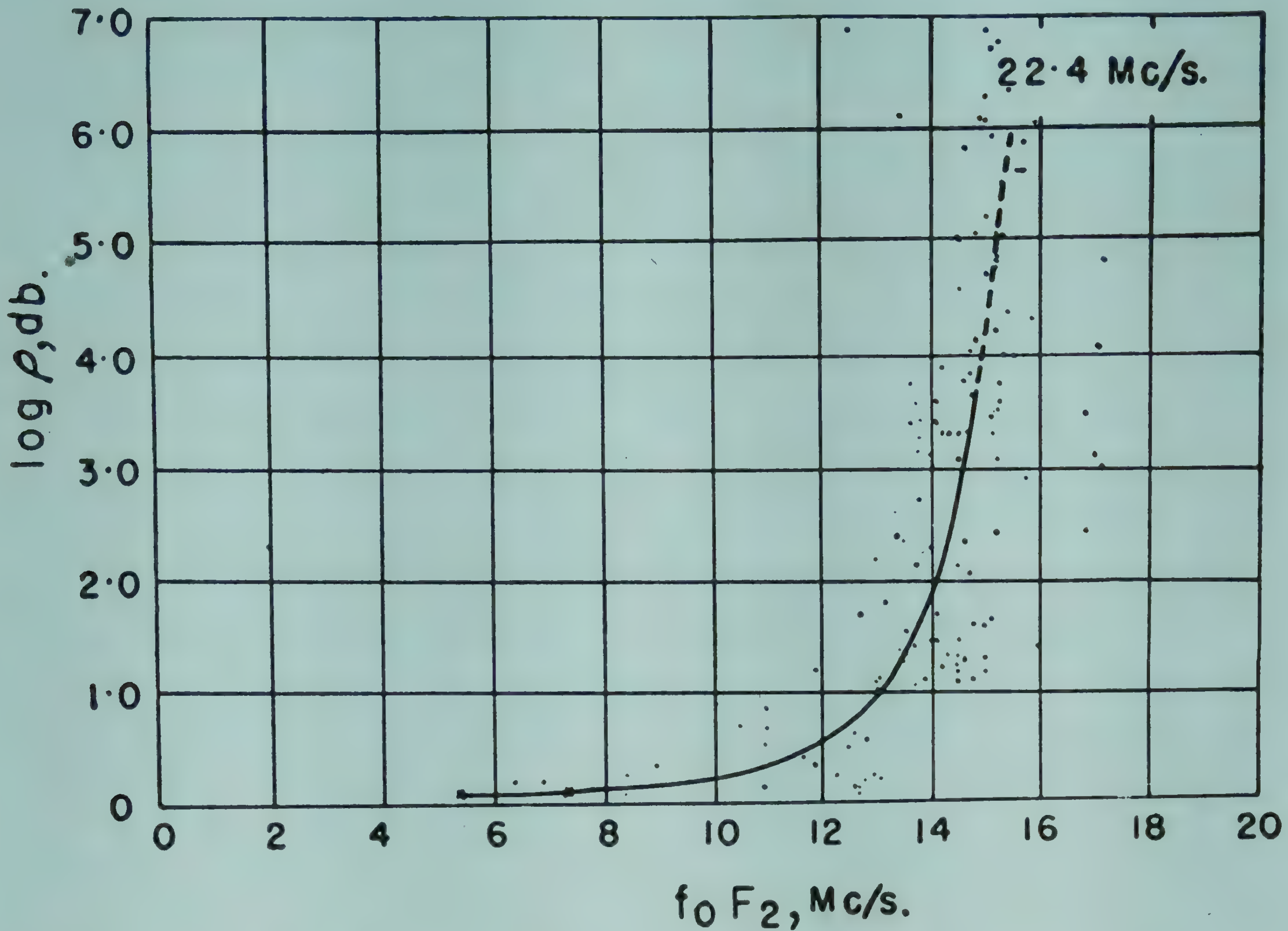

FIG. 4 — SCATTER DIAGRAM SHOWING THE INCREASE IN TOTAL ABSORPTION WITH f_0F_2

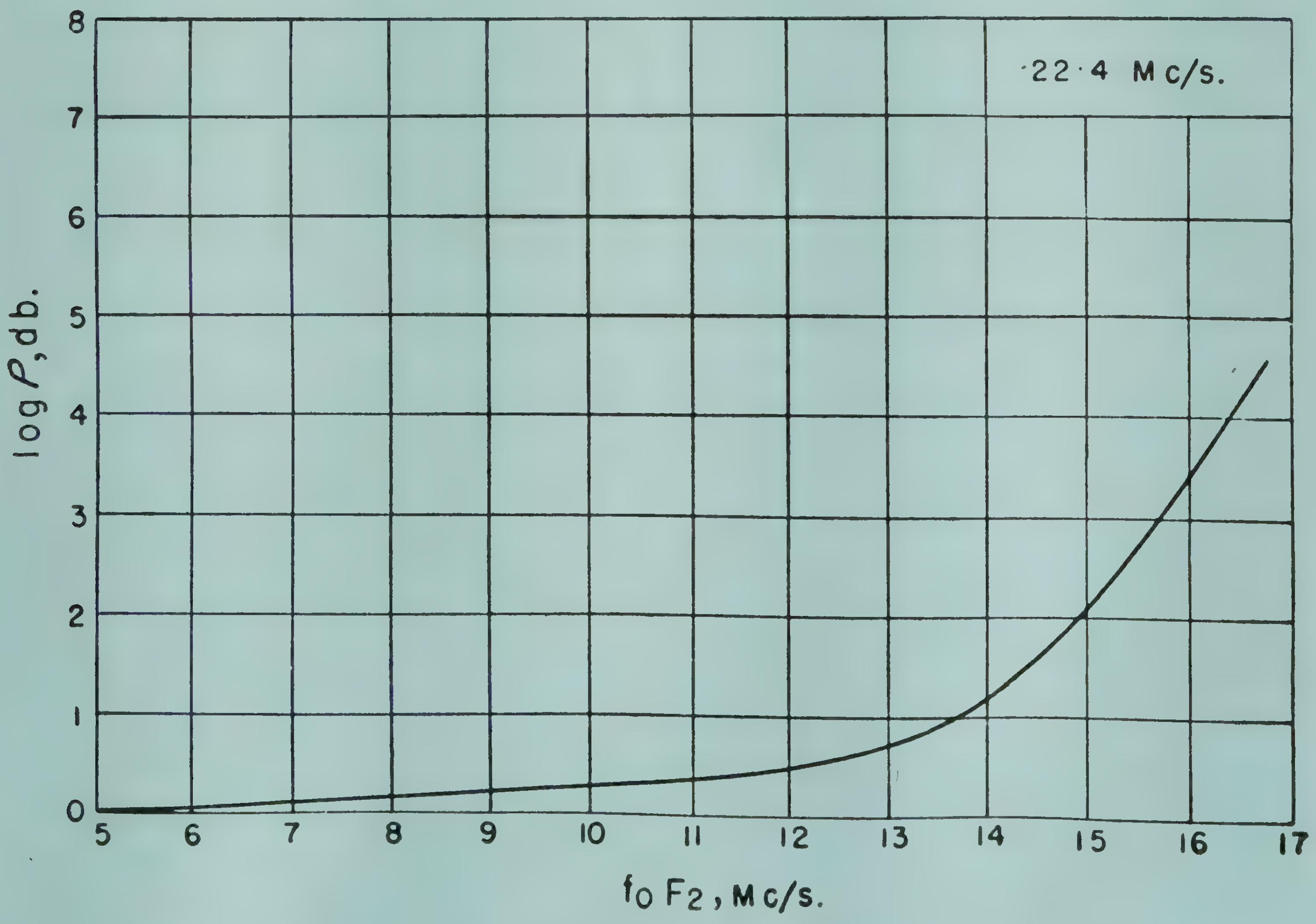

Fig. 5 — VARIATION OF ABSORPTION DUE TO REGION F WITH f_0F_2

It will be noted that the steep rise of F_2 absorption with f_0F_2 that was observed by Mitra and Shain for Hornsby observations continues for the higher values of f_0F_2. Similar results have been obtained by Bhonsle and Ramanathan[4] at 25 Mc/s., and by Warwick[5] for Boulder.

Mitra and Shain in their analysis of the Hornsby observations of cosmic radio noise have shown that the observed attenuation is practically independent of the F region height parameters $h'F_2$ or hpF_2, and that, for all practical purposes, one may consider the F region contribution to be dependent on f_0F_2 alone. Similar analysis with the authors' records have confirmed this conclusion; no appreciable variation of absorption was found to occur with changes in $h'F_2$ or hpF_2. These results would appear to indicate that either the effective collision frequency does not change much with height around the height of maximum ionization, as would indeed be the case if collisions at these levels are between electrons and ions or, because of a combination of circumstances, the product, which determines absorption at these heights, has little variation with height.

Absorption due to the Lower Ionosphere. As mentioned in the above section, the component of absorption which is independent of f_0F_2 is likely to be due to the lower ionosphere, comprising regions D and E. Of these, the E region contribution is expected to be small, so that the constant portion may be attributed predominantly to the D region. The relative contributions of the D and F_2 regions for the winter months, November and December 1957, are shown in Fig. 6. The D region absorption is approximately symmetrical about noon, and has a very large seasonal variation. The noon-time values for the summer, equinox and winter seasons are 3·4, 2·6 and 2·5 db. respectively.

It will be noted that the noon-time value is greatest in summer and least in winter, or in other words, the winter anomaly is absent.

Variation of D Region Absorption with cos χ. The nature of variation of the D region absorption with cos χ has been determined. An example is given in Fig. 7. It is found that the value of the cos χ exponent, n, ranges from 0·62 to 1·27, with an average of about 1·0. The morning values are slightly greater than the afternoon values, and the summer values are larger than the winter values. These values are compared with those obtained by others in Table 1.

While early determinations[6,7] gave values around 3/2, current values[8–15] tend to be around 3/4 for terrestrial techniques and around 1 for measurements involving cosmic noise[1,3,4]. There is thus some indication that the values obtained from cosmic noise observations are somewhat greater than those obtained by the terrestrial methods. The cosmic noise observations further show a progressive decrease of the value of n from summer to winter.

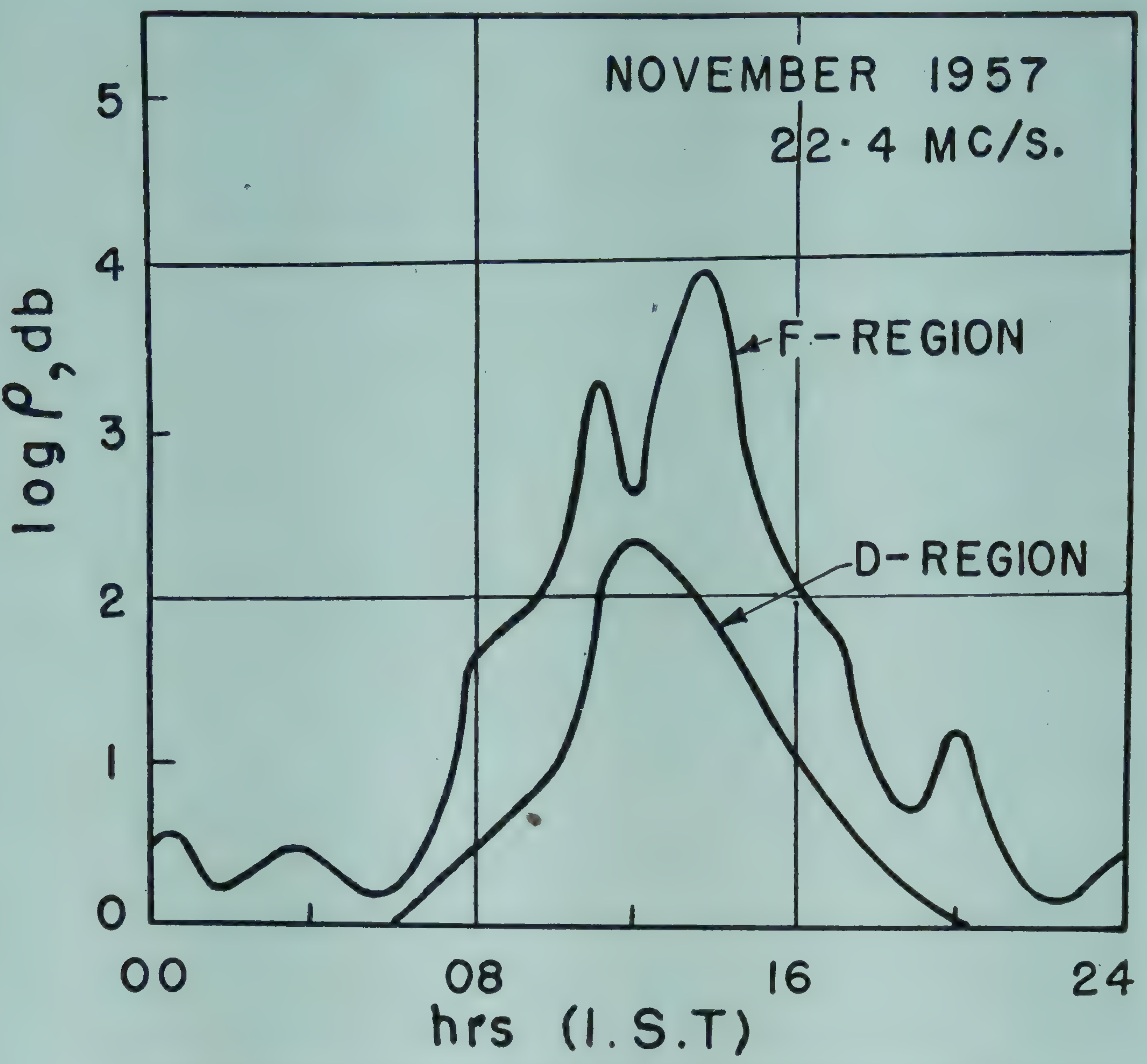

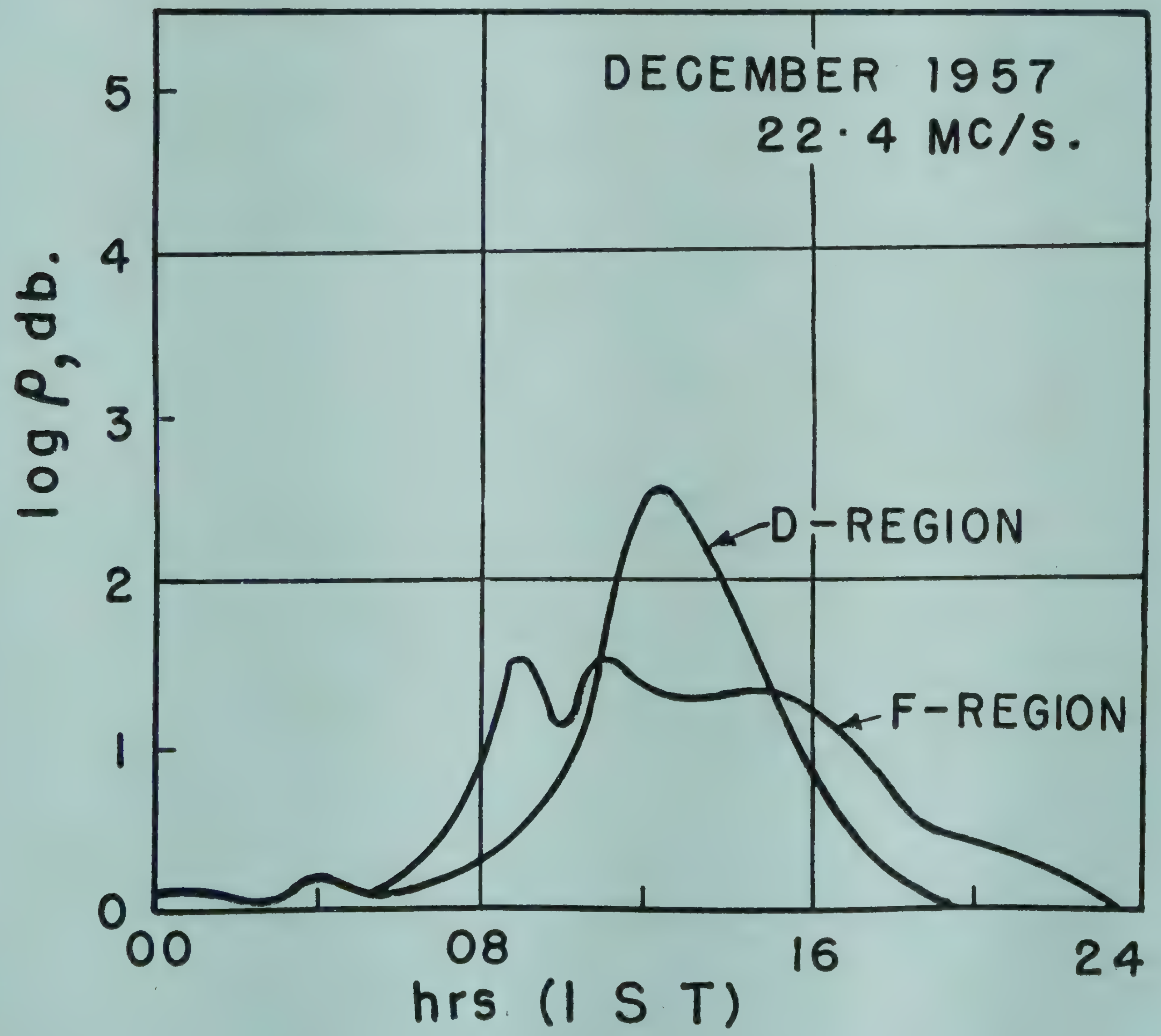

FIG. 6 — DIURNAL VARIATION OF D REGION ABSORPTION AND F_2 REGION ABSORPTION FOR DIFFERENT MONTHS

TABLE 1 — VALUES OF THE COS χ EXPONENT (n) OBTAINED BY DIFFERENT WORKERS FROM DIFFERENT TYPES OF ABSORPTION MEASUREMENTS

TYPE OF OBSERVATION	AUTHOR(S)	FREQUENCY Mc/s.	INDEX n	REMARKS
Terrestrial techniques	Best & Ratcliffe[6]	3·2–4·2	1·5	
	White & Straker[7]	5·6–7·5	1·76	
	Taylor[8]	2·0	0·87	
	Taylor[8]	4·3	1·07	
	Benner[9]	0·14	0·65	
	Bracewell *et al.*[10]	0·016	0·0	
	Appleton & Piggott[11]	1·6–5·5	0·75	
	Beynon & Davies[12]	2·0	0·82	
	Davies & Hagg[13]		0·5	
	Mitra & Mazumdar[14]	2·5, 5	0·62	
	Pillet[15]	3·4	0·8	
Cosmic radio noise	Mitra & Shain[1]	18·3	1·1	Summer
			0·9	Equinox
			0·5	Winter
	Bhonsle & Ramanathan[4]	25·0	1·1	Summer
			1·0	Equinox
			0·8	Winter
	Sarada & Mitra	22·4	1·1	Summer
			1·1	Equinox
			0·8	Winter

It may be recalled here that n is 3/2 in the simple theory[16] in which (i) $\nu^2<<(f+f_L)^2$, (ii) the absorbing layer is formed in an isothermal atmosphere of uniform composition, and (iii) the electronic recombination is independent of height.

The discrepancy between the value of 3/2 predicted by the simple theory and the observational values indicates that in the actual case the assumptions of the simple theory are not valid. Appleton and Piggott[11] have indicated the consequences of removing some of these assumptions. The removal of the condition $\nu^2<<(f+f_L)^2$, for example, shows that the value that n assumes depends greatly on the location of the absorbing layer. At the levels where $\nu^2<<(\omega+\omega_L)^2$, the exponent n will have a value of 3/2. At lower levels n rapidly decreases.

The picture is somewhat altered if the assumption of a constant recombination coefficient is also removed[11]. If the recombination coefficient is assumed to vary directly with pressure, then, even at levels where $\nu^2<<(\omega+\omega_L)^2$, l$n$ is 1, and at lower levels, it decreases again rapidly.

It has been earlier pointed out that there is some indication that the cosmic noise method yields a somewhat larger value of n than the pulse method.

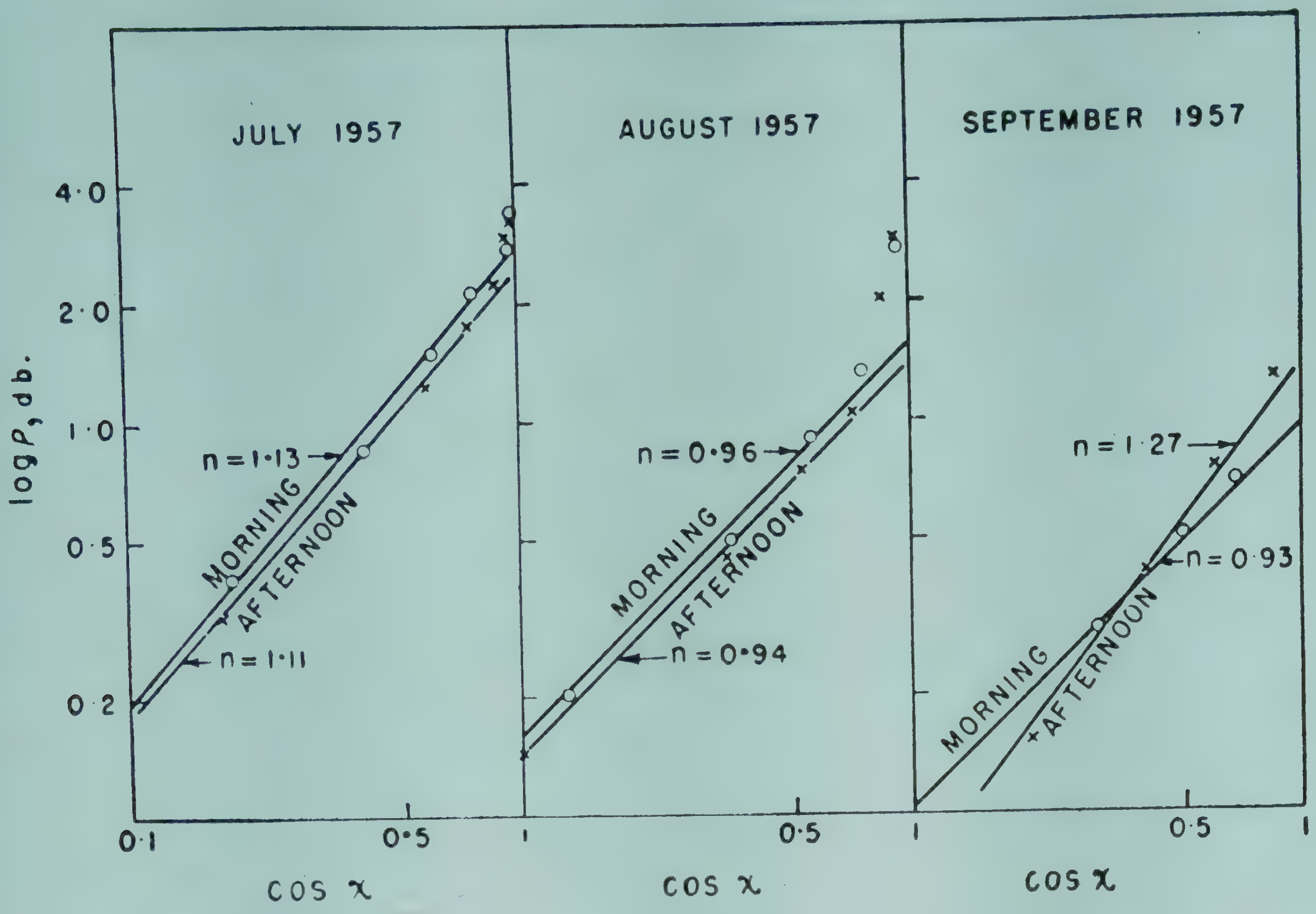

FIG. 7 — VARIATION OF D REGION ABSORPTION WITH cos χ FOR DIFFERENT MONTHS

This is expected to be the case, since the absorption attributed to region D in this method must also contain some absorption from region E, and the effective height of this combined absorption is, therefore, likely to be higher than that of the pulse method.

Variation of D Region Absorption with Frequency. The theory of ionospheric absorption indicates that absorption for a non-deviative region will vary as

$$[\nu^2+(\omega\pm\omega_L)^2]^{-1} \tag{1}$$

If, however, the absorbing layer is located at levels where $\nu^2 << (\omega+\omega_L)^2$, the frequency relationship becomes

$$\log \rho = \frac{A}{(f+f_L)^2} \tag{2}$$

where A is a constant for any set of conditions. Equation (2) may also be written as

$$\frac{1}{\sqrt{\log \rho}} = \frac{1}{\sqrt{A}}\,(f+f_L)^2 \tag{3}$$

Detailed analysis of absorption measurements obtained by the terrestrial techniques by a number of workers, and especially by Appleton and Piggott[11], have shown that for non-deviative absorption, the straight line relationship indicated by Equation (3) is obeyed. This relationship naturally breaks down if the operating frequency is near the critical frequency of any ionospheric layer, in which case the observed absorption includes an appreciable amount of deviative absorption. Appleton and Piggott further state that this inverse frequency relationship was obeyed on 30 per cent of the days on which multi-frequency measurements were made, the remaining days showed irregular variations which were mainly due to abnormal deviative absorption or scattering.

While the inverse frequency relationship appears to be generally obeyed, certain important anomalies have been observed. First, a certain number of stations during the IGY have found that with an equation of the type (2), one always obtained very high A-values on the higher frequency side and lower values for the lower frequencies, so that the median value of A depended on the set of frequencies used. Secondly, Skinner and Wright[16] reported that at the equatorial station, Ibadan (7°26′N: 3°54′E, mag. lat. 2·5°S), the experimental results were more consistent with an inverse frequency law rather than an inverse square law, except for frequencies very close to penetration. Thus at this station,

$$\log \rho \propto \frac{1}{(f+f_L)} \tag{4}$$

In view of the importance of the above results, and the somewhat surprising results of Skinner and Wright[16] for the equatorial station, it was considered desirable to investigate the frequency relationship of absorption at Delhi at some length. For this purpose, the cosmic radio noise observations reported in this work were combined with the observations made by the A.I.R., Delhi, using the pulse technique at frequencies of 5 and 7 Mc/s. Observations were also available from Ahmedabad at 25 Mc/s. (cosmic radio noise) and 2·5 Mc/s. (pulse technique). While, strictly speaking, such observations should not be combined with observations at Delhi, these were also used. Figs. 8 and 9 show plots of $1/\sqrt{\log \rho}$ against $(f+f_L)$ for these observations. It will be observed that the Delhi observations are quite consistent with the inverse frequency square law for all the cases investigated. Observations for Ahmedabad at 2·5 Mc/s. also fit with the curve, although the cosmic noise observations at 25 Mc/s. for this station consistently fall below it. A few estimates of the value of gyrofrequency made from the intercept in the frequency axis give results in consonance with the known values.

Sluggishness of the D Region. It has been observed that the maximum of many ionospheric parameters does not normally coincide with the time of local noon: the difference in time (τ), usually known as the relaxation time, varies with height, latitude, etc. The physical significance of τ is

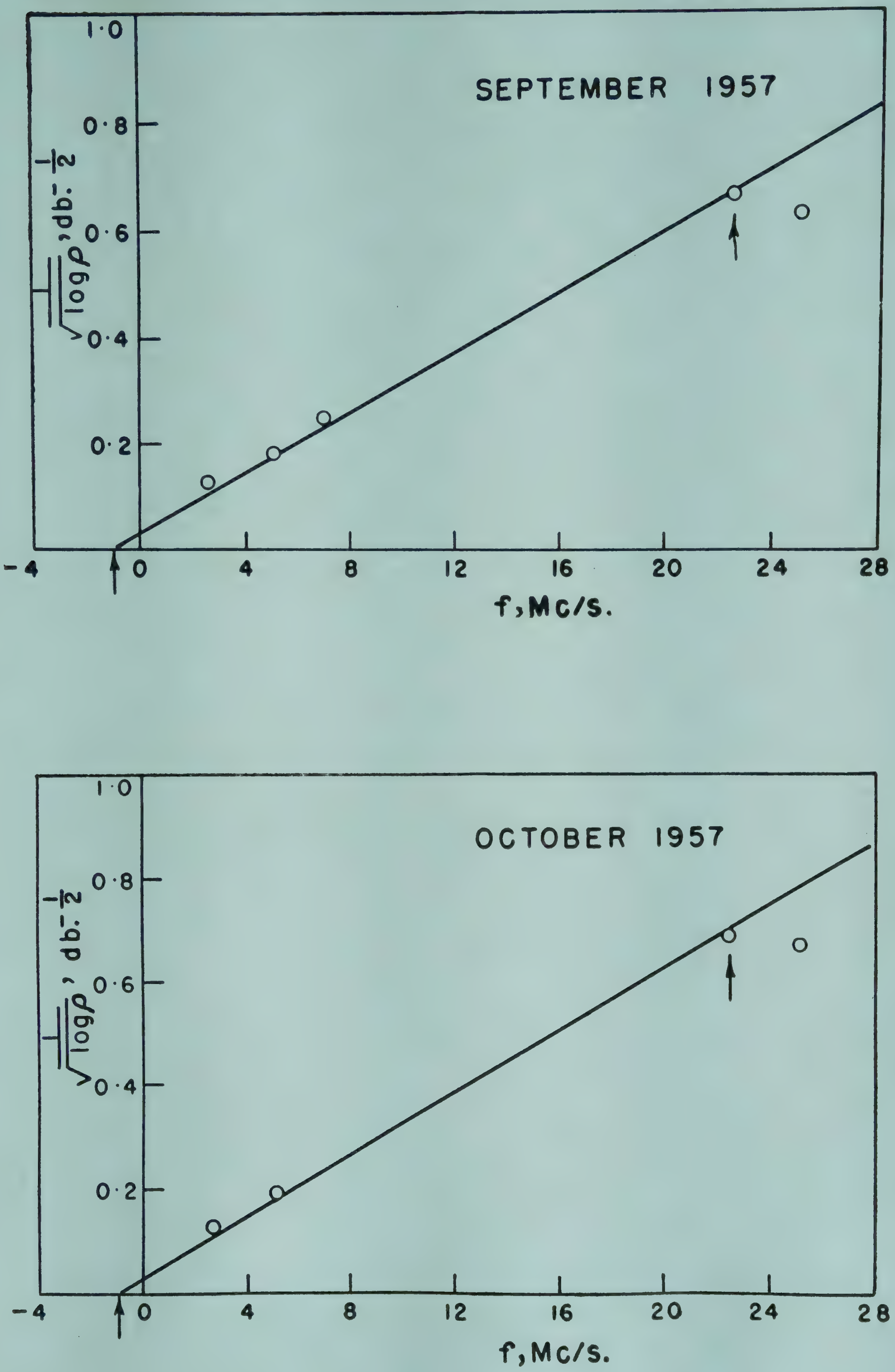

FIG. 8 — VARIATION OF D REGION ABSORPTION WITH THE FREQUENCY

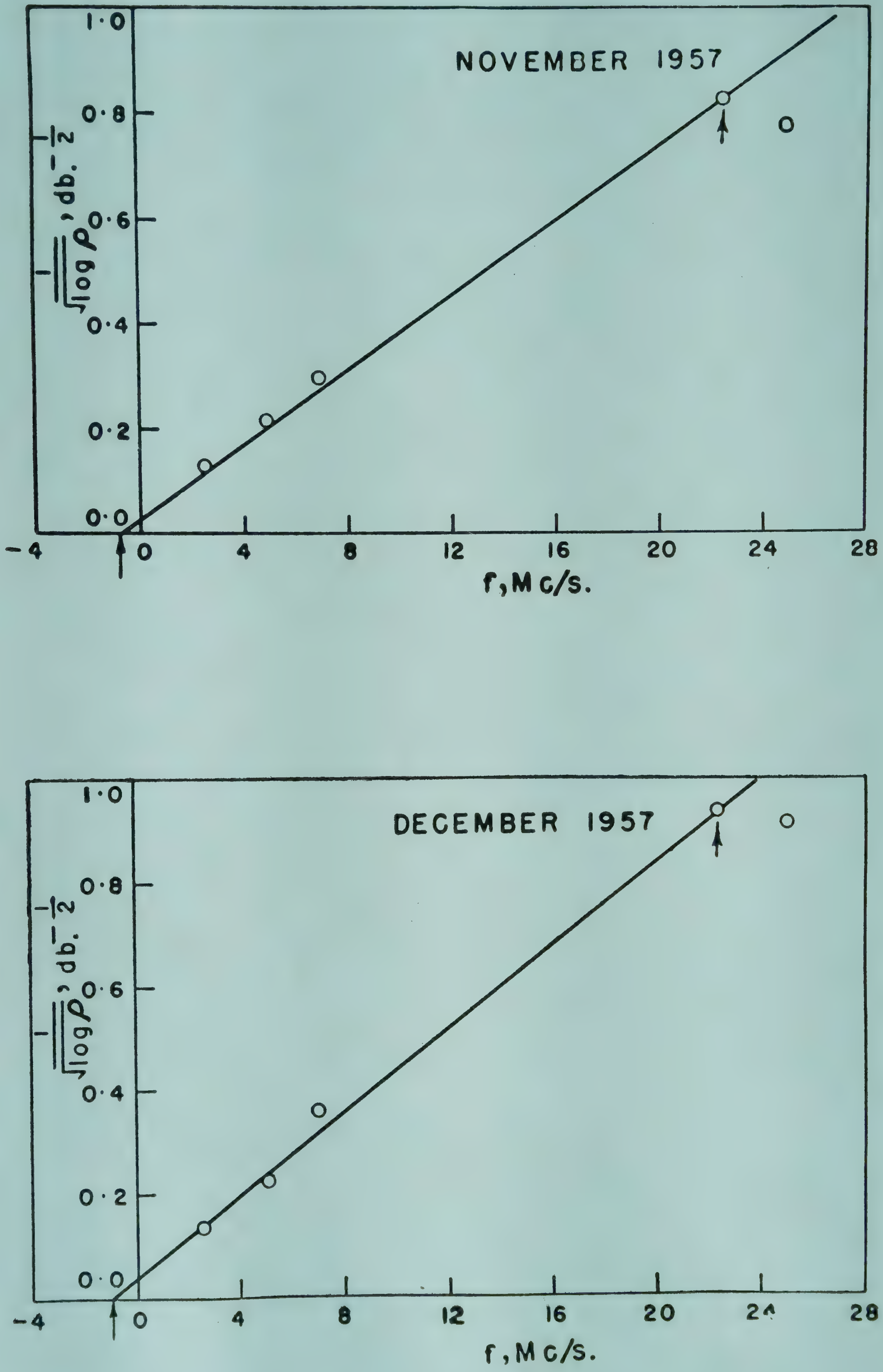

FIG. 9 — VARIATION OF D REGION ABSORPTION WITH THE FREQUENCY

provided by its relationship with the loss coefficient K and the electron density N by the expression

$$\tau = \frac{1}{[nKN^{n-1}]}$$

Estimates of the relaxation time are often obtained visually or by the constant ordinate method in which the times for the same value of N are noted. If the variation is truly parabolic, then τ is given by

$$T = \frac{|t_2| - |t_1|}{2}$$

A more accurate method, due to Aitkin, and described by Appleton and Lyon[17], is to use a five- or seven-point grid system, centred at noon, and to determine the best fitting parabola through these points.

Hence the Appleton-Lyon-Aitkin procedure to determine the relaxation time for the D region, using monthly average values of cosmic radio noise absorption attributed to region D has been used. For the period July to December 1957, the value of τ varied from 24 to 45 min. with an average of about 33 min. No systematic variation with season was observed.

It is of interest to compare this value with those obtained by other workers from absorption obtained either by the terrestrial technique using pulses or by the cosmic radio noise method. These values are summarized in Table 2.

It will be noted that the values determined by the various authors range within 20–40 min. approximately, and an average value of 30 min. is indicated.

It is not quite clear how much credence one may put on these estimates. While, on the average, the maximum is delayed by an amount given above,

TABLE 2 — RELAXATION TIMES FROM ABSORPTION DATA

METHOD	τ *min.*	EXPERIMENTAL DATA	AUTHOR(S)
Terrestrial technique	20	150 kc/s. absorption	Mitra[18]
	23	Shortwave absorption	Appleton & Piggott[11]
	45	Shortwave absorption	Mitra & Mazumdar[14]
Cosmic radio noise	27	18·3 Mc/s. absorption at Hornsby	Mitra & Shain[1]
	28	25 Mc/s. absorption at Ahmedabad	Bhonsle & Ramanathan[4]
	33	22·4 Mc/s. absorption at Delhi	Sarada & Mitra

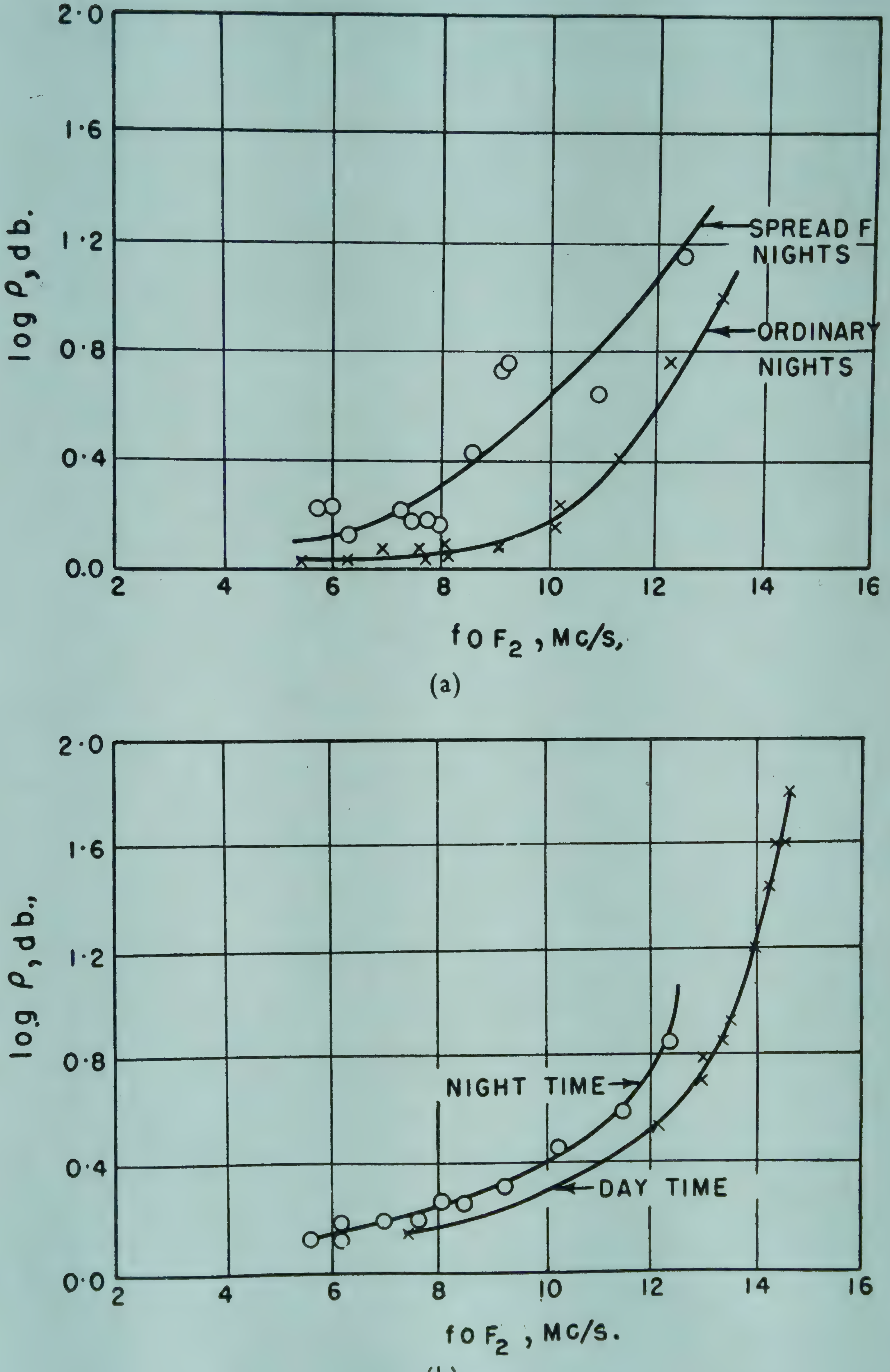

(a)

(b)

Fig. 10 — Diagrams showing additional absorption at night

individual cases in which the maximum occurs before noon are occasionally encountered. Such cases, however, are not frequent.

Night-time Absorption. It was noted that, for the same value of f_0F_2, the night-time absorption was often greater than the day-time value — a result in consonance with earlier observations of Mitra and Shain[1]. To examine the difference, values of log ρ were plotted against f_0F_2 separately for day and night. From the resulting curves shown in Fig. 10(b) it can be seen that the night curve is consistently above the day curve, indicating that at night an additional source of absorption exists. In the earlier work of Mitra and Shain[1], the slightly larger value of the night-time absorption was attributed to the occurrence of irregular clouds of ionization at night. To examine this possibility, the nights on which spread F occurred were distinguished from the nights for which spread F was absent. Variation of log ρ with f_0F_2 for these two types of nights are substantially different [Fig. 10(a)], absorption during the spread F nights being appreciably and consistently larger. It has, therefore, been concluded that the excess night-time absorption is caused by the same mechanism that causes spread F.

DISCUSSION

From the results given above, the following conclusions may be made:

(i) Absorption of extraterrestrial radio noise occurs principally in two regions of the ionosphere, one in the D region and another in the F region. The F region contribution is normally negligible for low values of f_0F_2, but is appreciable if f_0F_2 values are large.

(ii) The absorption occurring in the F region depends principally on the value of f_0F_2 and is apparently unaffected by the variation in the height of the layer.

(iii) The absorption occurring in region D varies with the solar zenith angle according to the law, log $\rho \propto \cos \chi$.

(iv) Relaxation time is around 30 min. at the height at which D region absorption is located.

(v) In general, the D region absorption varies with frequency according to an inverse square law.

(vi) The night-time F region absorption is larger than the corresponding day-time value. This excess absorption is associated with the occurrence of spread F at night.

A problem of some importance is the determination of the level of the D region absorption. In determining this, we make use of the following results: (i) the nature of variation of absorption with frequency and (ii) the value of the D region relaxation time.

Of these, the frequency criterion is somewhat critical. The validity of the inverse square law requires that at the level of absorption $\nu^2 << (\omega + \omega_L)^2$ with $f = 2{\cdot}5$ Mc/s. and $f_L = 1$ Mc/s., the criterion is $\nu << 3{\cdot}5 \times 10^6$/sec. With Nicolet's model of collision frequency[19] this requires that the absorbing layer should be located above 80 km.

We now consider the result concerning the D region relaxation time. Since the relaxation time is a function of height, the result may be used to obtain an estimate for the location of the absorbing layer, provided a reliable τ-h curve is available. Such a curve has recently been given by Mitra[18] on the basis of a detailed examination of the diurnal asymmetry of several experimental parameters from certain considerations of the ionospheric loss coefficient. A comparison with this curve shows that a relaxation time of 30 min. corresponds to heights around 85–95 km. Thus both the criteria give consistent results, indicating a level of about 90 km. for the absorbing layer. It is also the level of D region maximum.

ACKNOWLEDGEMENT

The authors wish to thank Shri R. Parthasarthy for his help during the phase of the design and installation of the equipment, and Shri C. V. Subramaniyam and Miss S. Aggarwal for help in the preparation of the paper.

REFERENCES

1. MITRA, A. P. & SHAIN, C. A., *J. atmos. terr. Phys.*, **4** (1953), 204.
2. SHAIN, C. A. & MITRA, A. P., *J. atmos. terr. Phys.*, **5** (1954), 116.
3. SARADA, K. A. & MITRA, A. P., *Some Ionospheric Results obtained during the International Geophysical Year* (Elsevier Publishing Co.), 1960, 270.
4. BHONSLE, R. V. & RAMANATHAN, K. R., *J. sci. industr. Res.*, **17A** (1956), 40.
5. WARWICK, J. W., *Science*, **127** (1958), 3305.
6. BEST, J. E. & RATCLIFFE, J. A., *Proc. phys. Soc. Lond.*, **50** (1938), 233.
7. WHITE, F. W. G. & STRAKER, T. W., *Proc. phys. Soc. Lond.*, **51** (1939), 865.
8. TAYLOR, E., *J. Res. nat. Bur. Stand.*, **41** (1948), 575.
9. BENNER, A. H., *Proc. Inst. Radio Engrs, N.Y.*, **39** (1951), 186.
10. BRACEWELL, R. N. *et al.*, *Proc. Instn elect. Engrs*, **98**, Pt III (1951), 221.
11. APPLETON, E. V. & PIGGOTT, W. R., *J. atmos. terr. Phys.*, **3** (1954), 141.
12. BEYNON, W. J. G. & DAVIES, K., *The Physics of the Ionosphere* (Physical Society), 1955, 40.
13. DAVIES, K. & HAGG, E. L., *J. atmos. terr. Phys.*, **6** (1955), 18.
14. MITRA, S. N. & MAZUMDAR, S. C., *J. atmos. terr. Phys.*, **10** (1957), 32.
15. PILLET, G., *Contribution à l'étude de l'absorption ionosphérique sur unefréquence fixe*, D.Sc. Thesis, University of Paris, 1960.
16. SKINNER, J. J. & WRIGHT, R. W., *J. atmos. terr. Phys.*, **9** (1956), 103.
17. APPLETON, E. V. & LYON, A. J., *J. atmos. terr. Phys.*, **10** (1957), 1.
18. MITRA, A. P., *The Pennsylvania State University, Ionosph. Res. Sci., Rep.* No. 119, April 1959.
19. NICOLET, M., *The Pennsylvania State University, Ionosph. Res. Sci., Rep.* No. 102, April 1958.

Ionospheric absorption using cosmic radio noise on 25 Mc/s. at Ahmedabad

R. V. BHONSLE

Physical Research Laboratory
Ahmedabad

The paper discusses the observations of ionospheric absorption using cosmic radio noise on 25 Mc/s. made at Ahmedabad during the period March 1957 to December 1959. The recording equipment used for measuring the intensity of the cosmic noise is briefly described. The total ionospheric attenuation is divided into three components: (i) a day-time symmetrical component depending on the solar zenith distance; (ii) a non-symmetrical component, which is a function of f_0F_2; and (iii) a late evening component apparently depending on F scatter associated with dispersal of high electron densities in F_2 region. The diurnal and seasonal variations of (i) and (ii) are discussed. Much larger attenuations than those recorded at other places have been observed at Ahmedabad in this period of high solar activity.

The most commonly used method for studying the structure and morphology of the ionosphere is by vertical soundings with pulsed transmissions of radio waves of varying frequencies. Another valuable method which is particularly useful for the study of ionospheric attenuation and scattering of radio waves is by measuring the variations of intensity of radio noise from the galaxy. This method has not received much attention in low latitudes.

Since the cosmic radio waves have to pass through the whole ionosphere, including the part above the level of maximum electron density of the F_2 layer, the method is a good supplement to the usual technique of studying the ionosphere by echo sounding.

In one of the earliest observations of cosmic radio noise on 20 Mc/s., Jansky[1] noticed that during day-time, the intensity of cosmic radio noise was lower than that during night and he attributed this to ionospheric absorption. In 1949, Shain[2] observed that the intensity of cosmic noise on 18·3 Mc/s. from any part of the sky was comparatively high when the critical frequency of the F_2 region at the time was less than 9 Mc/s. Mitra and Shain[3] made a detailed study of ionospheric absorption on 18·3 Mc/s. at Hornsby in Australia. They showed that the total attenuation could be divided into two components: (i) a symmetrical day-time effect with maximum at about noon which they attributed to absorption mainly in the D region, and (ii) an absorption in the F_2 region. The D region absorption showed diurnal and seasonal variations similar to those observed by other methods. The F_2 absorption depended on the critical frequency of F_2 but not on the height of base of the F_2 layer. They noticed an excess of night-time F_2 attenuation over day-time attenuation for the same value of the critical frequency of the F_2 region and attributed it to the scattering of radio waves by the irregularities in the electron distribution in the F_2 region.

Blum and others[4] working on 29·5 Mc/s. at Marcoussis found that the absorption varied linearly with f_0F_2, while according to Mitra and Shain, a curvilinear relation held good.

Warwick and Zirin[5] analysed the diurnal variation of cosmic noise on 18 Mc/s. at Colorado. Their absorption data did not allow them to separate the D region absorption from the absorption produced by the other layers of the ionosphere. Therefore, they used the absorption recordings to study the electron density of the D layer as a function of the local time and height of the D region, and derived the vertical distribution of the ionizable constituent, which was supposed to be nitric oxide.

In high latitudes, Little and Leinbach[6] in Alaska have been working on 65 and 30 Mc/s. and later on 27·6 Mc/s. Their work is mainly concerned with polar blackouts associated with geomagnetic storms and visible aurorae. Using riometers on 27·6 Mc/s. they have discovered the interesting phenomenon called Pre-SC Polar Cap Blackout which is caused by low energy cosmic ray protons emitted by the sun at the time of some flares and reaches the polar regions of the earth well before the commencement of a magnetic storm.

In tropical latitudes, observations on ionospheric absorption have been made with conventional pulse techniques at Singapore, Ibadan and Delhi, but until quite recently, no systematic work has been done on extraterrestrial radio noise. The Physical Research Laboratory, Ahmedabad (23°02′N: 72°38′E), started ionospheric absorption measurements in 1956 using cosmic radio noise on 25 Mc/s. as an extraterrestrial source of radio waves. The cosmic noise records have proved very useful for studying various aspects of ionospheric physics. Among the problems studied are: (i) the diurnal and seasonal variations of total ionospheric attenuation, and its analysis into a day-time component and a component associated with the F layer; (ii) sudden ionospheric disturbances (SID) associated with solar flares; and

(iii) changes in the ionospheric attenuation during geomagnetically disturbed periods.

The present paper embodies the results of the study of the ionospheric attenuation and its time variation from cosmic noise recordings at Ahmedabad during the years 1957–59, a period of high solar activity. Some of the points that have emerged from these studies have already been published[7-11].

EQUIPMENT

The equipment consists of a directional aerial connected to a communications-type receiver whose output, after second detection, is fed to a d.c. amplifier. After d.c. amplification, the output is recorded on a 0–1 ma. recording milliammeter. The output of the receiver is calibrated manually every day against the noise generated in a pure tungsten filament noise diode. The filament and high tension supplies are stabilized electronically. A cold resistor of 100 Ω is automatically substituted for the aerial for a period of about 2 min. at intervals of 45 min. by means of DPDT relay actuated by a synchronous motor. With this arrangement it is possible to make corrections for the unavoidable changes in the noise level of the receiver. The same resistor is used to load the impedance of the diode noise generator. The directional aerial consists of 16 half-wave dipoles spread in E–W direction in 4 rows and 4 columns. The aerial is backed by a parallel wire reflecting screen stretched along the ground at a distance of 0·2 wavelengths from the dipole elements. The aerial is directed vertically upwards and has an angular beam-width to half power points of about 30° in E–W and 40° in N–S planes. The power gain of this array over an isotropic radiator is estimated to be about 17 db.

EXPERIMENTAL RESULTS

The directional aerial scans the same strip of the sky once in a sidereal day owing to the diurnal rotation of the earth about its axis and the intensity of cosmic noise picked up by the aerial depends, firstly, upon the sidereal time and secondly, upon the transparency of the ionosphere, which is a function of the local time, and of disturbances in the ionosphere. The method of calculating ionospheric attenuation by the cosmic noise technique has been described elsewhere[8].

Total Ionospheric Attenuation. The total ionospheric attenuation has been computed for each hour on all possible days in different months during the period March 1957 to December 1959. The analysis of the cosmic noise data from March 1957 to February 1958 has already been published[8]. This preliminary study showed that a minimum of total attenuation invariably occurred between midnight and sunrise and this was true for all seasons. The day-time maximum in the total attenuation was reached at about 1400 hours (local time), the maximum value being slightly different in different months as set out in Table 1. Thereafter, the total attenuation decreased till about 1800 hours. In December 1957 which was an exceptional month, the day-time peak occurred in the forenoon at about 1100 hours. After sunset, the total attenuation showed two distinct types of variation, in one case it continued to decrease throughout the night and in another, it showed a temporary rise to a maximum somewhere between 2000 and 2100 hours (local time) followed by a steady decrease in the rest of the night. The pre-midnight peak in the total attenuation was pronounced during winter and equinoctial months while no such peculiarity was observable in summer. The occurrence of this pre-midnight peak was thought to be in some way connected with F scatter. In a recent communication Ramanathan and Bhonsle[9] have drawn attention to the new evidence that the additional night-time peak is related to F scatter in latitudes of F_2-peak-electron densities from the work of Bateman and others[12] who have discussed the observations of VHF scatter propagation during the IGY in the Philippines-Okinawa area. They observed anomalous enhancements, during evening hours of the signals transmitted at VHF between Philippines and Okinawa. The enhancements occurred with greatest frequency in September and October. They lasted several hours beginning at about 1900 hours at the midpoint of the transmission path. The signal intensity usually increased rapidly, then levelled off, and finally dropped back to the normal scatter level around midnight. They suggested that the enhanced signal was propagated via the F region and was enhanced when there was spread F in that region. Spread F echoes showed a maximum in the equinoxes of high sunspot years and a negative correlation with magnetic activity at Ahmedabad[13].

In Fig. 1 are plotted the monthly mean hourly values in db. of the total attenuation at Ahmedabad from March 1957 to December 1959. An examination of the diurnal curves shows that they reach a minimum in the late hours of the night in all the months. The diurnal variation also shows maxima either as a single hump which occurs early in the afternoon, or as a double hump, the second hump occurring between 1800 and 2400 hours (local time) in the winter and equinoctial months. The double hump is most prominent between March 1957 and June 1959 except summer. In the autumn of 1959 the second maximum is tending to merge with the afternoon hump. The maximum day-time attenuation in db. and mean time of its occurrence in hours (75° EMT) are set out in Table 1. In general, the day-time maximum of the total attenuation occurs between 1300 and 1500 hours. There are only two exceptional cases, namely December 1957 with a maximum at 1100 hours and July 1959 with a maximum at 1800 hours. The largest and smallest values of maximum day-time attenuation in the course

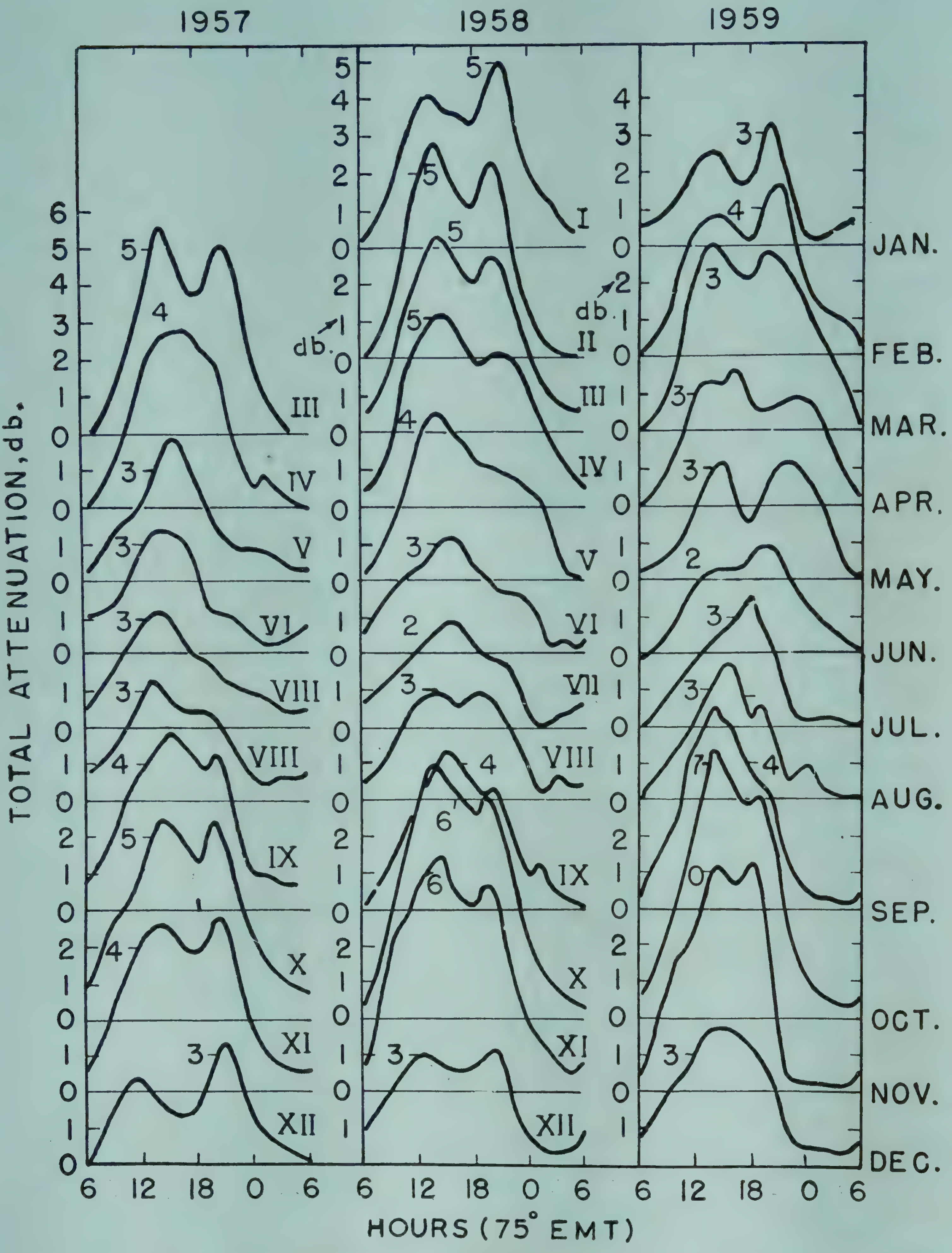

FIG. 1 — MONTHLY MEAN HOURLY VALUES IN DB. OF TOTAL IONOSPHERIC ATTENUATION OF COSMIC RADIO NOISE ON 25 Mc/s. AT AHMEDABAD: MARCH 1957 TO DECEMBER 1959

of three years are 7·3 and 2·4 db. in October 1959 and December 1957 respectively.

The observations of the second maximum of the total attenuation, which occurs in the early part of night, are summarized in Table 2. The second

TABLE 1 — MAXIMUM DAY-TIME TOTAL ATTENUATION IN DB. AND MEAN TIME OF ITS OCCURRENCE

(*A* — *Attenuation in db.*; *T* — *hours* 75° *EMT*)

YEAR		JAN.	FEB.	MAR.	APR.	MAY	JUNE	JULY	AUG.	SEPT.	OCT.	NOV.	DEC.
1957	A	No obser-		5·6	4·9	4·0	3·4	3·1	3·3	5·0	5·5	4·6	2·4
	T	vation		14	16	15	14	13	13	15	14	14	11
1958	A	4·1	5·8	5·3	5·2	4·5	3·2	2·9	3·0	4·3	6·9	6·4	3·1
	T	13	14	14	14	14	15	16	14	15	13	14	12
1959	A	2·5	3·8	5·0	3·7	3·1	2·2	3·5	3·7	5·4	7·3	6·1	3·7
	T	14	14	14	16	15	14	18	15	14	14	14	15

TABLE 2 — MAXIMUM NIGHT-TIME TOTAL ATTENUATION IN DB. AND MEAN TIME OF ITS OCCURRENCE

YEAR		JAN.	FEB.	MAR.	APR.	MAY	JUNE	JULY	AUG.	SEPT.	OCT.	NOV.	DEC.
1957	A	No obser-		5·1	—	—	—	—	—	4·3	5·5	4·8	3·3
	T	vation		21	—	—	—	—	—	20	20	20	21
1958	A	5·0	5·3	4·8	4·1	—	—	—	3·0	3·3	6·0	5·3	3·2
	T	21	20	20	21	—	—	—	19	20	19	19	20
1959	A	3·2	4·6	4·8	2·9	3·1	2·8	—	2·6	—	6·2	6·2	—
	T	20	21	20	23	22	20	—	19	—	19	18	—

hump occurs between 1800 and 2300 hours (local time). Its highest value was 6·2 db. and smallest 2·6 db. Blank spaces in Table 2 indicate absence of second hump.

Mean Monthly Variation of Total Attenuation. Fig. 2 shows the monthly mean values (mean of 24 hr) of the total attenuation for the period March 1957 to December 1959. The attenuation shows maxima in the equinoxes and minima in summer and winter. This is true for each of the three years, the maximum which occurs in October is stronger than the one occurring in March. The monthly mean total attenuation reached its highest value 3·8 db. in October 1958. In 1957, the attenuation remains at a low value during the whole summer from May to August. As against this, in 1958 and 1959 the minima are sharper.

Dependence of Attenuation on f_0F_2. Fig. 3 shows a scatter plot of the total attenuation during 1958 and 1959 against f_0F_2. Since a large amount of data over an extended period was available, the monthly median hourly values of f_0F_2 have been plotted to establish a relationship between them. Analysis by Bhonsle and Ramanathan[8] of the cosmic radio noise absorption

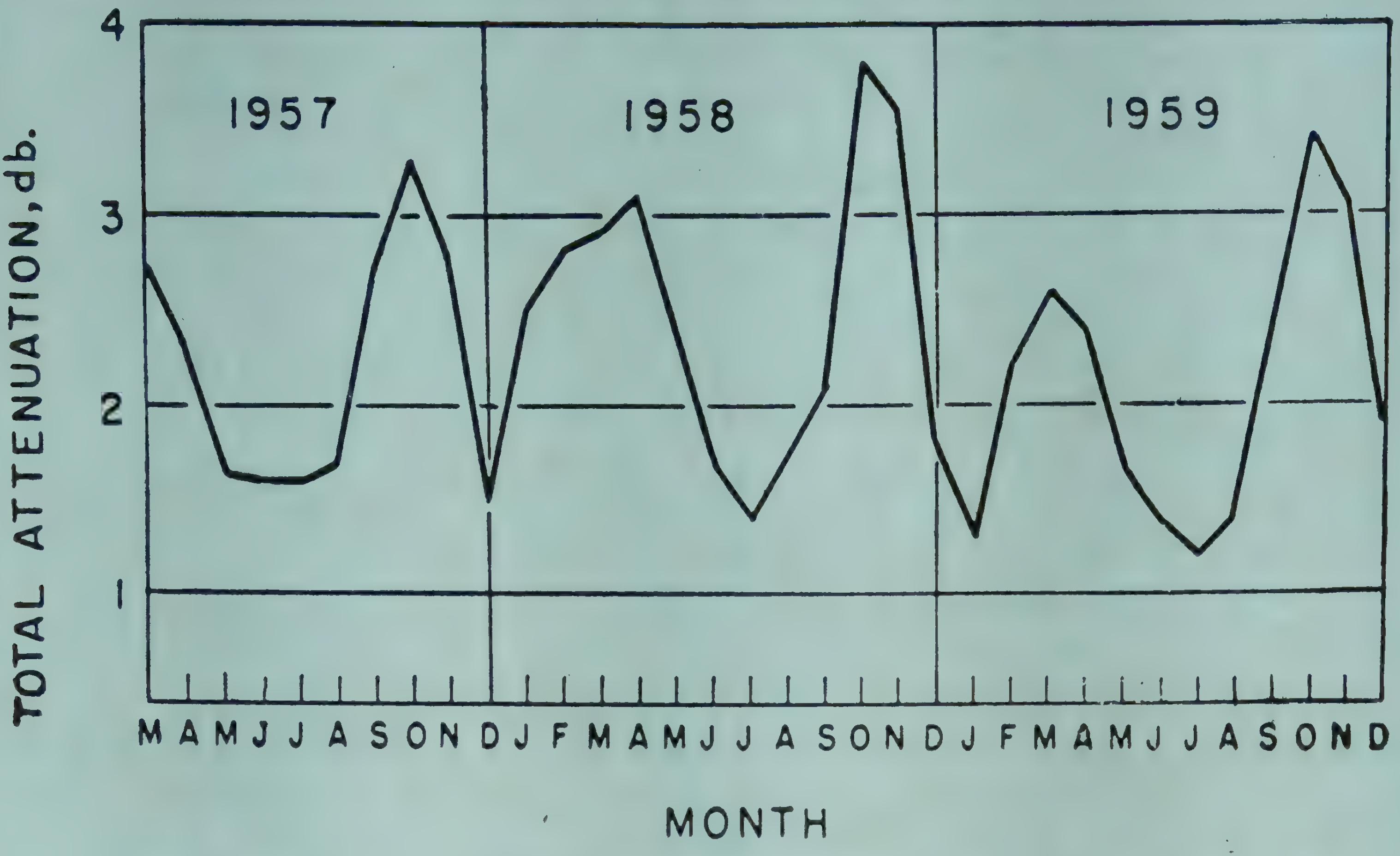

FIG. 2 — MONTHLY MEAN VALUES OF TOTAL ATTENUATION OF COSMIC RADIO NOISE AT AHMEDABAD: MARCH 1957 TO DECEMBER 1959

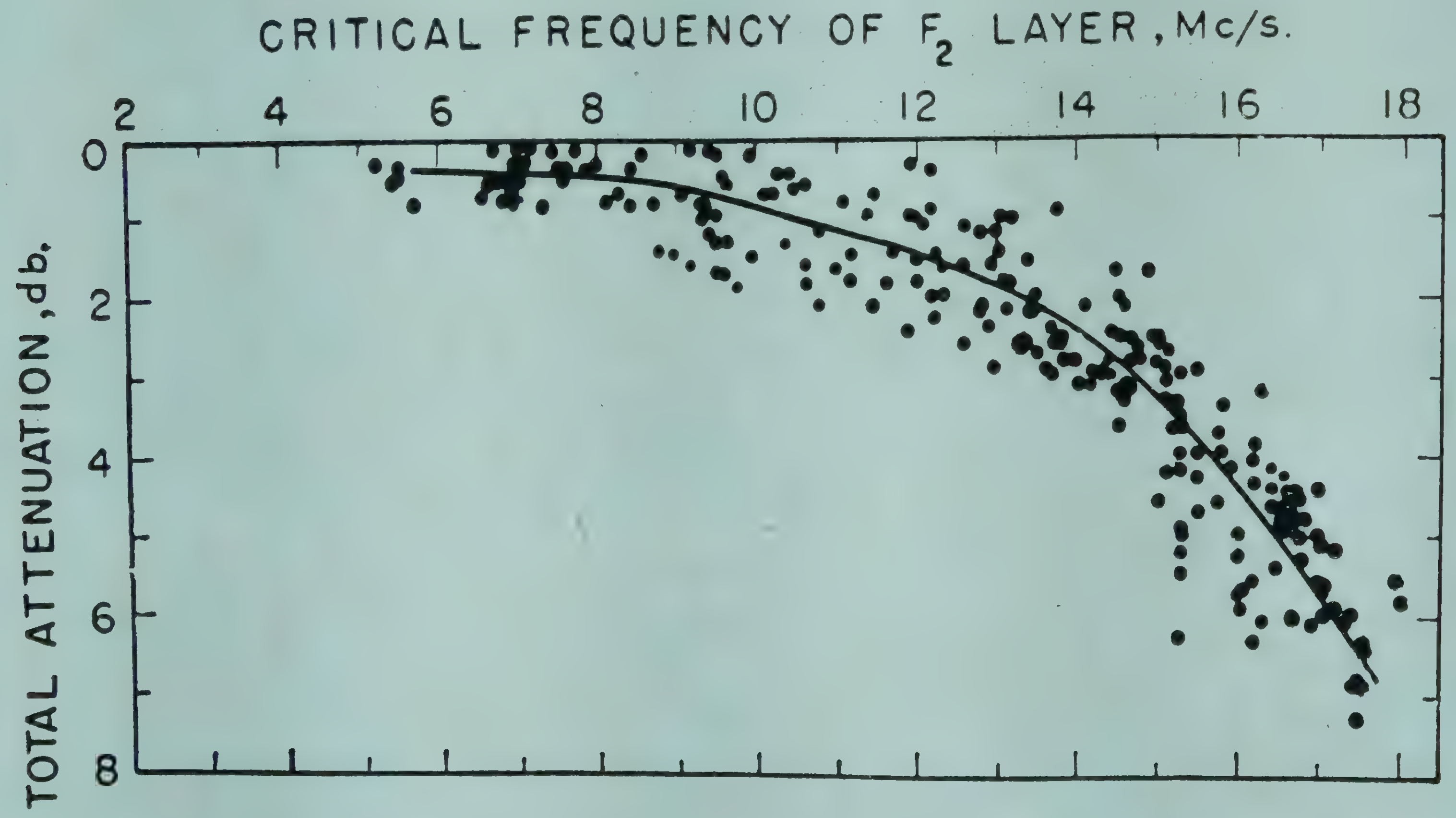

FIG. 3 — SCATTER PLOT OF TOTAL ATTENUATION AGAINST f_0F_2 DURING 1958 AND 1959

on 25 Mc/s. from March 1957 to February 1958 at Ahmedabad showed that in general when f_0F_2 exceeded 8 Mc/s. the attenuation increased rapidly with increasing f_0F_2. Earlier, Mitra and Shain had found from the Australian observations a correlation between the total absorption of cosmic noise on 18·3 Mc/s. and f_0F_2 values above 5 Mc/s. Blum[4] and others working on 30 Mc/s. in France showed that absorption varied linearly with f_0F_2. All these

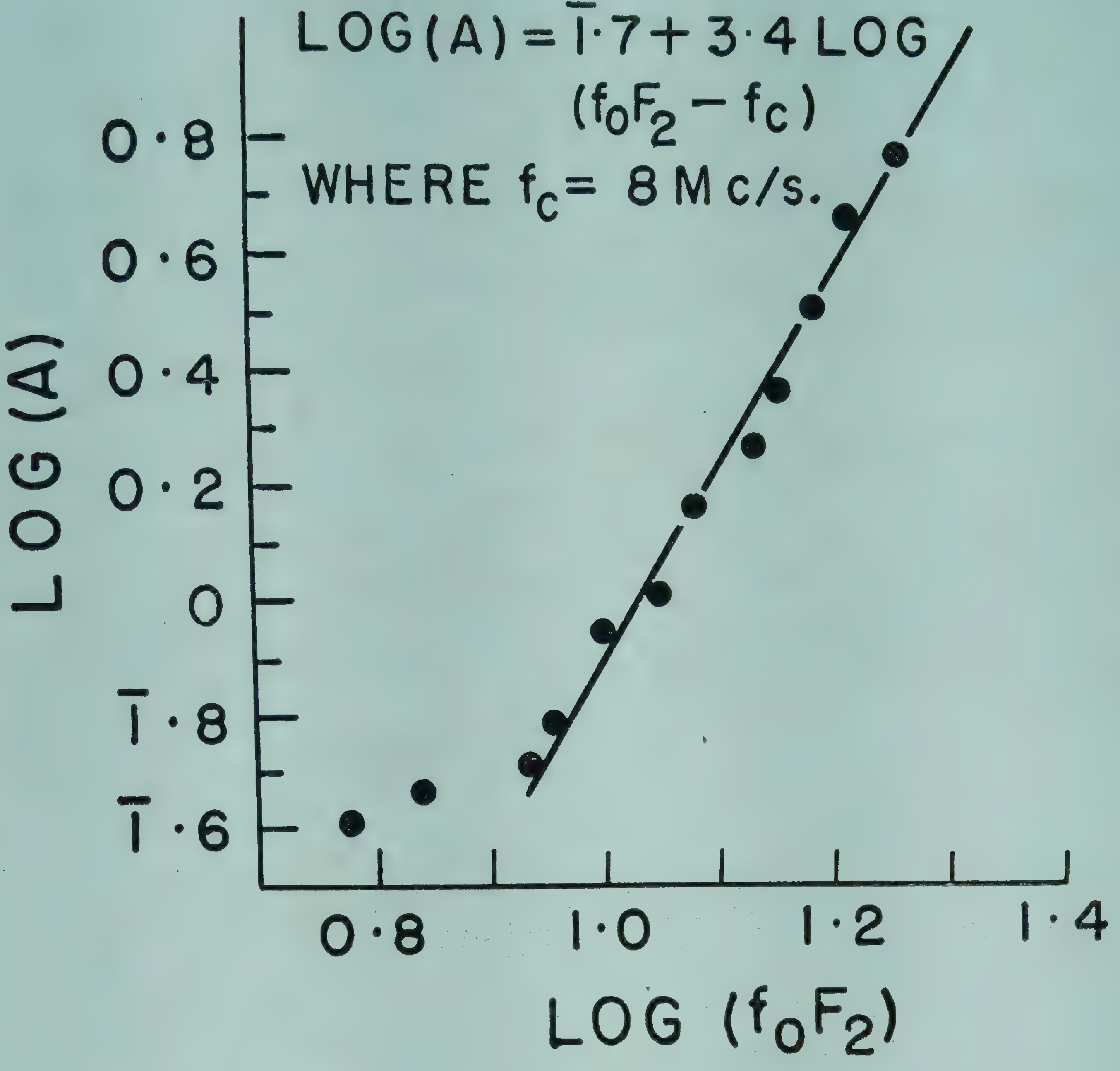

FIG. 4 — PLOT OF log (A) VERSUS log (f_0F_2)

show that a part of the total attenuation of cosmic noise takes place in the F region.

Fig. 4 shows the plot of $\log_{10} A$ against $\log_{10} f_0F_2$. The majority of the points lie on a straight line whose equation is given by

$$\log_{10} A = \bar{1}{\cdot}7 + K\ (\log_{10} f_0F_2 - \log_{10} 8) \tag{1}$$

where A = total attenuation in db.,
K = slope of line with a value near about 3·4, and
f_0F_2 = critical frequency of the F_2 region in Mc/s.

The equation may also be written in the simple form

$$A = \tfrac{1}{2}\left(\frac{f_0F_2}{8}\right)^{3\cdot 4} \tag{2}$$

This holds for frequencies greater than 8 Mc/s.

Separation of Day-time Component Symmetrical about Noon. It is expected both on theoretical grounds and from empirical data that an important fraction of the total attenuation would be a day-time effect depending on the solar zenith angle with maximum near noon and smaller values in the morning and evening. Mitra and Shain[3] devised a method to separate the F_2 region component of absorption from the total attenuation. Bhonsle and Ramanathan[8] analysed the cosmic noise absorption data of Ahmedabad for the period March 1957 to February 1958 and showed that below 8 Mc/s., the total attenuation showed little variation with f_0F_2. Bhonsle[14] extended the analysis to a later period till December 1959. Fig. 5 represents day-time symmetrical absorptions which have been separated from the absorptions depending on f_0F_2 for the period March 1957 to December 1959. They show reasonably good symmetry around local noon in each of the months. There is, however, a mean delay of about 28 min. beyond noon, which is in good agreement with Mitra and Shain's value of 27 min. It is clear that the diurnal variation of the day-time symmetrical component of absorption obeys a relation of the type $y = \cos^n\chi$. Averaging over different months, it is found that in 1957, n was 1·1 in summer, 1·0 in equinox and 0·8 in winter. The corresponding values of n in 1950 found by Mitra and Shain were 1·1 in summer, 0·9 in equinox and 0·5 in winter.

Seasonal Variation of Noon Absorption Corrected for F Attenuation. The noon value of $\cos^n\chi$ absorption was obtained for each month by extrapolating the total attenuation for low f_0F_2. These monthly values are plotted in Fig. 6. Although there is a progressive decrease from 1957 to 1959 in the noon values of absorption in summer and winter, the seasonal variation is not regular. In autumn, there occurs pronounced maxima of absorption in all the three years. If the noon absorption depended only on $\cos\chi$, maximum values in summer and minimum values in winter as indicated by the dotted line should have been expected. This suggests that although the day-time component of absorption shows symmetry around the local noon, a part of it may be contributed by the higher regions of the ionosphere.

F Attenuation. The symmetrical component of absorption which is under direct solar control is supposed to originate in the D, E and F_1 regions of the ionosphere. As these layers disappear soon after sunset and only the F_2 layer remains during the night, the attenuation observed during night has been attributed to the F_2 layer. Ahmedabad is situated in a belt of magnetic latitudes at which f_0F_2 reaches its peak value. Hence large attenuations of extraterrestrial radio noise correlated with f_0F_2 may be expected to occur. In winter and equinoctial months, another increase in f_0F_2 occurs after sunset which reaches a maximum about 2000–2200 hours. This may be due to F scatter which is common in this part of the day. If the symmetrical $\cos^n\chi$ component from the total attenuation is subtracted, then the remainder may be called the non-symmetrical component of attenuation which may arise in the F region or beyond.

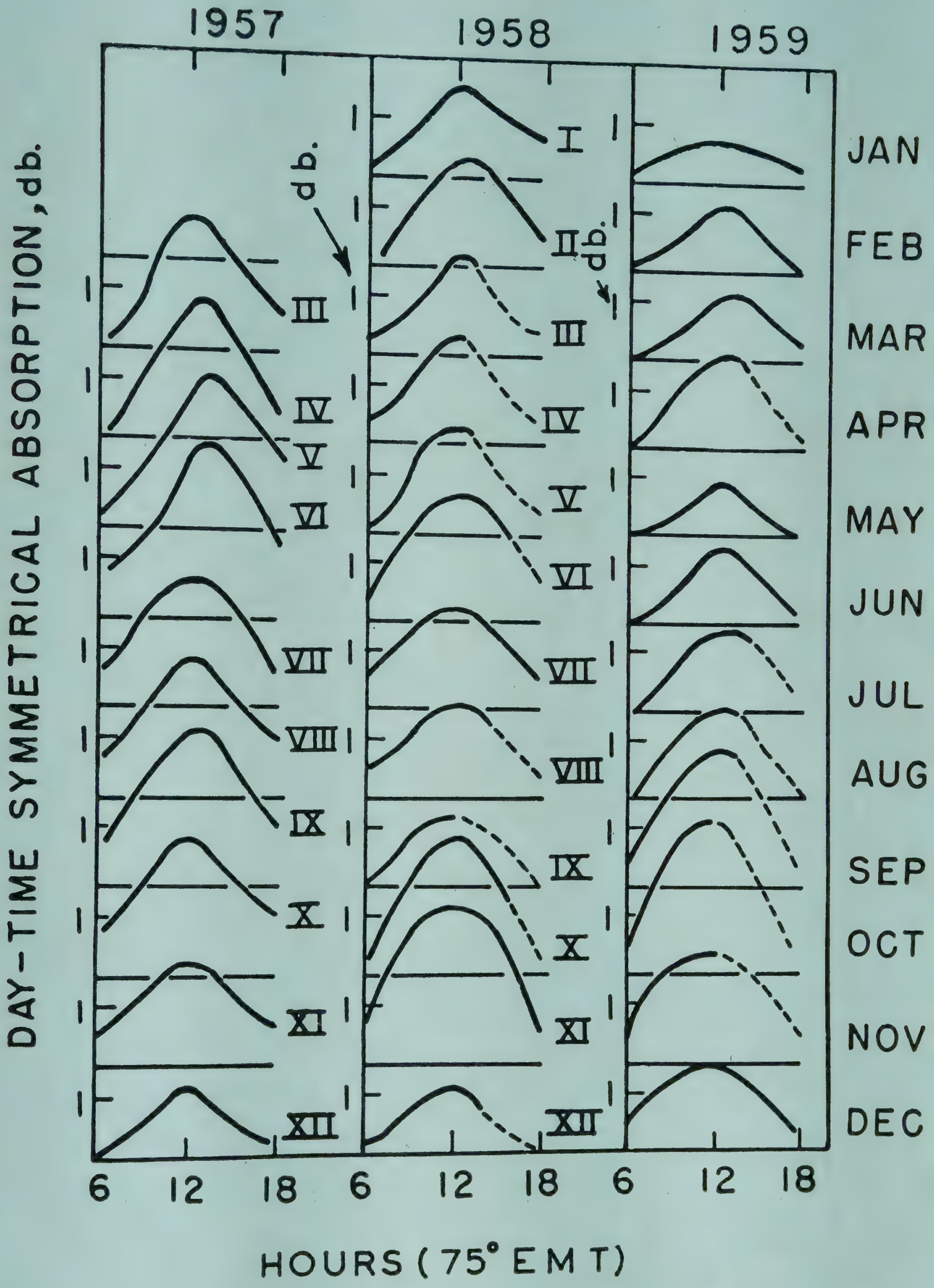

FIG. 5 — DAY-TIME COMPONENT OF ABSORPTION SYMMETRICAL AROUND NOON FOR THE PERIOD MARCH 1957 TO DECEMBER 1959

Fig. 7 shows the monthly mean hourly values in db. of the non-symmetrical component of attenuation (i.e. total attenuation minus the day-time symmetrical component) for March-April, June-July, October-November and

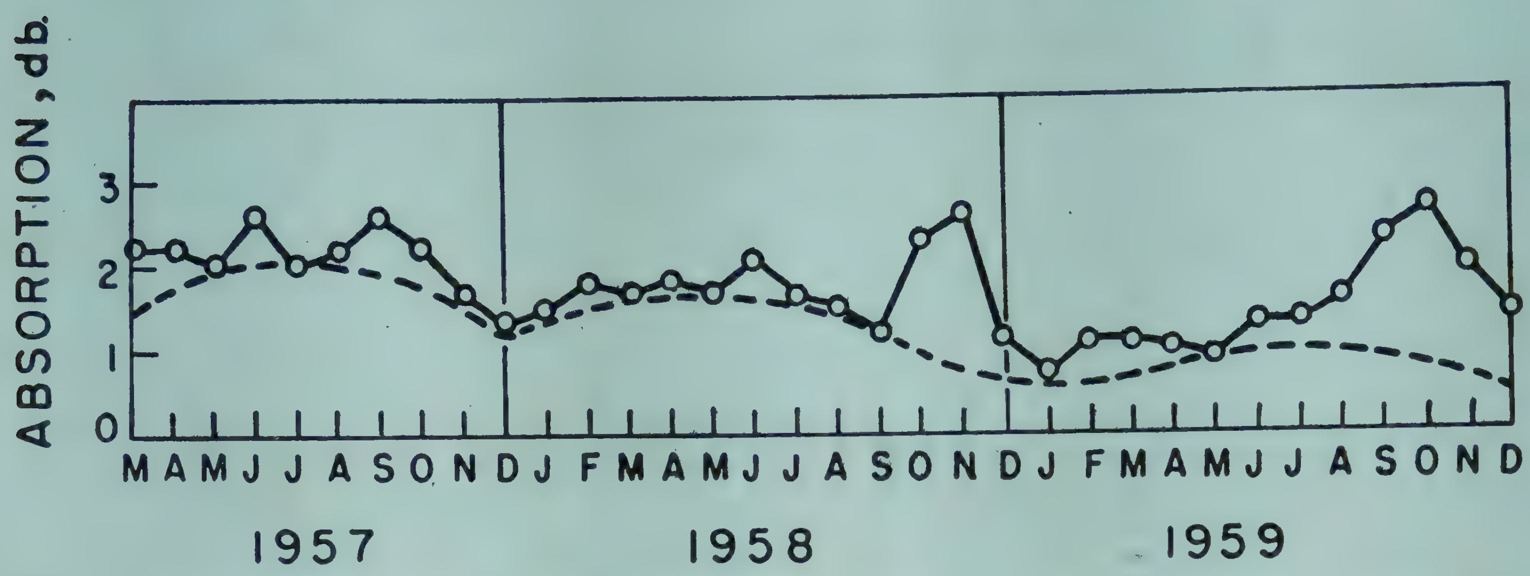

FIG. 6 — MONTHLY MEAN NOON ABSORPTION IN DB. CORRECTED FOR F ATTENUATION

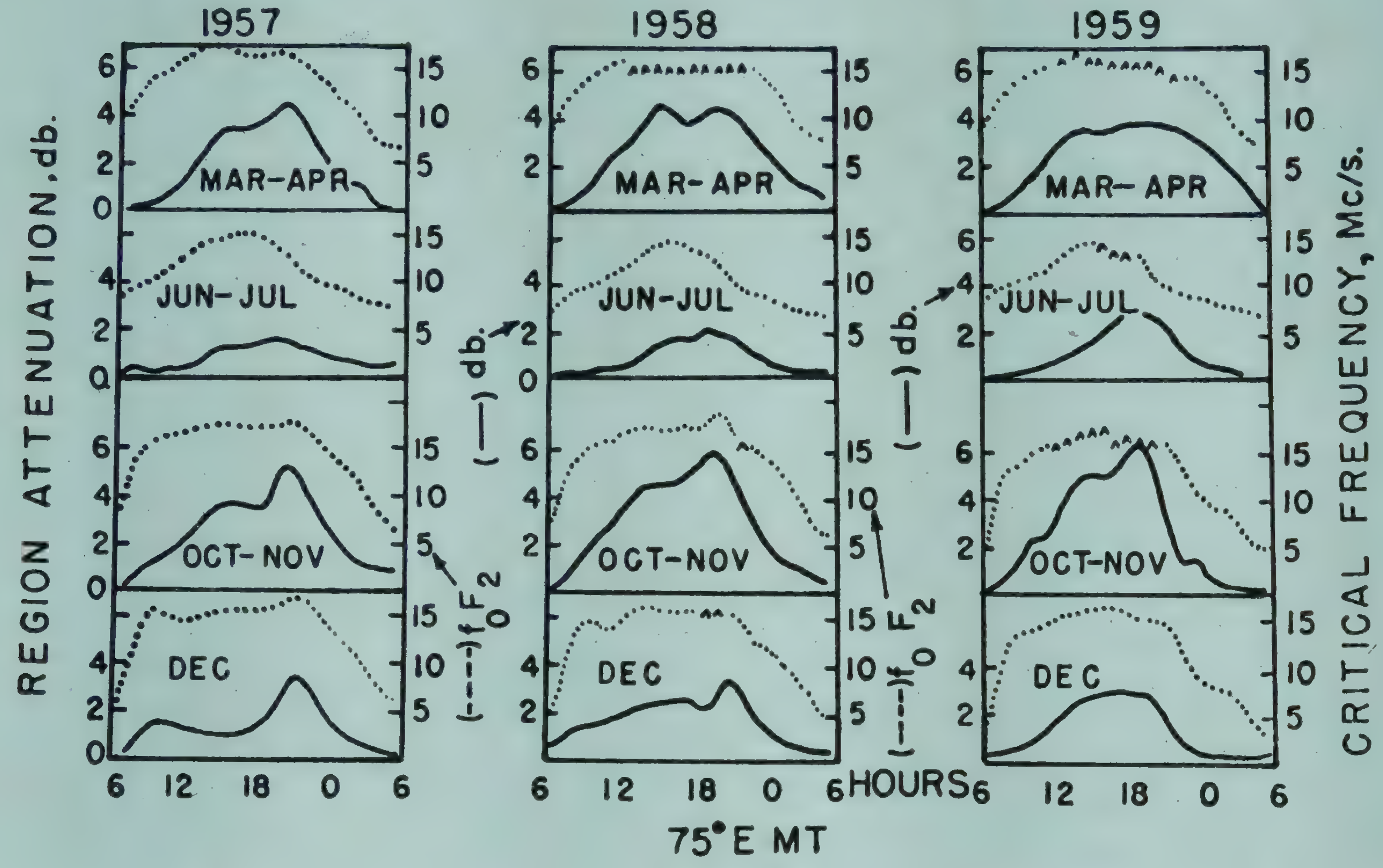

FIG. 7 — MONTHLY MEAN HOURLY VALUES IN DB. OF NON-SYMMETRICAL COMPONENT OF ATTENUATION FOR MARCH-APRIL, JUNE-JULY, OCTOBER-NOVEMBER AND DECEMBER IN 1957, 1958 AND 1959

December in 1957, 1958 and 1959. The corresponding monthly median values of f_0F_2 are also plotted and are shown by dotted lines. In June-July of each year, when the f_0F_2 values are low, low non-symmetrical attenuations are observed, whereas in October, November and December, large f_0F_2 values occur with correlated rise in attenuation. The early night values of f_0F_2 in summer are lower than those in equinoxes and winter.

The disparity between day and night attenuations for the same f_0F_2 can be seen clearly from Fig. 8 in which the attenuations at noon and 2000 hours are compared for all the months together with the corresponding values of f_0F_2. While the 12-hr attenuations follow the change in f_0F_2 rather closely,

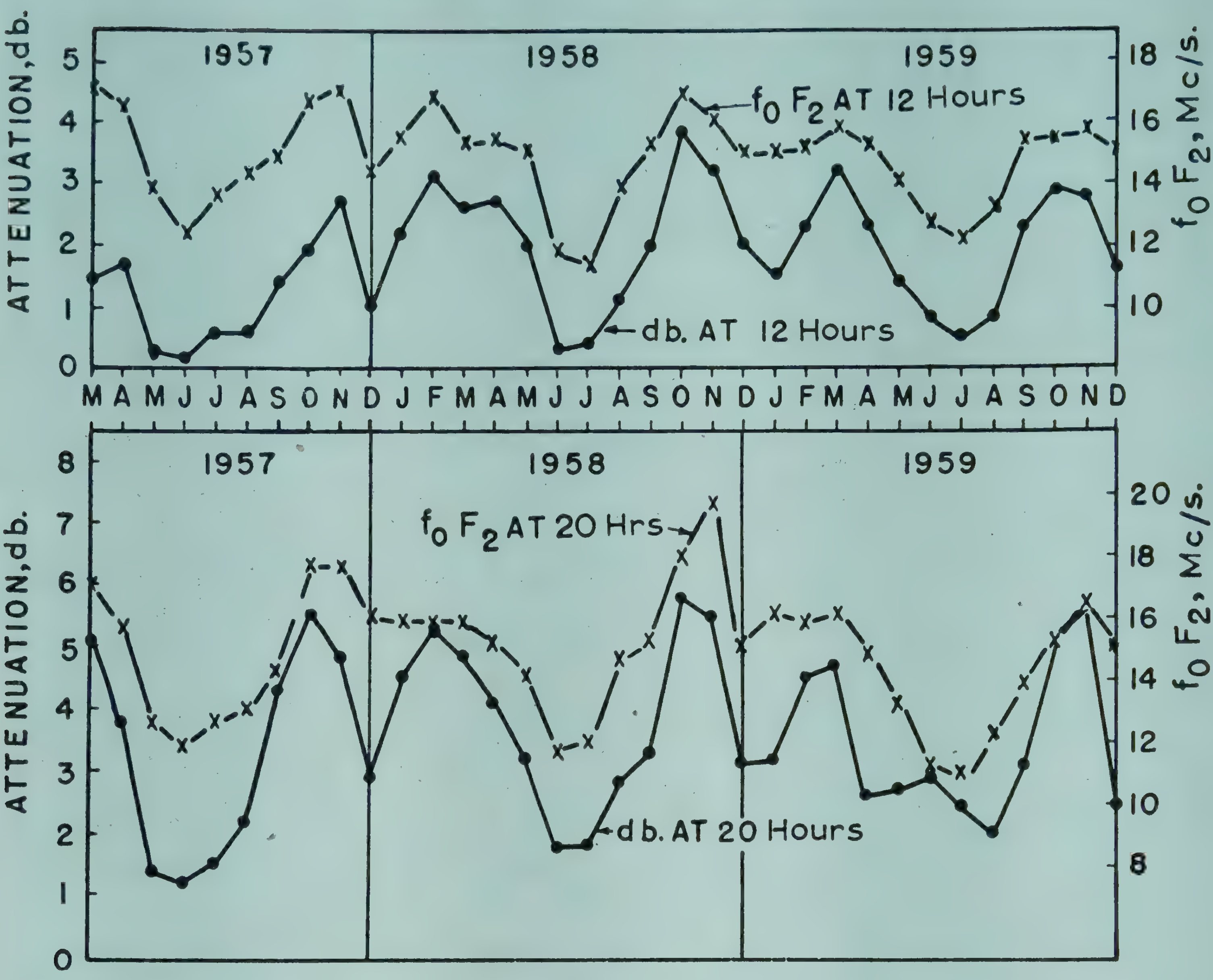

Fig. 8 — Monthly mean non-symmetrical component of absorption at 1200 and 2000 hours and corresponding values of f_0F_2

the 20-hr attenuations show abnormally high values, particularly in spring and autumn.

Noon Attenuations at Ahmedabad Compared with Similar Observations at other Stations. As the total attenuation of cosmic radio noise on 25 Mc/s. at Ahmedabad changes significantly with the local time and season, a comparison of the noon values of total attenuation in different seasons at Ahmedabad with similar observations made at other places is made. Table 3 gives a summary of the observations at various stations in different latitudes. The observations are not directly comparable since they have been made at different phases of the solar cycle and also on different frequencies, but it is still possible to get some idea of the orders of magnitude. Mitra and Shain analysed the cosmic radio noise data on 18·3 Mc/s. for selected periods in different seasons in 1950. They found that the maximum attenuation occurred in summer and it was somewhat less in both winter and equinoxes. Observations of Blum *et al.*[4] on 29·3 Mc/s. made in France in 1949 showed comparatively smaller attenuations.

Fredriksen and Dyce[15] worked with riometers for a short period in 1958 on 27·6 Mc/s. at Johnston Island, Hawaii and Bikini. The total attenuations

TABLE 3 — COMPARISON OF TOTAL NOON ATTENUATIONS OF COSMIC RADIO NOISE ON 25 Mc/s. AT AHMEDABAD WITH SIMILAR OBSERVATIONS MADE AT OTHER STATIONS

(*Total attenuation in db.*)

PLACE	LAT.	LONG.	YEAR	AUTHORS	FREQ. *Mc/s.*	SUMMER	EQUINOX	WINTER
Hornsby	34°S	151°E	1950 (6 months)	Mitra & Shain	18·3	1·3	0·85	0·9
Marcoussis	49°N	2°E	1949	Blum & others	29·5	0·5	—	—
Ahmedabad	23°02′N	72°38′E	1957	Bhonsle & Ramanathan	25	2·8	4	3·8
Ahmedabad	23°02′N	72°38′E	1958	Bhonsle & Ramanathan	25	2·7	4·5	3·6
Ahmedabad	23°02′N	72°38′E	1959	Bhonsle & Ramanathan	25	2·1	4·4	3·8
Hawaii	21°N	157°W	1958 (3 weeks)	Fredriksen & Dyce	27·6	0·75	—	—
Johnston Island	16°45′N	169°31′W	1958 (3 weeks)	Fredriksen & Dyce	27·6	0·4	—	—
Bikini	12°N	165°E	1958 (3 weeks)	Fredriksen & Dyce	27·6	—	1·25	—

at these stations were much smaller than those observed at Ahmedabad, even though the observations were made on nearly the same frequency.

Measurements made by the author on 25 Mc/s. at Ahmedabad, in a period of high solar activity, showed much larger values of attenuation than those observed by others. The situation of Ahmedabad on the belt of magnetic latitude, where the highest frequencies of the F_2 region occur, is probably responsible for the large attenuations which have been consistently observed from 1957 to 1959.

CONCLUSION

The studies of ionospheric absorption made at Ahmedabad using cosmic noise technique on 25 Mc/s. lead to the following conclusions:

(i) The total attenuation of cosmic radio noise on 25 Mc/s. at Ahmedabad can be divided into two components: (i) a day-time symmetrical component depending on the solar zenith distance and (ii) a non-symmetrical component, which does not depend on χ.

(ii) The total attenuation is a minimum usually between midnight and sunrise in all the seasons.

(iii) The total attenuation attains a maximum in the afternoon usually between 1400 and 1500 hours (local time). This is also the time when f_0F_2 reaches its maximum day-time value.

(iv) A second maximum is observed between 2000 and 2100 hours in certain months. This is probably due to F scatter.

(v) When f_0F_2 exceeds 8 Mc/s., the attenuation increases rapidly with increasing frequency and is empirically given by the following equation

$$A = \tfrac{1}{2}\left(\frac{f_0F_2}{8}\right)^{3\cdot 4}$$

where A = attenuation in db., and
f_0F_2 = critical frequency of F_2 region in Mc/s.

(vi) The monthly mean values of total attenuation show minima in summer and winter and maxima in the equinoxes; the maxima which occur in October-November are usually greater than those in March-April.

(vii) The symmetrical component of absorption reaches its maximum shortly after noon, the mean delay being 28 min.

(viii) The seasonal variation of non-symmetrical absorption shows maxima in equinoxes and minima in winter and summer.

(ix) The seasonal variation of the non-symmetrical component exhibits two minima similar to f_0F_2, one in summer and another in winter. The winter minima are more marked in the curves of attenuation.

ACKNOWLEDGEMENT

The author wishes to acknowledge the valuable guidance and encouragement he has received from Prof. K. R. Ramanathan during the course of this work. Thanks are also due to the Atomic Energy Commission of the Government of India for financial assistance and support.

REFERENCES

1. JANSKY, K. G., *Proc. Inst. Radio Engrs, N.Y.*, **20** (1932), 1920.
2. SHAIN, C. A., *Aust. J. sci. Res., Ser. A*, **4** (1951), 258.
3. MITRA, A. P. & SHAIN, C. A., *J. atmos. terr. Phys.*, **4** (1953), 204.
4. BLUM, DENISSE & STEINBERG, *C.R. Acad. Sci., Paris*, **238** (1954), 1695.
5. WARWICK, J. W. & ZIRIN, H. J., *J. atmos. terr. Phys.*, **11** (1957), 187.
6. LITTLE, C. G. & LEINBACH, H., *Proc. Inst. Radio Engrs, N.Y., A*, **47** (1958), 315.
7. RAMANATHAN, K. R. *et al.*, *Proc. Indian Acad. Sci.*, **43A** (1956), 306.
8. BHONSLE, R. V. & RAMANATHAN, K. R., *J. sci. industr. Res.*, **17A** (1958), 40.
9. RAMANATHAN, K. R. & BHONSLE, R. V., *J. geophys. Res.*, **64** (1959), 1635.
10. BHONSLE, R. V. & RAMANATHAN, K. R., *Planet. Space Sci.*, **2** (1960), 99.
11. BHONSLE, R. V., *Proc. Indian Acad. Sci.*, **51** (1960), 189.
12. BATEMAN, R. *et al.*, *J. geophys. Res.*, **64** (1959), 403.
13. KOTADIA, K. M. & RAMANATHAN, K. R., *Ann. IGY* (in press).
14. BHONSLE, R. V., Ph.D. Thesis, Gujarat University, 1960.
15. FREDRIKSEN, A. & DYCE, R. B., *J. geophys. Res.*, **65** (1960), 1177.

Ionospheric absorption over Delhi during IGY and IGC

M. K. RAO
S. C. MAZUMDAR
S. N. MITRA

Research Department, All India Radio
New Delhi

An automatic method of measuring ionospheric absorption was developed a few years ago at the Research Department, All India Radio, New Delhi (28°35′N : 77°5′E). The method used for measurements is more or less the same as that used by Appleton[1], with the difference that instead of measuring the amplitudes of successive echoes, suitable circuit techniques have been used to obtain directly the reflection coefficient on a logarithmic scale. The absorption can be directly recorded on a pen-and-ink recorder. The details of the experimental set-up and the circuit techniques have been published in another paper[2]. Regular measurements with the recorder were commenced in June 1954 and some preliminary results have been reported earlier[3].

During the IGY and IGC, measurements of absorption were intensified as per recommended schedules. Analysis of the data collected is the subject of this paper. The analysis pertains to diurnal variation of absorption, seasonal variation of absorption, relaxation time of the absorbing region and the night-time absorption. The measurements cover the period 0600–2300 hours LMT on frequencies 2·5, 5 and 7 Mc/s.

PRINCIPLE OF MEASUREMENT

Using the general nomenclature adopted by Appleton, the apparent reflection coefficient (ρ) may be defined as the ratio of the electric field of the polarized wave reflected from the layer to the electric field of the corresponding polarized wave incident on the layer, and $-\log \rho$ as the measure of absorption. The measurement of ionospheric absorption could be carried out by comparing the amplitude of successive echoes, taking advantage of the fact that such echoes arrive at distinct time intervals and can easily be separated when pulsed transmission is used.

At vertical incidence,

$$\rho = \frac{BR_1}{G} = \frac{2R_2}{\rho' R_1}$$

where B = constant, G = ground signal, R_1 = amplitude of the first echo, R_2 = amplitude of the second echo, and ρ' = apparent reflection coefficient of the ground for the wave frequency employed.

Thus,

$$\log \rho = \log B + \log \frac{R_1}{G}$$

$$= \log 2 - \log \rho' + \log \frac{R_2}{R_1}$$

One can evaluate $\log B$ from simultaneous measurements of $\log (R_1/G)$ and $\log (R_2/R_1)$. Knowing the value of $\log B$, $\log \rho$ could be determined on first reflection alone. This procedure has to be adopted, since in routine observations, often the first order reflection is alone present. It is also necessary to evaluate $\log B$ each time when any change in the experimental set-up is made.

The technique of measuring absorption is based on the above principles. A suitable pulsed signal from a signal generator adjusted to the same frequency is utilized in place of the ground signal for comparison.

Experimental Set-up. The experimental set-up is shown schematically in Fig. 1. A one-kW. pulsed transmitter connected to a vertical delta aerial acts as a signal source. The signal is received by a Hammerlund super pro receiver modified for pulsed reception[4]. The receiver is connected to another vertical delta aerial oriented at right angles to the transmitting

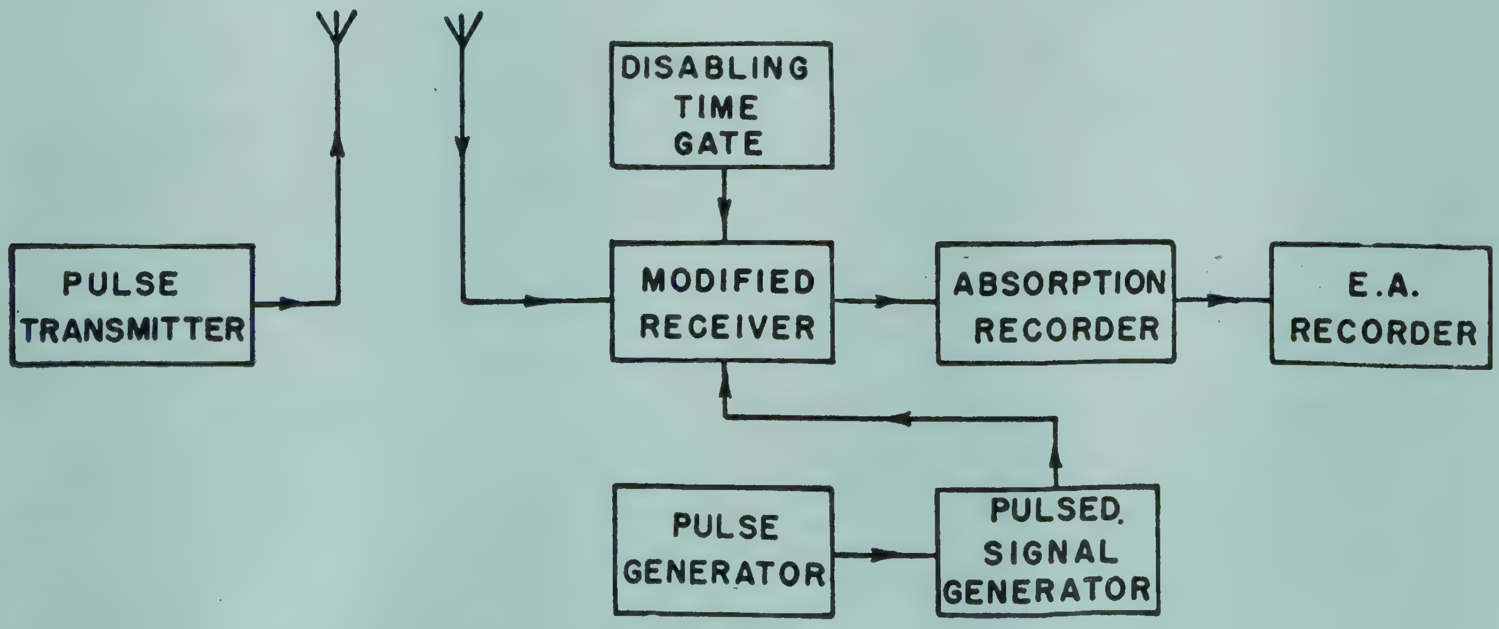

FIG. 1 — EXPERIMENTAL SET-UP FOR ABSORPTION MEASUREMENT

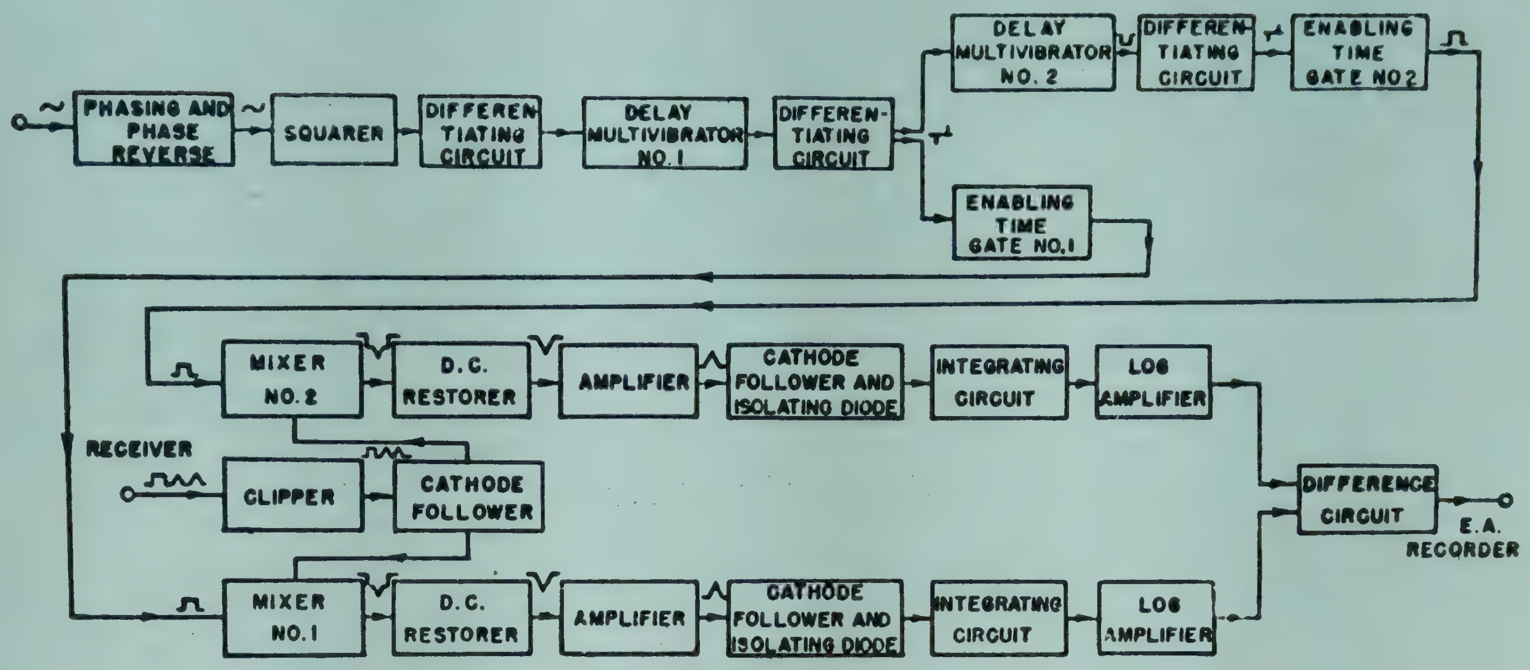
PHASING AND PHASE REVERSE
SQUARER
DIFFERENTIATING CIRCUIT
DELAY MULTIVIBRATOR NO. 1
DIFFERENTIATING CIRCUIT
DELAY MULTIVIBRATOR NO. 2
DIFFERENTIATING CIRCUIT
ENABLING TIME GATE NO 2
ENABLING TIME GATE NO. 1
MIXER NO. 2
D.C. RESTORER
AMPLIFIER
CATHODE FOLLOWER AND ISOLATING DIODE
INTEGRATING CIRCUIT
LOG AMPLIFIER
RECEIVER
CLIPPER
CATHODE FOLLOWER
DIFFERENCE CIRCUIT
E.A. RECORDER
MIXER NO. 1
D.C. RESTORER
AMPLIFIER
CATHODE FOLLOWER AND ISOLATING DIODE
INTEGRATING CIRCUIT
LOG AMPLIFIER

FIG. 2 — SCHEMATIC DIAGRAM OF ABSORPTION RECORDER

antenna. A suitable pulsed signal from a signal generator adjusted to the transmitter frequency is also injected to the input of the receiver. To minimize desensitization of the receiver by the strong ground pulse, the receiver is muted during the time interval occupied by the ground pulse by means of an externally generated disabling time-gate. The rectified video output of the receiver is then passed on to the absorption recorder.

The basic operating principles of the absorption recorder are as follows. An electronic gate of variable width and delay[5] selects the calibrating pulse (or the first echo, as the case may be). The gated echo is then passed on to a logarithm amplifier which gives $\log G$ (or $\log R_1$). Another electronic gate of independently variable width and delay selects the first echo (or the second reflection). The gated output is similarly passed on to a second independent logarithm amplifier, which gives $\log R_1$ (or $\log R_2$). The two logarithm outputs are combined in a difference circuit which gives $\log (R_1/G)$ [or $\log (R_2/R_1)$]. The d.c. output from the difference circuit is recorded on an Esterline Angus recorder which records the time variations of $\log \rho$. The circuit parameters are so adjusted that each division in the recorder chart represents 1 db. The absorption recorder is shown schematically in Fig. 2.

EXPERIMENTAL PROCEDURE AND ANALYSIS

The following procedure is followed in the evaluation of $|\log \rho|$ from the absorption records. Each record is taken for a period of 15 min. This record is then statistically analysed. About 200 readings are taken from each record and the median $|\log \rho|$ is evaluated. Thus the errors due to fading are eliminated. In order to enable the taking of measurements of ionospheric absorption even when the second order echo is very weak, the

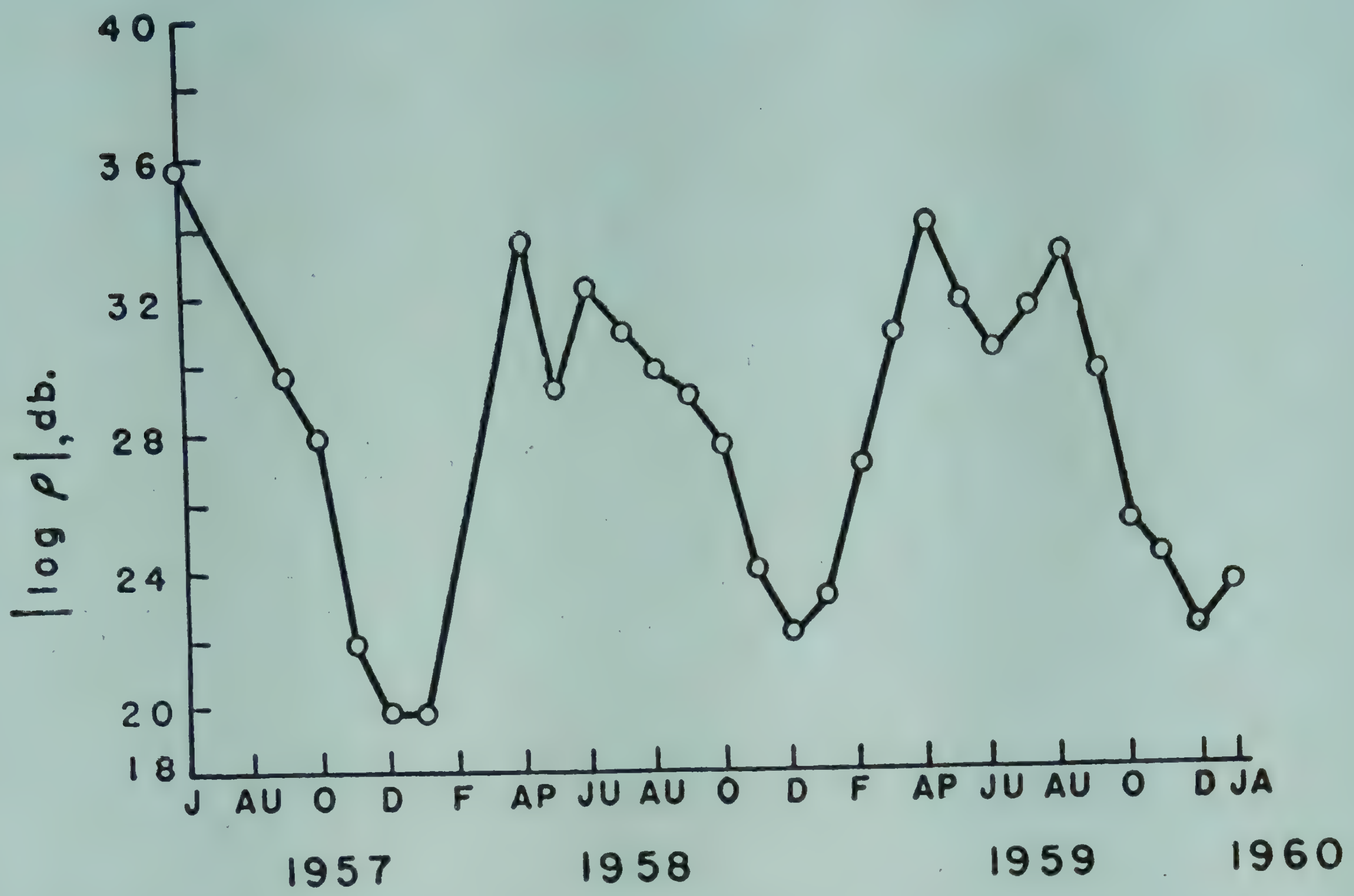

FIG. 3 — MONTHLY MEDIANS OF MIDDAY ABSORPTION ON 5 Mc/s.: JUNE 1957 TO JANUARY 1960

equipment is suitably calibrated on every frequency and the calibration constant determined. This is carried out during nights, when second order echo is present. Knowing the calibration constant, absorption at any frequency can be determined directly from the record even when the first order echo is alone present. For determining the calibration constant at any frequency, at least 20–30 sets of measurements have been taken. The following is the analysis of the data.

Midday Absorption. Regular measurements of absorption at midday have been carried out throughout the period. The exact time of local noon varies from about 1200 to 1240 hours IST depending upon the season. Observations were usually taken around the local noon during the different months as far as practicable. Fig. 3 shows the variation of the monthly medians against the different months for the 30-month period of IGY and IGC. It can be seen from the figure that $|\log \rho|$ varies from 20 to 35 db. and absorption during summer and equinox is higher than that during winter. The average midday absorptions during summer, equinox and winter are 31·5, 29·7 and 22·7 db. respectively.

Diurnal Variation of Absorption. Appleton[1] has shown that for a simple Chapman layer, the non-deviative absorption is given by

$$\int k.ds = |\log \rho| = 4{\cdot}13 \left(\frac{4\pi e^2}{mc}\right) \frac{N_0 \nu_0 H \, (\cos \chi)^{3/2}}{(p \pm |p_L|)^2} \tag{1}$$

Equation (1) can be written as

$$|\log \rho| \propto (\cos \chi)^{3/2} \tag{2}$$

when the other factors are kept constant.

It has been observed by workers in the field that Equation (2) is seldom valid. It may be expressed in a generalized form by

$$|\log \rho| \propto (\cos \chi)^{n} \tag{3}$$

Wide variations in the value of n have been reported by workers at different places. The values reported so far range from 1·76 to 0·5.

The authors have evaluated n in the following manner. The records of $|\log \rho|$ have been taken for durations of 15 min. each throughout the day at intervals of half-hour to one hour. The records have been statistically analysed and median $|\log \rho|$ has been evaluated. A curve is then plotted between $|\log \rho|$ and $\cos \chi$ on a logarithmic scale and n determined from the slope of the straight line thus obtained. The frequency used for these observations was 5 Mc/s. and the echoes from F layer only were utilized. Fig. 4 shows one such curve obtained on April 14, 1959. It can be seen from the figure that the relationship between $|\log \rho|$ and $\cos \chi$ on log scale is linear. In this particular case n comes out to be 0·99. About 40 sets of such observations have been obtained during the IGY and IGC. The values of n varied between 0·65 and 1·35 with an average of 0·95.

There is considerable variation in the value of n at different seasons. The average value of n during summer, equinox and winter works out to be 1·04, 0·96 and 0·88 respectively. Similar seasonal variations have been reported from temperate latitudes by Taylor[6].

The authors' observations have been taken on 5 Mc/s. during sunspot maximum. Due to high ionization density in the E layer, there will be contribution from E to the total non-deviative absorption. An attempt has been made to separate the effect of D and E layer absorption following a method given by Jaeger[7]. The details of this investigation are being published elsewhere. However, when the D and E layer effects are separately studied, the value of n for D layer (n_D) comes out to be 0·77, a value in close agreement with 0·75 found by Appleton and Piggott for England.

Seasonal Variation of $|\log \rho|$. The seasonal variation of $|\log \rho|$ has been investigated in the following manner. The mean of the absorption values at midday has been evaluated for each month. Then the mean midday $|\log \rho|$ values have been plotted on a logarithmic scale against the monthly mean values of $(\cos \chi)$ at noon. This relationship should be linear as indicated by Equation (3) and the slope of the straight line gives the value of n. Figs. 5 and 6 show the seasonal variations for 1958 and 1959 respectively. The relationship is substantially linear and the values of n obtained

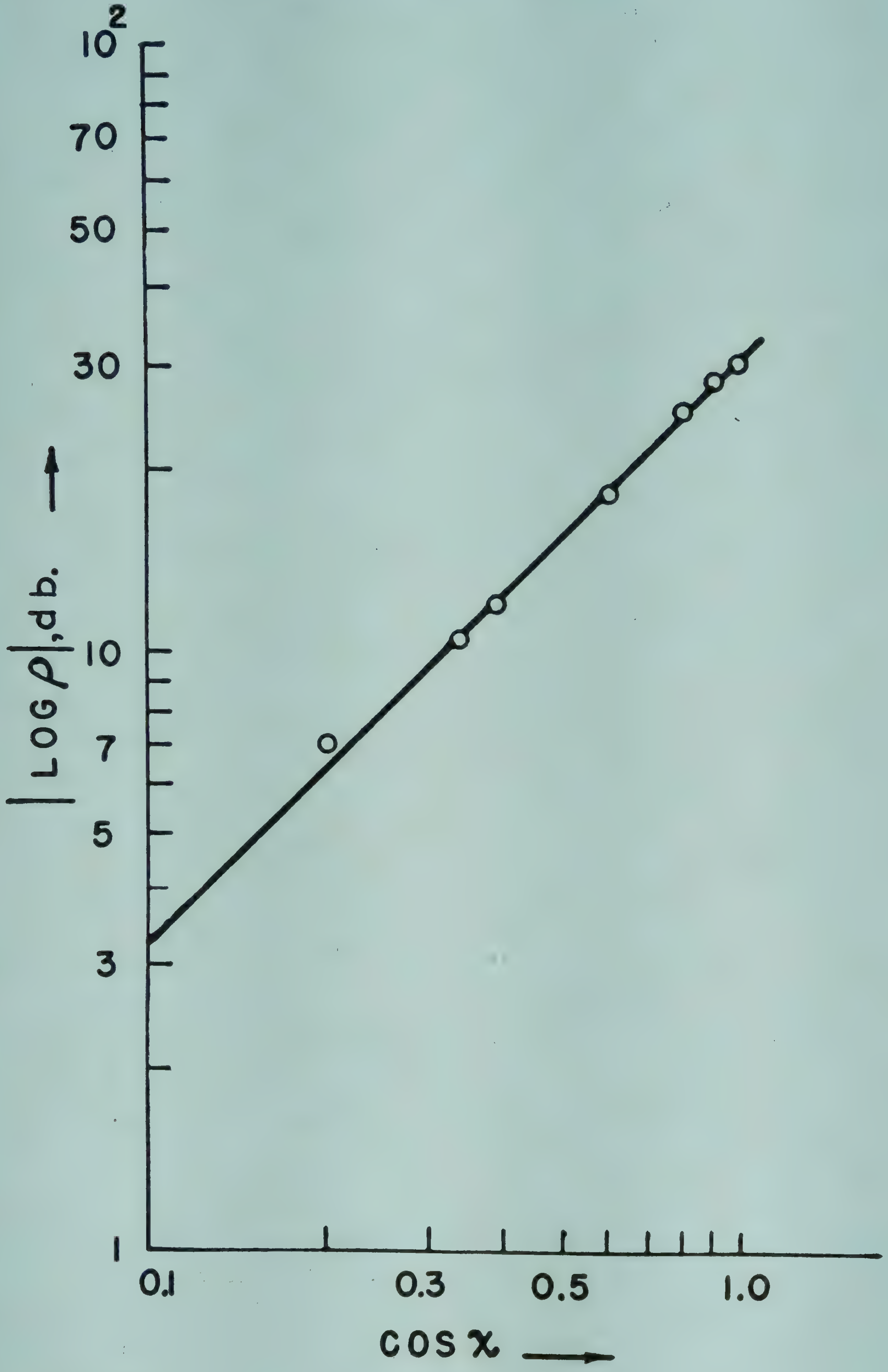

FIG. 4 — DIURNAL VARIATION OF | log ρ | ON 5 Mc/s. ON APRIL 14, 1959

from these curves are 0·78 and 0·83 as against the mean value of 0·95 found from the diurnal variation of | log ρ |. The diurnal variation factor is thus found to be higher than the seasonal variation factor. This indicates that the absorption in winter is slightly more than what is expected from

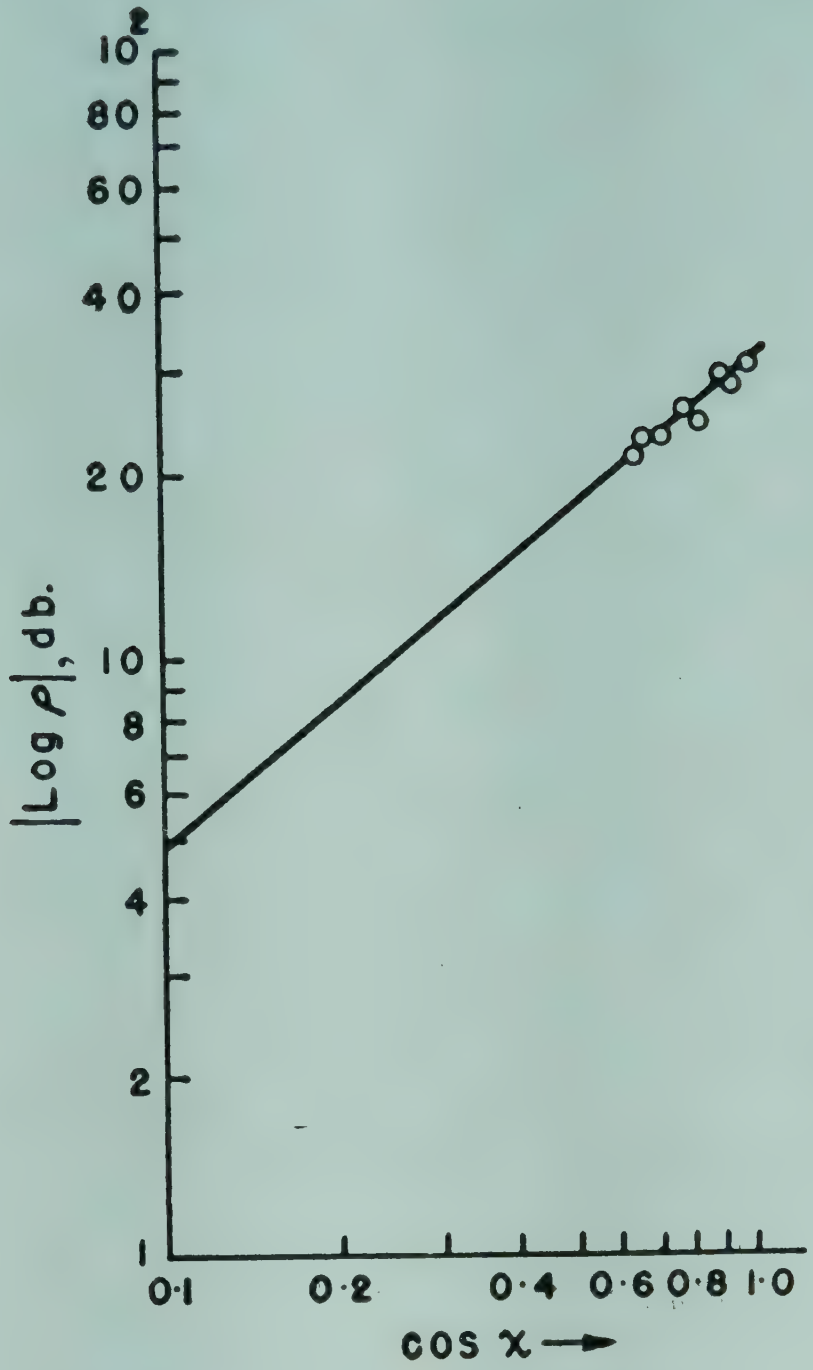

Fig. 5 — Seasonal variation of | log ρ | for the year 1958

$n = 0{\cdot}95$. This higher absorption in winter has also been observed at higher latitudes by Appleton and Piggott[8] and is known as the ‘ winter anomaly ’. However, at the latitude of Delhi this increase in absorption during winter is not very prominent as it is of the order of 2 db. only.

Relaxation Time. Appleton[9] has shown that the diurnal maximum in absorption is obtained not exactly at local noon but at a certain time afternoon. This delay time (τ) is known as the relaxation time of the absorbing region. To determine the value of τ, absorption records were taken continuously between 1000 and 1400 hours on many days. The value of τ varies from 6 to 79 min., the average being 37 min., if the most prominent maxima after local noon are considered. A distinct pre-noon maximum has, however, been obtained on most of the days, in addition to the post-noon maximum.

Night Absorption. Ionospheric absorption after sunset has been similarly investigated. These measurements have been carried out on 2·5 and 5 Mc/s.

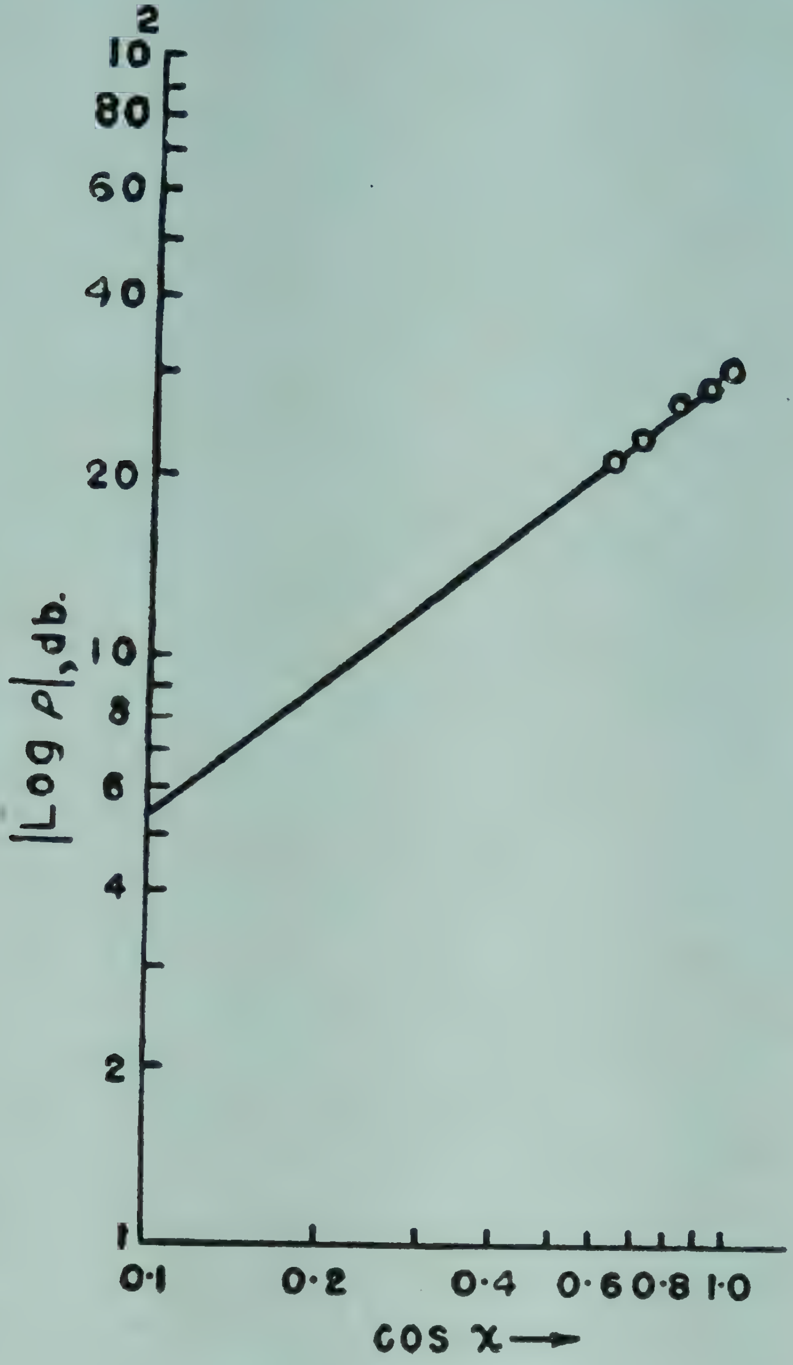

FIG. 6 — SEASONAL VARIATION OF | log ρ | FOR THE YEAR 1959

Absorption during night has been observed to be very low — of the order of 2–3 db. Fig. 7 indicates the fall of absorption after sunset on December 18, 1958. It can be seen from this figure, that the absorption decreases quickly after sunset and remains low for a considerable period in the night increasing gradually thereafter. This increase is presumably due to deviative absorption as the critical frequency comes down during this period.

Magnetic Activity and Ionospheric Absorption. In an attempt to investigate whether ionospheric absorption is influenced by changes in the geomagnetic field, magnetic data provided by Alibag Observatory have been used. The midday absorption values on various days corresponding to different midday magnetic K indices have been grouped together separately in different seasons. Thus, the variation of | log ρ | with magnetic activity has been studied. A plot of | log ρ | against K indices in different seasons is shown in Fig. 8. It may be seen from this figure that there is practically no correlation between the two at the latitude of Delhi.

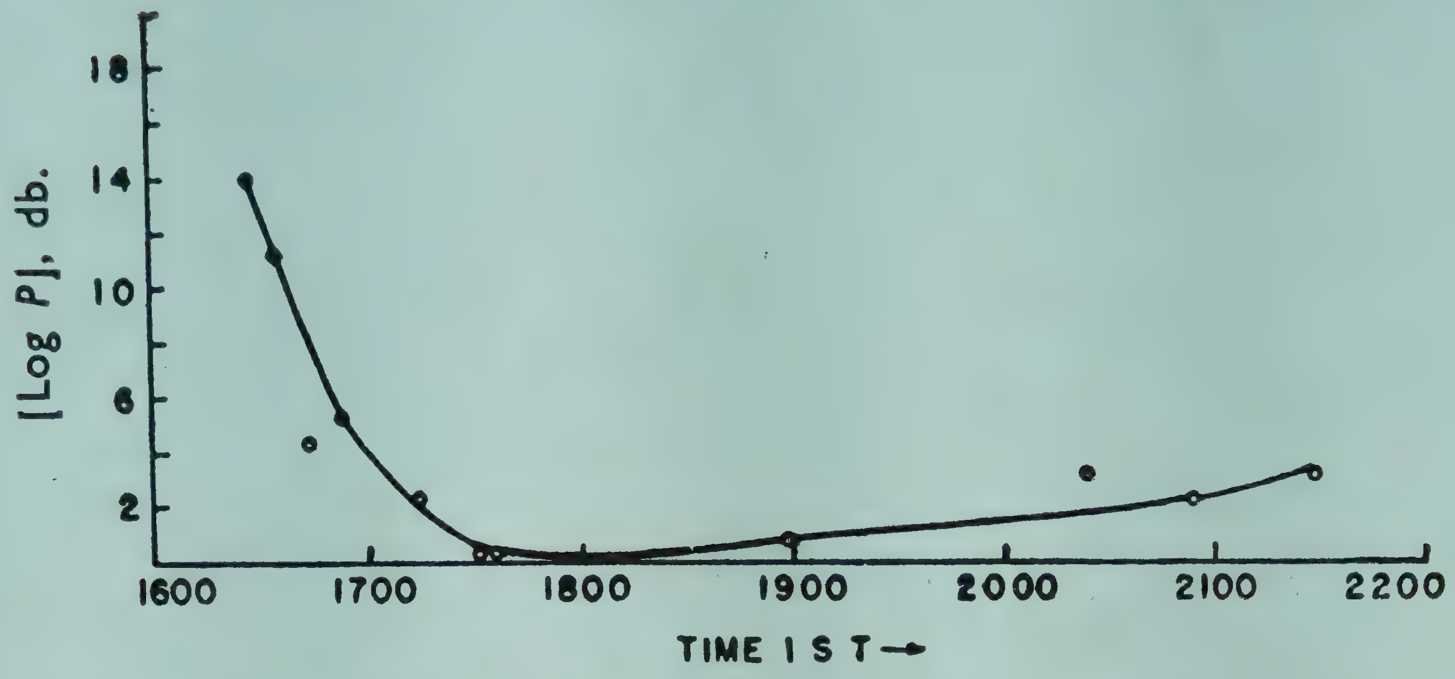

Fig. 7 — Night absorption on 2·5 Mc/s. on December 18, 1958

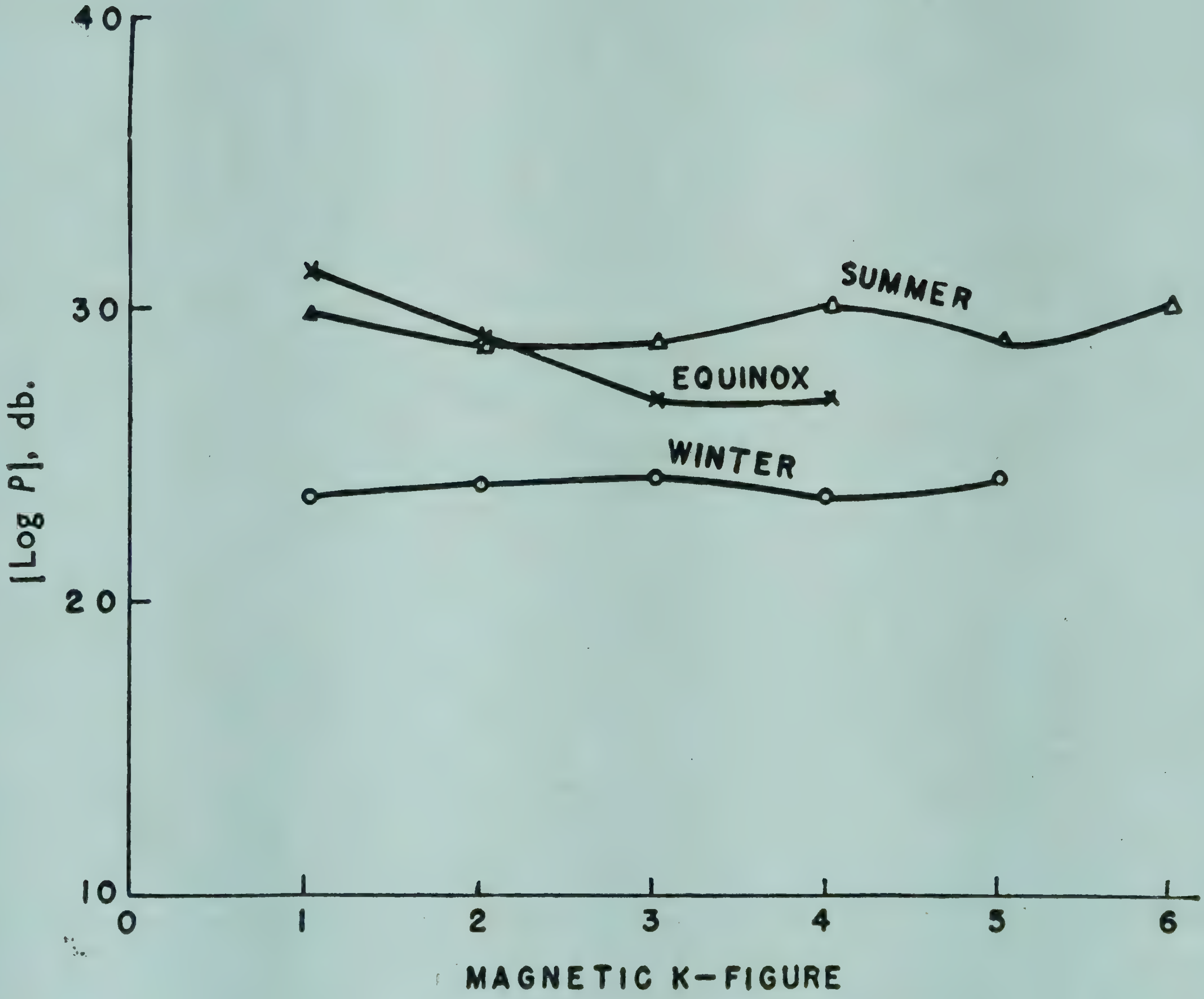

Fig. 8 — Plot of magnetic K indices against mean midday |log ρ|

Special Observations on Regular World Days. Diurnal variation of $|\log \rho|$ has been investigated on all the Regular World Days of IGY and IGC. It has been found that the absorption increases after sunrise, reaches a broad maximum around noon and falls off during the afternoon period.

CONCLUSIONS

The investigation of absorption at Delhi by vertical incidence pulsed sounding during the IGY leads to the following conclusions:

(i) The non-deviative absorption on 5 Mc/s. is quite high at Delhi and its midday value in different seasons lies within the approximate range of 20–35 db.

(ii) The diurnal variation factor n varies within wide range of 0·65–1·35. There is a distinct seasonal trend in the summer, equinox and winter, values being 1·04, 0·96 and 0·88 respectively. When the contribution to the total observed non-deviative absorption due to D and E layers are separated out, the value of n for D layer (n_D) comes out to be 0·77 which is in close agreement with 0·75 found by Appleton and Piggott for England.

(iii) The seasonal variation of absorption confirms the winter anomaly already reported by Appleton and Piggott. In other words, the absorption in winter is more than that expected from the observed diurnal variation factor, although for Delhi, the magnitude of this anomaly is only about 2 db.

(iv) Relaxation time of the absorbing region varies from 6 to 79 min., the average being about 37 min. A well-pronounced pre-noon maximum in absorption is often observed; this may be due to deviative absorption in the F_1 layer when its critical frequency is around 5 Mc/s., the exploring wave frequency.

(v) The absorption during night on 2·5 Mc/s. is very small, of the order of 2 db.

(vi) There is hardly any correspondence between magnetic K index and absorption at the latitude of Delhi.

(vii) From the frequency variation of absorption it appears that an inverse square law is approximately valid for the stations lying in the same latitude as Delhi.

ACKNOWLEDGEMENT

The authors' grateful thanks are due to the Chief Engineer, All India Radio, New Delhi, for permission to publish this paper.

REFERENCES

1. APPLETON, E. V., *Proc. roy. Soc.*, **162A** (1937), 451.
2. MAZUMDAR, S. C., *J. Instn Telecomm. Engrs*, **4** (1958), 81.
3. MITRA, S. N. & MAZUMDAR, S. C., *J. atmos. terr. Phys.*, **10** (1957), 32.
4. MITRA, S. N. & ROY, J. M., *Electrotechnics*, No. 23, (1951), 5.
5. MAZUMDAR, S. C. & MITRA, S. N., *Indian J. Phys.*, **28** (1954), 251.
6. TAYLOR, E. W., *Nat. Bur. Stand. J. Res.*, **41** (1948), 575.
7. JAEGER, J. C., *Proc. phys. Soc. Lond.*, **59** (1947), 87.
8. APPLETON, E. V. & PIGGOTT, W. R., *J. atmos. terr. Phys.*, **5** (1954), 141.
9. APPLETON, E. V., *J. atmos. terr. Phys.*, **3** (1953), 282.

Ionospheric absorption on 2.5/2.6 Mc/s. at Ahmedabad

J. S. SHIRKE

Physical Research Laboratory
Ahmedabad

Measurements of ionospheric absorption using vertical pulsed transmission were carried out at Ahmedabad on 2·5 Mc/s. from August 1957 to April 1958 and on 2·6 Mc/s. from May 1958 to February 1959.

The data show that the mean monthly values of absorption, L, obey a relation, $L \propto \cos^n \chi$, where χ is the zenith angle of the sun, the mean value of n being 0·70 for 2·5 Mc/s. and 0·80 for 2·6 Mc/s. The value of n was 0·86 for summer, 0·69 for winter and 0·74 for the equinoxes.

For removing the seasonal variations, the values of absorption were extrapolated to $\cos \chi = 1$. These extrapolated values showed a linear dependence on the sunspot number R. It was observed that $L' = L_0 (1+\beta R)$, where $L_0 = 47$ db. and $\beta = 0{\cdot}0020$ for 2·5 Mc/s.; and $L_0 = 45$ db. and $\beta = 0{\cdot}0018$ for 2·6 Mc/s.

Measurement of ionospheric absorption was carried out at Ahmedabad (23°0′N : 72°6′E) during the period August 1957 to February 1959 by measuring the intensities of vertical pulse reflections. The frequencies used were 2·5 Mc/s. from August 1957 to April 1958 and 2·6 Mc/s. later. The change was made in order to reduce the interference from the harmonics of the local broadcasting station. Vertical pulsed transmission was used in both the cases. The method of taking the measurements and some of the results obtained till July 1958 have been published[1]. The additional data for the period July 1958 to February 1959 have now been analysed. The results obtained confirm the earlier results.

It was shown in the previous paper that the monthly mean values of absorption obeyed a relation of the type $-\log \rho \propto \cos^n \chi$, where χ is the zenith angle of the sun and $-\log \rho$ the absorption in db. and n an approximate constant.

TABLE 1 — VALUES OF n FOR EACH MONTH FROM AUGUST 1957 TO FEBRUARY 1959

2·5 Mc/s.			2·6 Mc/s.		
	Month	n		Month	n
1957	Aug.	0·89	1958	May	0·72
	Sept.	0·64		June	0·87
	Oct.	0·65		July	0·87
	Nov.	0·64		Aug.	0·97
	Dec.	0·60		Sept.	0·93
1958	Jan.	0·74		Oct.	0·81
	Feb.	0·71		Nov.	0·76
	Mar.	0·64		Dec.	0·70
	Apr.	0·87	1959	Jan.	0·77
				Feb.	0·63
	Mean n	0·70		Mean n	0·80

A similar law is found to hold for each of the remaining months. Plots of monthly mean hourly values against the cosine of the solar zenith angle were made on logarithmic paper and found to fall on straight lines for each individual month. The slope of the line gives the index n for each month. Table 1 gives the values of n so obtained.

Tables 2 and 3 give the monthly mean values of absorption in db. for each hour of observations — Table 2 for the period August 1957 to April 1958 and Table 3 for May 1958 to February 1959. The cosine of the solar zenith angle for the corresponding hour on the 15th of each month is shown side by side with the measured absorption L. Since the data for August 1958 were centred around the 5th and that of September 1958 around the 23rd, the values of χ for these months correspond to the declination of the sun on the 5th and the 23rd. For the other months, they relate to the 15th day of the month.

From the two sets of the observations, it would be seen that the absorption corresponding to the higher frequency 2·6 Mc/s. was consistently lower than that for 2·5 Mc/s. However, because of the nearness of the frequencies, it would not be proper to derive any general relation.

The mean value of n is seen to be 0·70 for the frequency 2·5 Mc/s. and 0·80 for 2·6 Mc/s. The value of n for August and September 1958 is rather high; in these months the number of observations were small.

In calculating n, the values of absorption only for the hours when f_0E was greater than 3·5 Mc/s. were considered. This is to avoid any effect of additional attenuation which might be associated with the closeness of the

TABLE 2 — MONTHLY MEAN VALUE OF ABSORPTION FOR EACH HOUR OF OBSERVATION FROM AUGUST 1957 TO APRIL 1958

(*Frequency*, 2·5 *Mc/s.*; $T = 75°$ *EMT*; L = *absorption in db.*; *and* χ = *solar zenith angle*)

Month		Time, *hr*																			
		0830–0845		0910–0925		1010–1015		1115–1145		1210–1240		1310–1320		1410–1415		1510–1520		1610–1615		1710–1715	
		cos χ	L	cos χ	L	cos χ	L	cos χ	L	cos χ	L	cos χ	L	cos χ	L	cos χ	L	cos χ	L	cos χ	L
1957	Aug.	0·64	38	0·73	42	0·87	51	0·97	55	0·99	57	0·96	54	0·87	51	0·71	41	0·58	27	0·38	30
	Sept.	0·57	44	0·68	52	0·84	59	0·93	d63	0·94	d62	0·91	d61	0·81	d58	0·64	49	0·47	43	0·28	32
	Oct.	0·55	39	0·64	49	0·76	56	0·86	d62	0·85	d58	0·82	d59	0·72	52	0·53	46	0·34	36	0·12	28
	Nov.	0·37	36	0·56	43	0·67	51	0·74	57	0·74	58	0·69	55	0·60	46	0·44	38	0·24	31	0·04	27
	Dec.	0·35	31	0·47	43	0·60	48	0·69	52	0·69	53	0·66	53	0·56	48	0·42	39	0·23	32	0·05	23
1958	Jan.	0·35	29	0·45	33	0·58	42	0·71	52	0·71	52	0·69	48	0·61	46	0·49	39	0·30	29	0·12	23
	Feb.	0·43	30	0·52	38	0·66	44	0·79	52	0·81	52	0·79	51	0·70	46	0·59	37	0·39	31	0·20	21
	Mar.	0·53	42	0·62	46	0·76	52	0·89	d62	0·91	d62	0·88	d62	0·80	55	0·64	52	0·40	43	0·24	31
	Apr.	0·64	41	0·72	49	0·86	57	—	—	0·97	d62	0·95	60	0·85	59	0·69	52	0·50	40	0·28	32

d = greater than.

TABLE 3 — MONTHLY MEAN VALUE OF ABSORPTION FOR EACH HOUR OF OBSERVATION FROM MAY 1958 TO FEBRUARY 1959

(*Frequency, 2·6 Mc/s.; time = 75° EMT*; L = *absorption in db.; and* χ = *solar zenith angle*)

Month		Time, *hr*															
		0845		0915		1010		1315		1415		1510		1610		1710	
		$\cos \chi$	L	$\cos \chi$	L	$\cos \chi$	L	$\cos \chi$	L	$\cos \chi$	L	$\cos \chi$	L	$\cos \chi$	L	$\cos \chi$	L
1958	May	0·69	43	0·79	48	0·91	53	0·95	57	0·87	54	0·72	46	0·53	38	0·33	29
	June	0·69	39	0·77	45	0·90	50	0·97	54	0·88	51	0·74	45	0·56	35	0·37	27
	July	0·65	39	0·74	45	0·88	51	0·97	58	0·88	54	0·76	49	0·59	38	0·38	28
	Aug.	0·65	41	0·72	48	0·87	57	—	—	0·89	60	0·75	50	0·57	37	0·36	36
	Sept.	0·61	32	0·67	36	0·81	43	—	—	0·78	41	0·63	35	0·45	28	0·21	24
	Oct.	0·56	35	0·64	38	0·76	45	—	—	0·69	44	0·55	38	0·35	30	0·12	20
	Nov.	0·48	34	0·55	36	0·66	39	—	—	0·59	39	0·44	35	0·25	30	0·05	15
	Dec.	0·39	32	0·47	32	0·60	42	—	—	0·56	41	0·43	36	0·25	30	—	—
1959	Jan.	0·37	28	0·44	30	0·58	43	—	—	0·61	43	0·49	35	0·32	28	—	—
	Feb.	0·44	32	0·50	36	0·66	42	0·78	46	0·71	47	0·59	43	0·41	34	0·20	24

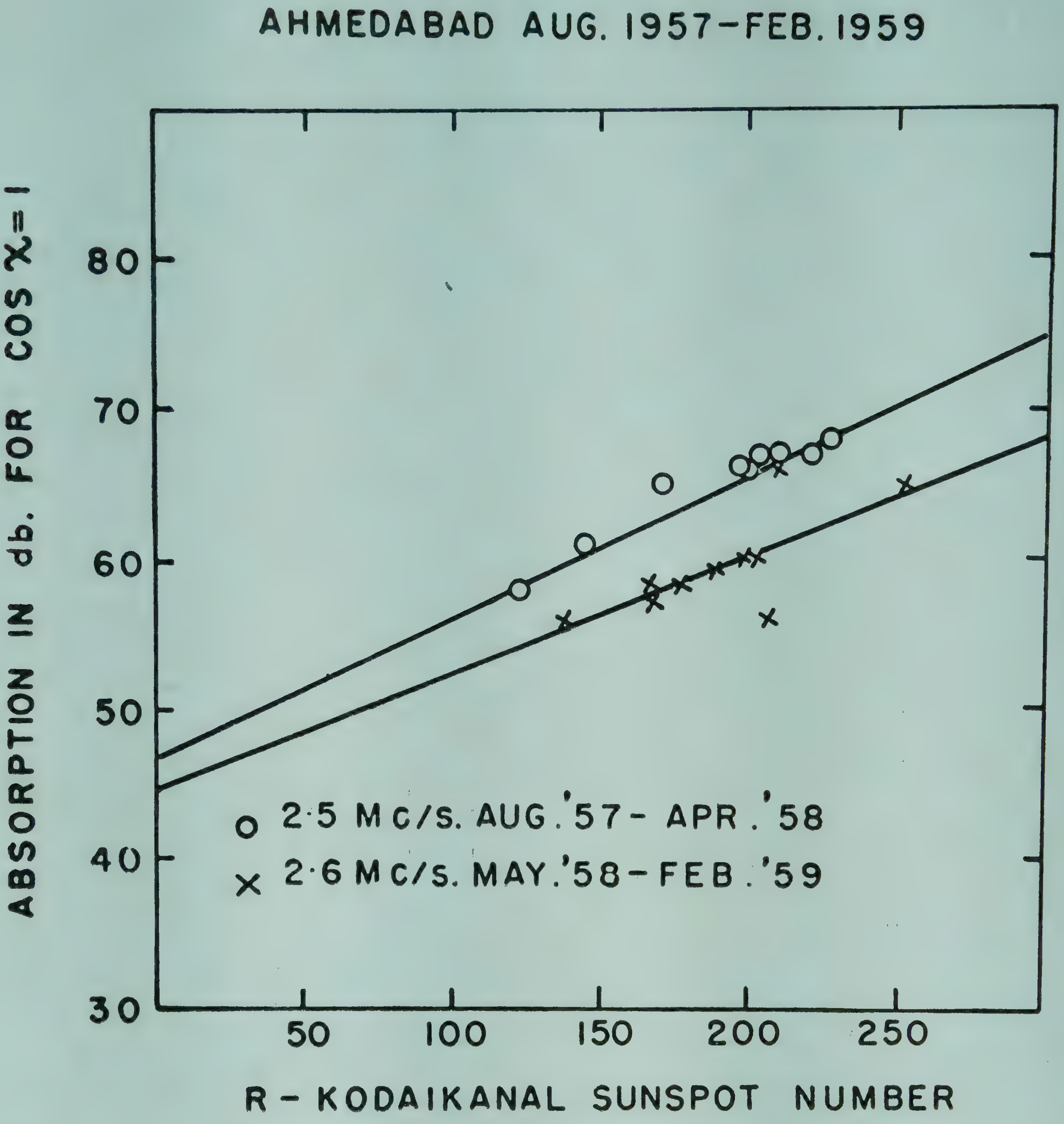

FIG. 1 — THE VARIATION WITH SUNSPOT NUMBER OF THE EXTRAPOLATED ABSORPTION FOR COS $\chi = 1$

exploring frequency to the critical frequency of the E layer. That the slopes of the lines are not affected by deviative absorption due to the E layer is evident from the fact that for the higher frequency, namely 2·6 Mc/s., the mean value of n has not decreased below the one shown by 2·5 Mc/s. Had there been a contribution from the deviative absorption it would have been larger on the higher frequency and would have decreased the slope rather than increased it.

Considering the fact that the data are available for 19 months only, it would be premature to draw conclusions on the seasonal variations in the value

TABLE 4 — VALUES FOR THE EXTRAPOLATED ABSORPTION L' FOR EACH MONTH AGAINST THE MONTHLY MEAN SUNSPOT NUMBERS

2·5 Mc/s.				2·6 Mc/s.			
	Month	L' db.	R		Month	L' db.	R
1957	Aug.	58	123	1958	May	58	167
	Sept.	65	171		June	59	189
	Oct.	67	211		July	60	202
	Nov.	66	198		Aug.	66	211
	Dec.	67	203		Sept.	56	207
1958	Jan.	68	227		Oct.	58	178
	Feb.	61	145		Nov.	57	168
	Mar.	66	200		Dec.	60	200
	Apr.	67	221	1959	Jan.	65	252
					Feb.	56	138

of n; however, it may be noted that the mean value of n for summer months works out to be 0·86, for winter it is 0·69 and 0·74 for the equinoxes. It is interesting to compare these with the values of n obtained by Bhonsle and Ramanathan[2] for D region absorption from the 25 Mc/s. cosmic noise measurements at Ahmedabad during 1957–58. They found that $n = 1{\cdot}1$ in summer, 1·0 in equinox and 0·8 in winter.

It may be noted that Appleton and Piggott[3], from a sequence of observations extending over two solar cycles, obtained a mean value of $n = 0{\cdot}75$ at Slough.

In order to remove the seasonal variations in the measured values of L, the line $\log \rho \propto \cos \chi$ corresponding to each month was extended to give the value of absorption L' corresponding to $\cos \chi = 1$. Table 4 gives for each month the value of the extrapolated absorption L'. Also shown in the table are the monthly mean sunspot numbers R provided by the Kodaikanal Astrophysical Observatory. Fig. 1 gives the graphs of L' versus R, the sunspot number for 2·5 and 2·6 Mc/s. They are straight lines.

The equation of the two straight lines can be written in the form

$$L' = L_0\,(1+\beta R)$$

where $L_0 = 47$ and $\beta = 0{\cdot}0020$ for 2·5 Mc/s.
and $L_0 = 45$ and $\beta = 0{\cdot}0018$ for 2·6 Mc/s.

The slope of the line is only slightly lower for the higher frequency, but the line is shifted down by a significant amount.

The points corresponding to August and September 1958 seem to fall outside the lower line.

It is interesting to note that though the monthly mean sunspot number is well correlated with the absorption in the D region, it is difficult to find a day-to-day correspondence between the two. There are days with fairly low absorption corresponding to large sunspot numbers and vice versa.

ACKNOWLEDGEMENT

The author is indebted to Prof. K. R. Ramanathan for guidance. Thanks are due to Sarvashri S. K. Alurkar, I. M. Gandotra and C. M. Patel for the help given in working the transmitter for the absorption measurements.

REFERENCES

1. SHIRKE, J. S., *J. Instn Telecomm. Engrs*, **5** (1959), 115.
2. BHONSLE, R. V. & RAMANATHAN, K. R., *J. sci. industr. Res.*, **17A** (1958), 40-45.
3. APPLETON, E. V. & PIGGOTT, W. R., *J. atmos. terr. Phys.*, **5** (1954), 144.

Collision frequency measurements in ionosphere at Waltair

K. V. V. RAMANA
B. RAMACHANDRA RAO

Ionospheric Laboratories, Physics Department
Andhra University, Waltair

The results of E and F region collision frequencies determined from absorption data are presented. The E region collisional frequencies are determined from 5·65 Mc/s. absorption data using Jaeger's method to separate out the D and E region contributions to the total absorption. An average value of $5{\cdot}3 \times 10^4$ c/s. is obtained for the E region collision frequency assuming a scale height of 7 km.

The electron collision frequencies in the F region are determined from deviative absorption data on several frequencies close to the F region critical frequency. The average value of the collision frequency for the F region is about $2{\cdot}4 \times 10^3$ c/s.

Several attempts have been made by earlier investigators like Eckersley[1], Farmer and Ratcliffe[2], White and Brown[3], Datta[4], Beynon and Davies[5], Schlapp[6] and Whitehead[7] to determine the electron collision frequencies in the E and F regions of the ionosphere from absorption data at various frequencies. But very little work has been done on the determination of electron collision frequency at low latitude stations. Hence, the absorption data on 5·65 Mc/s. have been utilized by the authors to determine the electron collision frequencies in the E region over Waltair, which is a low latitude station.

Special measurements were carried out on eight days to determine the electron collision frequencies in the F region from deviative absorption studies at various frequencies close to the critical penetration frequency. The results of these studies are presented in this paper.

The experimental technique used in these studies is the familiar vertical incidence pulse reflection method for absorption studies described earlier by Piggott[8] and others.

RESULTS AND DISCUSSION

E Region. Diurnal measurements of absorption on a frequency of 5·65 Mc/s. were taken for about ninety days during the years 1958 and 1959. The monthly mean daily variation of this absorption varied linearly with $F(f_0E/f) \cos \chi$, where $F(f_0E/f)$ is the Jaeger[9] function and χ is the solar zenith angle. The slope of the lines for the observations taken on each of the twenty months gives the value of $\nu_0 H/c$ for that particular month, where ν_0 is the electron collision frequency in the E region at the datum level h_0, which corresponds to a level of about 105 km., c the velocity of e-m waves and H, the scale height of the atmosphere at this level. Assuming values for H and c, the value of ν_0 can be calculated. Briggs[10] and Beynon and Davies[5] as well as several other investigators assumed a value of 10 km. for H. But, recent rocket measurements by Kaiser[11], Hulburt[12] and Horowitz and LaGow[13] show that the value of H appropriate to the E region at 105 km. is about 7 km. Assuming this value for the scale height, the values of ν_0 have been calculated for the observations of each month and the results are given in Table 1.

It is evident from this table that ν_0 varies between a minimum of about $3{\cdot}6 \times 10^4$ c/s. to a maximum of about $6{\cdot}4 \times 10^4$ c/s. giving an average value

TABLE 1 — ELECTRON COLLISION FREQUENCY FOR DIFFERENT MONTHS DURING 1958-59

	MONTH	$\bar{\nu}_0 \times 10^{-4}$ c/s.
1958	Mar.	6·30
	Apr.	5·36
	May	4·70
	June	4·80
	July	5·30
	Aug.	6·00
	Sept.	5·30
	Oct.	6·14
	Nov.	6·00
	Dec.	3·57
1959	Jan.	5·57
	Feb.	—
	Mar.	5·00
	Apr.	3·70
	May	4·70
	June	5·60
	July	6·43
	Aug.	5·14
	Sept.	5·30
	Oct.	5·71
	Nov.	6·00

TABLE 2 — COMPARATIVE STUDY OF ELECTRON COLLISION FREQUENCY DATA IN THE E REGION

AUTHOR(S)	HEIGHT *km.*	$\nu_0 \times 10^{-4}$ c/s.
Briggs	119	2·7
Nicolet	102	7·8*
Schlapp	105–120	2·0
Beynon & Davies	110	4·9
Whitehead	—	1·9±0·1
Ramana & Ramachandra Rao	105	5·3

*Theoretical value.

of $5{\cdot}3 \times 10^4$ c/s., which is found to be in reasonable agreement with those reported by previous investigators. The values of electron collision frequencies estimated by previous investigators along with the value obtained by the authors are presented in Table 2.

It is gratifying to note from Table 2 that the value of ν_0 obtained by the authors is in good agreement with that obtained by Beynon and Davies from similar studies. However, it must be noted that the differences in the values of ν_0 are mainly due to a discrepancy in the scale heights as ν_0 varies rapidly with height. It is well known that collision frequency rapidly increases with decrease of height. The low values obtained by some of the earlier investigators may be partly due to the higher level to which their results correspond.

F Region. It can be shown that the apparent reflection coefficient (ρ) of radio waves reflected from the ionosphere is related to the mean collision frequency $\bar{\nu}$ in the deviating zone by the relation

$$\log_e \rho = -\frac{\bar{\nu}}{2c}(P'-P) \tag{1}$$

if the operating frequency is close to the critical frequency of the region and if $\nu^2 << f^2$, and if the effect of the earth's magnetic field is neglected. In the above relation P' and P are the group and the phase paths respectively. As shown by Appleton[15], the above equation can be conveniently expressed in the form

$$\bar{\nu} = -c.f^{-1}\frac{\delta(f.\log_e \rho)}{\delta.h'} \tag{2}$$

This relation is used in the present investigation for determining collision frequencies in the F_2 region.

Experiments were conducted on eight days to determine the electron collision frequencies in the F region. In each experiment, observations of

TABLE 3 — MEAN COLLISION FREQUENCY WITH DATE AND TIME OF OBSERVATION AND VIRTUAL HEIGHT

DATE	TIME IST	h' *km.*	$\bar{\nu}\times10^{-3}$ c/s.
Dec. 29, 1958	0815	370	1·8
Dec. 30, 1958	0815	315	3·5
Jan. 1, 1959	0800	330	1·4
Jan. 2, 1959	0745	370	3·5
May 1, 1959	2115	450	1·6
June 7, 1959	2145	450	2·2
June 20, 1959	2130	550	2·7
July 7, 1959	2115	550	2·6
		Mean	2·4

TABLE 4 — COMPARATIVE STUDY OF ELECTRON COLLISION FREQUENCY DATA IN THE F REGION

AUTHOR(S)	HEIGHT* *km.*	$\bar{\nu}\times10^{-3}$ c/s.
Eckersley[1]	265	3·6
Farmer & Ratcliffe[2]	—	1·6 & 1·5
White & Brown[3]	250	5·0
Vilbig[16]	250–400	5·0–1·2
Ginsburg & Alpert[17]	300	3·0
Rawer, Bibl & Argence[18]	—	0·2
Datta[4]	—	3·8
Whitehead[7]	150–180	3·6±0·6
	180–200	3·0±0·6
Ramana & Ramachandra Rao	300	2·4

*Corresponds to true heights of reference.

amplitude were taken on six to seven frequencies and the absorption was calculated by using the relation

$$-\log_e \rho = \log_e F' - 2 \log_e F'' \tag{3}$$

where F' and F'' are the first and second hop reflection amplitudes. Graphs were plotted with h', the virtual height, as abscissa and $(f.\log_e \rho)$ as ordinate. From the graphs, the gradient $\delta(f.\log_e \rho)/\delta.h'$ was measured corresponding to any value of f. The values of $\bar{\nu}$, together with the date and time of observation and virtual height are presented in Table 3.

The values of $\bar{\nu}$ vary from a minimum of $1{\cdot}4\times10^3$ to a maximum of $3{\cdot}5\times10^3$, the average value being $2{\cdot}4\times10^3$ c/s.

It is interesting to make a comparative study of the results obtained by the authors with those of previous investigators. Table 4 presents the results of collision frequency studies conducted by various authors. From a study of this table, it can be seen that the results obtained by various investigators are in general agreement with one another with the exception of the result obtained by Rawer, Bibl and Argence[18], which is too low.

The electron collision frequency in the F region, as measured, is the sum of the various collisional frequencies and is given by

$$\nu = \nu_{(i,e)} + \nu_{(N_2+N,e)} + \nu_{(o,e)} + \nu_{(e,e)}$$

where $\nu_{(i,e)}$ is the frequency of ion-electron collisions, $\nu_{(N_2+N,e)}$ is the frequency of nitrogen particle-electron collisions, $\nu_{(o,e)}$ is the frequency of atomic oxygen-electron collisions and $\nu_{(e,e)}$ the electron-electron collision frequency. In the F region, the ion-electron collision term is much larger than the other terms. Theoretical analysis of Mazumdar's[19] expression for $\nu_{(i,e)}$ by Nicolet[14] and Gerson[20] shows that the value $\nu_{(i,e)}$ depends on electron concentration and to a larger extent on temperature. The theoretical expression, as given by Nicolet[21], is of the form

$$\nu_{(i,e)} = \left[34 + 8{\cdot}36 \log_{10} \frac{T^{3/2}}{N_e^{1/2}}\right] \times N_i \times T^{-3/2}$$

where T is the absolute temperature in the region, N_e is the electron density and N_i, the positive ion density. N_i can be taken as equal to $N_e(1+\lambda)$. For F_2 layer λ is nearly zero and hence $N_i \simeq N_e$.

Taking $f_0F_2 = 14$ Mc/s., which is the average value obtained during the period of observations on the eight days and $T = 1400$°K. for the F_2 layer at 300 km., a value given by Martyn[22], the $\nu_{(i,e)}$ comes out as $2{\cdot}2 \times 10^3$ for the F_2 layer, while the experimentally deduced average value of $\bar{\nu}$ is $2{\cdot}4 \times 10^3$. According to Nicolet, the value of $[\nu_{(N_2+N,e)} + \nu_{(o,e)}]$ is of the order of 100 at this level. Thus, the experimentally deduced value of $2{\cdot}4 \times 10^3$ c/s. is in very good agreement with the value obtained from theoretical considerations.

REFERENCES

1. ECKERSLEY, T. L., *Nature, Lond.*, **135** (1935), 435.
2. FARMER, F. T. & RATCLIFFE, J. A., *Nature, Lond.*, **135** (1935), 585; *Proc. phys. Soc. Lond.*, **48** (1936), 839.
3. WHITE, F. W. G. & BROWN, L. W., *Proc. roy. Soc.*, **153A** (1936), 639.
4. DATTA, S., *Res. Rep. Inst. Radio Phys. Electron.*, **8** (1955-56), 21.
5. BEYNON, W. J. G. & DAVIES, K., *The Physics of the Ionosphere*, Rep. Phys. Soc. Conf. Lond., 1955, 40.
6. SCHLAPP, D. M., *J. atmos. terr. Phys.*, **16** (1959), 340.
7. WHITEHEAD, J. D., *J. atmos. terr. Phys.*, **16** (1959), 283.
8. PIGGOTT, W. R., *Proc. Instn elect. Engrs*, **100** (1953), Pt III, 61.
9. JAEGER, J. C., *Proc. phys. Soc. Lond.*, **59** (1947), 87.
10. BRIGGS, B. H., D.Sc. Thesis, Cambridge University, 1951.
11. KAISER, T. R., *Rocket Exploration of the Upper Atmosphere* (Pergamon Press, London), Spec. Suppl., *J. atmos. terr. Phys.*, **1** (1954), 108.
12. HULBURT, E. O., *Advances in the Physics of the Upper Air Since* 1950, Naval Res. Lab. Rep. No. 4600, 1955.

13. Horowitz, R. & LaGow, H. E., *J. geophys. Res.*, **62** (1957), 57.
14. Nicolet, M., *J. atmos. terr. Phys.*, **3** (1953), 200.
15. Appleton, E. V., *Nature, Lond.*, **135** (1935), 618.
16. Vilbig, H. F., *Lehrbuch der Hoch-freqentz technic*: *I* (Akad Verlagsgesellschaft, Leipzig), 1944, 338.
17. Ginsburg, V. L. & Alpert, I. L., *Bull. Acad. Sci. U.R.S.S., Ser. Fiz.*, **8** (1944), 42.
18. Rawer, K., Bibl, K. & Argence, E., *Soc. Roy. Sci., Liège, Mémoires*, **12** (1952), 269.
19. Mazumdar, R. C., *Z. Phys.*, **107** (1937), 599.
20. Gerson, N. C., *Rep. Progr. Phys.*, **14** (1951), 316
21. Nicolet, M., *Physics of Fluids*, **2** (1959), 95.
22. Martyn, D. F., *Proc. Inst. Radio Engrs, N.Y.*, **47** (1959), 147.

Effect of magnetic activity on night-time absorption

K. V. V. RAMANA
Y. V. RAMANA MURTY
B. RAMACHANDRA RAO

Ionospheric Research Laboratories
Andhra University, Waltair

A study of the variation of night-time absorption with geomagnetic activity has been made. An important result of this study has been the observance of a linear relationship between $|\log_e \rho|$ for night-time data and geomagnetic K index.

Several previous investigators have studied the dependence of ionospheric absorption at high latitude stations on sunspot activity, magnetic activity, ionospheric storms, etc. Wells[1] and others pointed out that intense magnetic disturbances are accompanied by radio blackouts at high latitudes, but very few quantitative relationships have been established between magnetic activity and ionospheric absorption. Davies and Hagg[2] studied the correlation of midnight absorption on 2·0 Mc/s. with the magnetic K index and found that the absorption was independent of the K index up to $K = 5$ and that the absorption increased sharply with increase of K index above $K = 5$. In the light of this investigation, it was thought that it would be interesting to study the relationship between night-time absorption at Waltair and magnetic K index.

Vertical incidence pulse reflections on a frequency of 5·65 Mc/s. were received by a tuned dipole and fed to a BC 348Q receiver, modified for pulse reception, through a matched π-type attenuator. The detected output of the receiver was fed to the Y plates of a pulse oscillograph. Amplitude measurements were taken at 5-sec. intervals for about 10 min. and a mean of these measurements was taken for each sample. Thereby, the errors due to fading were minimized.

Results and Discussion

Absorption measurements during night were taken at Waltair (17°43′N: 83°18′E), a low latitude station, between March 1958 and February 1959.

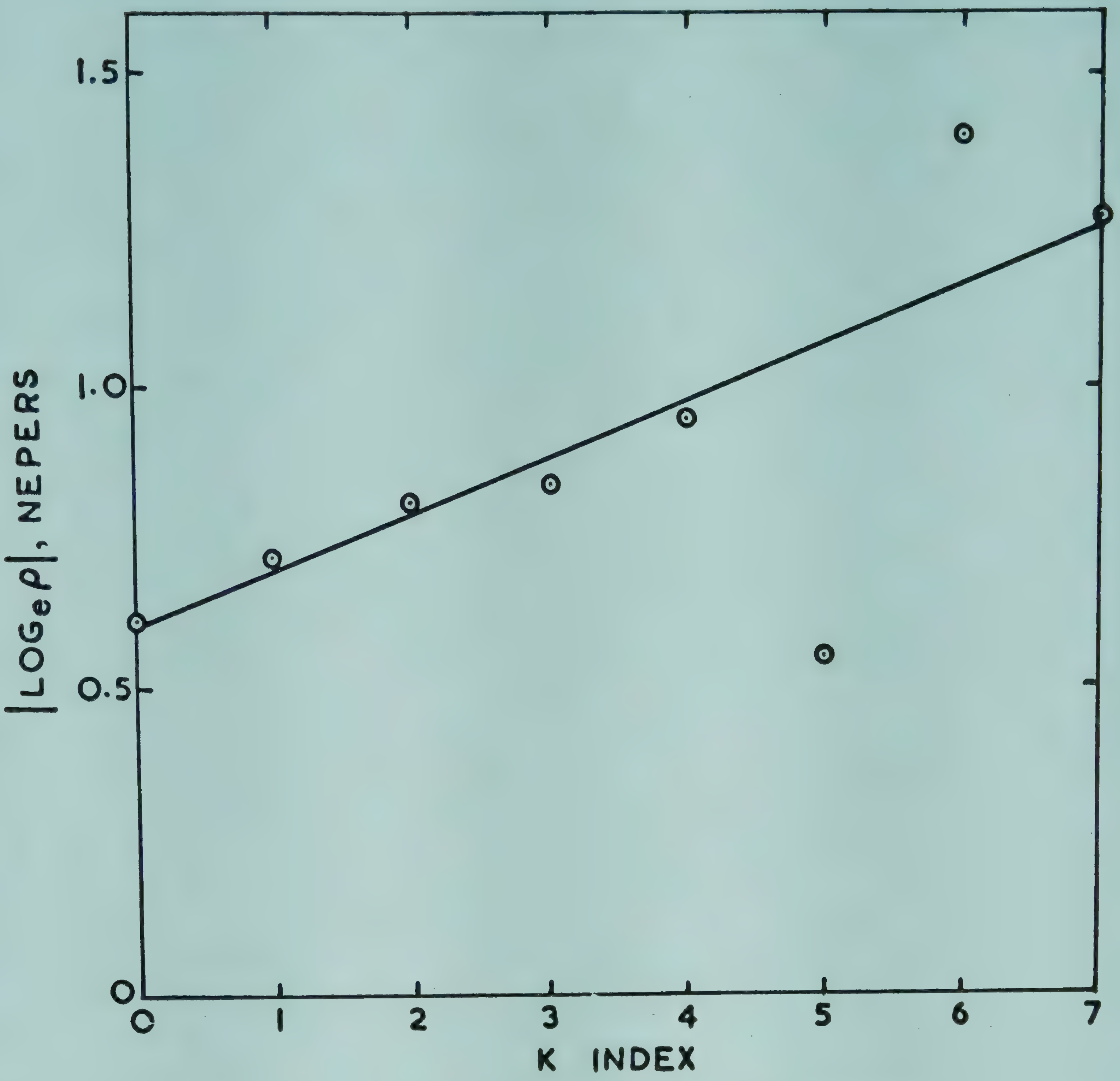

FIG. 1 — VARIATION OF NIGHT-TIME ABSORPTION WITH GEOMAGNETIC ACTIVITY

Measurements taken at hourly intervals were grouped into three-hour periods for which data of K indices are available. As no geomagnetic data are available for Waltair, the geomagnetic three-hour range K indices supplied by Alibag Observatory were used for this investigation. Alibag is situated on nearly the same geomagnetic latitude as Waltair. Values of $|\log_e \rho|$ which are excessive due to deviative absorption were eliminated from the study. Average of $|\log_e \rho|$ values were obtained for each of the three-hour periods. Values of $|\log_e \rho|$ corresponding to the same geomagnetic K index were summed up and the average value was obtained. A graph plotted with $|\log_e \rho|$ as ordinate and K index as abscissa is presented in Fig. 1. Out of eight mean values thus obtained, only two corresponding to values of 5 and 6 of K index depart somewhat significantly from the mean straight line which fits well with the other points in the plot. The departure of these values is understandable, considering the fact that they correspond to averages taken over lesser number of observations. It is of interest to note here that no such good linear relationship was obtained between noon values of $|\log_e \rho|$ and geomagnetic planetary K index, as the correlation coefficient in this case was only +0·36 as compared to a value of +0·75 for night-time $|\log_e \rho|$ and K index co-variation. However, Davies[3] found no significant correlation between geomagnetic activity and noon-time or midnight absorption.

The first important fact that emerges from this investigation is the higher correlation between night-time absorption and K index as compared to the noon-time absorption variation with K index.

The sharp increase of night-time absorption with K index observed by the authors and Davies and Hagg[2] lends support to the view that the night-time absorption is due to ionization in the lower ionosphere caused by corpuscular radiation which is responsible for the geomagnetic disturbances.

REFERENCES

1. WELLS, H. W., *Terr. Magn. atmos. Elect.*, **52** (1947), 315.
2. DAVIES, K. & HAGG, E. L., *J. atmos. terr. Phys.*, **6** (1955), 18.
3. DAVIES, K., *J. geophys. Res.*, **65** (1960), 2285.

* * *

Diurnal Variation of Absorption on 5·65 Mc/s. at Waltair. B. RAMACHANDRA RAO & K. V. V. RAMANA, Andhra University, Waltair [*J. sci. industr. Res.*, **17A** (Suppl.) (1958), 56].

Absorption measurements on 5·65 Mc/s. have been made at Waltair during the IGY period with a view to studying the variation of absorption with zenith angle. The values of the index of the cosine of zenith angle are found to vary from 0·88 to 1·75, the average being 1·25. A value of 2·2 is obtained for the average ratio of summer to winter noon absorption coefficient. (*Abstract*)

Sudden cosmic radio noise absorption associated with solar flares

K. A. SARADA
A. P. MITRA

National Physical Laboratory
New Delhi

The characteristics of flare-associated events in the cosmic noise records were examined. A study of about 100 such events, observed at both 22·4 and 30 Mc/s. during the IGY and IGC, lead to the following conclusions: (i) there is no one-to-one correspondence between the size or the occurrence of the SCNA and that of the optical flare; although larger SCNAs tend to be associated with the more intense flares; (ii) the SCNA follows generally the time curves of H_α line-width, but the maximum is delayed, on the average, by 2 min. and precedes the SEA by about 5 min.; (iii) the average time of growth of the SCNA is about 5 min.; (iv) the average sizes of the SCNAs corresponding to flares of class 2, 2^+ and 3 are around 2, 3 and 5 db. respectively at a frequency of 22·4 Mc/s.; and (v) the average magnitudes of ionization enhancements at the SCNA level for flares of class 2, 2^+ and 3 are around 3, 3·5 and 5 respectively.

Evidence is adduced to show that the SCNA is located at approximately the same level as the normal D region component of cosmic noise absorption.

The efficacy of the cosmic radio noise method as a tool for continuous flare patrol is now well known. Following the pioneering work of Shain and Mitra[1], this method has been used for both research and routine purposes in several countries, and during the IGY and IGC formed an accepted form of flare patrol. The effect is a fade-out and is similar to the Mögel-Dellinger effect, excepting that the entire time-curve can be drawn, making it thus an ideal curve for the study of ionospheric physics. Shain and Mitra[1] gave a larger number of such records, and showed that the SCNA effect was stronger for larger flares and that it began approximately at the same time as a visual flare, although the times of maxima and ends were not the same.

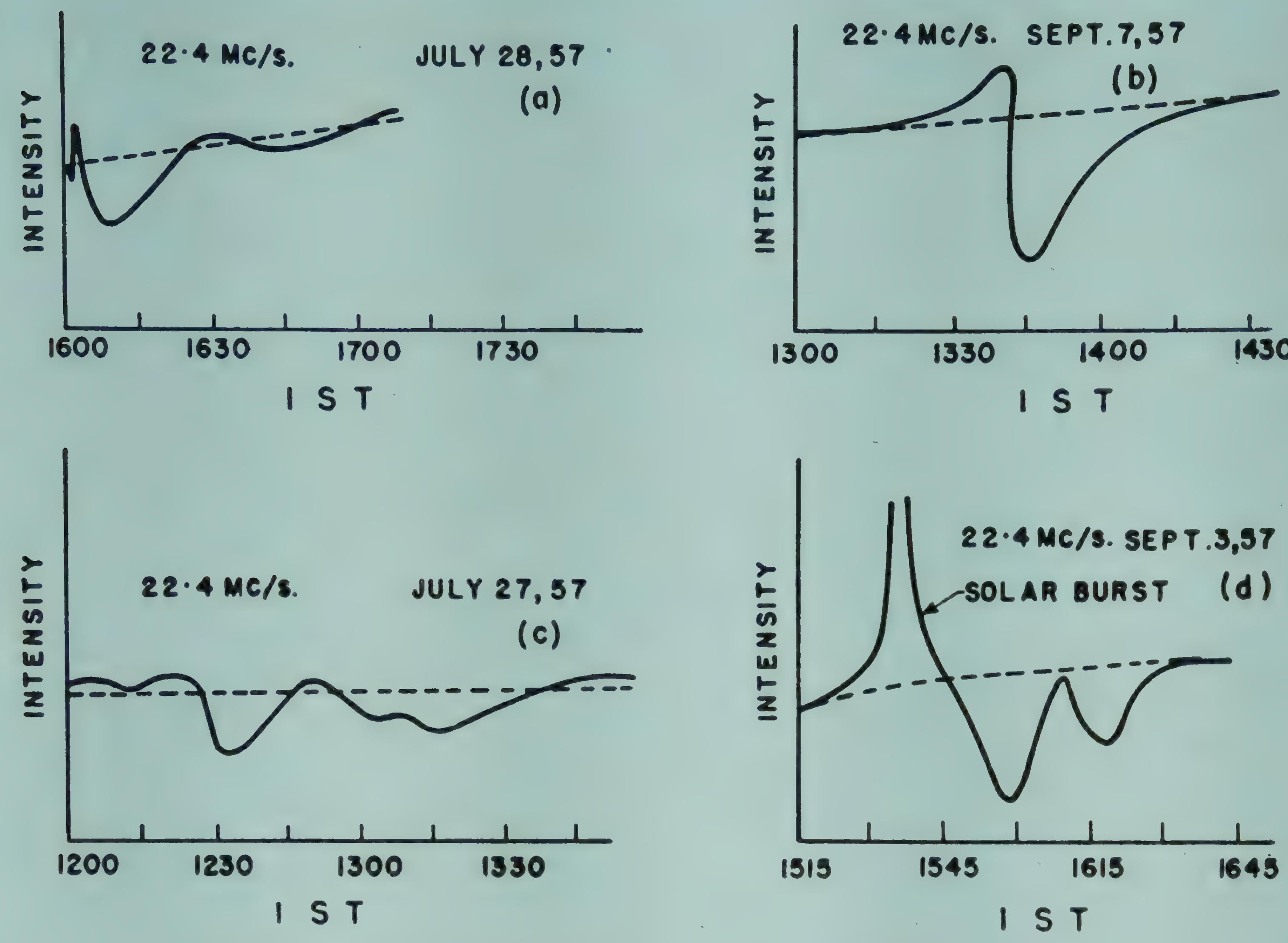

Fig. 1 — Different types of SCNAs observed at Delhi

The authors have used the cosmic noise observations for the study of solar flares using both the observations at 22·4 Mc/s. at Delhi and at 30 Mc/s. at Mussoorie. These studies have been supplemented by simultaneous radio flare patrol by the following additional techniques: (i) Rceording of SEA at frequencies of 27 and 100 kc/s., and (ii) quick-run ionospheric soundings by an automatic ionospheric recorder (C-4).

The objective of this work was twofold: (i) To examine the efficacy of the SCNA as a radio flare patrol service, and (ii) to investigate the changes occurring in the ionosphere during solar flares.

In this paper, the results obtained by the cosmic radio noise method are discussed.

Radio Flare Patrol at Delhi and Mussoorie

A large number of SCNAs have been observed. Some typical cases are shown in Fig. 1. Many of these were preceded by solar bursts. Of the 90 major SCNAs recorded, 60 coincided with solar flares.

For each SCNA, the following data were recorded: times of beginning, maximum and end of the effects and the maximum absorption in decibels. The time of end was defined as the time at which the absorption had fallen to

TABLE 1 — MAJOR SCNAs OBSERVED IN DELHI ON 22·4 Mc/s. ASSOCIATED WITH OPTICAL FLARES

MONTH	DATE	SCA			EXCESS ABSORPTION *db.*	OPTICAL FLARE			CLASS OF FLARE
		Beginning	Max. (UT)	End		Beginning	Max. (UT)	End	
July 1957	20	1426	1428	1435	5·6	1406	—	1503	1
	26	0917	0920	0930	0·9	—	—	—	—
	27	0658	0703	0715	3·4	0653	—	0808	2
	27	0730	0743	0805	1·8	—	—	0806	2
	28	1032	1041	1055	3·6	1023	—	1105	1
	30	2310	2317	—	2·3	2315	—	2327	1
Aug. 1957	1	0630	0643	0700	2·2	0614	—	—	2
	8	1121	1127	1150	2·1	1119	—	—	2
	31	0235	0238	0255	0·7	—	—	—	—
Sept. 1957	1	0200	0205	0230	8·1	—	—	—	—
	3	0758	0803	—	1·9	0754	0759	0841	2^+
	3	1022	1027	1050	11·0	1024	1028	1052	2
	4	0343	0343	0403	3·3	—	—	—	—
	7	0812	0816	0841	8·4	0811	0823	0831	2
	14	0725	0729	0810	2·5	—	—	—	—
	15	0336	0341	0415	1·9	0230	—	0300	2^+
	15	0430	0435	0445	2·2	0426	0428	0450	2
	17	0808	0815	—	1·1	0808	—	1000	2^+
	18	0630	0650	0730	2·3	0624	—	0708	2^+
	19	0402	0410	—	5·0	0400	0406	0500	3
	19	0753	0812	0840	—	0750	0809	1006	2^+
	20	0745	0800	—	3·0	—	—	—	—
	21	0412	0420	—	3·5	0410	—	0427	2
	22	1310	1315	1345	2·9	1248	—	1418	2^+
	23	0645	0655	—	4·0	0503	—	—	2^+
	30	0602	0605	—	4·1	—	—	—	—
Oct. 1957	20	0252	0255	—	3·5	—	—	—	—
	23	0625	0628	0643	3·4	0623	—	0645	3
	26	0348	0352	—	4·4	—	—	—	—
Dec. 1957	17	0558	0606	0615	2·0	—	—	—	—

10 per cent of its maximum value. Some of the major effects are listed in Tables 1 and 2.

The relation between the importance of a flare and the maximum excess absorption during the associated SCNA on the occasions when both were recorded are shown in Figs. 2(a) and 2(b) for 22·4 and 30 Mc/s. respectively. It is seen that the flares classed 2^+ or 3 are clearly associated with larger SCNAs. The average sizes of the SCNAs corresponding to flares of class 2, 2^+ and 3 are 2, 3 and 5 db. respectively.

TABLE 2 — MAJOR SCNAs OBSERVED IN MUSSOORIE ON 30 Mc/s. ASSOCIATED WITH OPTICAL FLARES

MONTH	DATE	SCA			EXCESS ABSORPTION *db.*	OPTICAL FLARE			CLASS OF FLARE
		Beginning	Max. (UT)	End		Beginning	Max. (UT)	End	
Feb. 1958	11	0828	0833	0945	1·3	0823	—	0837	2
	26	0550	0600	0630	1·9	0547	0548	0630	2
	28	0815	0835	0950	2·2	0800	—	0825	2
Mar. 1958	1	0910	0914	1010	4·0	0911	—	0938	3^+
	3	1014	1020	1120	11·0	1013	1018	1048	3
	7	0807	0813	0910	3·2	—	—	—	—
	7	1030	1045	1145	2·5	1030	—	1156	2
	9	0950	0955	1020	2·5	0946	0956	1032	2
	10	1105	1120	1200	0·9	1035	—	1345	2
	11	0810	0820	0850	1·7	—	—	0837	2
	19	1117	1123	1210	3·4	1114	—	1140	2
	20	1445	—	—	2·6	1445	—	—	2
	23	0950	(1040)	1245	>13·0	0951	1005	1200	3^+
	24	0755	0810	0840	0·8	0756	0758	0803	2
	27	1035	1040	1120	2·0	1042	—	1116	2^+
	28	1033	1035	—	4·1	1033	—	1114	2^+
	30	1005	1008	1105	2·1	1007	1020	1054	2
	30	0817	0825	—	2·3	0817	—	0846	2^+
	30	0838	0845	0910	1·5	0842	0844	0853	2
Apr. 1958	5	0755	0805	0850	2·5	0752	0809	0849	2^+
May 1958	28	0757	0802	0820	4·2	0805	0814	0817	2
July 1958	21	1125	1129	—	1·2	1125	—	1132	1
	26	0857	0902	0923	1·8	0858	—	0924	2
	28	0809	0815	—	1·8	0858	—	1016	2
	29	0300	0305	0400	6·0	0303	—	0359	3
	29	1145	1210	1300	3·1	1140	1143	1220	2^+
Aug. 1958	23	1015	1030	1110	3·6	1014	—	1048	2
	28	1035	—	1130	8·1	1032	—	1210	2^+
	30	1340	1350	1420	3·6	1412	—	1520	2
Sept. 1958	12	0702	0705	0750	1·1	0702	—	0730	2^+
	12	0915	0920	1000	1·4	0919	—	0956	2
	14	0840	—	0925	2·5	0831	—	1001	2^+
	15	0410	0420	0510	3·0	0406	—	0525	2^+
Nov. 1958	23	0751	0754	0825	3·8	0752	—	0825	2
	30	1145	1150	1205	2·1	1145	1152	1207	2^+
Dec. 1958	3	0700	0703	0730	2·4	0701	0703	0730	2
	3	0957	1002	1032	3·6	0958	—	1002	2^+
Apr. 1959	13	0832	0840	0915	2·3	0831	—	0923	3
	15	0834	0848	—	6·0	0832	—	0844	2

Fig. 3 shows histograms of time of growth of the SCNAs on 22·4 and 30 Mc/s. The medians for both cases were 5 min. This agrees with the previous value obtained by Shain and Mitra[1].

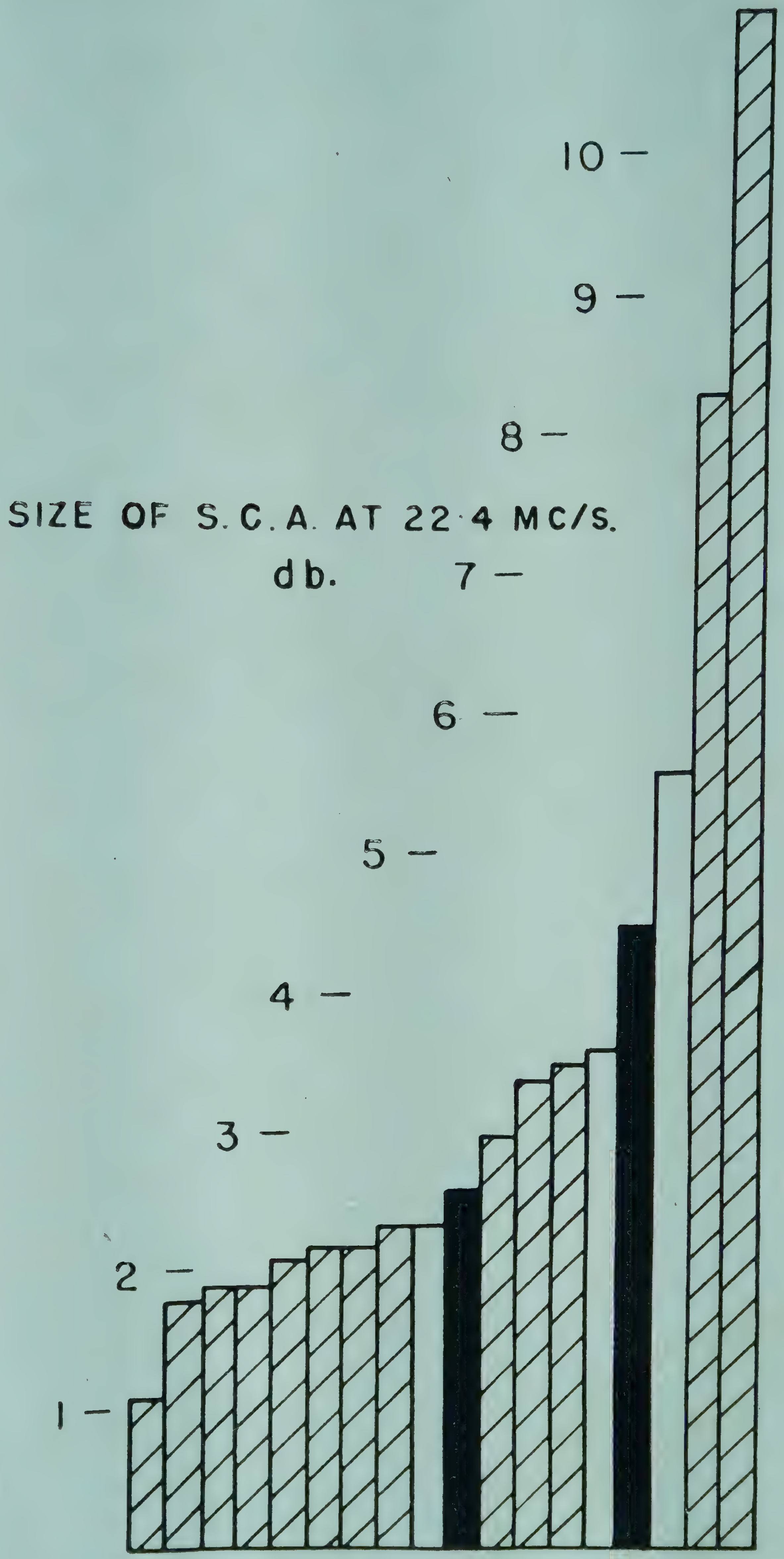

FIG. 2(a) — ASSOCIATION OF MAXIMUM ABSORPTION DURING SCNAs WITH THE FLARE IMPORTANCE FOR 22·4 Mc/s.

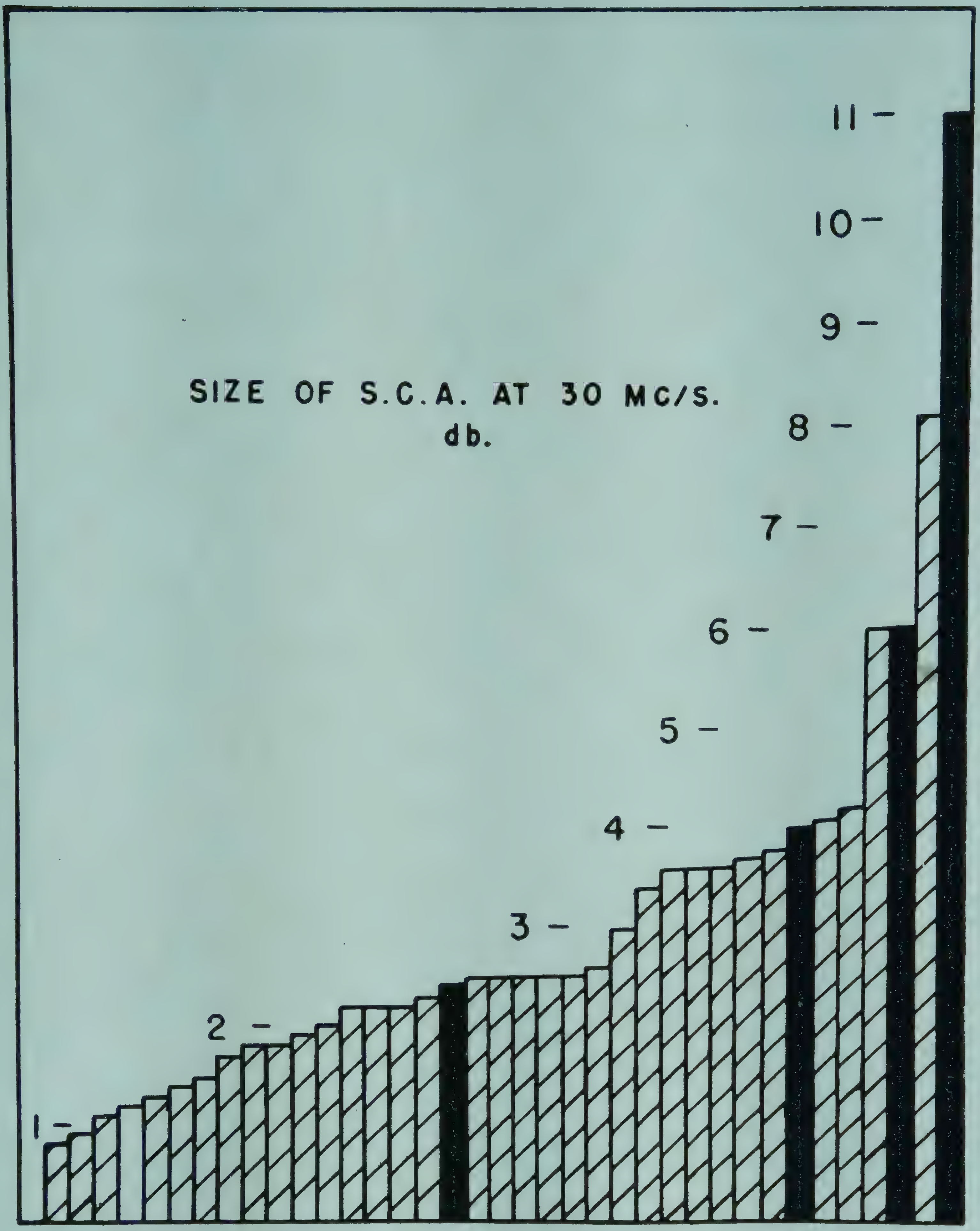

FIG. 2(b) — ASSOCIATION OF MAXIMUM ABSORPTION DURING SCNAS WITH THE FLARE IMPORTANCE FOR 30 Mc/s.

It has also been observed that larger SCNAs tend to have longer durations. However, cases of larger SCNAs having short lives are by no means rare.

In Fig. 4 temporal associations of SCNAs and flares are shown. Each SCNA is represented by a thin horizontal line proportional to its duration and the lines are arranged in order of increasing length. The time of maximum of

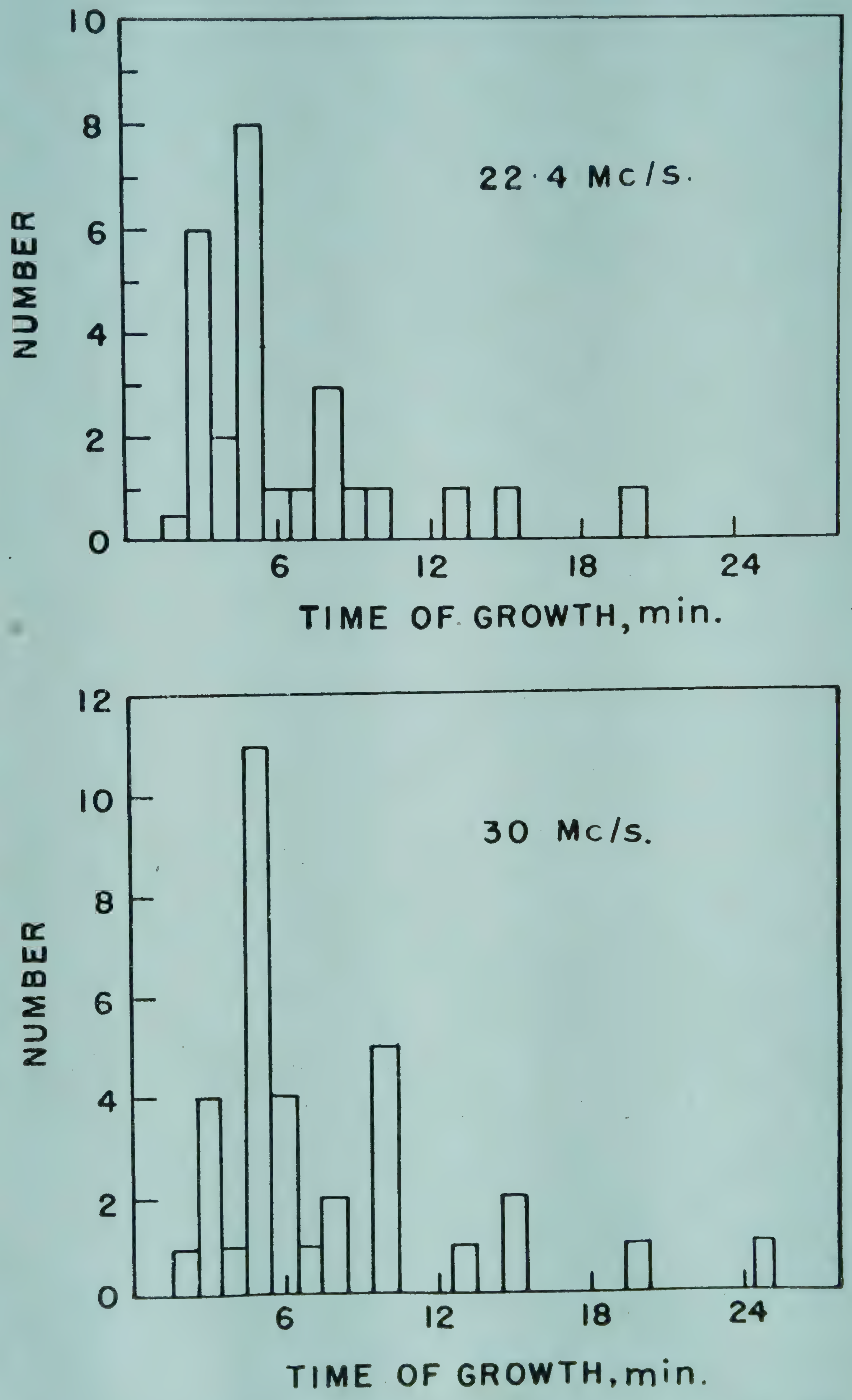

Fig. 3 — Histograms showing the relative occurrence of SCNAs with different times of growth

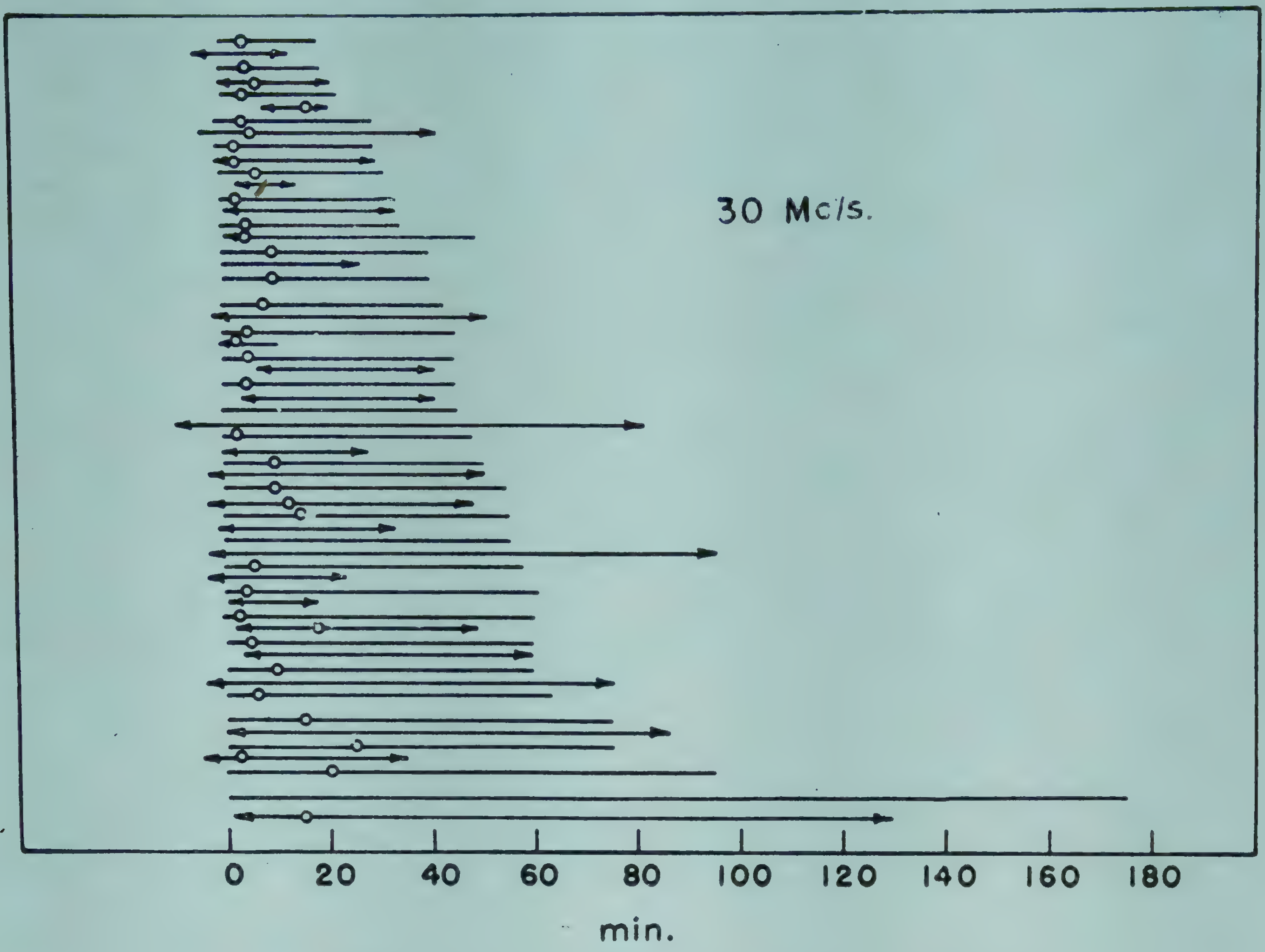

FIG. 4 — TEMPORAL ASSOCIATION OF SCNAs AND FLARES

SCNA is represented by a small circle. The accompanying flare is represented by a thick line just below. If the start or finish is seen, the line is terminated by an arrow; otherwise it is left blunt. A small circle marks the maximum when reported. The figure shows the close association between the SCNA and optical flares. When the times of start and maximum of the flare are given, the agreement with SCNAs is often close.

COMPARATIVE STUDY OF THE SCNA AND OTHER EFFECTS

The time curve of the SCNA is often remarkably similar to that of the H_α line-width. It is also similar to the time curves of other SID effects, such as SEA, SPA and magnetic crochet. However, there are small but important differences; the most striking difference is that the maxima of the SIDs occur a little later than the time of maximum of H_α line-width, and the decay curves are also somewhat displaced. Further, the time curves of different SIDs are not identical; some are more delayed than others. In Fig. 5, the time curves of several SIDs occurring on March 28, 1958 and April 13, 1959 are given. The SCNA curves are reproduced from the authors' own observations (taken at Mussoorie on 30 Mc/s.); those of SEA, SWF, magnetic crochets and light curves are reproduced from a report by Ellison, McKenna and Reid[2]. It will be noted that in both cases the SCNA maximizes at nearly the same time as the optical flare, but the magnetic crochets and the SEAs maximize

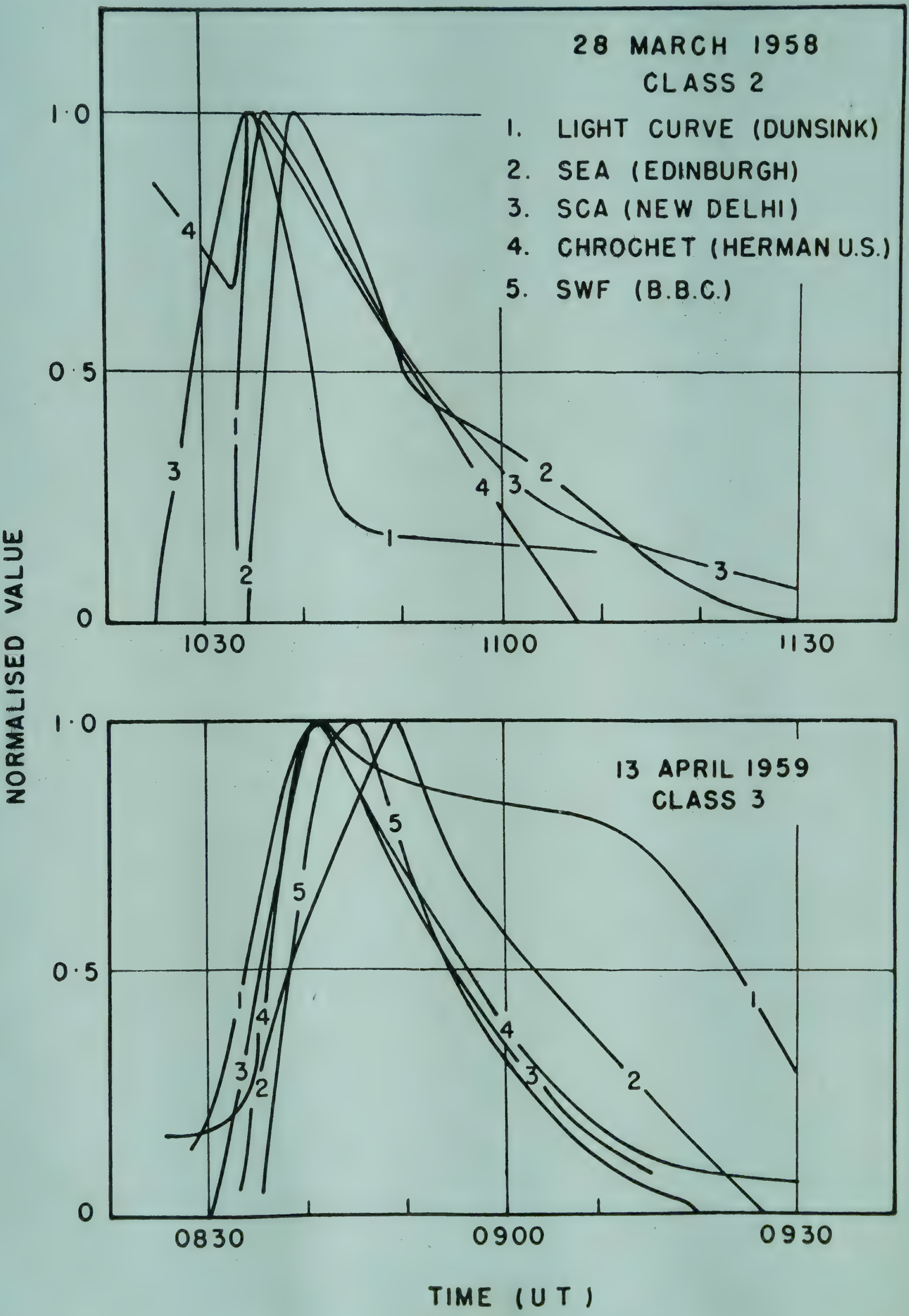

Fig. 5 — Time curves of different SIDs

about 2 and 8 min. later. These values are found to be fairly typical. A detailed examination of the authors' SCNAs indicate that, on the average, the time lag of the SCNA (from the maximum of H_α emission) is about 2 min. Quite often the SCNA maximum precedes the H_α maximum. The SEAs, on the other hand, maximize some 7 min. after H_α maximum. The decay curve of the SEA also consistently lags behind that of the SCNA.

There is thus a real difference in the sluggishness of the two effects.

ANALYSIS OF SCNA TIME CURVES

It is generally believed that all the SIDs originate because of an additional ionization produced in the D region, presumably confined within the heights 50–100 km. This ionization causes improved reflectivity for the low and very low frequency radio waves and produces greater absorption for medium and short waves.

The actual magnitude and distribution of the fade-out ionization is not reliably known. It was formerly believed that such ionization is the result of an enhancement of the L_α radiation responsible for the normal D region. Recent observations by U.S. Naval Research Laboratory[3], however, strongly suggest that at least part of the flare ionization is produced by X-rays in the range 1·5–8 Å. It has also been suggested that the flare ionization may be composite, with X-rays providing ionization at the base of the D layer and L_α providing ionization at the level of the SCNA[4].

It is possible to obtain some information on the fade-out ionization from an analysis of the characteristics of SCNAs. It is also possible, provided certain assumptions are made, to obtain information about the recombination coefficient, or alternatively of the quiet day ionization at the level of the SCNA. Methods used for such analysis and the results obtained are outlined below.

The methods of analysis given by Appleton and Piggott[5] and by Mitra[6] have been used.

The equation for electron density during the decay of the flare is

$$\frac{dN_x}{dt} = q_x - \alpha N_x^2 - 2\alpha N_x N_0 \tag{1}$$

where N_x is the excess electron density at any time during the flare.

If one leaves out the initial position of the decay curve so that for the period of analysis q_x is zero or small, then

$$\frac{dN_x/dt}{N_x} = -\alpha(N_f+N_0) = -Q \tag{2}$$

If, therefore, $N_f >> N_0$, then

$$\frac{1}{N_x} = \frac{1}{N_{x_0}} + \alpha t \tag{3}$$

Now, if, during the course of the flare, the level of the absorbing layer remains practically unchanged, then the excess absorption $\Delta \log \rho$ is proportional to N_x, so that

$$\frac{(\log \rho)_f}{(\log \rho)_0} = \frac{N_f}{N_0} = K \tag{4}$$

and

$$\frac{1}{\Delta \log \rho} = \frac{1}{(\Delta \log \rho)_0} + \frac{\alpha}{G} t \tag{5}$$

where G is a constant relating absorption with electron density.

If, however, N_x is small in comparison with N_0 so that it is possible to ignore N_x^2 compared with $2N_0N_x$, then, for $q_x = 0$

$$N_x = N_{x_0} \exp. [-2\alpha N_0 t] \tag{6}$$

In the more general case where N_x and N_0 are comparable[6]

$$N_x = N_{x_0} \left[\frac{2N_0}{N_{x_0}(e^{2\alpha N_0 t} - 1) + 2\alpha N_0 e^{2\alpha N_0 t}} \right] \tag{7}$$

Equation (7) may be rewritten as

$$(2\alpha N_0)^{-1} = \tau_0 = t/P \tag{8}$$

where

$$P = \log_e \left[\frac{N_{x_0}}{N_x} + \frac{N_{x_0}}{2N_0} \right] - \log_e \left[1 + \frac{N_{x_0}}{N_0} \right]$$

Thus it is possible to determine normal day relaxation time from flare time observations of absorption.

The above equations are also applicable to all parameters which are proportional to N and may, therefore, be used for SCNAs. The following results have been derived.

Location of Fade-out Ionization. In the past, it has been generally accepted that the fade-out ionization occurs principally in the D region and is a one-layer effect. This is confirmed by the authors' observations. Consider the decay curves of excess absorption for medium and short waves and for SCNAs. It is found that the reciprocal of the excess absorption, in the majority of cases, varies linearly with time during most of the decay period. Fig. 6 shows the time variations of $(\Delta \log \rho)^{-1}$ for a medium wave fade-out reported by Appleton and Piggott[5] and two SCNAs 22·4 and 30 Mc/s. recorded by the authors. Such linear relationships are compatible only with absorption occurring at one level.

It is possible to give limits to the height between which this layer must be located. It is found that in most cases (both SCNA and fade-out), $\alpha(N_f + N_0)$ decreases asymptotically to a value of about 5×10^{-4}/sec. near the end of the flare. For the fade-out absorption, therefore,

$$2\alpha N_0 = 5 \times 10^{-4}/\text{sec.}$$

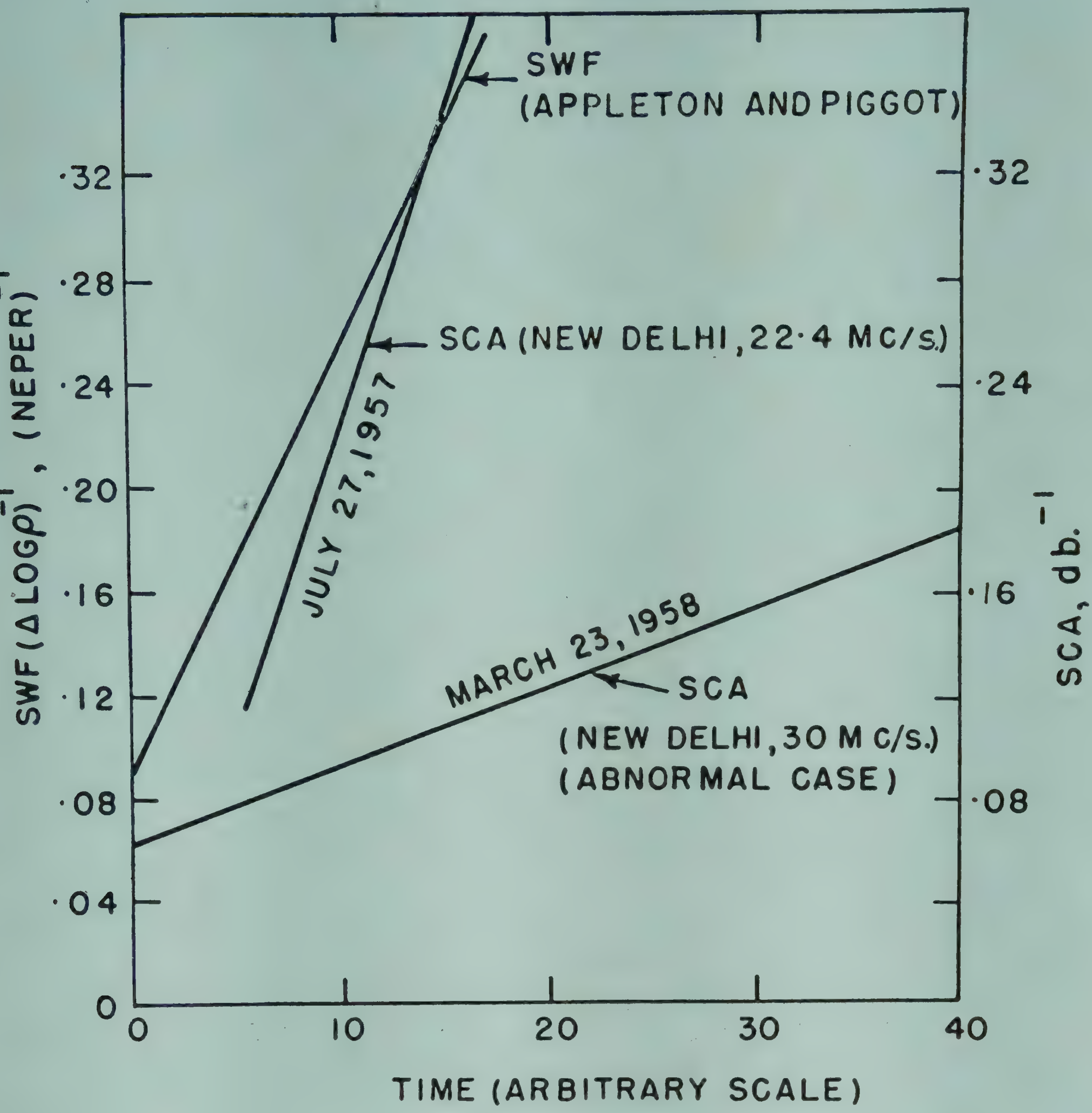

FIG. 6 — VARIATION OF THE RECIPROCAL OF ABSORPTION WITH TIME DURING THE DECAY PERIOD OF A FLARE

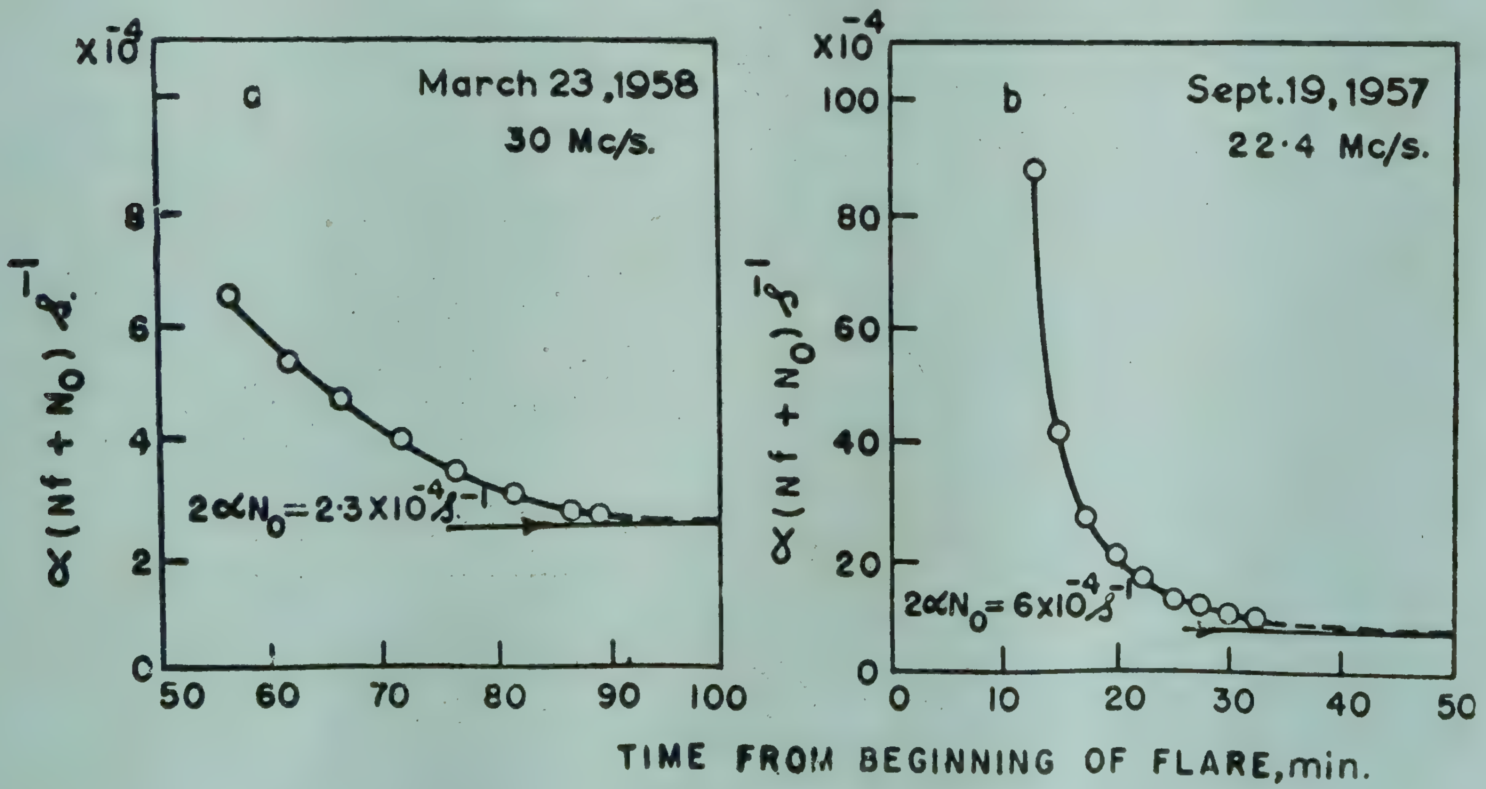

FIG. 7 — TIME VARIATION OF $\alpha(N_f+N_0)$ DURING SCNAs

TABLE 3 — ESTIMATES OF IONIZATION ENHANCEMENT

AUTHORS	METHOD	FREQUENCY Mc/s.	IONIZATION ENHANCEMENTS	REMARKS
Shain & Mitra	Cosmic noise	18·3	2·5 (class 1)	
			4·5 (class 2)	
			7·0 (class 3)	
Sarada & Mitra	Cosmic noise	22·4	3·0 (class 2)	
		30·0	3·5 (class 2)	
			5·0 (class 3)	
Appleton & Piggott	Pulse technique		5–10	

This is also the value for the normal absorption level. It may, therefore, be concluded that the fade-out absorption is located at approximately the same level as normal absorption (that is, around 90 km.).

Magnitude of Ionization Enhancements. If the above conclusion is accepted, then it becomes justified to use Equation (4) in determining the parameter (N_f/N_0). The values normally range between 2 and 9, the larger values occurring for more intense flares. For flares of class 2, 2^+ and 3, the average magnitudes of (N_f/N_0) are 3, 3·5 and 5 respectively.

Estimates of ionization enhancement are given in Table 3.

Variation of $\alpha(N_f+N_0)$ during Flares. The variation of ionization during the decay position of the flares was obtained by using Equation (2) for a number of SCNAs. Two cases are shown in Fig. 7(a, b). The SCNA of September 19, a typical case, shows that the value of $\alpha(N_f+N_0)$ varies from 80×10^{-4}/sec. near the peak of the flare to about 6×10^{-4}/sec. near the end of the flare. Most SCNAs give values similar to those of Fig. 7(b).

ACKNOWLEDGEMENT

The authors wish to thank Shri R. Parthasarathy for his help during the phase of the design and installation of the equipment, and Shri C. V. Subramaniyam and Miss S. Aggarwal for help in the preparation of the paper.

REFERENCES

1. SHAIN, C. A. & MITRA, A. P., *J. atmos. terr. Phys.*, **5** (1954), 116.
2. ELLISON, M. A. *et al.*, *Dunsink Observatory Publications*, **1**(1) (1960), 1.
3. FRIEDMAN, H. *et al.*, *IGY Rocket Rep.* No. **1** (1958), 179.
4. MITRA, A. P., *The Pennsylvania State University, Ionospheric Res. Sci. Rep.* No. 142, Dec. 1960.
5. APPLETON, E. V. & PIGGOTT, W. R., *J. atmos. terr. Phys.*, **5** (1954), 141.
6. MITRA, A. P., *The Pennsylvania State University, Ionospheric Res. Sci. Rep.* No. 112, Oct. 1958.

Effect of solar flares on E region drifts at Waltair

R. RAGHAVA RAO
B. RAMACHANDRA RAO

Ionospheric Research Laboratories
Physics Department, Andhra University
Waltair

The effect of two solar flares on E region drifts at Waltair has been studied. An increase in the amplitude of steady and 24-hourly components has been observed on solar flare days. Both the 24- and 12-hourly components have shown a more definite clockwise rotation on flare days compared to the quiet days. The results are discussed in the light of earlier work on solar flare effects.

Some solar flares are usually accompanied by sudden ionospheric disturbances (SID) and magnetic storms due to the augmentation of ionization in E and D regions. Recently Toubenheim[1] has quantitatively shown the enhancement of E layer critical frequency during SID. Vallard and Toubenheim[2] found a phase difference of 15°–30° between s.f.e. current and S_q current systems and it was suggested that the s.f.e. current system must be situated below S_q current system. Mitra and Jones[3] also suggested that the s.f.e. current system flows either in or below E layer. Vestine[4] has deduced tentative wind systems which could produce the observed magnetic storms and pointed out the necessity of experimental measurement of ionospheric movements to check up the dynamo theory of disturbances. The effect of solar flares on ionospheric drifts in the E region has not yet been studied by earlier investigators. The authors have, therefore, undertaken a study of the solar flare effects on drifts using the observations taken during IGY and IGC periods. Though quite a number of solar flares were reported during the IGY periods, in most of the cases there was much of absorption particularly for the major part of the period around noon, that sufficient number of E region drift observations could not be obtained. However, on two disturbed days, namely October 23 and 24, 1958, which were declared as Special World Intervals during IGY, sufficient number of observations were available to enable this study to be made. On both these days solar flares of importance 1–2 have been reported by several observatories[5].

RESULTS AND DISCUSSIONS

The horizontal drifts on these flare days were measured by the similar fades method which was suitably modified and described in an earlier paper[6]. The data for quiet days in this month have already been reported recently by the authors[7] in a detailed paper on quiet day drifts at Waltair covering a period of observation of two years. The diurnal variation of N–S and E–W components of E region drifts at Waltair for the data of both these flare days put together is shown in Fig. 1 along with the curves for the data of the quiet days in that month. The results of the harmonic analysis for these curves are given below:

$$\text{s.f.e. days}\quad \begin{cases} \text{N–S} & -33{\cdot}0+73\sin(t+256)+37\sin(2t+62)\\ \text{E–W} & 35{\cdot}1+81\sin(t+101)+34\sin(2t+296)\end{cases}$$

$$\text{quiet days}\quad \begin{cases} \text{N–S} & -14{\cdot}1+5{\cdot}2\sin(t+71)+56\sin(2t+68)\\ \text{E–W} & 24{\cdot}1+73\sin(t+65)+17\sin(2t+252)\end{cases}$$

A polar plot of the steady, 24-hourly and 12-hourly components is also presented in Fig. 2 for both disturbed and quiet days. The most striking difference observed between the s.f.e. and quiet day curves is the predominant increase in the amplitudes of the steady and 24-hourly components on s.f.e. days. There is no significant change in the direction of the steady vector between s.f.e. and quiet days. The N–S component of the 24-hourly drift vector is very small on quiet days in this month, but on disturbed days the N–S component has increased in amplitude to nearly the same value as the amplitude of the E–W component. The phase difference between N–S and E–W components is such that more definite clockwise rotation is indicated on s.f.e. days compared to quiet days. No significant difference in the amplitude of the 12-hourly components of the s.f.e. and quiet days is noticed, but the phase angle difference has decreased on s.f.e. days indicating a definite clockwise rotation. A peculiar feature of the quiet day drift behaviour during this month is that there is a certain amount of uncertainty in the sense of drift vector for both 24- and 12-hourly components as the phase angle difference between the N–S and E–W components is close to 180°. The s.f.e. curves have no such uncertainty and show a definite clockwise rotation with more amplitude of drift for the 24-hourly component.

An interesting feature of the 24-hourly periodic component of the drifts is the large phase difference of about 3 hr between drift vector on s.f.e. and quiet days. The 24-hourly s.f.e. drift vector is always ahead in phase compared to S_q drift vector. This large difference in phase between the quiet day and disturbed day 24-hourly periodic component may be regarded as

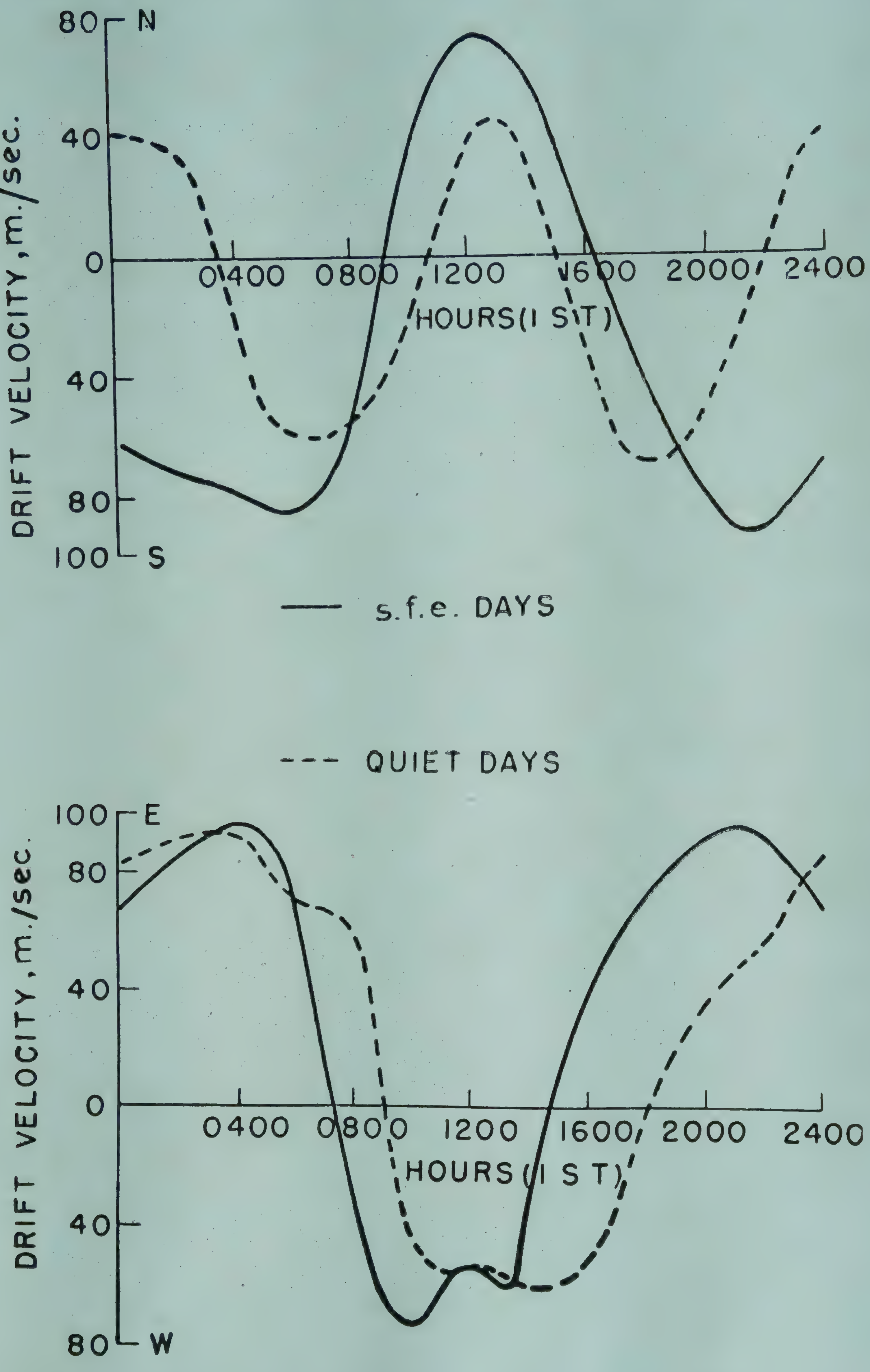

Fig. 1 — Comparison of diurnal variation of N–S and E–W components for s.f.e. and quiet days

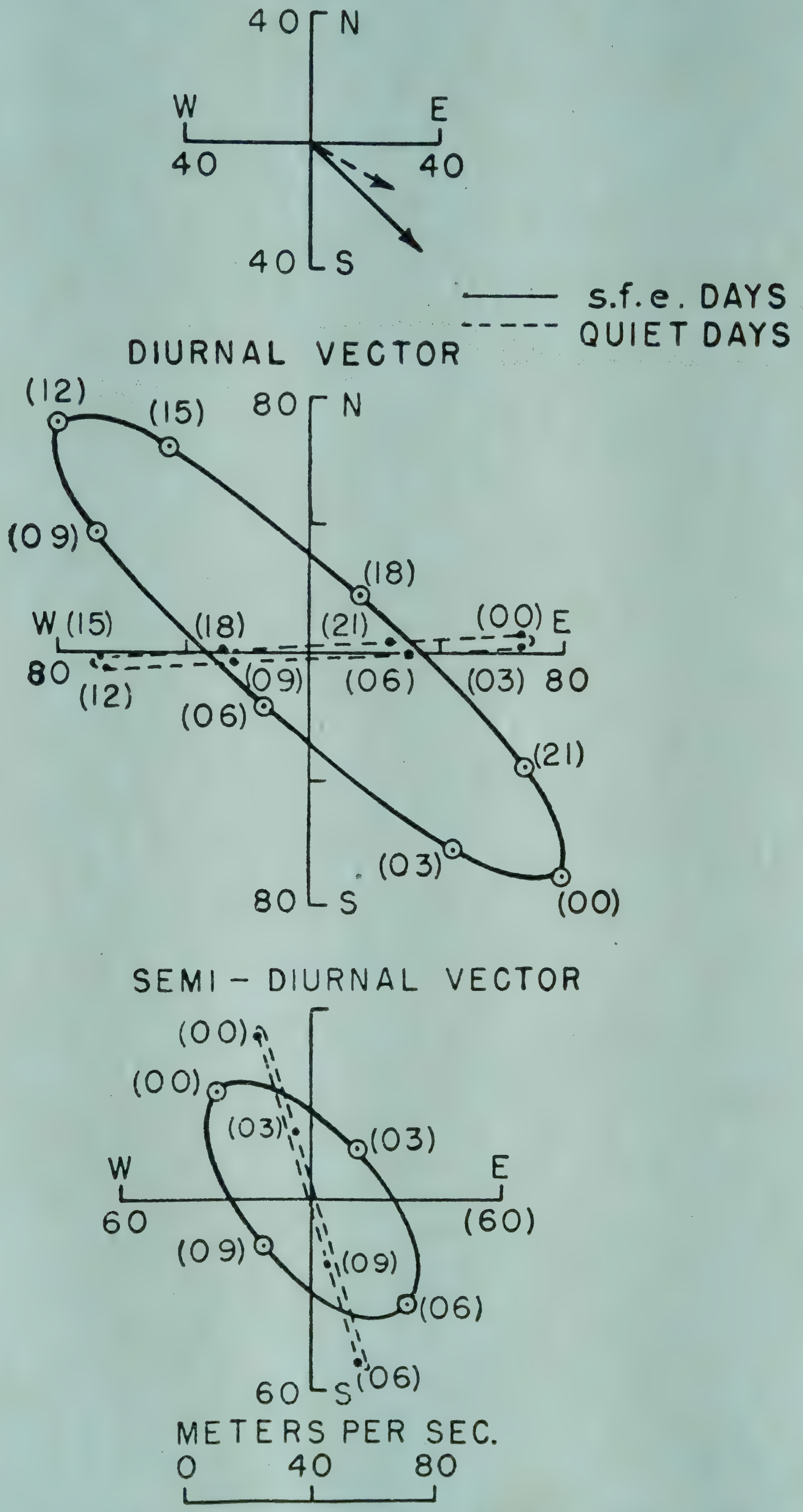

Fig. 2 — Polar plot of steady, 24-hourly and 12-hourly drift vectors for s.f.e. and quiet days

an evidence that the drift systems for these two cases are situated at different levels. In view of the fact that the drift measurements taken by using reflections from E region might be considerably affected by the enhanced ionization in the lower levels during solar flares, it appears likely that the drift results on these days refer to lower levels in the E region or higher levels in the D region. Recent work by Vollard and Toubenheim and others indicate that the disturbed day current system may also extend down to the D region. It is, therefore, quite likely that the 24-hourly component of the drifts recorded by the spaced receiver method arises from levels below the level of reflection in the E region on s.f.e. days. It appears quite likely that the enhanced amplitude of the 24-hourly harmonic may be due to the enhanced conductivity in the region responsible for the drifts on s.f.e. days.

REFERENCES

1. TOUBENHEIM, J., *J. atmos. terr. Phys.*, **11** (1957), 14.
2. VOLLARD, H. & TOUBENHEIM, J., *J. atmos. terr. Phys.*, **12** (1958), 258.
3. MITRA, A. P. & JONES, R. E., *J. atmos. terr. Phys.*, **4** (1953), 141.
4. VESTINE, E. H., *J. geophys. Res.*, **59** (1954), 93.
5. Central Radio Propagation Laboratory, F. 171 Part B (NBC, Boulder, Colarado), November 1958,
6. RAO, B. R., RAO, M. S. & MURTY, D. S. N., *J. sci. industr. Res.*, **15A** (1956), 75.
7. RAGHAVA RAO, R. & RAMACHANDRA RAO, B., *J. atmos. terr. Phys.*, **22** (1961), 81.

Effect of geomagnetic disturbances on F_2 layer of the ionosphere in low and middle latitudes

K. M. KOTADIA*
K. R. RAMANATHAN

Physical Research Laboratory
Ahmedabad

A statistical study of F_2 layer data over a period of five years from sunspot minimum (1953) to sunspot maximum (1957) has been made to find SD and D_{st} variations of f_0F_2 in low latitudes in the eastern zone. These have been then compared with similar variations at equatorial and higher latitudes obtained by other workers. The meridional profiles of f_0F_2 from 0600 hours to midnight are drawn both for normal and disturbed days, which show on disturbed days, (i) a morning rise of f_0F_2 which is a common feature for all latitudes in the range 0°-45° magnetic dip, and (ii) a day-time rise of f_0F_2 at places with magnetic dip from 0° to 20°, as against a fall of f_0F_2 during day-time and in the early night at places with magnetic dip from 20° to 60°. This fall is particularly marked at about 35° magnetic dip. As a consequence, the intensity of equatorial trough in f_0F_2 during these hours is reduced on disturbed days. A few individual cases of severe SC type disturbances have been discussed in relation to f_0F_2 changes in the East Asiatic Zone.

The changes in f_0F_2 and in cosmic radio noise absorption on 25 Mc/s. at Ahmedabad have been correlated. A study of spread F occurrence over a period of 2 years has shown that while spread F occurrence on disturbed days is reduced to $\frac{1}{3}$ of its value on normal days at Ahmedabad, it increases at Slough to nearly $2\frac{1}{2}$ times the normal. The change-over from decrease to increase takes place at about 44° magnetic dip.

A preliminary report on the study of the effect of geomagnetic storms on the F_2 layer of the ionosphere in low latitudes was given at the CSAGI meetings held in Moscow in August 1958[1]. An extended study of the subject is presented in this paper.

---

*Present address: Physics Department, Gujarat University, Ahmedabad

The changes in the F_2 layer associated with geomagnetic disturbances have been studied by a number of workers[2–8]. Their studies have covered a large range of latitudes and longitudes. Martyn, adopting the method of analysis introduced by Moos[9] and Chapman[10] for the study of magnetic disturbances, separated the storm time and local time variations of disturbance at several places.

The data used in this paper relate mostly to stations in the Asiatic Zone along nearly the same meridian, as it was considered desirable to separate out the local time effects and compare the variations in different latitudes as clearly as possible.

As shown in an earlier study, the values of midday f_0F_2 (1000–1400 hours) at Delhi and Ahmedabad are depressed on magnetically disturbed days, while at Tiruchirapalli and Madras they show an increase. The change-over from decrease to increase takes place at about magnetic dip 20°. For making this analysis, the superposed epoch method was followed, taking as zero epoch the day on which the noon value of f_0F_2 at Ahmedabad or Delhi was depressed by more than 10 per cent of corresponding monthly median value. The changes in f_0F_2 during a disturbance were expressed as ratios of the value on the disturbed day [or $D(f_0F_2)$] to the corresponding monthly median value at the same hour. In the present paper, a study of the D_{st} and SD variations of f_0F_2 in low latitude stations in India has been made and the results are compared with the data of some stations in middle latitudes. Disturbance variations of f_0F_2 in the East Asian Zone are compared for four SC type magnetic storms. Finally some relations between spread F, cosmic radio noise absorption on 25 Mc/s. and magnetic activity are briefly discussed. The term equator used in this paper means magnetic dip equator unless otherwise stated.

Equatorial Trough in f_0F_2. It has been known for some time that the value of day-time f_0F_2 has a peak near magnetic dip 30° and that there is a valley near the magnetic equator. The peaks get broader and the valley shallower in years of high solar activity[11]. In 1954, the peak of f_0F_2 was between Ahmedabad and Bombay[12], while in 1957 (a high sunspot year), it shifted to a position slightly to the north of Ahmedabad (magnetic dip 35°). Table 1 gives the difference $\Delta(f_0F_2)$ between f_0F_2 at Ahmedabad and Kodaikanal ($I = 3{\cdot}5°$N) at different hours of the day in 1954 and 1957. The equatorial trough is particularly pronounced in the winter months.

In 1954, the equatorial trough changed into a ridge by about 2100 hours, while in 1957 the trough continued to be pronounced even up to midnight. The earlier development of the trough in autumn and winter and its continuation until midnight in a year of high sunspot activity are respectively due to (i) the increased ionization rate and upward electrodynamic drift of

TABLE 1 — DEPTH OF EQUATORIAL TROUGH IN f_0F_2 AT DIFFERENT HOURS OF THE DAY IN 1954 AND 1957 — $\Delta(f_0F_2)$ in Mc/s. (AHMEDABAD-KODAIKANAL)

TIME	1954				1957			
	Jan.	Apr.	July	Oct.	Jan.	Apr.	July	Oct.
0900	0·6	0·5	0·3	0·3	2·6	−1·1	−1·2	1·0
1200	3·7	4·2	2·2	3·8	2·6	4·7	2·8	4·5
1500	4·5	4·4	2·1	4·6	5·2	5·5	3·6	5·1
1800	3·8	0·9	0·0	2·0	6·5	5·9	4·8	5·7
2100	1·0	—	—	—	7·8	5·2	0·5	7·1
2400	No data at Kodaikanal or Tiruchirapalli				1·0	2·1	−1·4	2·8

the electrons in the F region near the equator, and (ii) the lower loss rate at the increased heights of the F_2 region. The negative values at 0900 hours in April and July 1957 mean that the increase of electron production at Kodaikanal was more than sufficient to compensate for the fall in density due to upward drift in the summer of high solar activity. Appleton[13] has discussed the development and extinction of the equatorial anomaly in equinoxes of a low sunspot year.

What happens to the said anomaly during disturbed days is shown in Fig. 1 which gives the mean diurnal variation of f_0F_2 on disturbed and normal days at Ahmedabad and Kodaikanal in the year 1956 (47 days). It is seen that while f_0F_2 at Ahmedabad decreases on disturbed days between 0800 and 2300 hours, at Kodaikanal it increases. The tendency of the disturbance is to flatten out the equatorial trough. Though the midday 'bite-out' in f_0F_2 at Kodaikanal is removed, the diurnal variation on disturbed days is still not of the Chapman layer type. Another interesting feature is that on disturbed days, the normal post-sunset rise in f_0F_2 at Ahmedabad at about 2000 hours is suppressed. The reduction in the depth of the equatorial trough of f_0F_2 is shown by the shaded part in Fig. 1(b), while the curves (A′–A) and (K′–K) give the disturbance diurnal variation at Ahmedabad and Kodaikanal.

The normal and disturbed day profiles of f_0F_2 over a range of latitudes with magnetic dip 60°N–0° were obtained by taking the mean of the values on days having $\Sigma K > 25$ and the monthly median values, with due weight given to the number of disturbed days in a particular month. The analysis was made for the year 1956 at stations in the eastern zone for 0600, 0900, 1200, 1500, 1800, 2100 and zero hours. Forty-three days with $\Sigma K > 25$ were studied for which data were available at all the places. The results of this analysis given in Fig. 2 show clearly that f_0F_2 is depressed on disturbed days at all the places north of magnetic dip 20° and is enhanced at places south of it from 0900 to 2100 hours. It may also be noted that the

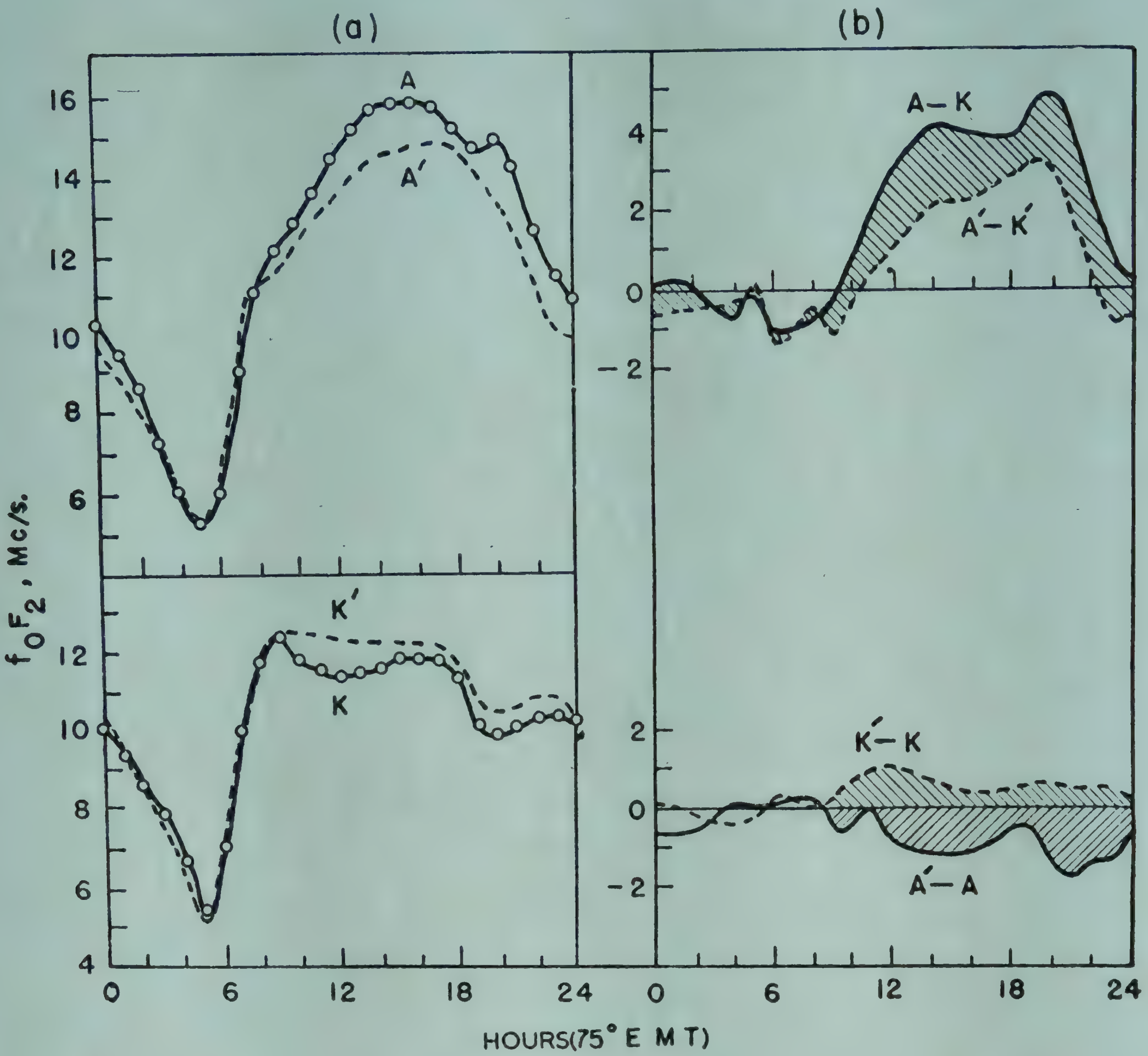

Fig. 1 — (a) Mean diurnal variation of f_0F_2 at Ahmedabad (A and A′) and Kodaikanal (K and K′) on normal days together with mean disturbed day variation (47 days) in 1956. Primed letter refers to disturbed days. (b) Difference (A–K) and (A′–K′) showing change in depth of equatorial trough of f_0F_2; SD variation of f_0F_2 at Ahmedabad and Kodaikanal expressed as $\Delta(f_0F_2)$ or deviation from normal (47 days, 1956)

depression is maximum at the place of f_0F_2 peak. The morning rise of f_0F_2 on disturbed days is a feature common at all the places with magnetic dip less than 45°. The profiles bring out the reduction of the equatorial anomaly in f_0F_2 on disturbed days.

Disturbance Diurnal Variation or SD Variation of f_0F_2. To find the effect of the disturbance on the diurnal variation of f_0F_2, hourly ratios of disturbed day f_0F_2 to monthly median f_0F_2 were calculated for 47 days with $\Sigma K > 25$ during the year 1956 for Ahmedabad, Bombay and Kodaikanal [Fig. 3(a)]. At Kodaikanal 24-hourly observations were begun in August 1955 and at Bombay they were begun only in 1958. The figure shows that the changes at Ahmedabad and Kodaikanal are in opposite directions from 0800 to 2300 hours, while at Bombay the effect of the disturbance

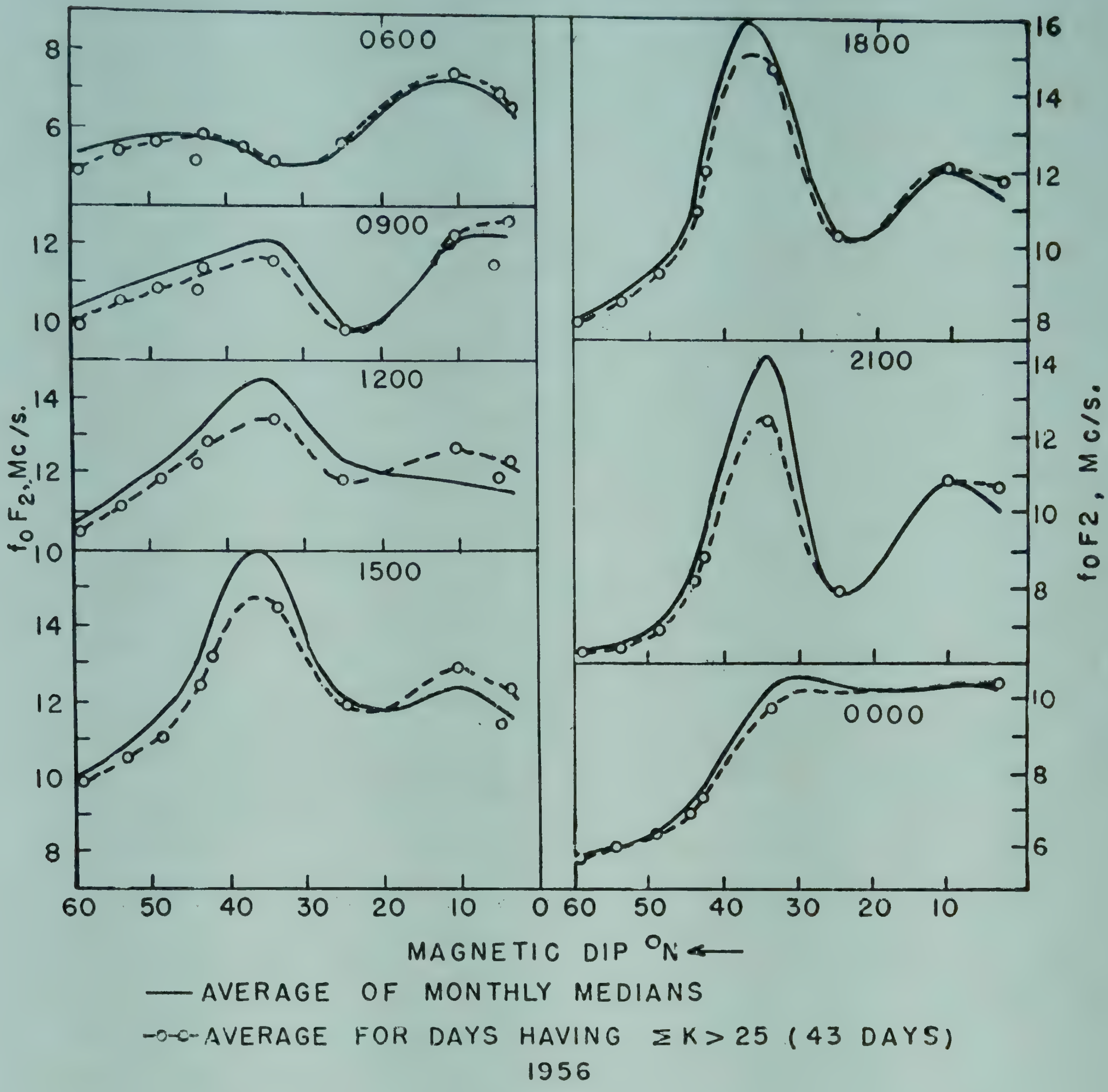

FIG. 2 — MERIDIONAL PROFILES OF f_0F_2 IN THE NORTHERN HEMISPHERE OF THE EASTERN ZONE, AT 3-HOURLY INTERVALS FROM 0600 TO 2400 HOURS IN NORMAL AND DISTURBED CONDITIONS

is small, and indicative of a transition from the equatorial zone. Sharp rises in f_0F_2 are observed in the morning both at Ahmedabad and Kodaikanal but values higher than normal continue throughout the day near the equator only.

As both Ahmedabad and Delhi had a longer series of data, the above analysis was carried out for 90 days over a period of 4 years (1953–56) with a view to finding the SD variations of f_0F_2 at these two places [Fig. 3(b)]. The curves are very similar, the only difference being that the amplitude at Ahmedabad is larger than that at Delhi. Figs. 2 and 3 prove that the phase reversal in disturbance variation of f_0F_2 during day hours takes place at about magnetic dip 20°. It is interesting to note that the lunar tidal variation of f_0F_2 also reverses in phase at about the same magnetic dip[14].

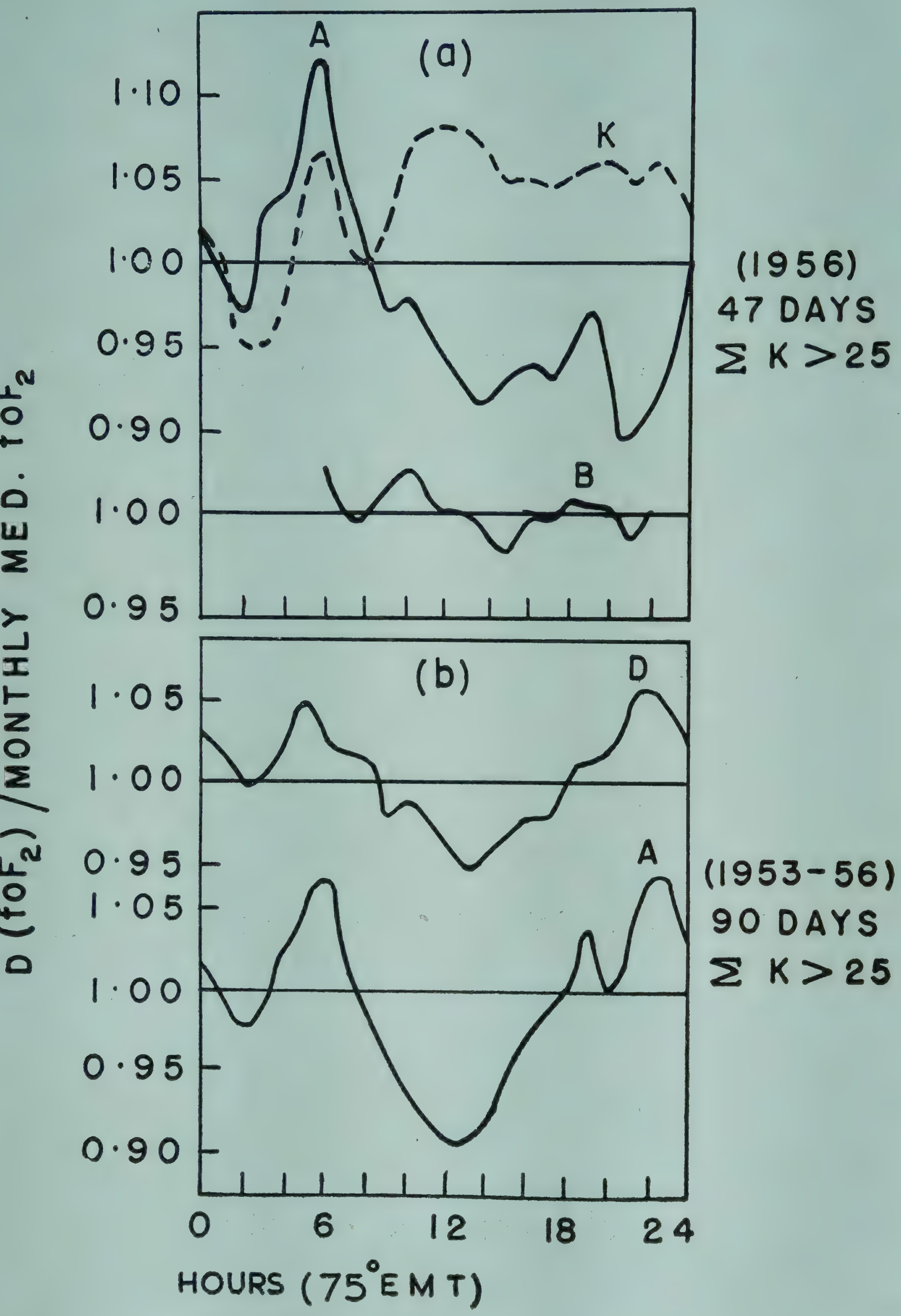

Fig. 3 — (a) SD variation of f_0F_2 at Ahmedabad, Bombay and Kodaikanal expressed as ratio $D(f_0F_2)$/monthly median f_0F_2 (1956). (b) SD variation of f_0F_2 at Ahmedabad and Delhi (1953–56)

One difference in the SD variation of f_0F_2 at Ahmedabad during 1956 from that for the longer period 1953–56 may be noted. The negative phase extends well into the night in 1956, while taking the data of the whole period, it is mainly confined to day-time. This will be further considered in the next section.

Dependence of SD (f_0F_2) on Local Time of the Commencement of the Magnetic Storm at Ahmedabad. All the SC type magnetic storms were then grouped according as they commenced in each of the four quarters of the day to find the associated variations in f_0F_2 over an interval of about 50 hr after the SC. This was done for a period of five years (1953–57). Sixty-five SC type storms were found of which 16 commenced in the quarter 0000–0500 hours, 15 in the quarter 0600–1100 hours, 20 in the quarter 1200–1700 hours and 14 in the last quarter. The mean ratio $D(f_0F_2)/(\text{med. } f_0F_2)$ was then plotted separately for each of the above groups against local time. Fig. 4 gives these curves and the lowest curve gives the average SD variation on the day following the SC. The mean curve in each group starts at a time round which SCs were most frequent. There is a clear dependence of the SD variation of f_0F_2 on the local time of commencement of the storm.

It can be seen at once that the variation on the second day of the storms commencing in the interval 0600–1100 hours is similar to that obtained in 1956 on the basis of days with $\Sigma K > 25$. Further examination revealed that majority of storms in 1956 commenced in the interval 0600–1100 hours.

The arrangement of data in Fig. 4 has brought out sharply the morning rise of f_0F_2 for each group. It is also seen that f_0F_2 is more depressed during the second 24 hr of the storm, and that storms commencing in the afternoon and pre-midnight hours have the effect of initially increasing f_0F_2 above normal, whereas those commencing in the early morning and forenoon hours have the opposite effect. The maximum disturbance in f_0F_2 is created by storms commencing in the forenoon. Those commencing in the evening hours cause the least disturbance. The mean SD curve of Fig. 4 shows a maximum positive change of 7 per cent at 0500–0600 hours and a maximum negative change of 7 per cent at 1400 hours. Positive changes are found only during 5 hr in the morning. Its difference from the mean curve for 90 days in 1953–56 [Fig. 3(b)] which showed a positive phase in the first half of the night is due to the fact that the latter included the first and second 24 hr of all types of storms, many of which were weak.

Comparison of SD (f_0F_2) Variations at Middle and Low Latitudes. Martyn[15] analysed the SD variations of f_0F_2 for seven places from near the boundary of the auroral zone to the magnetic equator. There were some gaps in low latitudes, the filling up of which would elucidate the progression

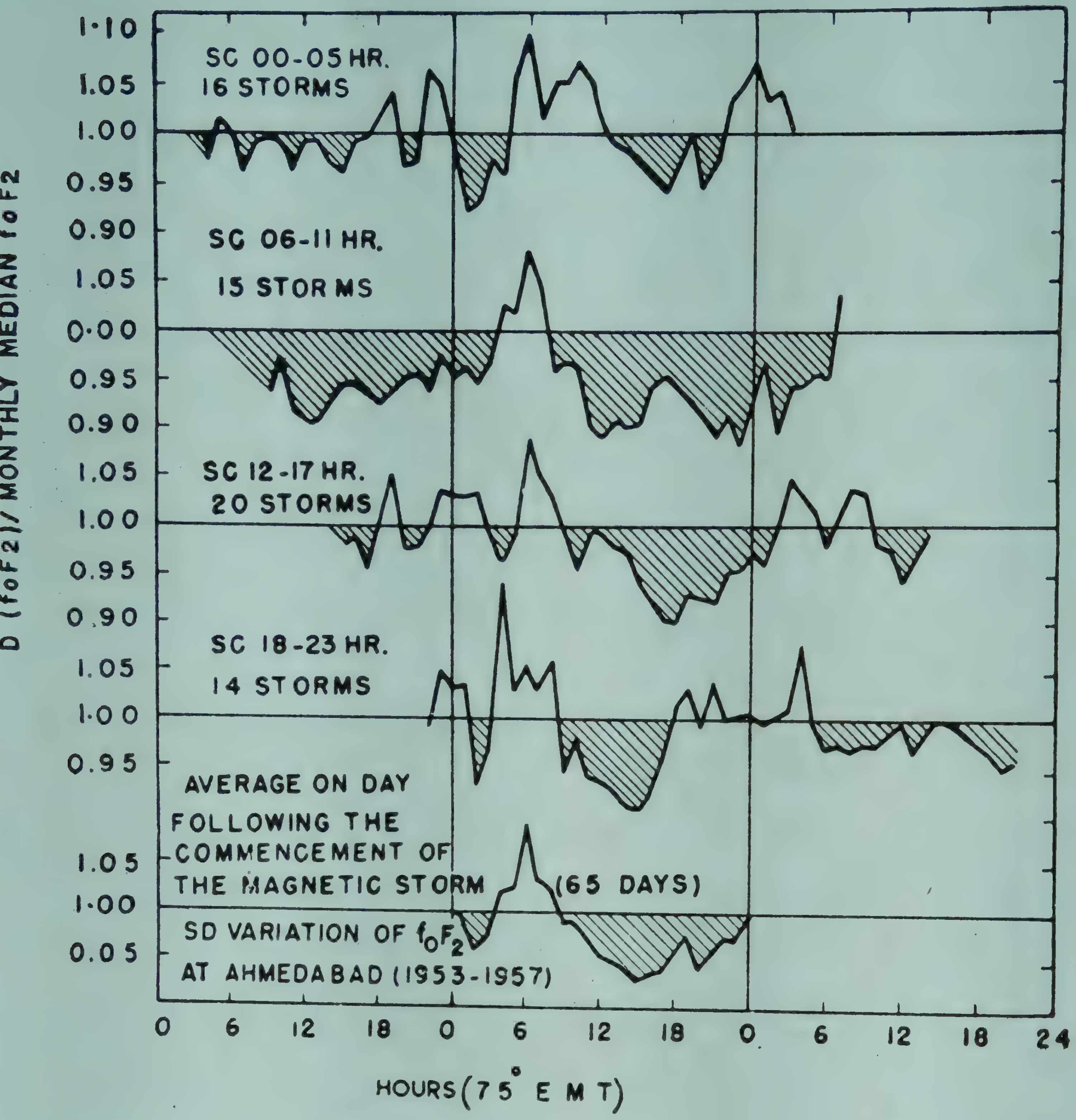

Fig. 4 — Disturbance variations of f_0F_2 during magnetic storms grouped according to their times of commencement in each quarter of the day. Shown at the bottom is the mean SD variation of f_0F_2 at Ahmedabad

of changes as the equator is approached. In Fig. 5 are reproduced SD (f_0F_2) curves for Washington[16], Wakkanai[17], Yamagawa[5] and Ibadan[6]. They are compared with those at Delhi, Ahmedabad and Kodaikanal. The curves reproduced here for middle latitudes relate to winter, but they are similar to the mean for all the seasons, with only a small difference in amplitude.

The comparative study brings out the following facts:

(i) While the curves for Washington and Wakkanai are similar, an important change of phase during morning hours takes place at Yamagawa and the change involving a morning rise in f_0F_2 is continued right up to the equator.

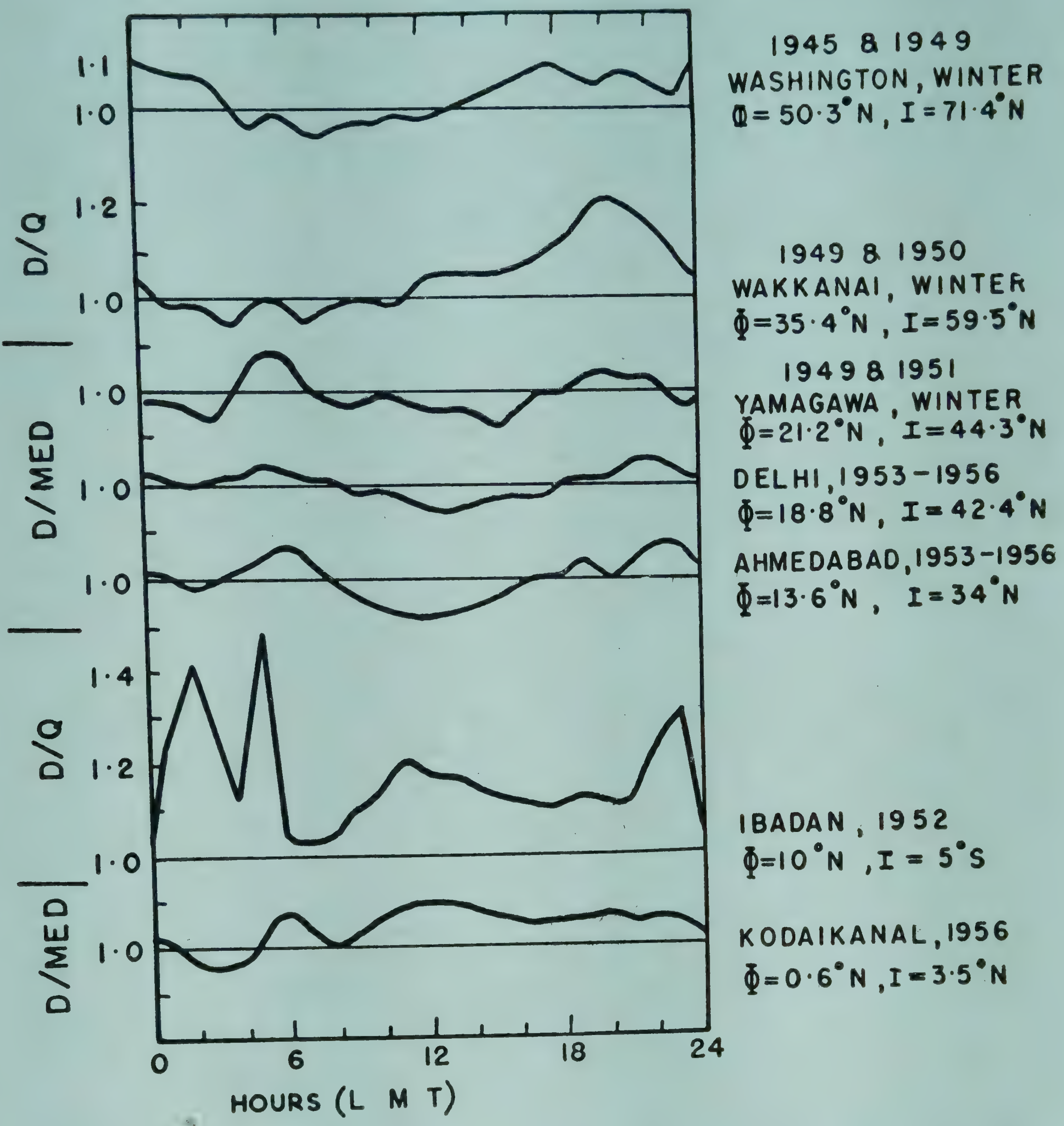

FIG. 5 — COMPARISON OF SD VARIATION OF f_0F_2 AT SOME OF THE STATIONS IN MAGNETIC DIP RANGE 0°–72°

(ii) Another change occurs during day hours on the equatorial side of Ahmedabad, viz. there is an increase of f_0F_2 near the equator corresponding to its decrease in the sub-tropics. As mentioned earlier, this change takes place at about magnetic dip 20°.

(iii) From sunset to midnight, all the stations show increased f_0F_2 during disturbance. Near the magnetic equator, $D(f_0F_2)$ is above normal throughout the day except for 2–3 hr in the night.

(iv) The difference in the amplitudes of the SD curves at Ibadan ($I = 6°S$) and Kodaikanal ($I = 3{\cdot}5°N$) may be due to the fact that a smaller number of days with $\Sigma K > 30$ were considered at Ibadan. At Kodaikanal, more days with $\Sigma K > 25$ were considered.

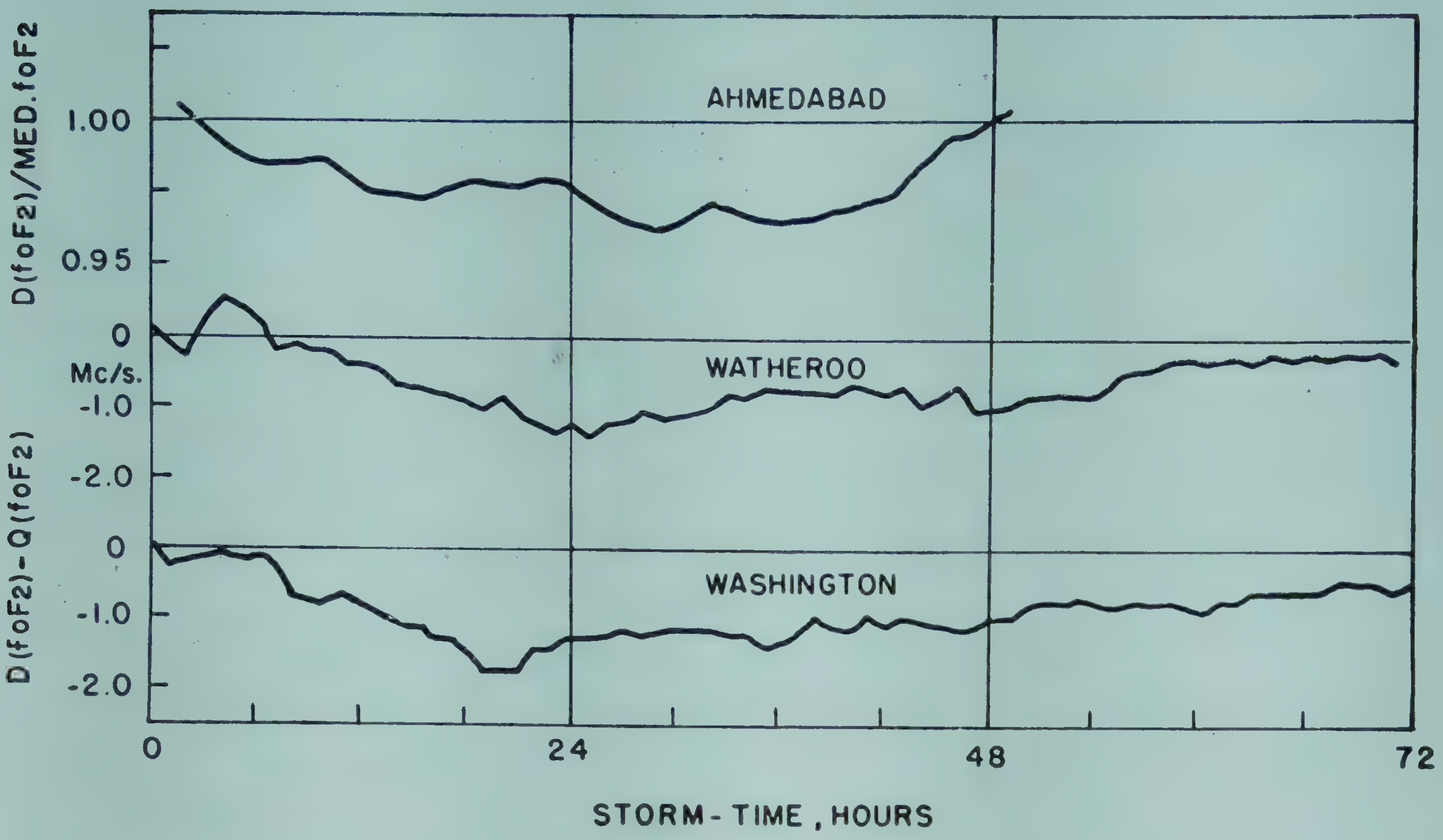

FIG. 6 — STORM TIME OR Dst VARIATION OF f_0F_2 AT AHMEDABAD (65 SC STORMS, 1953–57) COMPARED WITH THOSE AT WATHEROO (I = 64°S, 90 SC's, 1939–50) AND WASHINGTON (I = 71·4°N, 81 SC's, 1941–50) DUE TO MARTYN[4]

Storm Time Variation of f_0F_2 in Low and Middle Latitudes. Here, the hourly ratios $D(f_0F_2)$/med. f_0F_2 are arranged according to storm time, taking the hour nearest to the SC time as zero hour, and plotting the above ratios for 50 or more hours after the SC time. When a large number of SCs are available and their times are evenly distributed during 24 hr of the day, the superposed SD variation will be reduced to small proportions in the averaged D_{st} variation. Fig. 6 gives a smoothed curve of D_{st} variation of f_0F_2 at Ahmedabad for a duration of 50 hr after the SC, and it is compared with those at Washington and Watheroo[4] of middle latitudes.

(i) It may be noted that storm time effect is a reduction of f_0F_2 below normal at all these places. The maximum negative change at Ahmedabad is only 5 per cent as against 7 per cent in SD variation. The variations at the other two places are expressed as simple deviations, but one can see that when they are expressed as percentages, the depressions would be larger than those found at Ahmedabad.

(ii) The storm time effect on f_0F_2 attains its maximum value at a later hour in lower latitudes, e.g. it is maximum at 28 hr after SC at Ahmedabad, 24 hr at Watheroo and 20 hr at Washington. On the contrary, the recovery to normal takes place later at higher latitudes, i.e. the disturbance conditions prevail for a longer time at higher latitudes after the sudden commencement. The effect of the disturbance is more marked on the second day of the storm.

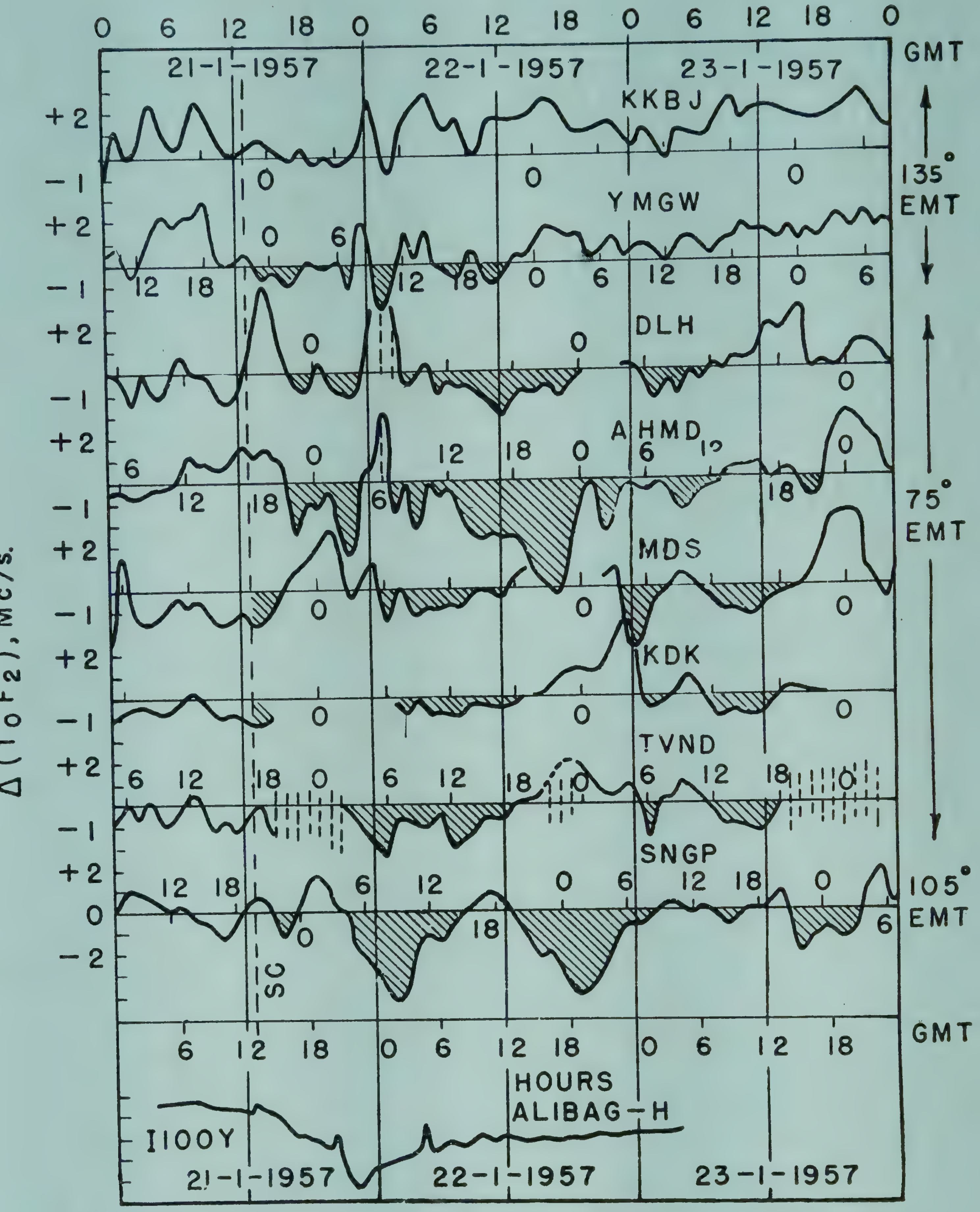

Fig. 7 — Storm time variations of f_0F_2 expressed as simple deviations from normal at various places from equator to magnetic dip 49°N in the East Zone, during the SC type magnetic storm of January 21, 1957

Some Instances of f_0F_2 Variations Associated with Severe SC type Magnetic Storms. In Figs. 7–10 are shown the simultaneous changes in f_0F_2 at various places in the eastern zone. In these figures, $\Delta(f_0F_2)$, the deviation in Mc/s. of the observed f_0F_2 from the monthly median value at the same hour are plotted. At the bottom of the figure is given the smoothed magnetogram of the horizontal component of the earth's magnetic field at Alibag, which has magnetic observatory nearest to Ahmedabad.

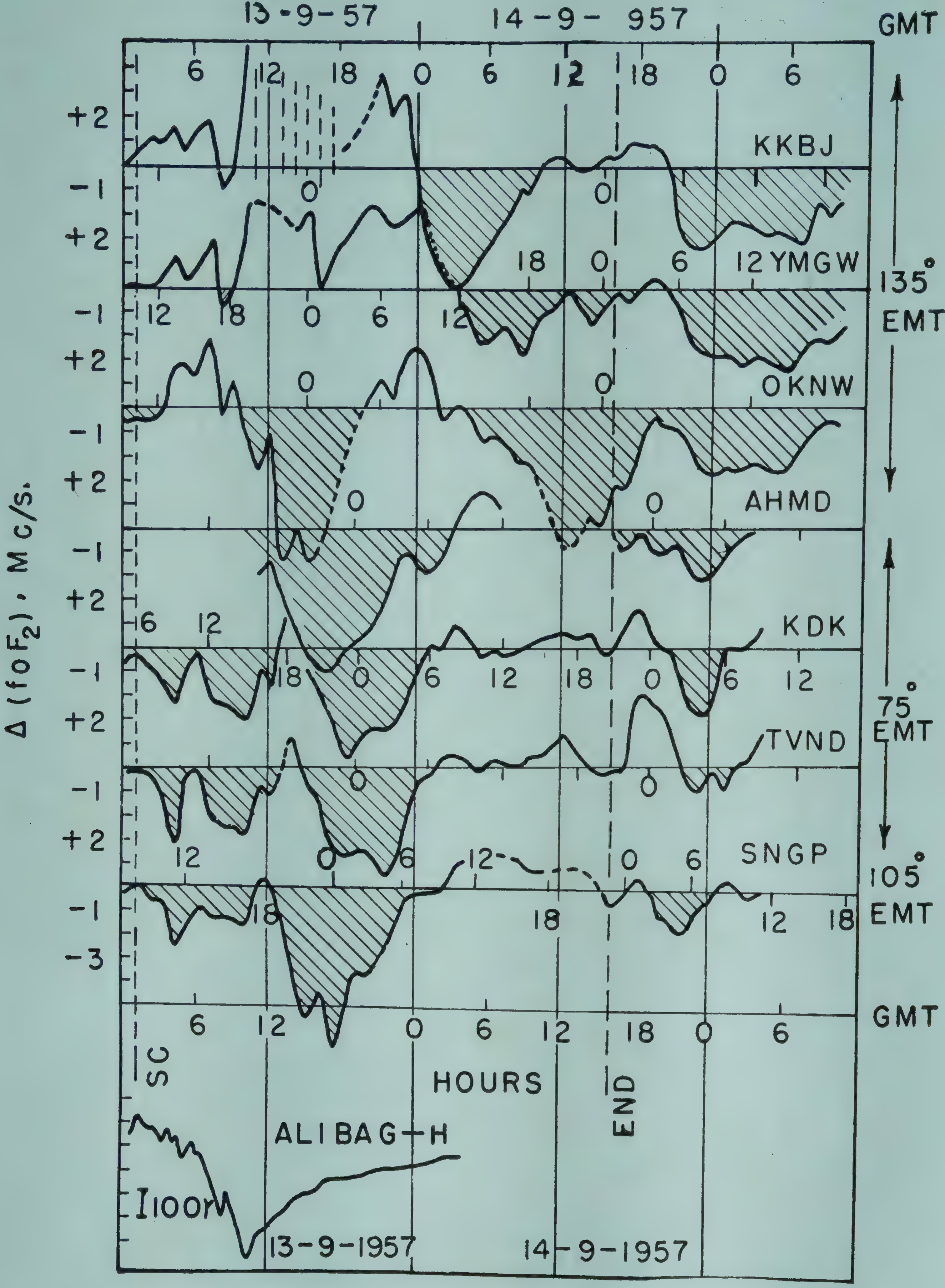

Fig. 8 — Storm time variations of f_0F_2 expressed as simple deviations from normal at various places from equator to magnetic dip 49°N in the East Zone, during the SC type magnetic storm of September 13, 1957

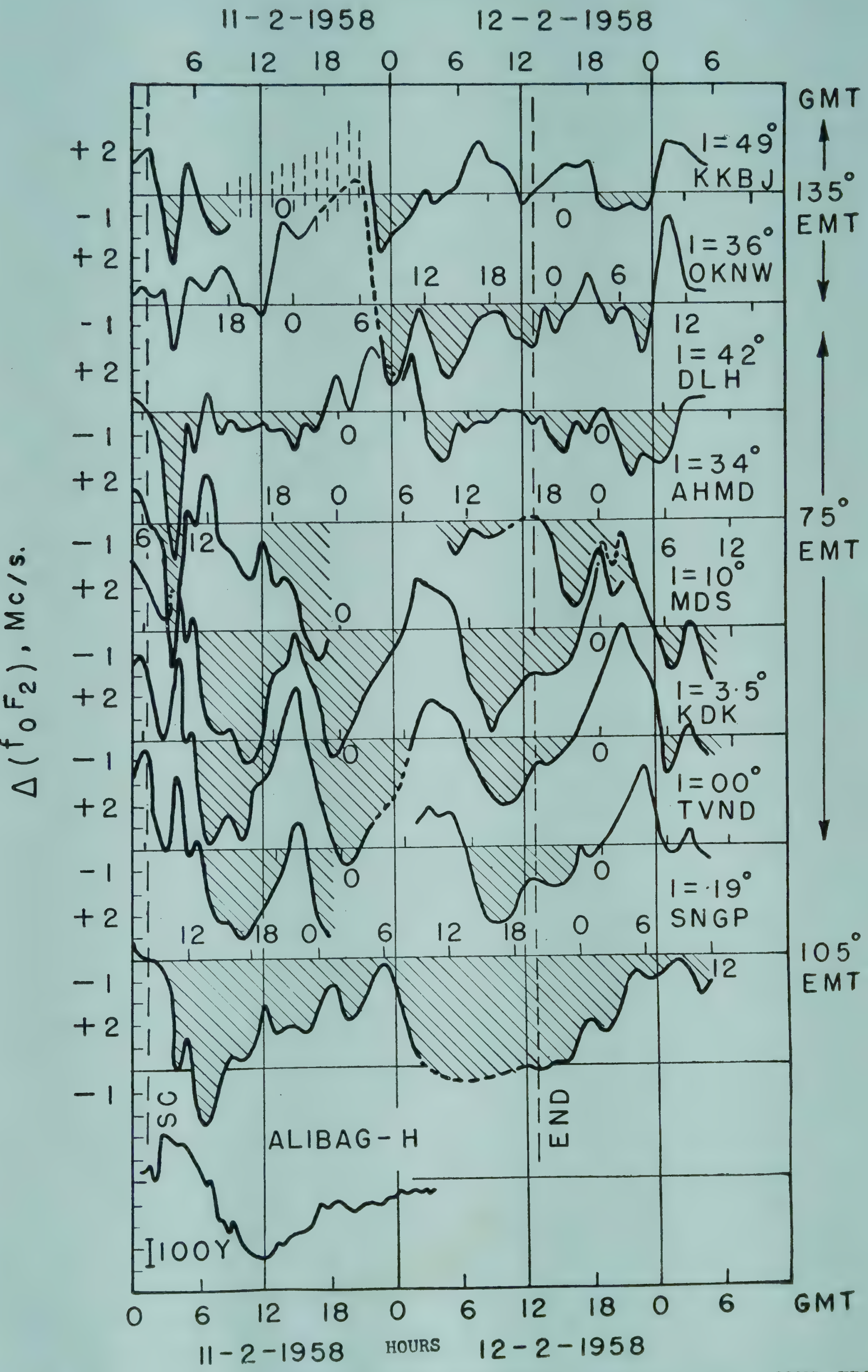

Fig. 9 — Storm time variations of f_0F_2 expressed as simple deviations from normal at various places from equator to magnetic dip 49°N in the east zone, during the SC type magnetic storm of February 11, 1958

TABLE 2 — SOLAR FLARE AND MAGNETIC STORM DATA

DATE AND TIME (UT) OF SC	INTENSITY OF STORM	RANGE ΔH AT KODAIKANAL *gammas*	ASSOCIATED SOLAR FLARE OR RADIO BURST
Jan. 21, 1957 1253	Severe	410	SF 2^+ Jan. 20, 1957 1850
Sept. 13, 1957 0049	Severe	710	Aug. 11, 1957 Type IV burst 0300
Feb. 11, 1958 0125	Severe	813	SF 2^+ Feb. 9, 1958 2053
July 8, 1958 0751	Severe	710	SF 3^+ July 7, 1958 0048

Table 2 gives some details of the storms included here.

All the storms followed intense solar flares within 28 hr. In the storm of January 21, 1957, the difference between the two events was about 18 hr.

(i) The amplitude and sign of changes in f_0F_2 after the sudden commencement depend on the latitude of the place and also on the local time of commencement. Large changes begin 8–10 hr after the SC and the maximum disturbance in f_0F_2 is observed 20–24 hr later. This maximum change in f_0F_2 does not necessarily coincide with the time of maximum magnetic disturbance. There is no evidence of a sudden commencement in the ionosphere corresponding to that observed in the H field. Plots against UT give an idea of the storm time changes, but superposed on them are the SD variations. To recognize SD from D_{st}, the local times are also marked on the zero axis of each station in Figs. 7–10.

(ii) At the Japanese stations the values of f_0F_2 are higher than normal in winter, though at low latitude stations, they are below normal even in winter. A large difference has been observed between the effects at the Japanese stations of the storms on February 11, 1958 and September 13, 1957, although the SC times in both the events were nearly the same.

(iii) In all cases when the magnetic storm commenced in the morning hours, the usual midday ‘ bite-out ’ in f_0F_2 at the equator was enhanced on the day of the SC. On the following day, however, higher values of f_0F_2 were observed during day-time. The storm of February 11, 1958 was so severe that even on the second day, abnormally low values of f_0F_2 continued near the equator. Large initial drops in f_0F_2 were recorded on a world-wide scale within 2–3 hr of SC. Because of its special features, the storm of February 11, 1958 has been studied in greater detail in a separate paper.

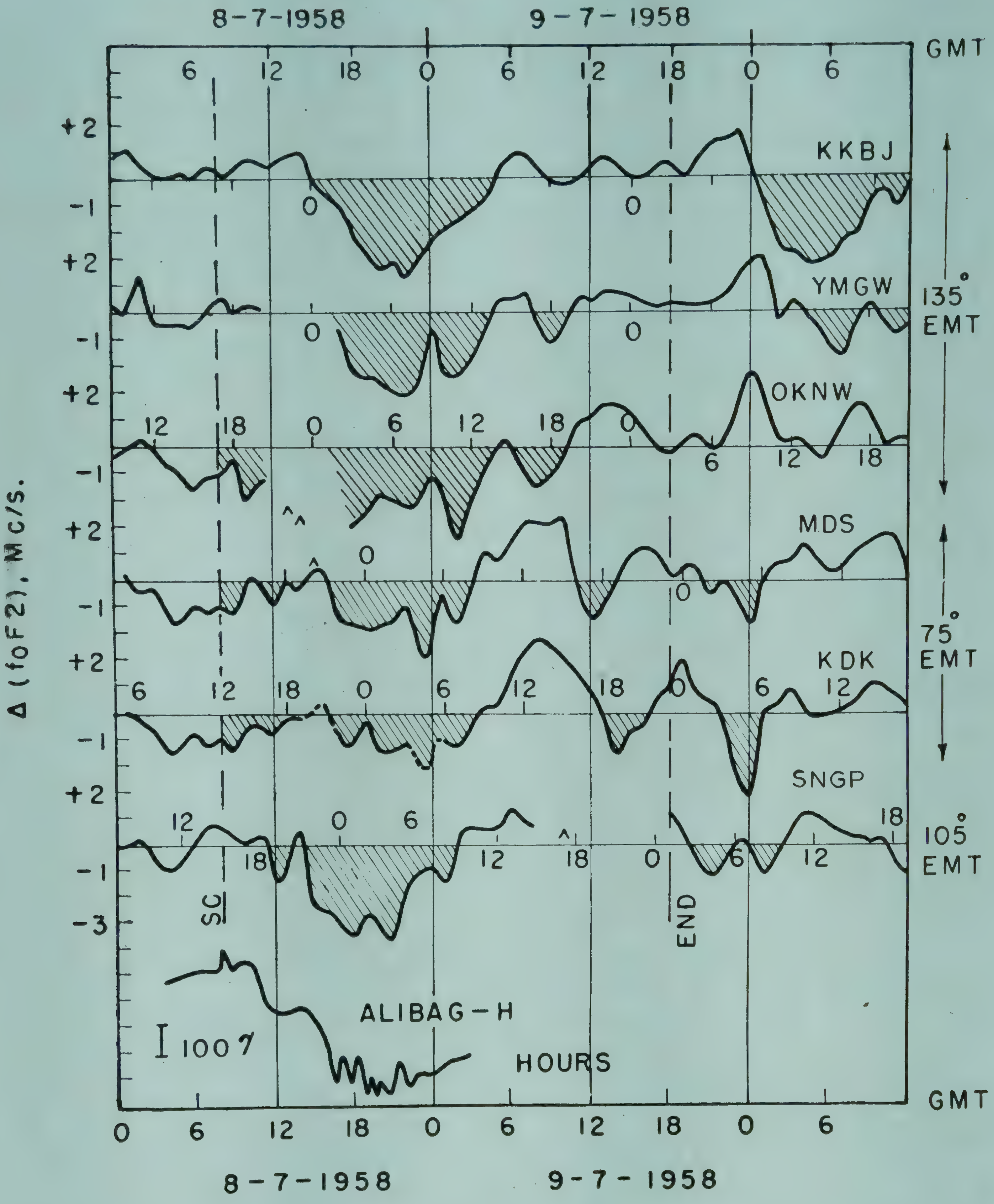

Fig. 10 — Storm time variations of f_0F_2 expressed as simple deviations from normal at various places from equator to magnetic dip 49°N in the East Zone, during the SC type magnetic storm of July 8, 1958

(iv) A comparison of the time variations of f_0F_2 at different stations shows that Madras (I = 10°N), Kodaikanal (I = 3·5°N) and Trivandrum (I = 0°) fall in the equatorial group; while Ahmedabad (I = 34°N), Okinawa (I = 36°N) and Delhi (I = 42°N) in the sub-tropics form another group. The three Japanese stations, viz. Kokubunji (I = 49°N), Akita (I = 54°N) and Wakkanai (I = 60°N) form a third group in middle latitudes. Yamagawa (I = 44°N) stands as an intermediate station between the sub-tropics and

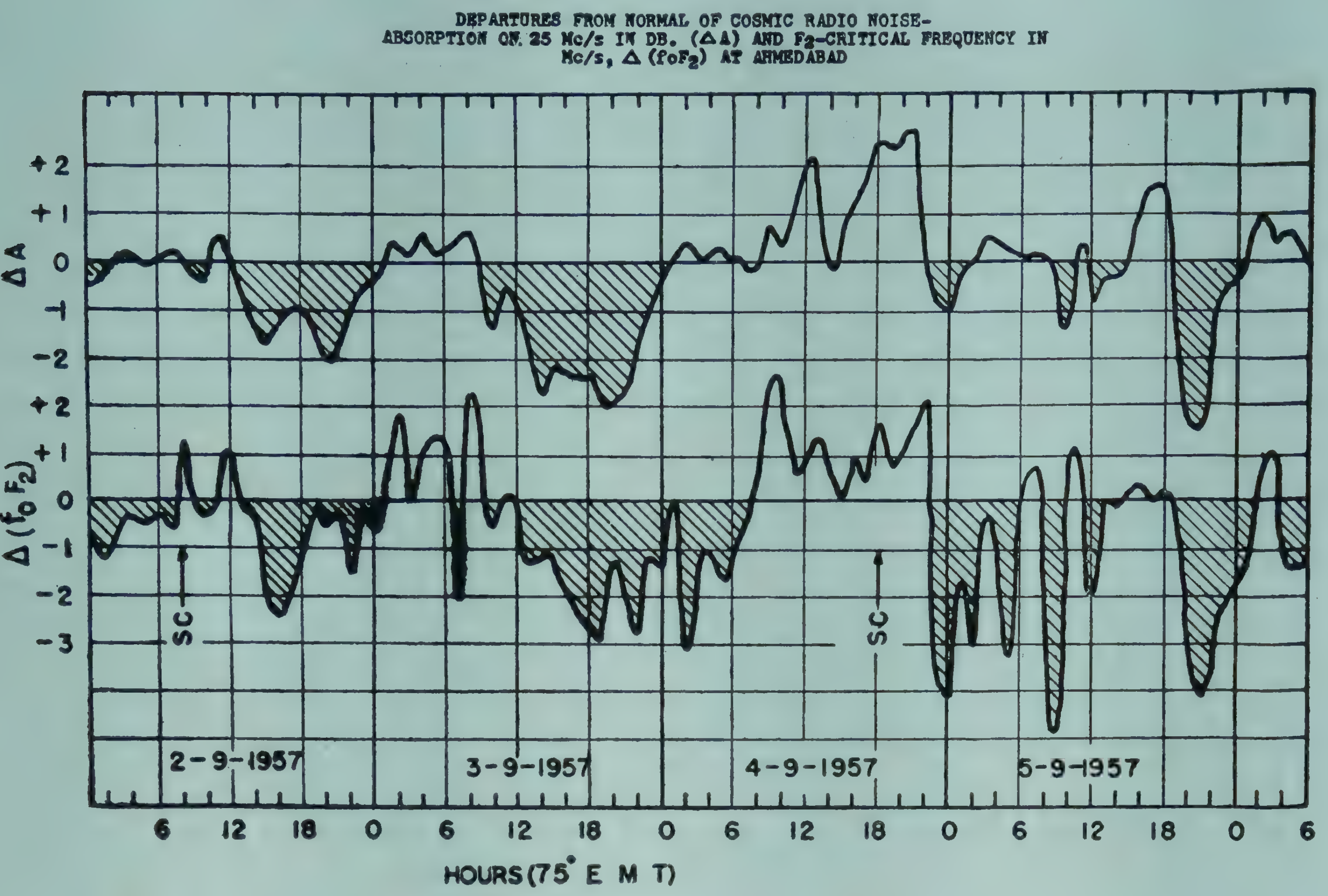

Fig. 11 — Correlation of $\Delta(f_0F_2)$ and ΔA of cosmic radio noise absorption during a magnetically disturbed period, September 2–5, 1957

mid-latitudes, while Baguio ($I = 19°N$) and Singapore ($I = 18°S$) are located near the transition between tropical and equatorial stations. The data show two reversals in phase of $\Delta(f_0F_2)$, one near magnetic dip 45° and the other near magnetic dip 20°.

The increased number of stations in low latitudes has helped in marking out the boundary of the zone of positive $\Delta(f_0F_2)$ near the magnetic equator with some precision.

Matsushita[7] divides the whole hemisphere into 8 zones to show the sequential changes in $D(f_0F_2)$. His analysis shows that an increase of f_0F_2 occurs at high latitudes immediately after SC.

f_0F_2 and Cosmic Radio Noise on 25 Mc/s. at Ahmedabad during a Magnetic Storm. It has been shown by Bhonsle and Ramanathan[18] that cosmic radio noise absorption (CRNA) on 25 Mc/s. at Ahmedabad is reduced on magnetically disturbed days. The cosmic radio noise as measured at ground level undergoes attenuation in its passage through the ionosphere. The absorption due to the D layer is fairly regular and is not affected much by magnetic disturbances. In the F_2 region, however, the changes in electron density are large and the layer is very much affected. On this ground, one can expect changes in CRNA (ΔA) corresponding to changes in f_0F_2. This is illustrated in Fig. 11 which shows a comparison of $\Delta(f_0F_2)$ and ΔA

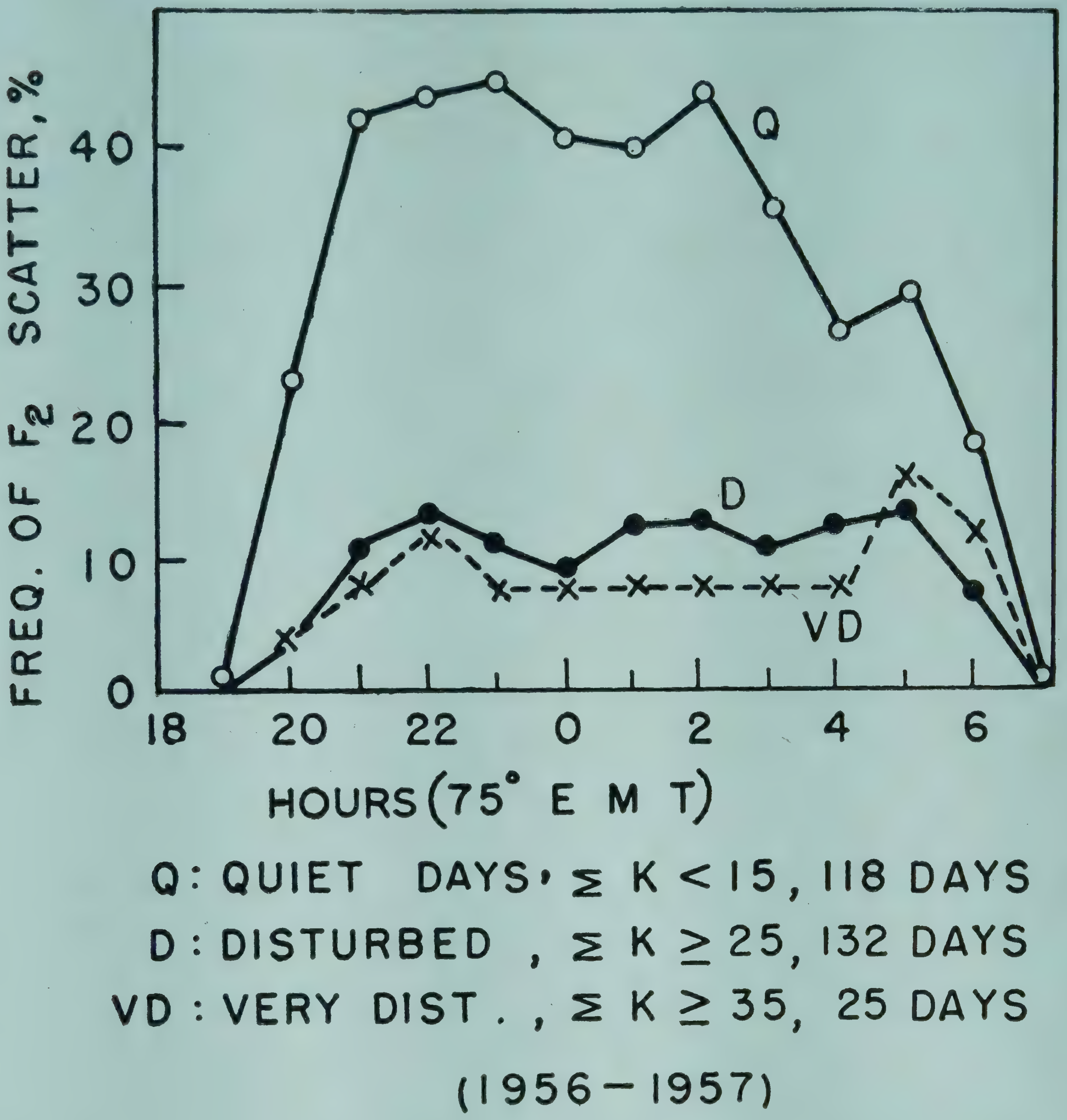

Fig. 12 — Variation during night hours of the occurrence of spread F echoes on magnetically quiet and disturbed days

during a prolonged disturbed period when severe SC type magnetic storms commenced on September 2 and 4, 1957. It should be noted that on all these days spread F echoes were absent. It is clear that ΔA and $\Delta(f_0F_2)$ show good correspondence from 0900 hours till midnight, after which f_0F_2 was so low that cosmic radio noise was not influenced. It has been observed that in general electron concentrations corresponding to $f_0F_2 = 8$ Mc/s. are not effective in causing CRNA on 25 Mc/s. at Ahmedabad.

An important feature shown by ionospheric records near the magnetic equator is that f_0F_2 increases during increased magnetic activity, but spread F echoes are rare. At Ahmedabad, both f_0F_2 and spread F decrease during a disturbance. An interesting question arises as to the relative contributions

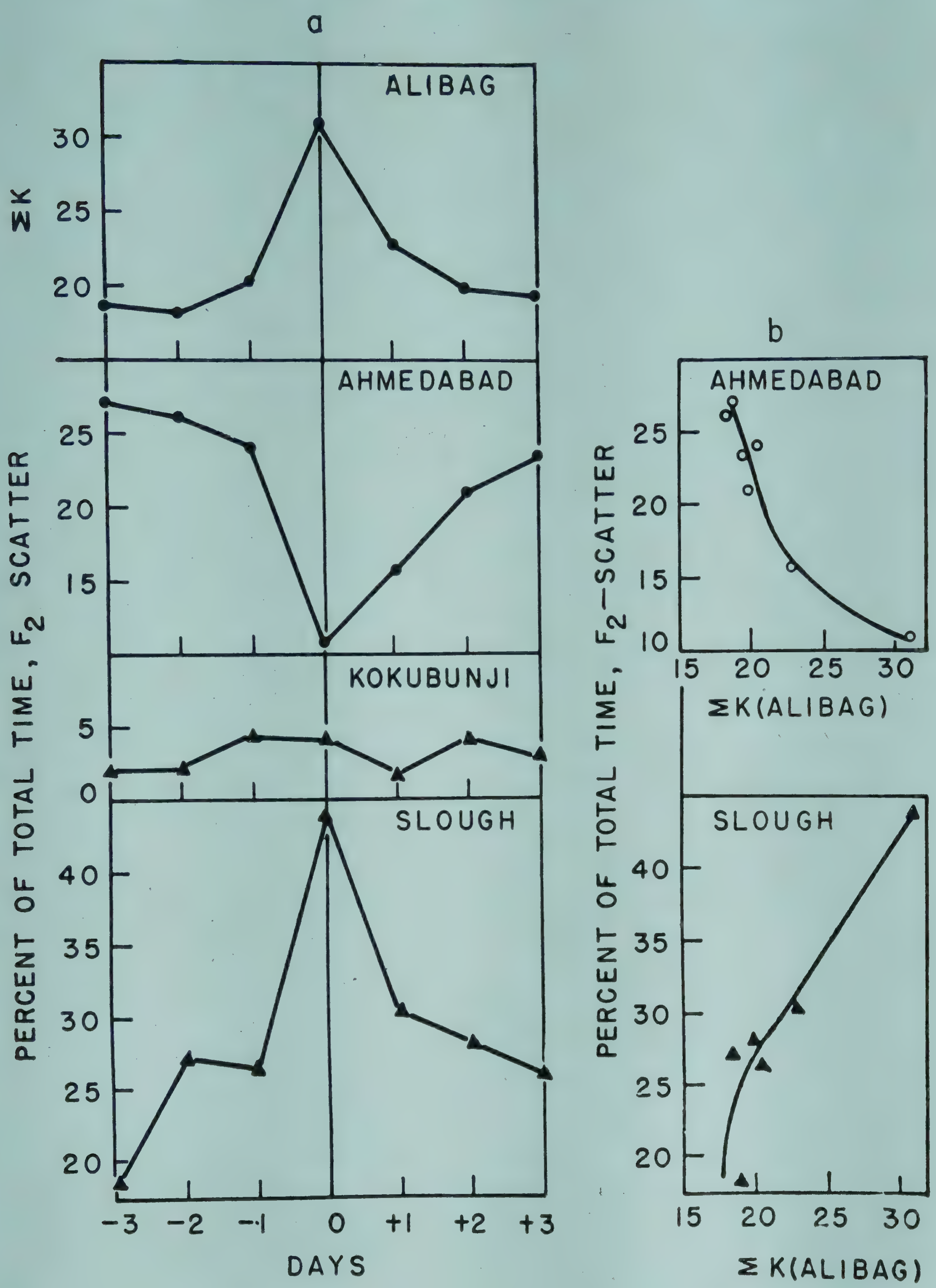

FIG. 13 — SUPERPOSED EPOCH DISTURBANCE VARIATION OF SPREAD F ACTIVITY AT AHMEDABAD, KOKUBUNJI (I = 49°N) AND SLOUGH (I = 67°N). K INDEX SUM OF MAGNETIC ACTIVITY AT ALIBAG IS ALSO SHOWN. 81 EPOCHS, 0 DAYS WITH $\Sigma K > 25$ (1956–57)

to cosmic radio noise attenuation from electron collisions in the ionosphere and F scatter. It should be possible to elucidate this by making measurements on CRNA near the magnetic equator.

Spread F and Magnetic Activity. It has been shown by one of the authors[19] that spread F was less frequent over Ahmedabad on days of increased magnetic activity and that this was also true for all stations having magnetic dip 0°–44°, though the decrease was not in the same proportion at different latitudes. The solar cycle variation of the occurrence of spread F also showed a decrease with increased magnetic character figure. In Fig. 12 are given the changes in the occurrence of spread F on (i) quiet days when $\Sigma K < 15$, (ii) disturbed days when $\Sigma K > 25$, and (iii) very disturbed days when $\Sigma K > 35$. They clearly show that spread F frequency on disturbed days is about $\frac{1}{3}$ of its value on quiet days at Ahmedabad. Days with $\Sigma K > 35$ are few in number and the percentage changes in this case cannot be given much weight. A similar reduction in spread F over Ibadan, particularly in winter, was obtained by Wright and others[20].

A further statistical analysis of spread F data was carried out by the superposed epoch method. The stations studied were Ahmedabad, Kokubunji and Slough and the zero epoch day was selected as one with $\Sigma K > 25$. When ΣK was high consecutively for 3–4 days, the day with the highest value of ΣK was taken as the zero day. The K indices of magnetic activity used in this analysis were from the Alibag Observatory. During the years 1956–57, 81 epochs could be collected and the mean percentage occurrence of spread F during the interval 2000–0600 hours on the epoch day and on 3 days before and 3 days after the epoch day were computed. The results are shown in Fig. 13a. It is found that the occurrence of spread F on a disturbed day is reduced to $\frac{1}{3}$ of its normal value at Ahmedabad for an increase of about 80 per cent in ΣK, while it increases to about $2\frac{1}{2}$ times the normal at Slough. At a place like Kokubunji, there is no appreciable change in spread F activity from quiet to disturbed period. In Fig. 13b, curves of spread F against ΣK are drawn for Ahmedabad and Slough. The change from a decrease in spread F in low latitudes to an increase in middle latitudes during magnetically disturbed periods takes place near magnetic dip 49°. Lyon and others[21] showed that in the southern hemisphere, such a change in the variation of spread F with magnetic character figure, Cp, took place at geographic latitude 20° or magnetic dip 54°. From the study of some individual storms it was found that while spread F occurrence was quite high at Kokubunji, Akita and Wakkanai after the storm commencements, it was not so at Yamagawa and other low latitude stations.

CONCLUSIONS

The following are the main conclusions on the various aspects of the disturbances in the F_2 layer of the ionosphere associated with geomagnetic storms which have been studied not only at Ahmedabad but also at other stations in lower and higher latitudes mainly in the eastern zone:

(i) The meridional profiles of f_0F_2 during quiet and disturbed periods show that in the range of latitudes with magnetic dip 0°–60°N, the maximum decrease in f_0F_2 takes place at about magnetic dip 35° on disturbed days. There is a morning rise in f_0F_2 at all the stations with magnetic dip 0°–45°. The equatorial trough of low f_0F_2 is removed to a certain extent during magnetic disturbances. The cross-over from negative to positive change in f_0F_2 takes place at about magnetic dip 20°.

(ii) Two reversals in the phase of SD(f_0F_2) variation take place, one in the morning hours near magnetic dip 45° and the other at midday hours near magnetic dip 20°. This is different from the SD variation of the horizontal component of the earth's magnetic field, which changes its phase at about magnetic dip 71° (or mag. lat. 55°).

(iii) The disturbance variations of f_0F_2 greatly depend on the local time of the commencement of the magnetic storm. Those commencing in the second quarter of the day produce maximum disturbance in F_2 at Ahmedabad, while those commencing in the evening hours cause the minimum effect.

(iv) The storm time or D_{st} variation of f_0F_2 continues for a longer period at higher latitudes. Sharp changes in f_0F_2 begin only after about 8 hr after the SC and the maximum depression of f_0F_2 occurs at later hours near the f_0F_2 peak. The maximum D_{st} variation of f_0F_2 does not occur simultaneously with that of H.

(v) Changes in cosmic radio noise absorption on 25 Mc/s. at Ahmedabad on magnetically disturbed days show correlation with changes in the maximum electron concentration in the F_2 layer.

(vi) Spread F echoes are less frequent on disturbed days at Ahmedabad. This is opposite to what is observed at Slough. The change-over from decrease to increase of spread F occurs at about magnetic dip 45°.

The disturbance effects on the F_2 layer of the ionosphere are of a complex character and for their elucidation, synoptic studies are required of true N-h profiles at a number of stations. There is reason to believe that magnetic storms disturb the whole of the ionosphere including the Van Allen belts.

ACKNOWLEDGEMENT

The authors' thanks are due to the Directors of Radio Research Station, Slough; the Radio Research Laboratories, Japan; the Magnetic Observatory, Alibag; the Astrophysical Observatory, Kodaikanal; and the Chief Engineer, All India Radio, who have kindly supplied ionospheric and magnetic data.

REFERENCES

1. KOTADIA, K. M. & RAMANATHAN, K. R., *Ann. IGY*, **11** (1958), 68.
2. BERKNER, L. V. & SEATON, S. L., *Terr. Mag. Atmos. Electr.*, **45** (1940), 393 & 419.
3. APPLETON, E. V. & PIGGOTT, W. R., *J. atmos. terr. Phys.*, **2** (1952), 236.
4. MARTYN, D. F., *Proc. roy. Soc.*, **218A** (1953), 1.
5. SINNO, K., *Rep. Ionos. Res. Japan*, **7** (1953), T.
6. SKINNER, N. J. & WRIGHT, R. W., *J. atmos. terr. Phys.*, **6** (1955), 177.
7. MATSUSHITA, S., *J. geophys. Res.*, **64** (1959), 305.
8. OBAYASHI, T., *J. Radio Res. Lab. Japan*, **6** (1959), 410.
9. MOOS, J. A. F., *Colaba Mag. Charts, Bombay*, (1910), 1846–1905.
10. CHAPMAN, S. & BARTELS, J., *Geomagnetism* (Clarendon Press, Oxford), 1940, 279.
11. RASTOGI, R. G., *J. atmos. terr. Phys.*, **14** (1959), 31.
12. RAMANATHAN, K. R. & KOTADIA, K. M., *Indian J. Met. Geophys.*, **5** (1954), 117.
13. APPLETON, E. V., *J. atmos. terr. Phys.*, **5** (1954), 348.
14. KOTADIA, K. M. & RAMANATHAN, K. R., *Proc. Indian Acad. Sci.*, **43** (1956), 394.
15. MARTYN, D. F., *Nature, Lond.*, **171** (1953), 14.
16. APPLETON, E. V., *Vistas in Astronomy*, Vol. 2 (Pergamon Press, London), 1956, 1.
17. APPLETON, E. V. & PIGGOTT, W. R., *J. atmos. terr. Phys.*, **3** (1953), 121.
18. BHONSLE, R. V. & RAMANATHAN, K. R., *Planet. Space Sci.*, **2** (1960), 99.
19. KOTADIA, K. M., *Proc. Indian Acad. Sci.*, **50** (1959), 259.
20. WRIGHT, R. W., KOSTER, J. H. & SKINNER, N. J., *J. atmos. terr. Phys.*, **8** (1956), 240.
21. LYON, A. J., SKINNER, N. J. & WRIGHT, R. W., *Nature, Lond.*, **181** (1958), 1724.

Geomagnetic disturbance effects in equatorial E_s

B. N. BHARGAVA
R. V. SUBRAHMANYAN

Astrophysical Observatory
Kodaikanal

Geomagnetic disturbance effects on day-time equatorial E_s at Kodaikanal which have been found to exist in addition to lunar effects are discussed. Sudden disappearances of sporadic E found to occur simultaneously with sudden decrease in horizontal and vertical force during the main phases of magnetic storms are described and discussed in relation to current systems responsible for intense equatorial E_s and those for storm time variations.

It has been known for some time that at equatorial stations where the quiet day solar magnetic variation S_q in horizontal force is large, day-time sporadic E has some remarkable characteristics. It is very regular in its diurnal variation with the critical frequency following the $\cos\chi$ law. It is also abnormally intense and often masks out the regular E layer in routine h′-f soundings. The lunar influence on this type of E_s has been discussed by Matsushita[1]. He has shown that at Huancayo the layer often disappears suddenly for varying intervals during day-time when these intervals are between zero and 0300 hours or between 1200 and 1500 hours lunar time. He also found that this disappearance occurred earlier than usual in the vicinity of new and full moon, particularly during winter, and that the phenomenon occurred during the first half of the periods when the lunar electric current flow in the equatorial regions was westward. Knecht[2] found, also at Huancayo, a lunar dependence of first appearance of E_s; during equinoxes and December solstice, E_s appeared earlier during new and full moon. Skinner and Wright[3] from Ibadan data observed that abnormally low values of fE_s occurred simultaneously with reduced horizontal and vertical force.

At Kodaikanal (mag. lat.: 1·75°N; geomag. lat.: 0·6°N) in addition to the lunar influence, a rather remarkable association of magnetic disturbances

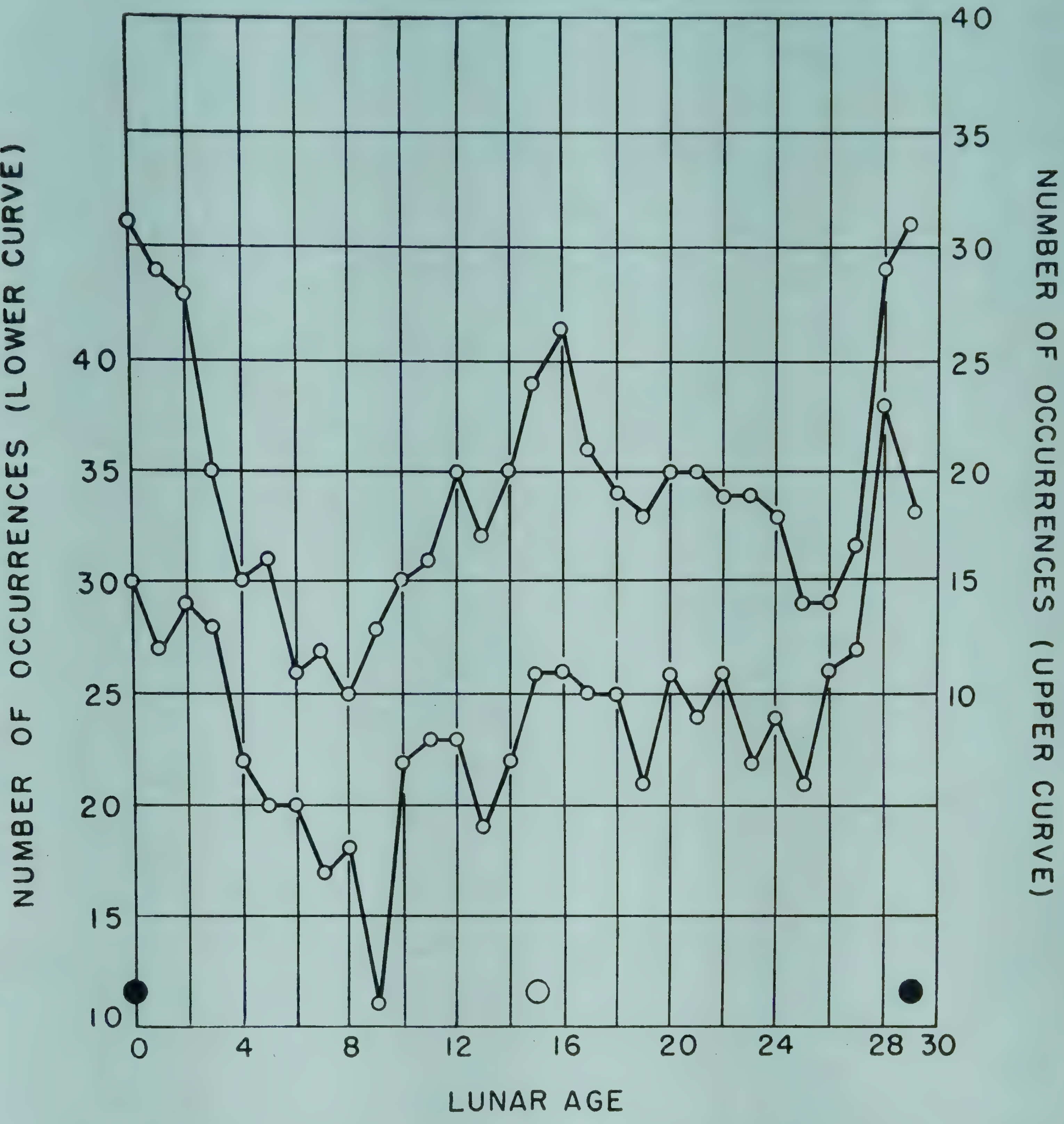

FIG. 1 — VARIATION OF NUMBER OF SUDDEN DISAPPEARANCE OF E_S WITH LUNAR PHASE, FOR ALL DAYS (LOWER CURVE), FOR DAYS AFTER EXCLUDING MAGNETICALLY DISTURBED PERIODS (UPPER CURVE)

with sporadic E has been noticed by the authors. It has been observed that during the main phases of most magnetic storms, when the horizontal force was considerably subnormal, E_s disappeared suddenly. While the main features of this phenomenon were similar to those associated with lunar currents, the length of time for which E_s remained absent during storm perturbations were, on the average, considerably in excess of those associated with the lunar effect.

In order to see how the effects could be separated from those associated with the lunar current, half-hourly day-time (0730–1700 hours, 75°E time) ionosonde records at Kodaikanal for a three-year period (June 1957 to May 1960) were scrutinized. To start with, all cases of E_s disappearance were grouped according to the age of the moon. The number of occurrences in each group were plotted against lunar age. It will be seen from the resulting curve (Fig. 1, lower curve) that the frequency of occurrence of the phenomenon was, in general, maximum around new and full moon with a certain amount of extraneous irregular variation. Next, when the process was repeated, with data for all disturbed days excluded, the behaviour (Fig. 1, upper curve) was more systematic with regard to the age of moon resulting in better maxima around new and full moon and minima around first and third quarter. This is an indication that the disappearance of E_s is, to a considerable extent, associated with geomagnetic storm perturbations at irregular intervals, irrespective of the lunar age.

According to Matsushita[4] the occurrence of intense E_s in equatorial regions has a connection with the large diurnal range in H at these stations. These ranges are restricted to a narrow belt centred on ‘ zero ’ dip equator and are explained by the occurrence of an intense eastward current, the so-called electrojet, superposed on the normal current responsible for the daily S_q magnetic variation. The E_s disappearance at Huancayo is, according to Matsushita, caused by the westward lunar current which opposes the eastward electrojet. This is confirmed from observations of solar times of E_s disappearance at Kodaikanal where the frequency of disappearance is found to be minimum around 1100 hours which is the time at which the normal S_q and electrojet effects are maximum as seen from Kodaikanal magnetic variations.

In order to obtain preliminary results on the effects of magnetic storms on E_s, a superposed epoch analysis was carried out. From inspection of ionograms at half-hour intervals the time of first disappearance of E_s was taken as zero epoch and the deviations ΔfE_s were obtained for an eight-hour period around zero epoch. This process was carried out for 27 storms recorded during the three-year period. For the same period, departures in horizontal force and vertical force were also obtained and these together with departures in fE_s are plotted in Fig. 2. It will be seen that there is considerable correspondence between E_s disappearance and subnormal values of H and Z. The horizontal force drops by over 175 gammas and vertical force by about 18 gammas on the average, simultaneously with E_s disappearance.

It is known that the large effective conductivity in the dynamo region during daylight (due to inhibition of the Hall currents) associated with abnormally large solar daily magnetic variation S_q and electrojet is responsible for the formation of equatorial type E_s. While the westward current responsible for lunar daily magnetic variation weakens, the eastward currents

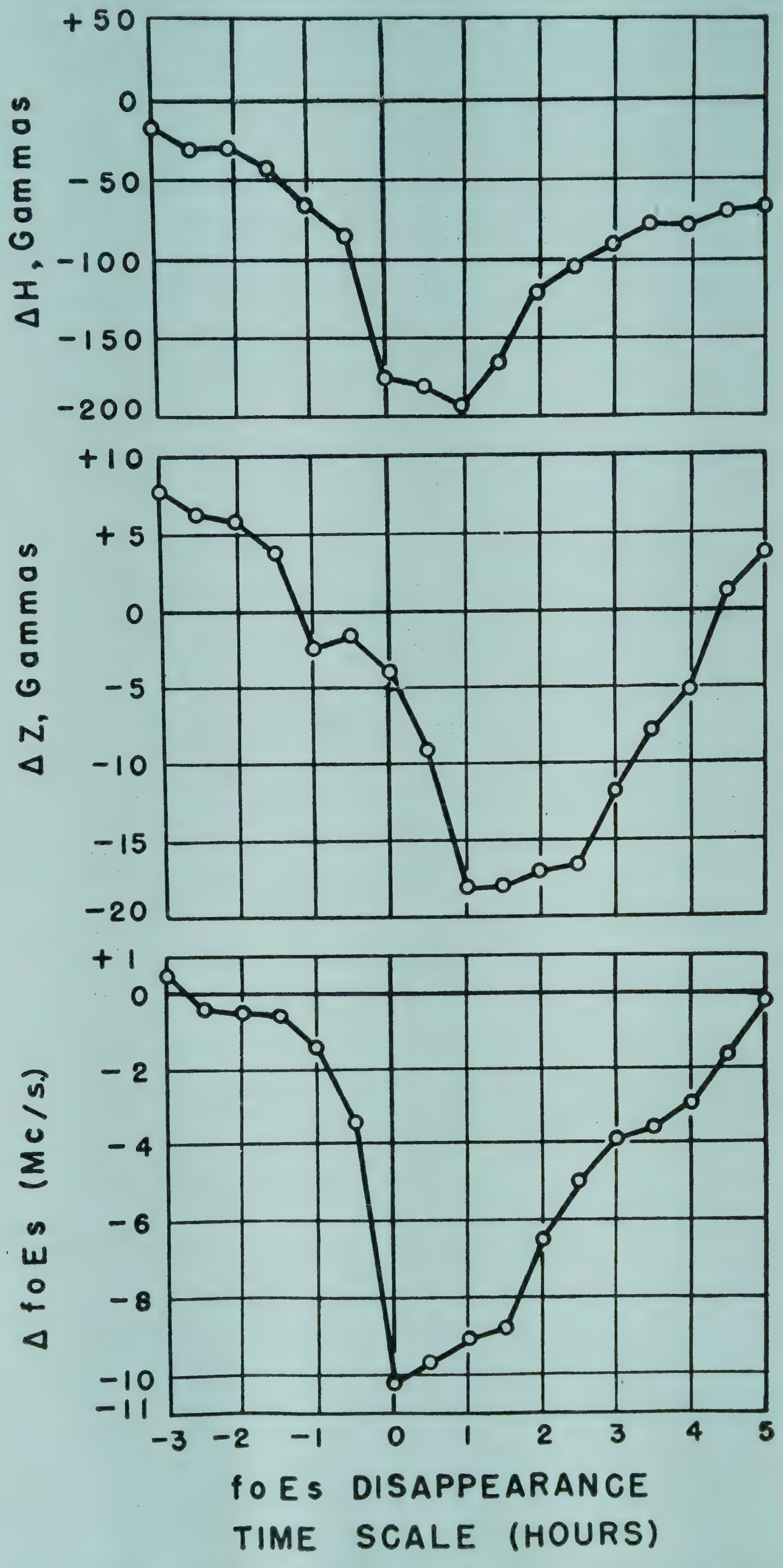

FIG. 2 — DEPARTURES IN H AND Z COMPONENTS OF EARTH'S MAGNETIC FIELD WITH THOSE IN fEs

resulting in E_s disappearance, the ring current responsible for D_{st} variation, which is also westward, appears to prevent favourable conditions for the inhibition of the Hall currents at equatorial stations. It appears that this causes a considerable drop in the effective conductivity in the dynamo region and results in weakening of the S_q and electrojet currents; consequently, subnormal values of H and Z and the disappearance of E_s for several hours during the main phase of a magnetic storm have been observed.

A detailed study covering a period of over half a solar cycle is in progress and the results will be published in due course.

REFERENCES

1. MATSUSHITA, S., *J. atmos. terr. Phys.*, **10** (1957), 163.
2. KNECHT, R. W., *J. atmos. terr. Phys.*, **14** (1959), 348.
3. SKINNER, N. J. & WRIGHT, R. W., *Proc. phys. Soc.*, **70B** (1957), 833.
4. MATSUSHITA, S., *J. Geomag. Geoelectr.*, **3** (1951), 44.

Effect of magnetic activity on E region drifts at Waltair

R. RAGHAVA RAO
B. RAMACHANDRA RAO

Ionospheric Research Laboratories
Andhra University, Waltair

This paper embodies results of the study of the effect of magnetic activity on E region drifts at Waltair. Analysis of all the observations taken over a period of two years shows a definite positive correlation between mean drift speed and magnetic K index. The mean drift speed has been found to increase more or less linearly with increase of K index.

Several investigators have studied the relation between the horizontal drifts in the E region and magnetic activity and reported that there is no systematic variation within the K index range 0–5, although for higher values of K indices (which occur rarely) higher drift speeds were recorded. Chapman[1] found no correlation between E region drift speed and K index until K exceeds 4. Briggs and Spencer[2] observed no dependence of E region drift speed on K index for values up to 5. However, they recorded on one occasion drift speed of the order of 500 m./sec. in the E region when there was a magnetic storm. In the present investigation E region drift data obtained at Waltair between June 1957 and May 1959 covering the IGY and part of the IGC periods have been utilized to study the nature and extent of the dependence of E region drift speeds on the magnetic K indices.

PROCEDURE

The E region drifts at Waltair were measured by the space receiver method which has been suitably modified by using a triple beam oscillograph for recording the fading patterns. This method has been described in a previous communication[3]. All the drift records were taken on a frequency of 2·5 Mc/s. at hourly intervals or at least six days including the World Days in each month. All the observations were made at a virtual height range of reflection of 100–105 km. Only day-time drift data were utilized in this investigation as there was not much variation in the regular quiet day variation in the magnitude of drift speed. Night-time results were not taken into consideration as there were fewer observations and as the values of drift speeds were generally higher than those taken during day-time. Three-hourly magnetic K indices provided by the Alibag Observatory (K index 9 corresponds 300γ) were utilized as this is the nearest magnetic observatory situated on nearly the same geomagnetic latitude. The average of the drift speeds in each of the three-hour periods corresponding to the K indices was obtained.

RESULTS AND DISCUSSION

Data for each year 1957–58 and 1958–59 were analysed separately to study if there was any change in the effect of magnetic activity from year to year. The mean drift speeds thus obtained are plotted against the corresponding K indices for observations of each year separately as shown in Fig. 1(a) and (b). A final plot of mean drift speed against K indices for all the data is also given in Fig. 1(c). Altogether about 600 observations have been utilized for this analysis. Mean straight lines are drawn to pass through the points which fit fairly on the line indicating the general linear relation existing between mean drift speed and magnetic K index. An interesting

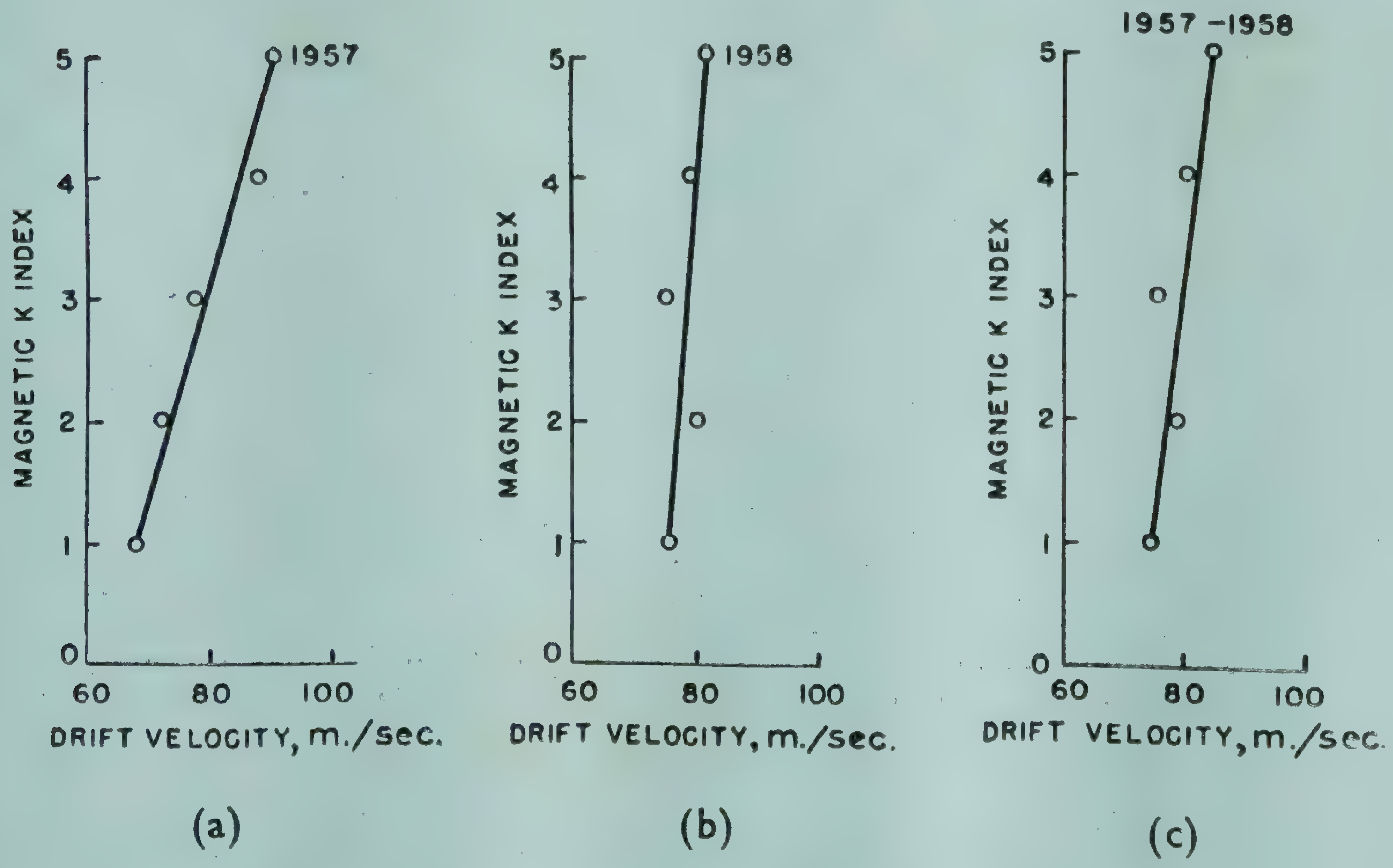

Fig. 1 — Relation between magnetic K index and drift velocity

observation is the larger effect of K index on drift speed from the data taken during 1957–58. It follows from this study that there is a well-defined positive correlation between E region drift speed and magnetic K index in the range 0–5. It may be noted here that the magnetic K indices reported from Alibag rarely exceeded the value of 5. The drift observations available against the K index values of 6 were few and hence they have not been utilized in this study.

No other similar investigation was carried out at any other low latitude station to compare the results obtained by the authors. It will be, however, interesting to examine the results in the light of earlier investigations at high latitude stations. Chapman[1], Harange and Pederson[4] and Briggs and Spencer[2] reported that E region drift speed is independent of K index up to a value of 4–5 for the observation at high latitude station, although on some occasions they noticed a large increase in drift speed for higher values of K indices and disturbed conditions in the ionosphere. In view of these earlier findings of absence of definite correlation between K index and E region drift speed, the authors' observation of a definite positive correlation at Waltair is of considerable significance particularly for the theoretical work on the origin of drifts. It may be noted that this positive correlation of E region drifts and magnetic activity is in marked contrast to the well-established negative correlation observed by Rao *et al.*[5] between F_2 region drifts and magnetic activity at Waltair. It is interesting to note that the drifts in the E and F regions at Waltair, which is one of the low latitude stations, differ significantly from those observed at high latitude stations not only in their diurnal and seasonal behaviour but also in their relation to magnetic activity. Martyn[6] has given a theory of the electro-dynamic origin of F_2 region drifts and predicted the significant differences in the phase of the drifts expected for the low and high latitude stations, but so far no satisfactory explanation has been given for the difference in the drift variation with magnetic activity observed at low and high latitude stations. Detailed work in this direction is in progress in this laboratory.

REFERENCES

1. CHAPMAN, J. H., *Canad. J. Phys.*, **31** (1953), 120.
2. BRIGGS, B. H. & SPENCER, M., *Rep. Progr. Phys.*, **17** (1954), 245.
3. RAO, B. R., RAO, M. S. & MURTY, D. S., *J. sci. industr. Res.*, **15A** (1956), 75.
4. HARANG, L. & PEDERSON, K., *J. geophys. Res.*, **62** (1957), 183.
5. RAO, B. R., RAO, E. B. & MURTY, Y. V. R., *Nature, Lond.*, **183** (1959), 667.
6. MARTYN, D. F., *Physics of the Ionosphere* (Physical Society, London), 1955, 163.

Effect of magnetic activity on horizontal drifts in F_2 region

B. RAMACHANDRA RAO
E. BHAGIRATHA RAO
Y. V. RAMANA MURTY

Ionospheric Research Laboratories
Physics Department, Andhra University
Waltair

The results of the study of the effect of magnetic activity on F_2 region drifts at Waltair are recorded. It is found that the drift speed decreases more or less linearly with increase in magnetic K index. The effect of magnetic activity is least on the N-S component and maximum on E-W component.

Systematic studies on geomagnetic variations and the different ionospheric parameters have revealed that they are intimately associated with the activity of the sun. Since, according to Martyn[1], the drifts in the F_2 region of the ionosphere are caused by the current system in the lower ionosphere, it is to be expected that the magnetic activity and the movements in the F_2 region are interdependent. The drift data for E and F_2 regions were examined by several investigators with a view to studying the effect of magnetic activity on drift speed and direction. Briggs and Spencer[2] have examined data from high latitude stations and concluded that the F_2 region drift speeds increase with magnetic K index. Examinations of drift data obtained by radio star scintillation method by some investigators[3,4] also led to the same conclusion. As the authors have found that the F_2 region drifts at Waltair (17°43′N : 83°18′E and mag. lat. 9°30′N) show a significantly different behaviour from those at high latitude stations, the drift data for F_2 region at Waltair were carefully examined with a view to ascertaining the nature and extent of this dependence of F_2 region drifts on magnetic activity and a note was published[5]. Details of the investigation are described in this paper.

PROGRAMME OF OBSERVATIONS

The drift measurements were made by the spaced receiver method of Mitra[6] using a slightly modified technique described in an earlier paper[7]. The F_2

region drift velocities obtained by the spaced receiver method on a frequency of about 6·0 Mc/s. for a period of 36 months from February 1956 to December 1958 (which includes the IGY period) were utilized for this investigation. Most of the observations were taken at 0900, 1200 and 1500 hours for three or four days in a week during the period. For those days on which drift data were available for all the 24 hr, the mean of the three observations around these three particular hours was taken to give smoothed and representative values for these hours. K indices published by the Alibag Magnetic Observatory were taken as an index of magnetic activity at Waltair as the geomagnetic latitude for these two stations is nearly the same.

In order to compare the drift velocity with magnetic K index, average of large number of drift speeds and the corresponding K indices extending over the period mentioned above were taken, as comparison of individual observations may not be justified due to the fact that several other factors are likely to influence the instantaneous values of both the quantities. Since the three hours at which F_2 drift observations were taken happen to be 0900, 1200 and 1500 hours IST which correspond to 0330, 0630, 0930 hours GMT, the average of the first two K indices was taken to represent the magnetic activity at 0900 hours IST and so on. Altogether about 500 observations were utilized for this analysis.

RESULTS AND DISCUSSION

Variation of Drift Speed with K Index. In the first instance the dependence of drift speed on magnetic K index was examined by taking the observations for all the three hours grouped together. Drift speeds corresponding to different K indices were then separated out and the average drift speed for each value of K index was obtained.

Fig. 1(a) shows a plot of the drift speed versus K index for all the observations. It is clearly seen from this figure that a mean straight line can be drawn to fit the observations fairly well. It may be concluded from this plot that the drift speed in the F_2 region decreases more or less linearly with increase of magnetic K index in the range 0–6. This result is exactly opposite to the variation of F_2 region drift speed with magnetic index observed at high latitude stations.

Results of drift measurements from this station reported in an earlier communication[8] revealed the interesting feature that the F_2 region drift speed varies systematically over a day, reaching a maximum value at about noon and midnight. In view of this diurnal variation of speed, the effect of magnetic activity on the drift speeds taken at the three hours separately has been studied. For this analysis, the average drift speed corresponding to each K index for the observations at each of the three hours were obtained taking approximately equal number of observations for the three hours.

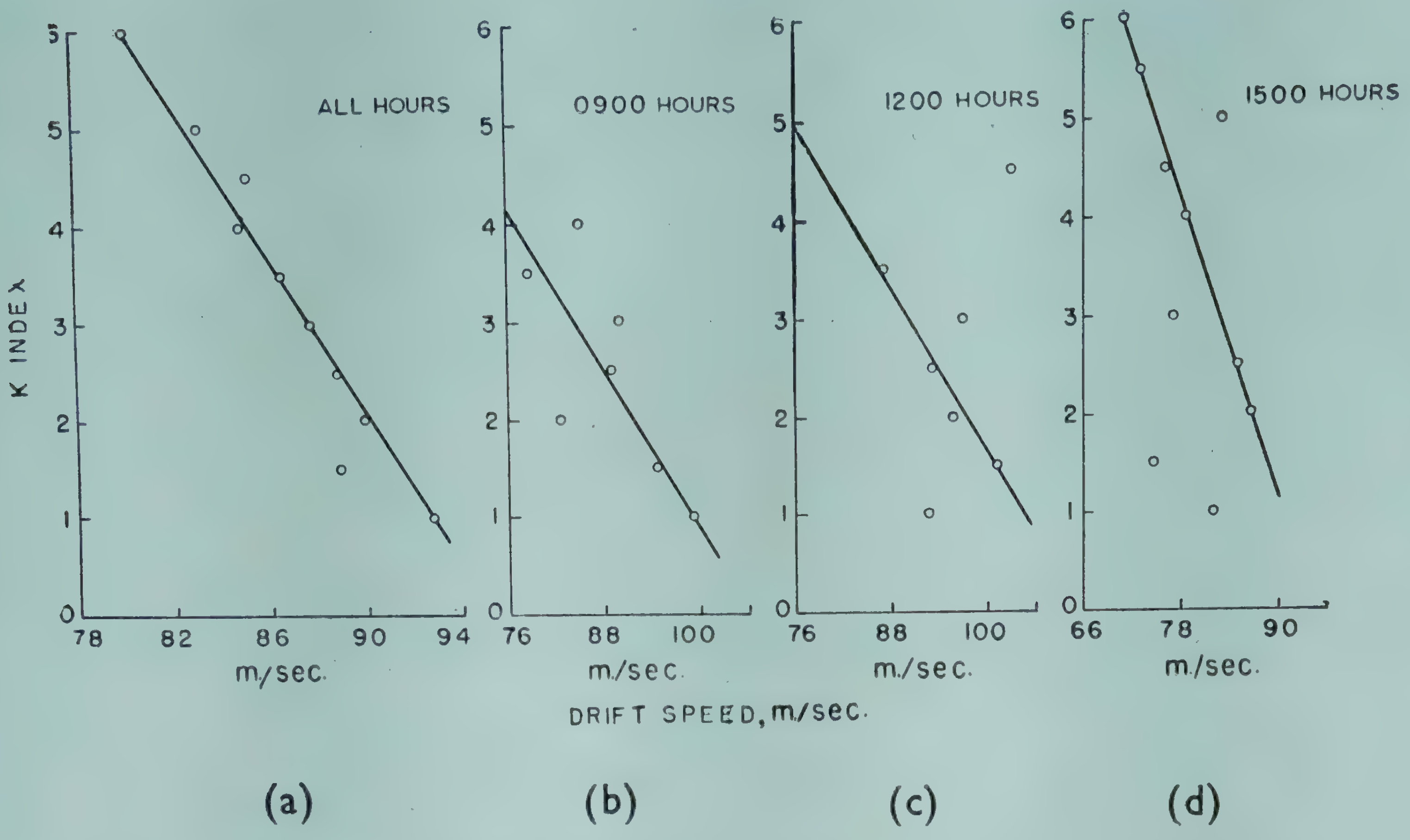

FIG. 1 — ALIBAG K INDEX VERSUS F_2 REGION DRIFT SPEED AT WALTAIR

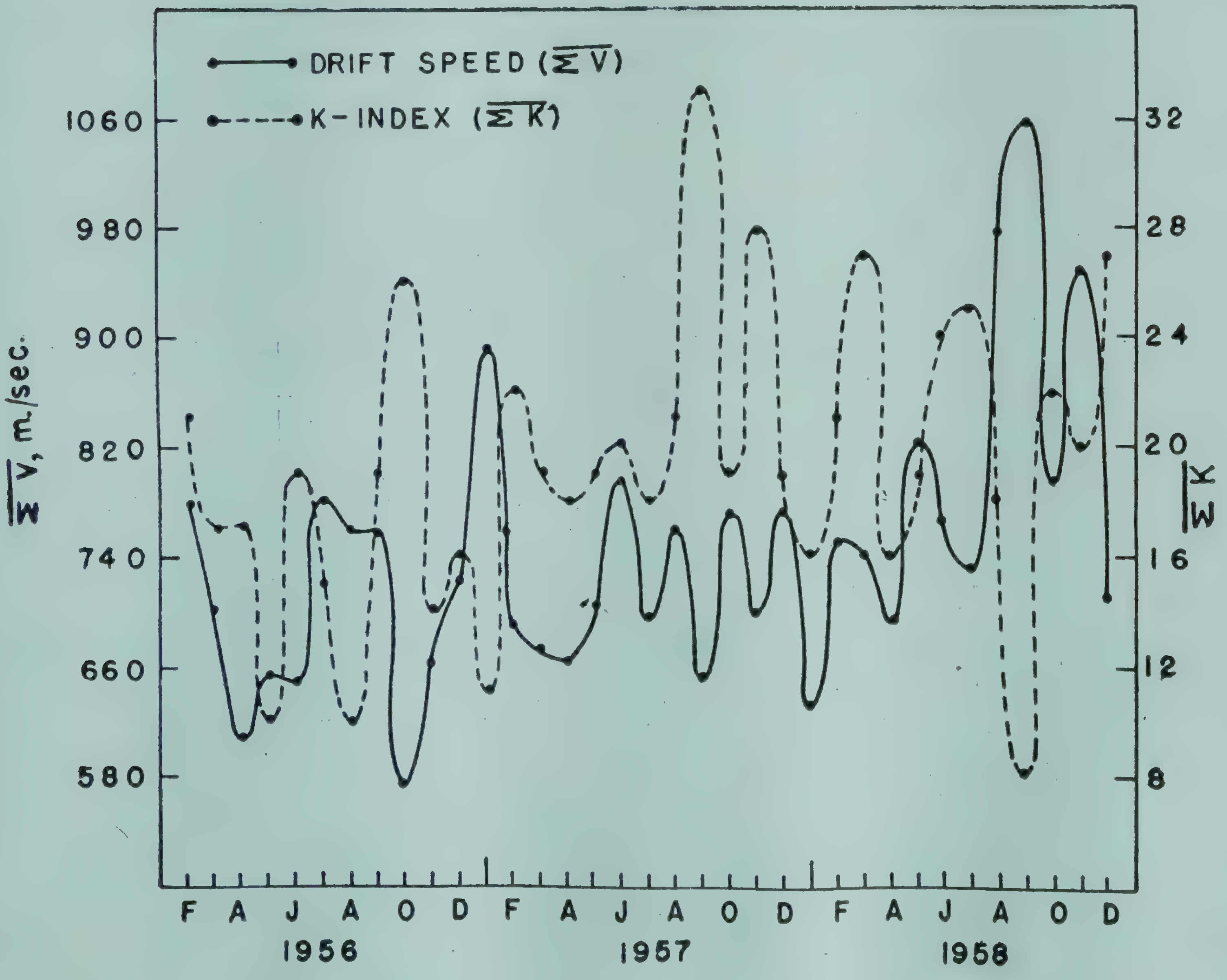

FIG. 2— VALUES OF DRIFT SPEED IN THE F_2 REGION AND ALIBAG K INDICES FOR DIFFERENT MONTHS DURING 1956–58

Plots of the K indices versus the average drift speed for the observations taken at the three hours — 0900, 1200 and 1500 — are shown in Figs. 1(b), 1(c) and 1(d) respectively. It will be clearly seen from these figures and from the mean straight lines drawn to pass through the points, that the drift speed decreases with increase of K index. Also, observations for the individual hours show a wider scatter when compared to the plot of the total observations shown in Fig. 1(a). This may be due to the fact that the number of observations is limited when considering the data taken at each hour separately. However, straight line graphs could be drawn to fit almost all the points except those that are obtained by averaging limited number of observations. It may be noticed that the rate of decrease of drift speed with K index is nearly the same for observations taken at 0900 and 1200 hours, while it is considerably less for observations taken at 1500 hours.

Besides the observations taken for at 0900, 1200 and 1500 hours, the authors have also taken 24-hourly observations on about 3–4 days in each month, especially on the World Days during the IGY period. The observations thus obtained were subjected to a slightly different method of analysis to establish the inverse correlation between drift speeds and magnetic activity. The sum of eight K indices $\overline{\Sigma K}$ and the sum of eight average drift speeds $\overline{\Sigma V}$ during the 3-hr intervals were first determined for each day on which diurnal variation records were available. Average values of K and V for each month were thus obtained by using the data available for some days in each month.

Fig. 2 shows the values of $\overline{\Sigma K}$ and $\overline{\Sigma V}$ values thus obtained plotted against the month in the same graph in order to compare the variation in these parameters. The data thus obtained cover the period from February 1956 to December 1958. Smooth curves are drawn through all the observations to depict the general trend of variation. A close study of these two curves in Fig. 2 reveals the interesting feature that the average value of $\overline{\Sigma V}$ varies inversely as the magnetic sum index $\overline{\Sigma K}$. It will be noticed that during some months this inverse correlation is particularly prominent as a large change in $\overline{\Sigma K}$ is associated with an equally large change in $\overline{\Sigma V}$ in the opposite sense. The negative correlation coefficient between $\overline{\Sigma V}$ and $\overline{\Sigma K}$ for the entire period is quite significant. Thus, it may be seen that this result once again establishes the conclusion from the previous study that, at low latitude stations, F_2 region drift speed and magnetic K index are inversely correlated. Beynon and Thomas[9] have investigated the effect of magnetic activity on the speed of travelling disturbances at high latitude stations on similar lines and found that they are positively correlated.

As there is no previous study of the effect of magnetic activity on F_2 region drifts at low latitude stations, the results obtained by the authors have been

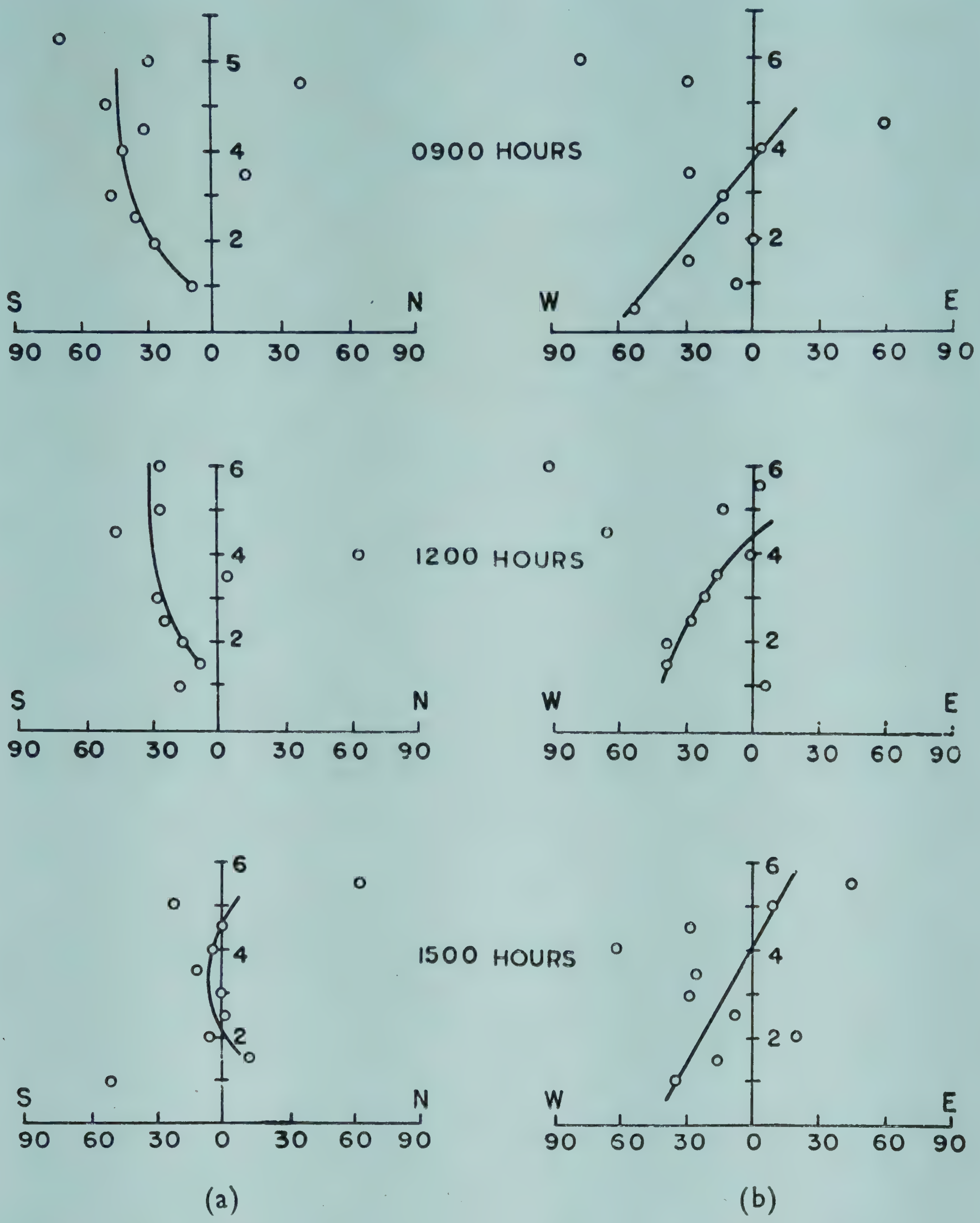

FIG. 3 — RELATION BETWEEN MAGNETIC K INDEX AND DRIFT SPEED AT WALTAIR AT DIFFERENT HOURS: (a) N–S COMPONENT AND (b) E–W COMPONENT

examined in the light of the work done at high latitude stations. The observations at a level of about 300 km. of Chapman for Ottawa[10] and Montreal and of Briggs and Spencer[2] for Cambridge show conclusively that F_2 drift speed increases with magnetic activity. Dagg[4] and others compared the drift speeds estimated by radio star scintillation method which refer to the F_2 region with magnetic K indices and showed that there is a rapid increase of drift speed with increase of magnetic activity. In view of the overwhelming evidence of a definite positive correlation between F_2 region drift speed and magnetic K index at high latitude, the opposite result obtained by the authors is of particular significance for the current theories of the origin of the F_2 region drifts.

Variation of N-S and E-W Components with K Index. In order to study the variation of N–S and E–W components of drift with K index all the drift speeds taken at the three timings, 0900, 1200 and 1500 hours, were resolved into N–S and E–W components and the average values of N–S and E–W components for each value of K index were arrived at by taking the sign into account. Drift movements towards north and east were taken as positive. Approximately equal number of observations were used for each of the three timings for various values of K index. The values thus obtained are plotted and shown in Fig. 3. Even though the availability of a limited number of observations for each hour results in some scatter of the points in this figure, it was possible to draw mean curves to cover maximum number of points. From an examination of the graphs it will be clear that for all the three hours the N–S component shows very little variation with magnetic K index, on the other hand, the E–W component, which is towards west on quiet days for all the three hours, shows a strikingly rapid decrease in the westward amplitude with K index. This decrease is not the same for all the three hours, being more rapid for data taken at 0900 hours. For K indices above 4 there is a tendency for the E–W component to change from west to east, the transition occurring for K index value of about 4.

The results of this study are compared with those of Briggs and Spencer who studied the effect of magnetic activity on N–S and E–W components of F region drifts. They have found that the predominant effect is on the E–W component, whereas the N–S component remains almost constant up to K index value of 5 and only shows a tendency to southward movement for higher K figures. Thus the result that the E–W component at this latitude is the one which is most effected is in agreement with the Cambridge result. But the E–W component which is towards west at Cambridge tends to increase in magnitude for higher K indices, whereas the E–W component which is towards west during the day-time at our latitude begins to decrease in magnitude with K index. The tendency for the E–W component to reverse its direction for higher values of K index, which was observed by Briggs and Spencer at Cambridge was also observed by the authors from an analysis of data obtained at Waltair although sufficient number of observations are not available at this low latitude station to confirm this point. But it may be mentioned that the variation of E–W component with increase in magnetic activity observed by the authors bears some similarity to the reversal of drift from west to east observed by Hewish[11] from radio star scintillation study at Cambridge.

Conclusions

It may be noted that the effect of magnetic activity on F_2 region at low latitude station is uniquely different from that observed at high latitude stations. This is of particular interest in view of the fact that the phase of F_2 drifts at low latitude stations is exactly opposite to that at high latitudes, an effect which has been satisfactorily explained by Martyn in his theory of the electrodynamic origin of the F_2 drift. It will be therefore interesting to examine Martyn's theory in detail to see if a theoretical explanation can be offered for the unusual result of the decrease of the F_2 region drift speed with increase of magnetic activity observed at this low latitude station.

References

1. Martyn, D. F., *Physics of the Ionosphere* (Physical Society, London), **260** (1955), 163.
2. Briggs, B. H. & Spencer, M., *Rep. Progr. Phys.*, **17** (1954), 245.
3. Maxwell, A., *Physics of the Ionosphere* (Physical Society, London), 1955, 166.
4. Dagg, M., *J. atmos. terr. Phys.*, **11** (1957), 133.
5. Rao, B. R., Rao, E. B. & Murty, Y. V. R., *Nature, Lond.*, **183** (1957), 667.
6. Mitra, S. N., *Proc. Instn elect. Engrs*, **96** (1949), Pt III, 441.
7. Rao, B. R., Rao, M. S. & Murty, D. S., *J. sci. industr. Res.*, **15A** (1956), 75.
8. Rao, B. R. & Rao, E. B., *J. atmos. terr. Phys.*, **14** (1959), 94.
9. Beynon, W. J. G. & Thomas, L., *Rocket Exploration of the Upper Atmosphere* (Pergamon Press, London), 1954, 131.
10. Phillips, G. J., *J. atmos. terr. Phys.*, **2** (1952), 141.
11. Hewish, A., *Proc. roy. Soc.*, **209A** (1951), 81; **214** (1952), 494.

Some characteristics of enhanced solar radio emission at 28.6 Mc/s.

M. KRISHNAMURTHI
S. RAMAKRISHNA

Director's Research Laboratory
Indian Institute of Science
Bangalore

A comparative study of enhanced solar radio emission has been carried out using two independent systems of aerials designed to receive mutually perpendicular planes of polarization at 28·6 Mc/s. This study has revealed certain polarization characteristics of the various types of solar bursts which do not seem to conform to the general pattern of observations made by other workers.

Solar radio bursts are being studied at present at various radio observatories using the swept frequency technique[1,2]. This technique is helpful in recording the starting time and intensity of a radio burst over a continuous range of frequencies. On the basis of these observations, it is now well established that enhanced solar radio emission can be classified into five categories[3]. Of these, the so-called Type I, Type II and Type IV are of interest at metre wavelengths. Studies of these different types of bursts at fixed frequencies have been made to determine their polarization characteristics[4–6], as these observations are very necessary to determine the origin of these radiations. Some preliminary results of the studies on solar radio noise outbursts made at 28·6 Mc/s. at Bangalore (13°N : 77°35′E) are given in this paper.

A broadside array of thirty full-wave dipoles has been set up for carrying out a survey of the sky at 28·6 Mc/s. This has a beam-width between half power points of 10·7° in E–W direction and 16·7° in N–S direction. In this array, the aerials are stretched in the N–S direction. Therefore it will be sensitive only to radio waves with the electric vector component in a plane perpendicular to this direction. Besides receiving the general background cosmic noise, the aerial array will be able to detect noise from a localized source, provided it is sufficiently intense in comparison with the background. The undisturbed sun is not sufficiently intense to produce any such impression on the background radio noise record, but the enhanced emissions from the sun have been recorded on several occasions.

A second system of aerials in the form of an interferometer has been set up specially to study enhanced solar radio emission. This consists of two groups, of four full-wave dipoles each, separated by a distance of 15λ along an E–W base line. Each set of four dipoles forms a broadside array of two by two dipoles in E–W and N–S directions all connected in phase. In this case, the aerials are stretched in the E–W direction and, therefore, are oriented to receive radio waves polarized in a plane perpendicular to that which the thirty dipole broadside array is capable of receiving. The beamwidth between half power points of each four-element group is 25° in E–W and 28° in N–S directions, but due to interference between the two groups which are separated by 15λ, there are fifteen nulls on each side of the vertical. They are approximately 4° apart, being slightly closer at inclinations close to the vertical and getting further apart towards the horizon. An intense point source, such as a disturbed region of the sun, as it passes over the aerial pattern produces maxima and minima provided the disturbance persists for a sufficiently long time. Short duration bursts do not produce any interference pattern but are merely recorded as sudden increases in the noise level. A comparative study of the records obtained by the broadside array and the interferometer will give a general idea of the nature and extent of polarization of the incoming radiation. For a complete study of polarization characteristics, however, it is not enough to determine the amplitude of the two mutually perpendicular components. The percentage of polarization and the phase angle between the two components also have to be determined. Methods of measuring these are now being developed. Some of the results that have been obtained with the present system are interesting and are given below.

Results and Discussion

The period covered by the present study is the month of September 1960. On four days of this month intense solar radio emission was observed both on the broadside array and the interferometer records.

September 1, 1960. A noise storm (Fig. 1) consisting almost entirely of a series of short duration bursts lasting not more than a few seconds each was recorded for about 90 min. around noon. These are obviously the Type I bursts. At present, it is not possible to say whether they are randomly polarized or circularly polarized (fully or partly), because in either case they can be split into two equal, mutually perpendicular plane polarized components. It is generally believed that these are circularly polarized for the most part. While many of these bursts are found in both types

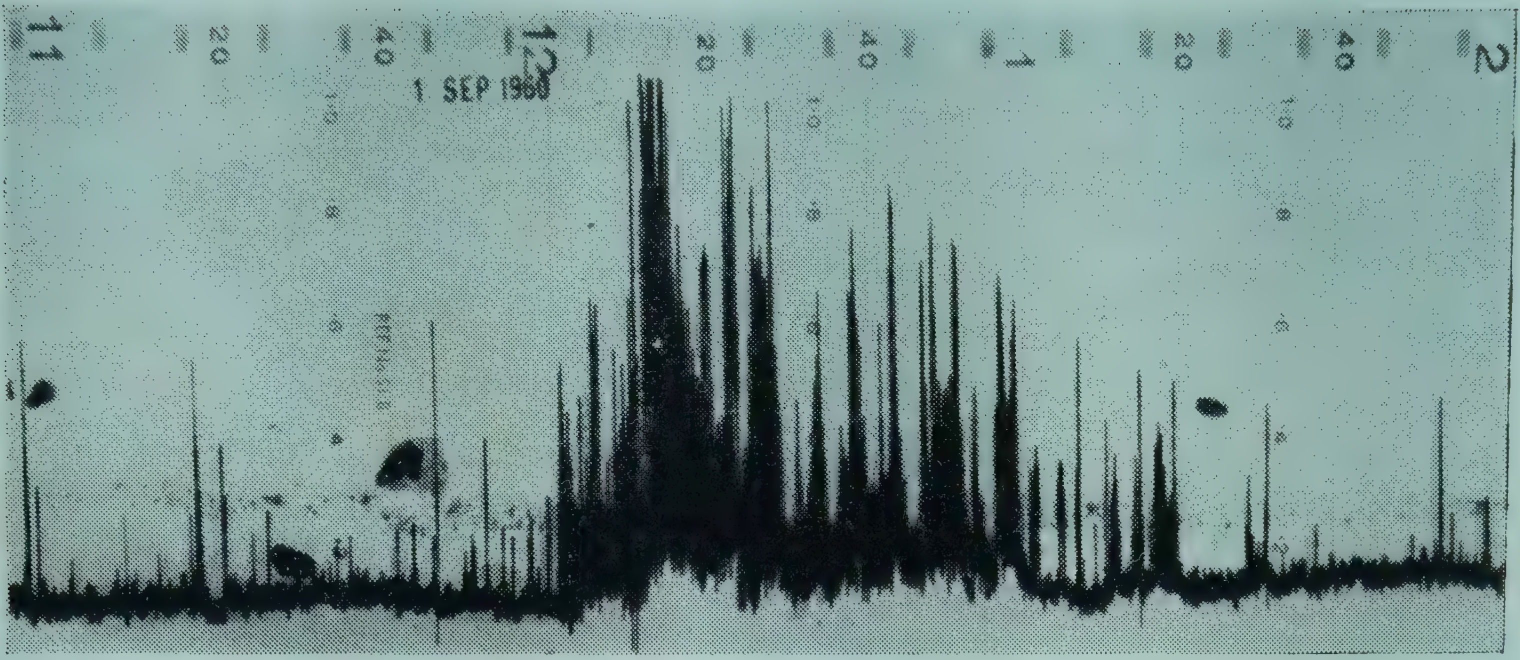

Fig. 1— Type I solar noise storm recorded on September 1, 1960

of record, there is a significant interval of about 10 min. in which the interferometer recorded a much larger number of Type I bursts, than the broadside array. This indicates that these particular bursts must have been highly elliptically polarized or, in the extreme case, linearly polarized.

September 2, 1960. A number of noise bursts of Type I were once again observed. Besides these, quite a few bursts each lasting for about 1–2 min. or more and a general increase in the noise level lasting about 25 min. also were recorded. From both the interferometer and the broadside array records, it can be inferred that the source responsible for the increased noise is the sun. Based on the classification already referred to, the increase in base level would correspond to a Type IV noise storm and the bursts of a few minutes duration to Type II bursts. All the Type I and Type II bursts occur simultaneously on the two records with a single exception. This occurred about an hour before local noon. A sudden and large increase in the noise level lasting nearly 10 min. (probably Type IV) was recorded at this time. On this, a number of very short duration bursts of Type I were superposed. The time of commencement of this particular event was definitely about 90 sec. earlier on the interferometer record than on the other one. This means that this particular event started off with a highly elliptically or even linearly polarized burst very soon becoming circularly or randomly polarized.

September 3, 1960. A somewhat similar phenomenon was observed with the difference that this time the broadside array started recording enhanced continuum noise nearly 10 min. prior to the interferometer (Fig. 2). In the figure, arrows marked *a* and *b* indicate the starting times of the noise storm on the broadside and interferometer records. All the other events were observed to occur simultaneously on the two records on this day also.

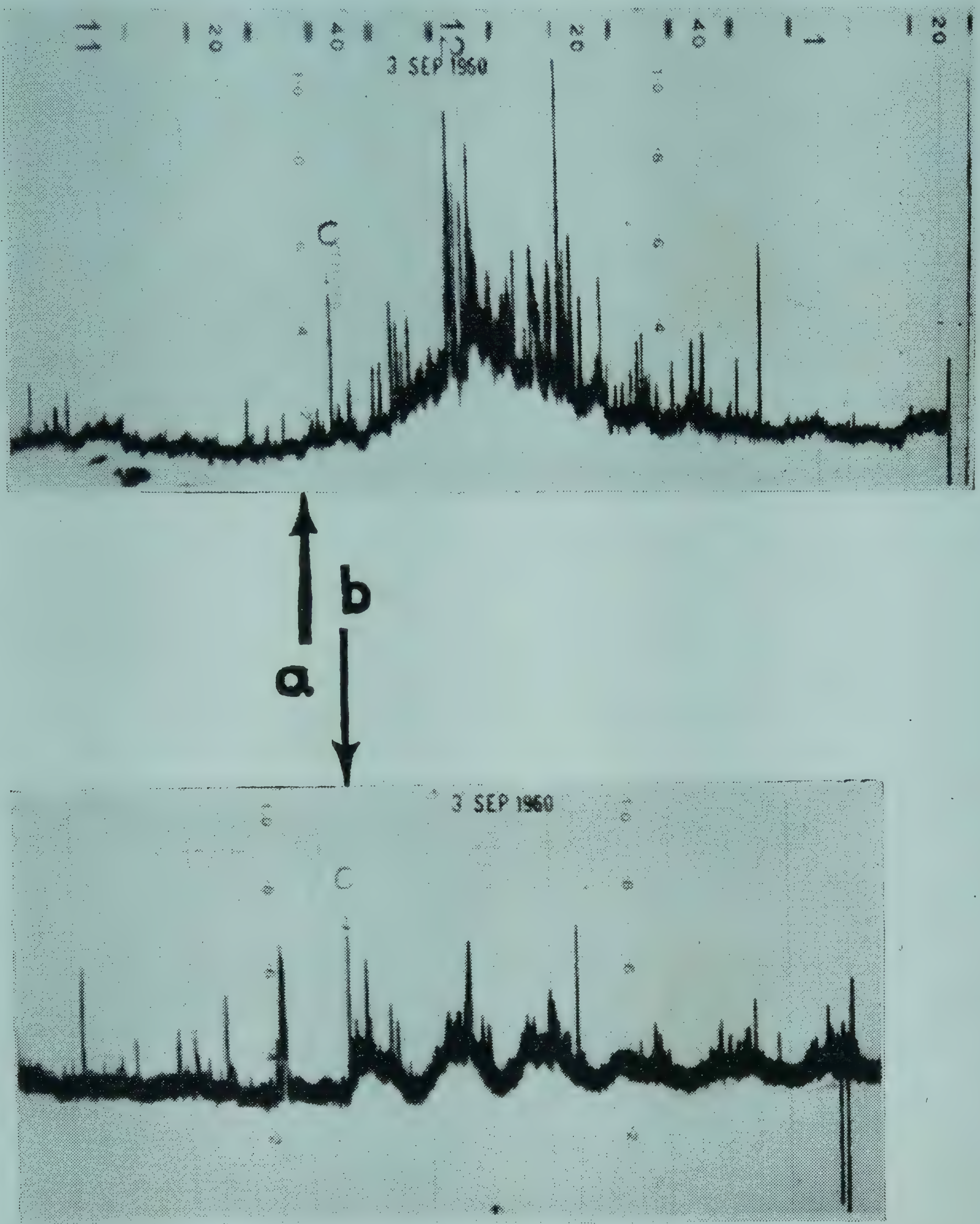

Fig. 2 — Broadside array and interferometer records of solar noise storm (Types I, II and IV) of September 3, 1960

If it is assumed that most of this radiation is either circularly polarized or unpolarized from the general nature of the records and also because of the observations made by several other workers, the two events described above seem to be rather exceptional. Firstly, enhanced radiation originating from an active region of the sun is generally observed to have the same sense of polarization throughout. Secondly, it is more usual for radiation to start as weakly and irregularly polarized but subsequently develop a strongly

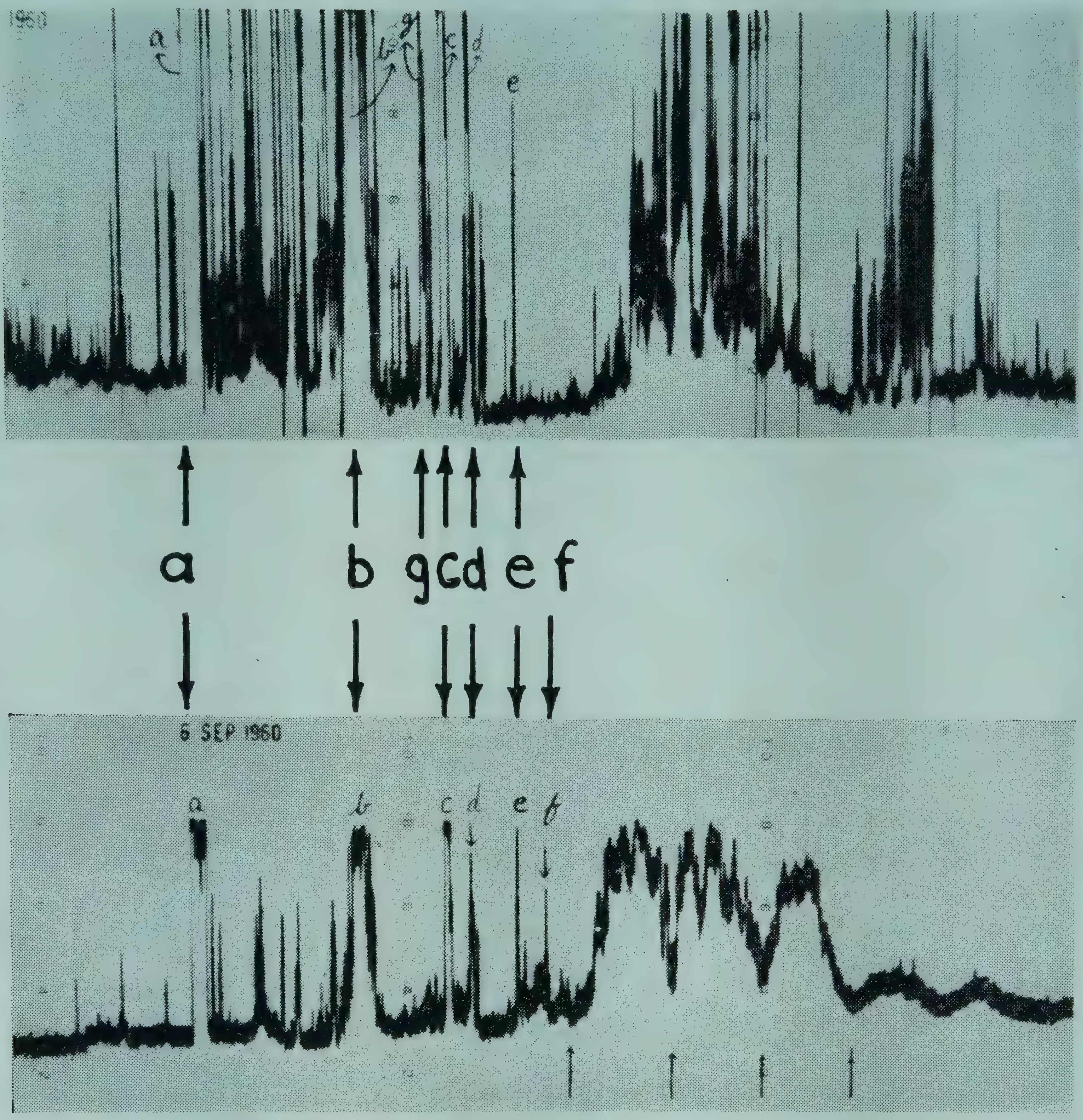

FIG. 3 — BROADSIDE ARRAY AND INTERFEROMETER RECORDS OF SOLAR NOISE STORM (TYPES I, II AND IV) OF SEPTEMBER 6, 1960

uniform polarization. The reverse case of a noise storm gradually becoming unpolarized has not been observed. The events of September 2 and 3 do not conform to these general observations. Similarly, the fact that some of the very short duration bursts on September 1 were not recorded on the broadside array while they were on the interferometer is not in accordance with the general observations.

September 6, 1960. On this day also, a number of Type I and Type II bursts occurred, and were recorded both on the interferometer record and broadside array record (Fig. 3). Some of the more intense bursts are identified in the above figure. Burst *f* is absent in the interferometer record, while burst *g* is absent in the broadside array record, suggesting that these were highly polarized bursts, such as were observed on the earlier days.

Another event of interest occurred on September 6. A very large increase in solar noise consisting of both Type I and Type IV was observed from 1300 to 1420 hours. Although by then the sun was in the minor lobe in the broadside array and beyond the half power point of the interferometer system, extremely high intensity was recorded. The main point of interest is, however, the interferometer record. Whereas on all previous occasions, the recorded noise returned to the average base level at the interference null positions, the minima were quite above the base level in this particular case. This means that even at the null positions noise from the sun was recorded. An obvious conclusion would be that the angular size of the source producing this enhanced emission from the sun is of the order of 1°, so that before it passes one lobe completely it is already partly in the next lobe. But such a large sized active region does not seem very likely from what is known of solar activity. It seems safer to assume that there were two separate regions on the sun's disc which became active simultaneously. In such a case while one region may be at the null point, the other might be contributing energy to the aerial system.

The correlation of the above observations with optical features on the sun's disc will be undertaken when data on this aspect become available.

Acknowledgement

The authors wish to thank Prof. S. Bhagavantam for his inspiring guidance during the course of the investigations.

References

1. Wild, J. P., Murray, J. D. & Rowe, W. C., *Aust. J. Phys.*, **7** (1954), 439.
2. Maxwell, A., Swarup, G. & Thompson, A. R., *Proc. Inst. Radio Engrs, N.Y.*, **46** (1958), 142.
3. de Jager, C., *Handbuch der Physik*, **52** (1959), 302.
4. Hatanaka, J., Suzuki, S. & Tscuchiya, A., *Proc. Japan Acad.*, **31** (1955), 81.
5. Cohen, M. H., *Proc. Inst. Radio Engrs, N.Y.*, **46** (1958), 172.
6. Alekseev, U. J. & Vitkevich, V. V., *Paris Symposium on Radio Astronomy*, 1959, 259.

A Study of Sudden Enhancement of Atmospherics on 27 kc/s. Band. M. W. CHIPLONKAR & R. N. KAREKAR, Department of Physics, Poona University, Poona.

A study of sudden enhancement of atmospherics (SEA) on 27 kc/s. at a station in low latitudes carried out during 1958–59, which is considered to be of importance for the world morphology of SEA, is reported. It is found that SEA shows maximum association with magnetic chrochet. The chances of occurrence of SEA are practically the same for most of the day hours. The rise time and decay time of SEA have average ratio of about 1: 4, with a total duration of about 40 min. The rise times cluster around two distinct values of 5 min. and 15 min. The total duration of SEA increases with its amplitude, whereas the rise time does not increase with amplitude. With rise time greater than about 13 min., the values of SEA are more in the forenoon than in the afternoon. (*Abstract*)

Changes in the Electron Density Distribution in the Ionosphere over Ahmedabad Associated with Solar Flares and Magnetic Storms: Part I—July 10-20, 1959. S. S. DEGAONKAR, Physical Research Laboratory, Ahmedabad [*Proc. Indian Acad. Sci.*, **54** (1961), 24].

Using the data from the vertical soundings made at Ahmedabad, the results of calculation of electron density-height profiles of the ionosphere in a highly disturbed period in July 1959 are discussed. After a brief account of the method of calculation (following Schmerling and Thomas), tables of coefficients for calculating the true heights from the h′-f curves of Ahmedabad are given. Charts of equal electron density at intervals of 2×10^5 electrons/cu. cm. are presented for each day during the period July 10–20. The following are the main conclusions:

(i) The perturbations produced by magnetic storms in low latitudes are mainly in the F region. The ionosphere below 200 km. remains relatively undisturbed.

(ii) During a magnetic storm, the layer heights go up, accompanied by sharp falls in electron densities. The total electron content in a vertical column also undergoes corresponding fluctuations. There is comparatively little or no F scatter during the storm period.

(iii) During day-time hmF is lower by 50–60 km. than hpF_2, but the difference between hpF_2 and hmF is not great at night hours. In general, this is true both for storm days and quiet days.

An appendix giving the hourly values of maximum electron density (NmF) and total electron content (n_T) for all the days is included. (*Abstract*)

Spread F and Geomagnetic Activity. C. V. S. Rao & S. N. Mitra, Research Department, All India Radio, New Delhi [*J. geophys., Res.*, **67** (1962)].

Ionospheric observations on the occurrence of spread F at Trivandrum for the period March 1957 to February 1960 have been analysed to study the correlation between geomagnetic activity and spread F. A definite inverse correlation has been found to exist between the two parameters. The relationship can be expressed by a linear equation. On all quiet days spread F starts after sunset and rapidly reaches a peak at about 2000 hours (75° EMT) falling off slowly towards morning. On disturbed days, spread F is decisively less than that on quiet days and the diurnal characteristics tend to attain a second peak after midnight. On magnetically stormy days the phenomenon is absent in the earlier part of the night and occurs only after midnight ultimately disappearing as sunrise approaches. These phenomena are discussed in the light of the theory of spread F recently developed by Martyn. The observed features over Trivandrum are in agreement with the theoretical interpretations. (*Abstract*)

Geomagnetic Field and Ionospheric Drift. S. N. Mitra & K. K. Vij, Research Department, All India Radio, New Delhi. [*J. Instn Telecomm. Engrs*, **6** (1960), 90].

Investigation of ionospheric drift by the well-known spaced receiver technique utilizing fading on pulsed transmission is in progress at the Research Department, All India Radio, since January 1958 and forms part of its programme of IGY. There is some uncertainty as to the origin of this drift system at ionospheric heights. If the drifts were due to the effect of solar and lunar gravitational tides upon a uniformly rotating sphere, one would expect the drift vector to exhibit a predominant semi-diurnal periodicity. Observation indicates that this is not always so. In fact, there is hardly any regular behaviour in diurnal variation of the phase of the drift system. One would, therefore, like to enquire whether earth's magnetic field exercises any influence on the drift system and is responsible for irregular variation of its phase. It is likely that such an influence exists, as the ionosphere consists of charged particles. The study has, however, shown that the magnitude of the drift velocity is fairly independent of K; in fact, large magnetic storms have failed to produce any significant change in the magnitude of the drift velocity. The variation of E–W and N–S components of the drift velocity during a quiet day does not indicate any correlation with K; but on disturbed days, the northward velocity of the N–S component increases in synchronism with increase in K. (*Abstract*)

Magnetic Storms and Cosmic Radio Noise on 25 Mc/s. at Ahmedabad. R. V. Bhonsle & K. R. Ramanathan, Physical Research Laboratory, Ahmedabad [*J. Planet. Space Sci.*, **2** (1960), 99].

Analysis of the intensities of cosmic radio noise on 25 Mc/s. at Ahmedabad shows that during days of magnetic storms there is, in addition to the usual variation of intensity due to the diurnal changes in D region ionization of F region absorption, a further variation. This shows itself as a decrease in the attenuation on the first two days of the storm and an increase in the attenuation on the third day. The decreased attenuation is most clearly seen in the first half of the night on the first and second days after the commencement of a storm and is associated with a decrease in F scatter. (*Abstract*)

Variation of angle of arrival of downcoming radio waves and irregularities in the ionosphere

S. S. BANERJEE
P. K. MUKHERJEE

Engineering College, Banaras Hindu University
Varanasi

It has been established during recent times that variation in the angle of arrival is closely related to the irregularities in the ionosphere[1,2]. In this laboratory also, observation on the angle of arrival of radio waves from the ionosphere by means of vertical and frame aerial was started some years ago in connection with the study of the intensity variation of the received radio signals. A few years later further observations were recorded by Srivastava and Rajan[3] in view of the anomalous variations of these angles of arrival. Much of the anomaly was, however, explained by taking into account the magneto-ionic interference of the incoming waves. The present communication shows the variation of the angle of arrival of the downcoming radio waves by means of two spaced aerials. The method of calculating the parameters of the irregularities in the ionosphere and that of estimating the angular spread in the downcoming rays have also been discussed.

METHOD OF MEASUREMENT

The method adopted for the measurement of the angle of arrival of downcoming waves is similar to that used by Wilkins[4].

Two similar horizontally spaced horizontal dipole aerials were placed equally above the terrace of the building. The aerials were connected to twin-matched superheterodyne receivers having a common oscillator. The outputs from the receivers were fed to the deflecting plates of a cathode ray oscillograph which produced the phase ellipses on its screen from which angles of arrival were calculated from Equation (1).

$$\cos\theta = \frac{\lambda}{\pi d}\tan^{-1} b/a \tag{1}$$

where θ = angle of arrival of the downcoming ray, λ = wavelength of the signals received, d = aerial spacing, and a and b are the lengths of the major and minor axis of the ellipses respectively.

It may, however, be mentioned here that the above equation holds good if the inclination of the major axis of these ellipses is 45°. But during the anomalous variation of the angle of arrival this inclination is seldom found to be constant. On such occasions phase difference from these ellipses were calculated by the method suggested by Vincent[5].

THEORETICAL CONSIDERATIONS

(i) Change in the angle of arrival due to ionospheric tilt.

Let the transmitter and the receiver be situated at the points $T(-\tfrac{1}{2}D, O)$ and $R(\tfrac{1}{2}D, O)$ respectively in a right-handed rectangular coordinate system with y axis vertically upwards as shown in Fig. 1. Let the height of the reflecting layer be such that when this is horizontal the reflecting point is $P(O, h)$.

Let the surface of the ionosphere be plane but tilted through a small angle ψ about a horizontal axis. Then, the point of reflection will shift to P' the coordinate of which is $(-x_1, h)$. The slope of the ionospheric plane passing through P' is $\tan\psi$ which may be taken as ψ for small angles. Slope of the normal $P'O'$ through P' will then be $-1/\tan\psi = -1/\psi$.

Now $\tan T\hat{P}'O' = \tan O'\hat{P}'R$

or

$$\frac{-\frac{1}{\psi}-\frac{h}{D/2-x_1}}{1+\left(-\frac{1}{\psi}\right)\left(\frac{h}{D/2-x_1}\right)} = \frac{\frac{-h}{D/2+x_1}+\frac{1}{\psi}}{1+\frac{h}{\psi(D/2+x_1)}} \tag{2}$$

Solving and neglecting ψ^2,

$$\psi x_1^2 + x_1 h - \psi\left(h^2+\frac{D^2}{4}\right) = 0 \tag{3}$$

$$\therefore\quad x_1 = \frac{-h \pm \sqrt{h^2+4\psi^2(h^2+D^2/4)}}{2\psi} \tag{4}$$

$$= \frac{-h \pm h[1+2\psi^2(1+D^2/4h^2)]}{2\psi} \tag{5}$$

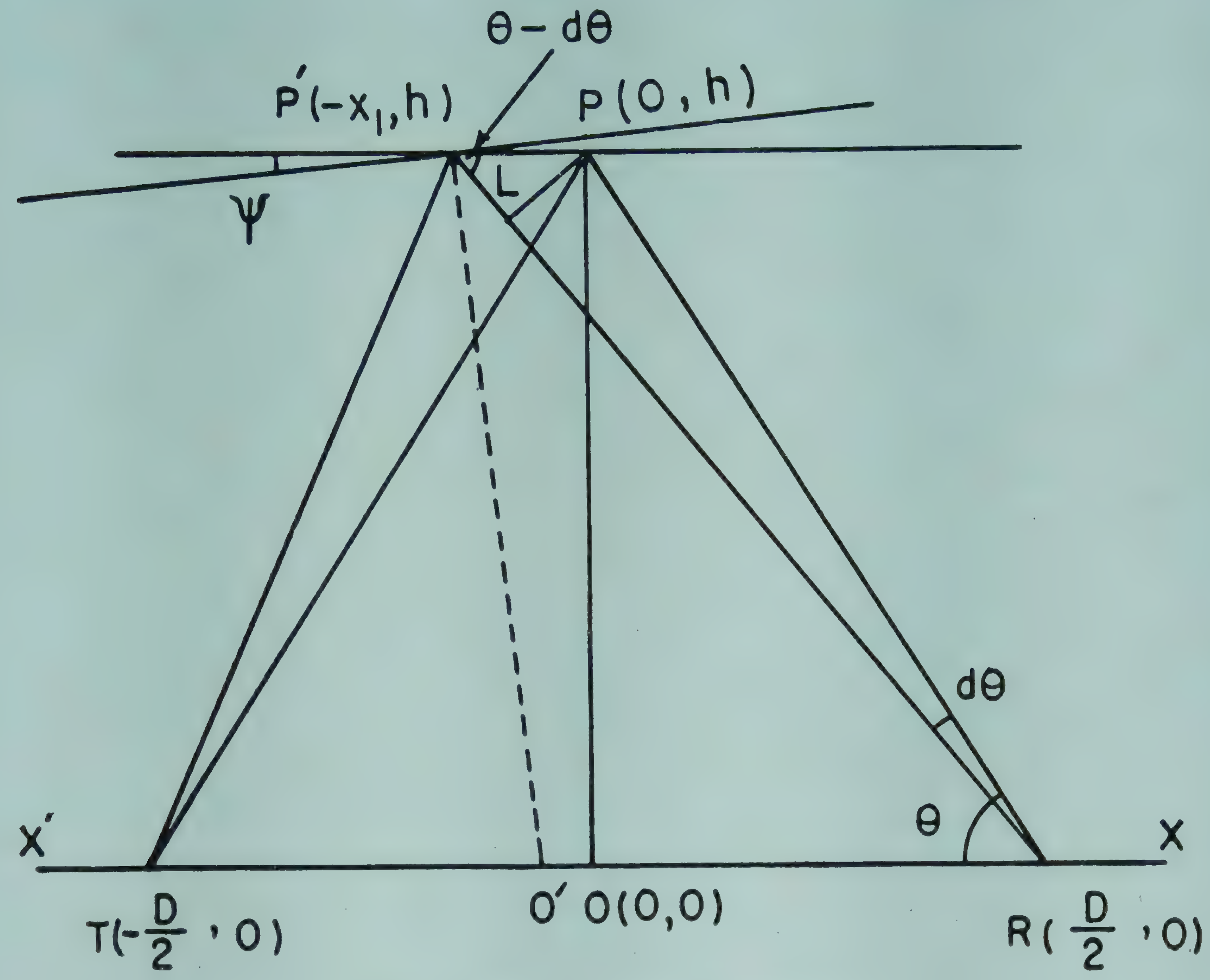

FIG. 1 — TILT IN THE IONOSPHERE

Accepting the +ve sign, the −ve sign being inadmissible we get

$$x_1 = \psi(h+D^2/4h) \tag{6}$$

$$= \psi\frac{\gamma^2}{h}, \quad \text{where } \gamma = RP = \frac{4h^2+D^2}{4}$$

Now $R\overset{\wedge}{P'}P = \theta - d\theta$ and $P'P \sin R\overset{\wedge}{P'}P = PL$, where PL is the perpendicular dropped on RP' from P.

$$\therefore \quad \psi\frac{\gamma^2}{h}[\sin(\theta - d\theta)] = \gamma d\theta \tag{7}$$

or

$$\frac{\psi\gamma^2}{h}\left[\frac{h}{\gamma} - \frac{D/2}{\gamma}d\theta\right] = \gamma d\theta \tag{8}$$

or

$$\psi = \frac{2hd\theta}{2h - Dd\theta} \tag{9}$$

(ii) Change in the angle of arrival due to undulations and method for calculation of their parameters.

Now let us imagine the ionosphere to contain sinusoidal undulations or ripples of wavelength λ and vertical amplitude A along the direction OX

in Fig. 1, the expressions for which have been derived below in terms of known parameters for the calculations.

Now the wave motion may be represented by Equation (10).

$$y = A \cos \frac{2\pi}{\lambda} (x \pm d) \tag{10}$$

where $d = nt\lambda$ determines the phase of the sine wave with respect to the coordinate axis and sign before it determines the direction of propagations.

The equation for the ionospheric undulation may be, therefore, written as

$$y = h + A \cos \frac{2\pi}{\lambda} (x \pm d) \tag{11}$$

If the system of ripples moves with a speed V along OX the substitution $d = nt\lambda = Vt$ gives the value of y in terms of x and t. Then the downward slope at $P'(x_1, y_1)$ on the ripple is given by

$$\tan \psi = \psi = dy/dx = \frac{2\pi A}{\lambda} \sin \frac{2\pi}{\lambda} (x_1 \pm d) \tag{12}$$

Now, as A is generally very small compared to λ (which has been subsequently shown), the height of the reflecting layer may be assumed to remain constant.

Then substituting the value of ψ from Equation (12) in Equation (6), we get

$$x_1 = \frac{2\pi A}{\lambda} \left(h + \frac{D^2}{4h} \right) \sin \left[\frac{2\pi}{\lambda} \cdot (x_1 \pm d) \right] \tag{13}$$

$$= \frac{2\pi A}{\lambda} \left(h + \frac{D^2}{4h} \right) \sin \alpha \tag{14}$$

where

$$\alpha = \frac{2\pi}{\lambda} (x_1 \pm d) \tag{15}$$

Then from Equation (15) we get

$$x_1 = \frac{\lambda}{2\pi} \left(\alpha \mp \frac{2\pi}{\lambda} \cdot d \right) \tag{16}$$

Comparing Equations (13) and (16) the following transcendental equation is obtained from which variation of sin α may be studied:

$$\sin \alpha = K \left[\alpha \mp \frac{2\pi}{\lambda} \cdot d \right] \tag{17}$$

where

$$K = \left[h + \frac{D^2}{4h} \right]^{-1} \times \frac{\lambda^2}{4\pi^2 A} \tag{18}$$

The variation of sin α with t, which is contained in d, for different values of K may be plotted from Equation (17) as shown in curves in Figs. 2–4.

Now the observed variations in the angles of arrival at R are proportional to x_1 which is proportional to sin α as shown in Equation (14). Thus that value of K for which sin α shows similar variations as in the angle of arrival will be chosen to determine the value of λ^2/A from Equation (18).

From Equation (18) we have

$$\frac{\lambda^2}{A} = 4\pi^2 K\,[h+D^2/4h] \tag{19}$$

From Equation (12), maximum value of ψ is $2\pi A/\lambda$ which will occur for maximum value of $d\theta$ (change in the angle of elevation) which may be represented by $d\phi$.

Therefore, from Equations (9) and (12) we get

$$\frac{2\pi A}{\lambda} = \frac{2hd\phi}{2h-Dd\phi} \tag{20}$$

From Equations (19) and (20), we get

$$\lambda = 2\pi K \frac{2hd\phi}{2h-Dd\phi}\left[h+\frac{D^2}{4h}\right] \tag{21}$$

and

$$A = K.\frac{(2hd\phi)^2}{(2h-Dd\phi)^2}\left[h+\frac{D^2}{4h}\right] \tag{22}$$

Thus from Equations (21) and (22), λ and A may be calculated.

(iii) Rapid fluctuations in the angle of arrival.

Bramley[6] has shown that for a single downcoming wave from the ionosphere it seems appropriate to consider a fairly narrow continuous angular distribution, symmetrical about some mean direction, θ_0, which may be deduced by smoothing out the rapid fluctuations which are assumed to be due to interference between the various component waves.

Bramley has shown that standard deviation of the angular spread of the downcoming waves α_0 is given by

$$\alpha_0 = \frac{\lambda\,|d\bar{\phi}|}{2\pi d \sin\theta_0} \tag{23}$$

where $|\bar{\phi}|$ = mean deviation of the phase difference in the two aerials. The above equation may also be written in terms of the variation in the angle of arrival.

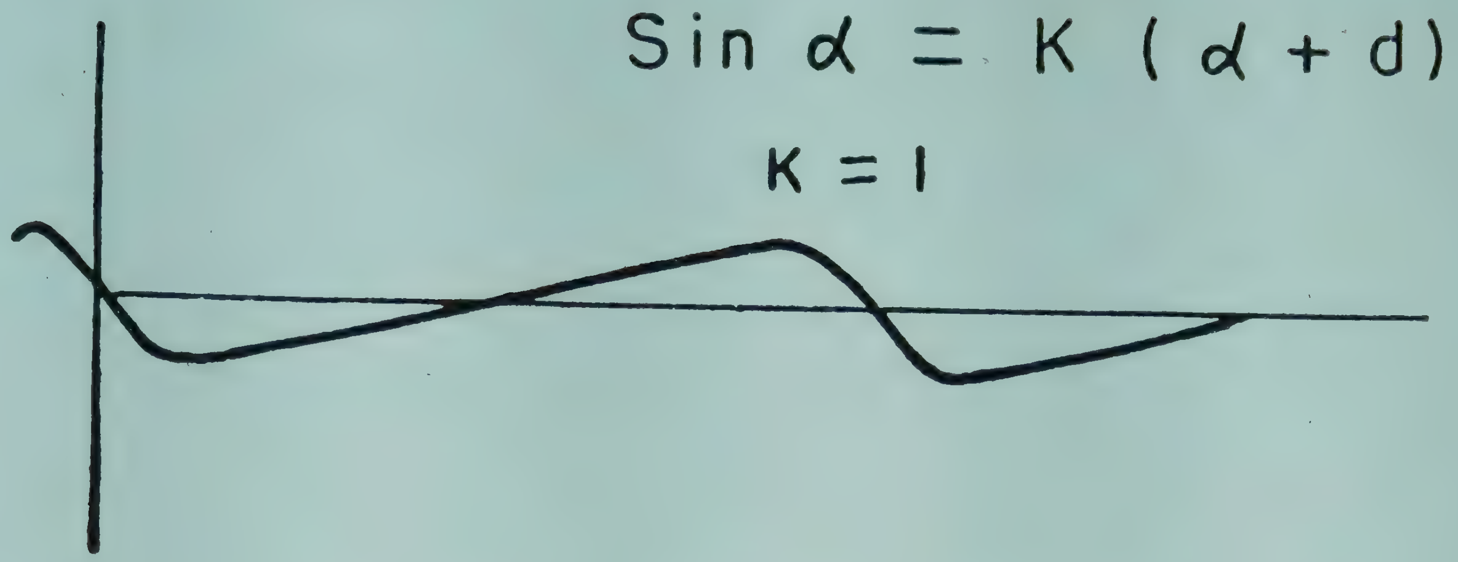

Fig. 2 — Variation of sin α with t

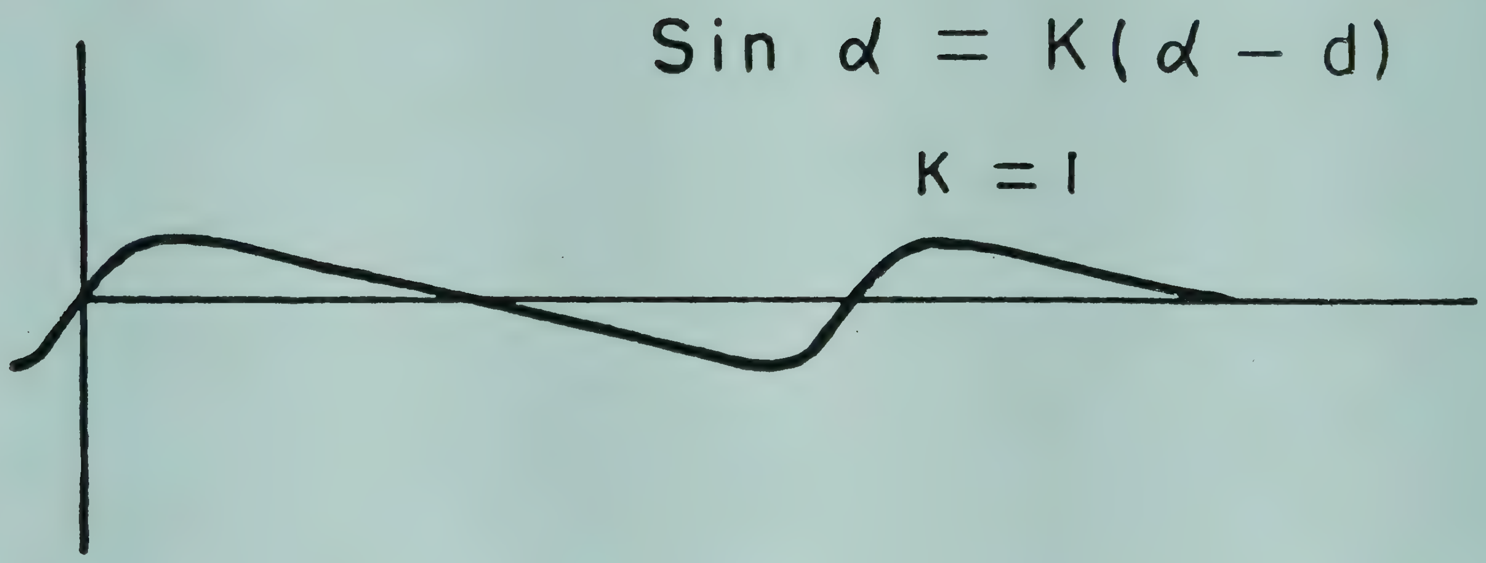

Fig. 3 — Variation of sin α with t

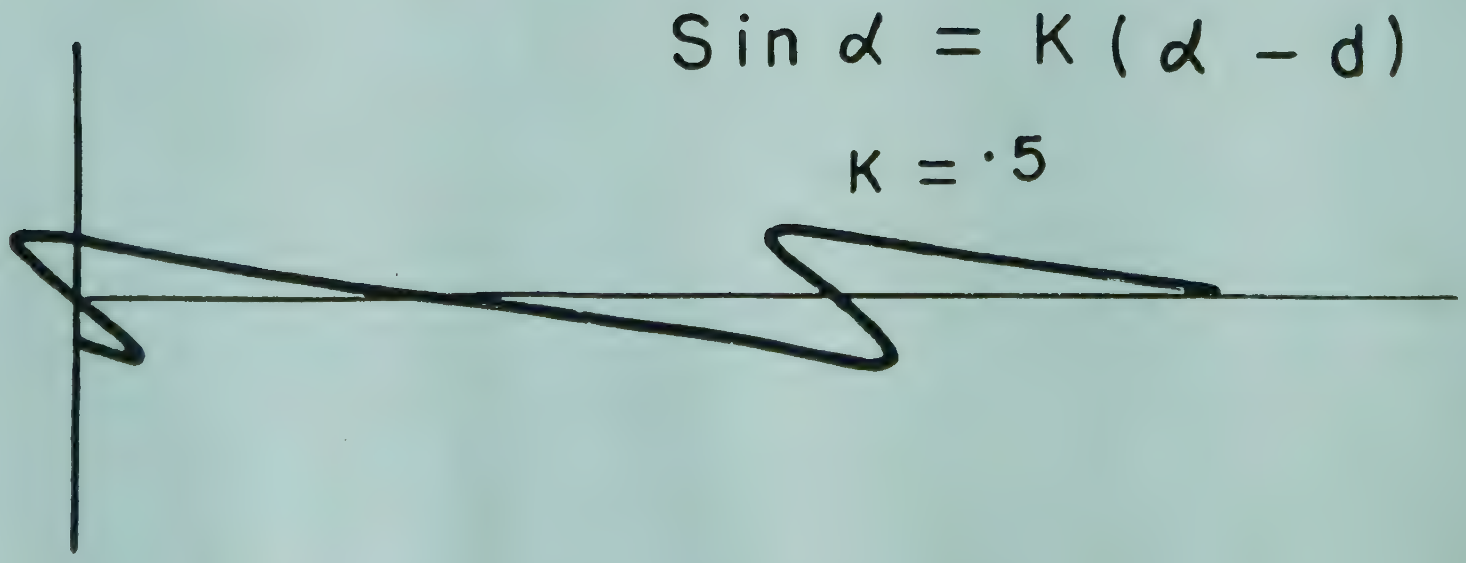

Fig. 4 — Variation of sin α with t

We know

$$\cos\theta_0 = \frac{\lambda}{2\pi d}\cdot\phi$$

Differentiating and neglecting sign,

$$d\theta = \frac{\lambda}{2\pi d\sin\theta_0}\cdot d\phi$$

$$\therefore\ |\overline{d\theta}| = \frac{\lambda}{2\pi d\sin\theta_0}\cdot|\overline{d\phi}|$$

$$=\alpha_0 \text{ from Equation (23)} \qquad (24)$$

∴ Arithmetic mean of the fluctuations in the angle of arrival gives the standard deviation of the angular spread α, which is an indication of the degree of roughness of the ionosphere at the frequency concerned.

(iv) Variation in the angle of arrival when more than one ray is incident on the aerial.

If more than one transmission paths be possible between the transmitter and the receiver, the voltage induced in the aerial P can be

$$y_1 = a_1\sin wt + a_2\sin(wt-\phi) \qquad (25)$$

where ϕ is the initial phase difference between the two transmission paths the number of which has been taken to be two only for simplicity. The voltage induced in the other spaced aerial

$$y_2 = a_1\sin(wt-\alpha)+a_2\sin(wt-\phi-\gamma) \qquad (26)$$

where $\alpha =$ phase difference due to spacing for rays following one transmission path, $\gamma =$ phase difference due to spacing for rays following the other transmission path.

Equation (25) may be written as

$$y_1 = a\sin(wt-\theta) \qquad (27)$$

where $$\tan\theta = \frac{a_2\sin\phi}{a_1+a_2\cos\phi}$$

and from Equation (26), $y_2 = A\sin(wt-\psi)$

where $$\tan\psi = \frac{a_1\sin\alpha+a_2\sin\beta}{a_1\cos\alpha+a_2\cos\beta}$$ taking $\phi+\gamma=\beta$.

Then phase difference between the waves in the two aerials is given by $\tan(\psi-\theta)$

$$=\frac{(a_1+a_2\cos\phi)(a_1\sin\alpha+a_2\sin\beta)-a_2\sin\phi(a_1\cos\alpha+a_2\cos\beta)}{(a_1\cos\alpha+a_2\cos\beta)(a_1+a_2\cos\phi)+a_2\sin\phi(a\ \sin\alpha+a_2\sin\beta)} \qquad (28)$$

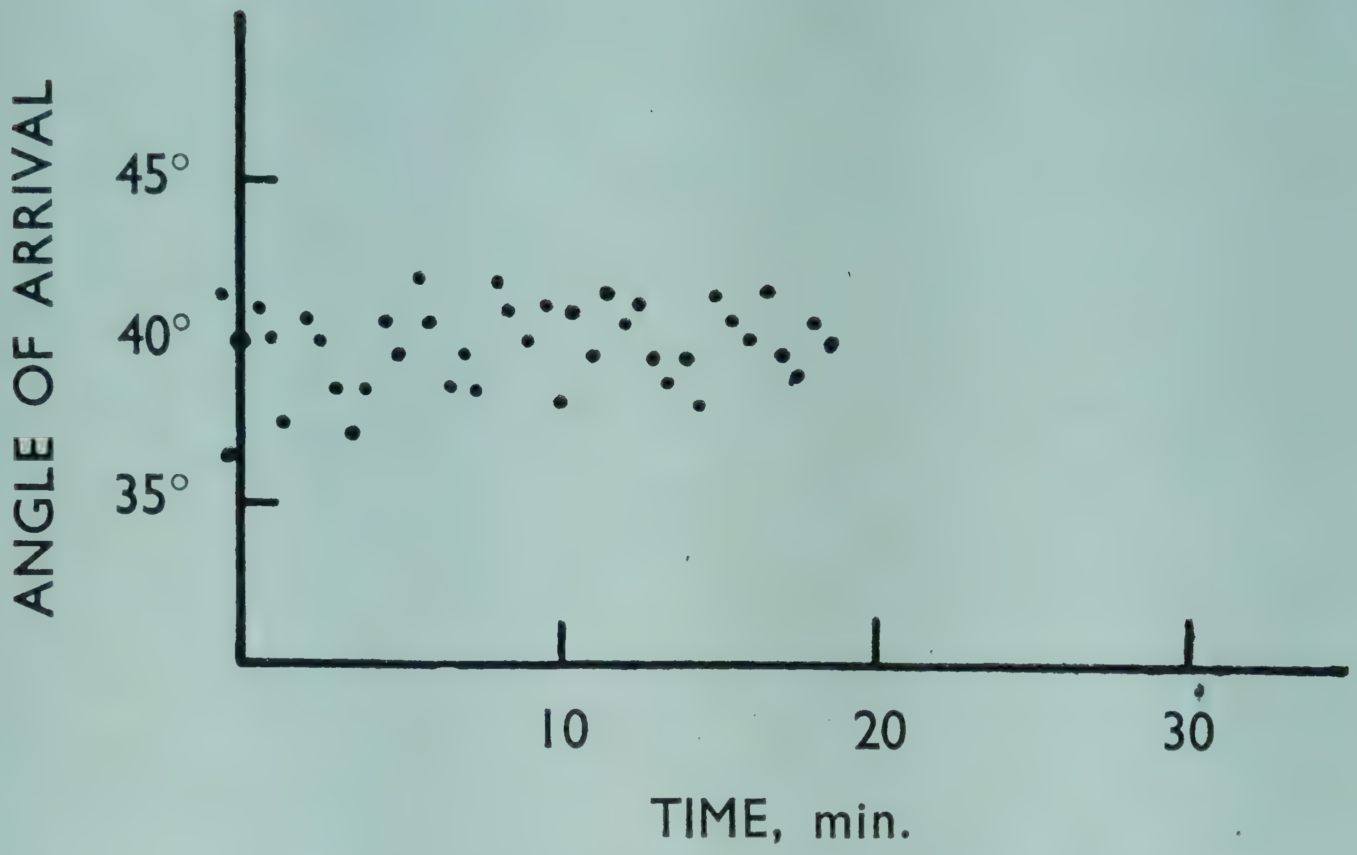

FIG. 5 — VARIATION OF ANGLE OF ELEVATION (ARRIVAL) WITH TIME

From Equation (28) it is clear that, when $a_2 = 0$

$(\psi-\theta) = \alpha$, i.e. the angle calculated from the resulting ellipse will correspond to that due to one transmission path and when $a_1 = 0$

$(\psi-\theta) = \gamma$, i.e. the angle calculated from the resulting ellipse will correspond to that due to the other transmission path.

In general when both types of transmissions are possible the resulting phase differences will be a function of relative amplitude a_1 and a_2 of the waves and angle of arrival will vary between two fixed angles corresponding to the two possible transmission paths.

Observations. Variation in the angle of arrival of single hop ordinary wave transmissions from Delhi at noon was studied from time to time. It was observed that angle of arrival undergoes slow changes which are of two types, random slow changes and periodic slow changes.

The rapid fluctuations have been always found superimposed on slow changes.

(i) Random slow changes: Angles were calculated from Equation (1), where $\lambda = 19{\cdot}86$ m. and $d = 23{\cdot}10$ m.

The phase ellipses were recorded photographically at an interval of 30 sec. and angles of elevation from ground showed variations with time a typical example of which has been shown in Fig. 5.

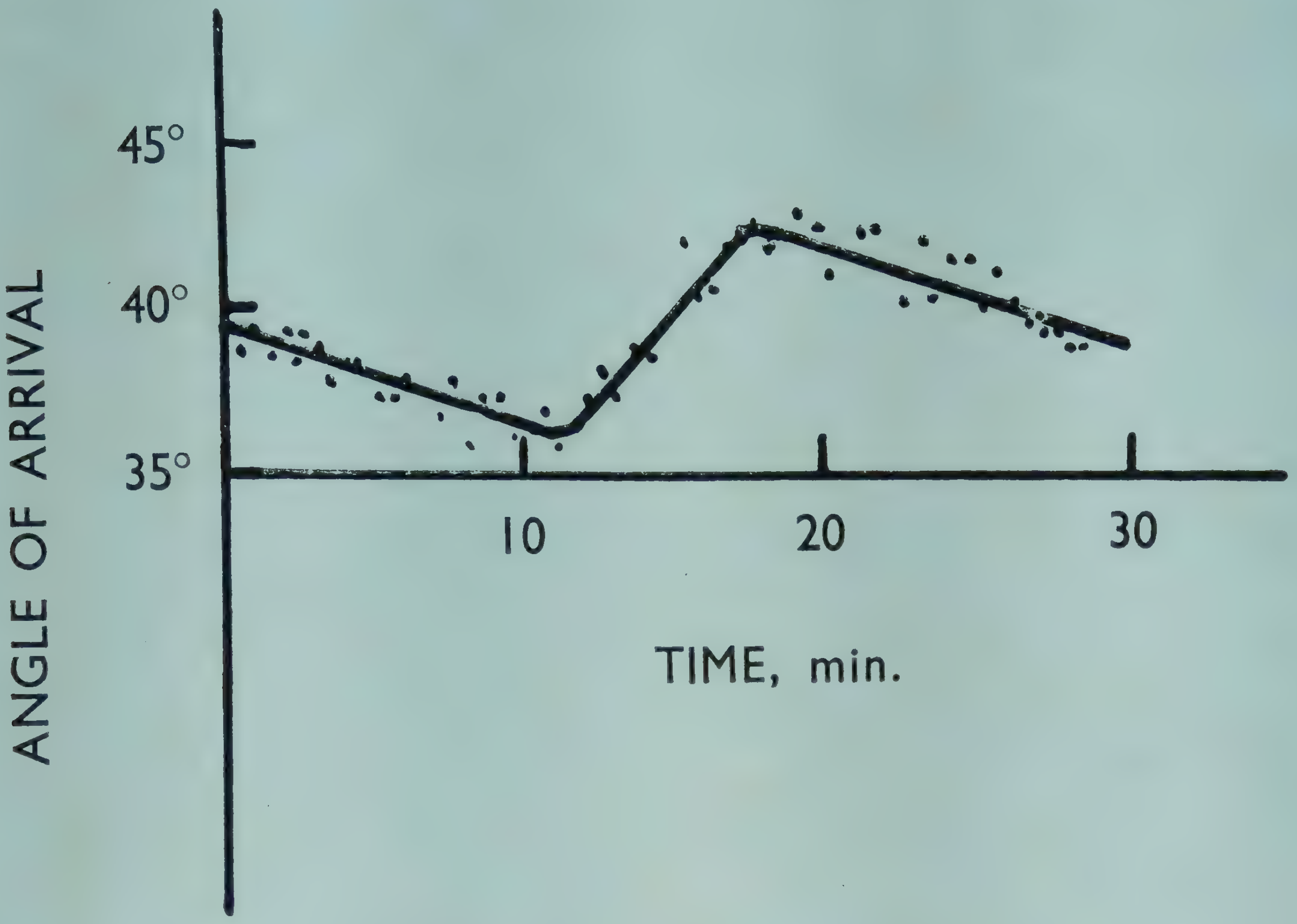

FIG. 6 — PERIODIC VARIATION OF ANGLE OF ARRIVAL WITH TIME

(ii) Periodic slow changes: Angles were calculated from Equation (1), where $\lambda = 19{\cdot}86$ m. and $d = 23{\cdot}10$ m.

The angles of elevation were calculated from photographed ellipses recorded at the interval of 30 sec. The periodic variations of the angle of arrival with time in a typical case has been shown in Fig. 6.

(iii) Rapid changes: Angles were calculated from Equation (1), where $\lambda = 19{\cdot}86$ m. and $d = 23{\cdot}10$ m.

In order to study the changes in greater detail the ellipses were photographed at an interval of 5 sec. One of the typical series of observations has been shown in Fig. 7.

(iv) Random variation due to multiple transmission path:

Theoretically the phase angles for different angles of arrival have been calculated from Equation (1) as shown in Table 1.

The angle of arrival for single and double hop transmissions for various ionospheric height lies in the range 35–40° and 60–65° respectively. Thus, when both are simultaneously received any angle between these two limits is possible and the resulting phase ellipses will be found to change orientation from one quadrant to the other as can be seen in Table 1. Such observations are shown in Fig. 8. Sometimes changes are wide and random but

TABLE 1 — PHASE ANGLES FOR DIFFERENT ANGLES OF ARRIVAL

ANGLE OF ARRIVAL *deg.*	PHASE DIFFERENCE	MINOR/MAJOR AXIS
65	176°55′	36·99
60	209°24′	3·8118
55	240°10′	1·7251
50	269°9′	1·01
45	296°6′	0·6236
40	320°42′	0·3571
35	342°47′	0·1515
30	362°35′	0·0224

ellipse does not change quadrant. In such cases the transmission by one of the hops is not absent but present with a feeble strength.

Calculation of the Undulation Parameters. Fig. 6 shows the observed periodic variation in the angle of elevation of radio waves with time. A number of theoretical curves were drawn from Equation (17) so as to fit in with the experimental curve. It was observed that observed variation resembled the theoretical curve shown in Fig. 3 plotted from the equation

$$\sin \alpha = \alpha - \frac{2\pi}{\lambda} \cdot d$$

which is obtained from Equation (17) by putting $K = 1$ and by taking negative sign before d. Also from the observed variations shown in Fig. 6, the value of $d\phi$ is found to be 3°. Average height of the ionosphere was taken to be 250 km. and the distance between the transmitter (Delhi) and the receiver (Banaras) was 680 km. Substituting these values in Equations (21) and (22), we get

$$\lambda = 247{\cdot}4 \text{ km. and } A = 8{\cdot}4 \text{ km.}$$

The period of the variations was found to be 28 min. as found from Fig. 6.

Thus, the speed of the travelling disturbances is given by

$$V = \frac{\lambda}{T} = 147{\cdot}2 \text{ m. per sec.}$$

The equation of curve 3 which resembles the observed variations in curve 6 shows that sign before d is negative which signifies a progressive wave travelling towards the negative side of the x axis from the origin. Thus the disturbance in our case was travelling from Banaras towards Delhi.

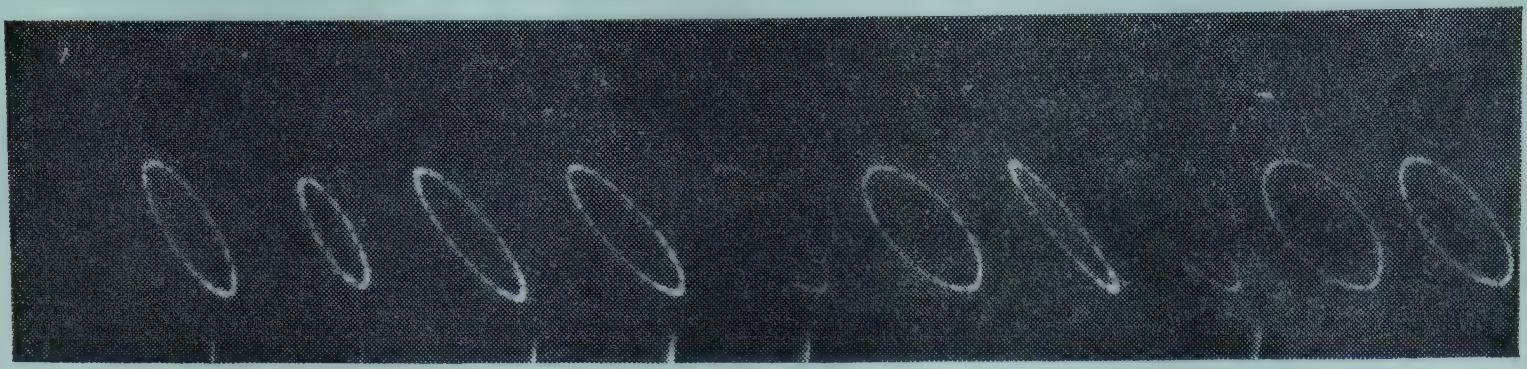

FIG. 7 — PHASE ELLIPSES AT INTERVALS OF 5 SECONDS

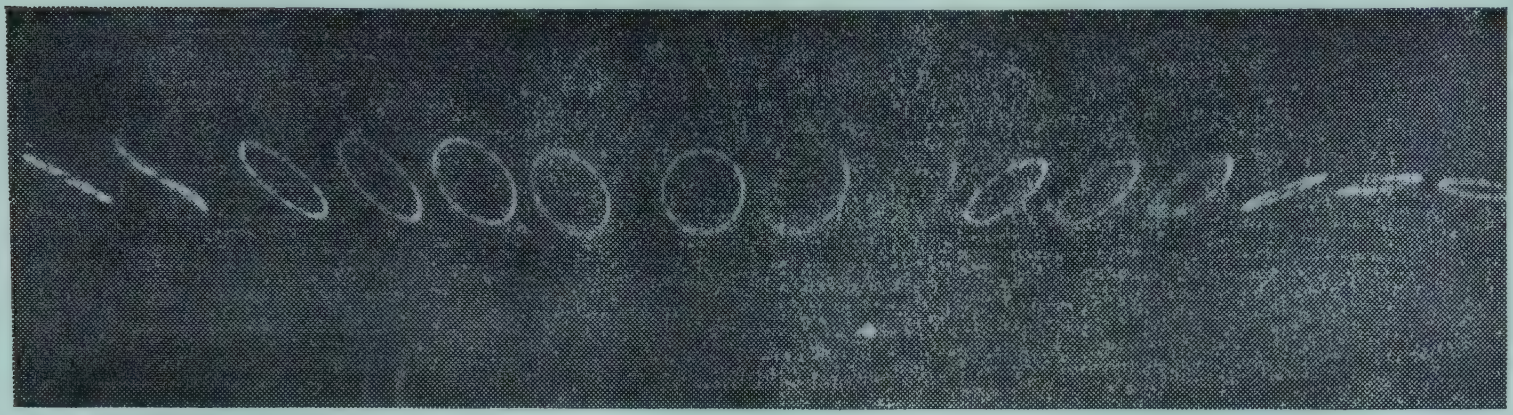

FIG. 8 — CHANGE OF ORIENTATION OF PHASE ELLIPSES

Calculation of the Angular Spread of the Downcoming Waves. The mean angle for the observation of Fig. 7 was found to have a mean value of 37·5°. The arithmetic mean of the deviations (neglecting sign) from this mean value of 37·5° for 37 observations was calculated to be 2°. The number of observations were deliberately restricted so as to eliminate the effect of slow changes on which these changes are supposed to be superimposed. Thus angular spread of the downcoming rays was found to be 2° as given by Equation (24).

SUMMARY

It has been observed that slow random variations in the angle of arrival of downcoming radio waves are due to tilts in the surface of the ionosphere and the periodic variations may be interpreted as the result of large scale ionospheric irregularities or undulations in the ionosphere which give rise to drift velocity in these regions. Various parameters of the undulations and the drift velocity have been calculated from these periodic variations in the angle of arrival. Assuming the incident wave to have a continuous narrow symmetrical distribution, the angular spread in these downcoming rays has been calculated from the rapid fluctuations in the angle of arrival. It is also shown that rotation of the ellipse in the absence of magneto-ionic interference may be explained on the basis of multiple hop transmission.

References

1. Bramley, E. N. & Ross, W., *Proc. roy. Soc.*, **207A** (1951), 251.
2. Bramley, E. N., *Proc. roy. Soc.*, **220A** (1953), 39.
3. Srivastava, J. P. & Rajan, V. D., *Indian J. Phys.*, **25** (1951), 287.
4. Wilkins, A. F., *J. Inst. elect. Engrs*, **74** (1934), 582.
5. Vincient, C. H., *Wireless Engineer*, (1956), 113.
6. Bramley, E. N., *Proc. Instn elect. Engrs*, **98** (1951), Pt III, 19.

Focussing effects due to large scale irregularities in F_2 layer

G. SIVARAMA SASTRY
T. SESHAGIRI RAO
M. KRISHNAMURTHI*

Department of Physics, Osmania University
Hyderabad

Prominent maxima observed in the level of cosmic radio noise records at a wavelength of ten metres have been interpreted as due to focussing effects caused by large scale lens-like formations in the F_2 layer. An approximate calculation has shown that their sizes lie in the range 60-240 km.

The irregularities of the ionosphere have been studied by two principal methods, one involving the reflection of radio waves transmitted from the earth and the other based on observations on the scintillations of radio sources. Mitra[1] and several later workers have used the spaced receiver method for the investigation of the drifts of small scale irregularities in the ionosphere. Experiments of Bramley and Ross[2] and Bramley[3], in which the angle of arrival of short radio waves reflected from the ionosphere is measured, have revealed the existence of large scale irregularities of the order of 50–400 km., moving with speeds up to 350 m./sec. Whitehead[4] has reported focussing effects due to irregularities of the order of 15 km. and travelling with an average velocity of about 100 m./sec.

The radio star scintillation method has been used among others by Ryle and Hewish[5], Little and Maxwell[6,7], Maxwell and Dagg[8], and Wild and Roberts[9]. Booker[10] has reviewed these observations and has shown that these radio scintillations are produced by irregularities of electron density, of the order of a kilometre. The purpose of the present communication is to report focussing effects due to large scale irregularities observed at a wavelength of 10 m. using the background cosmic radio noise instead of localized sources of such noise.

---

*Present address: Indian Institute of Science, Bangalore

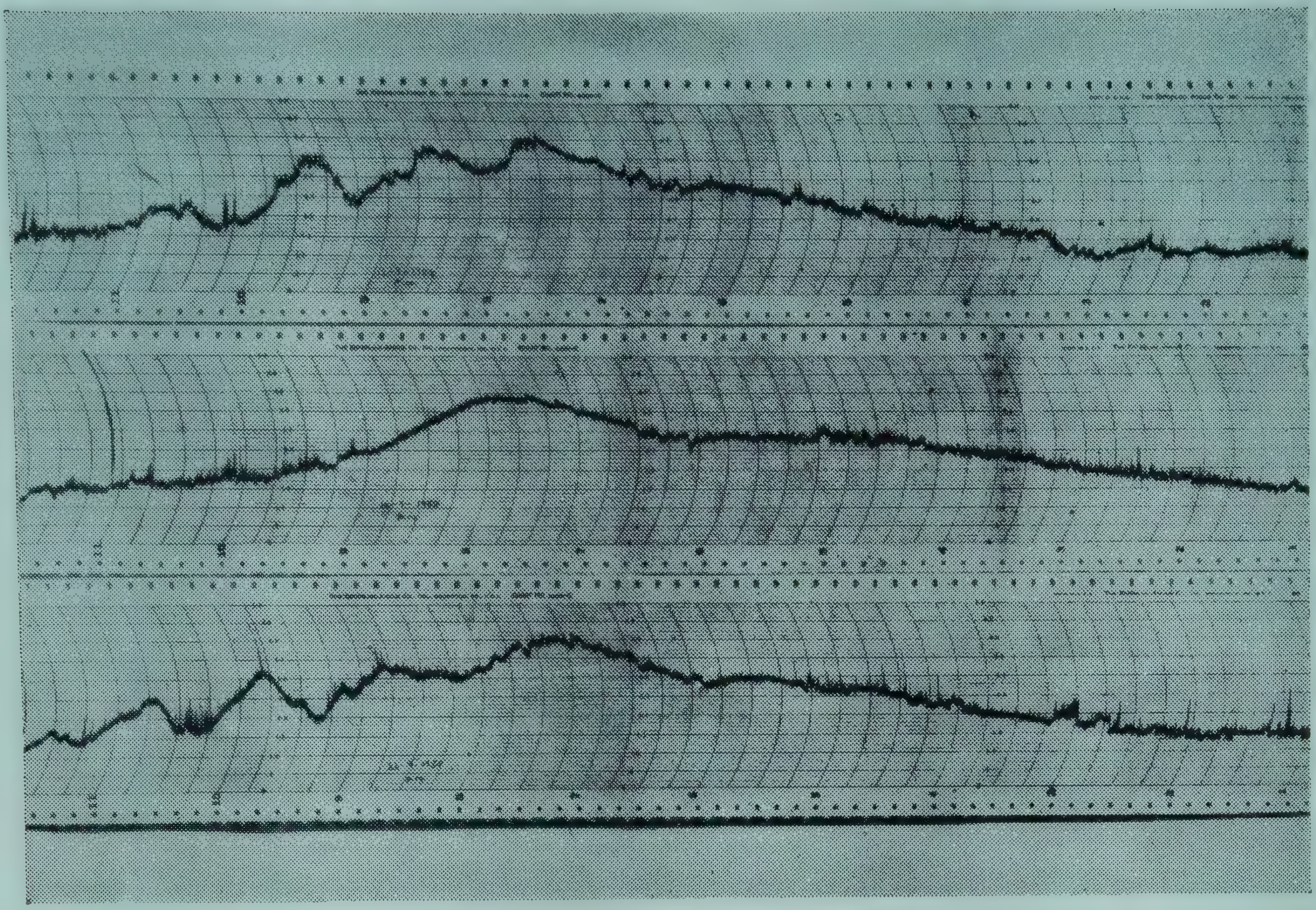

FIG. 1 — COSMIC NOISE RECORDS OBTAINED ON SEPTEMBER 12, 16 AND 22, 1958

EXPERIMENTAL SET-UP

The experimental set-up consists of a broadside array of 30 full-wave dipoles producing a half power beam-width of 8·4° in the E–W direction and 18° in the N–S direction and directed at the zenith. This aerial is connected to the input of a Marconi communication receiver type CR 150/3, the i.f. output of which is further amplified and detected. The d.c. output is fed to an Esterline Angus pen recorder through a GR type 715-AS2 d.c. amplifier. The gain of the receiving system is calibrated by a noise generator using a noise diode type CV 2171.

RESULTS AND DISCUSSION

The cosmic noise over a strip of the sky scanned by the aerial has been continuously recorded since January 1958. During certain winter nights in the years 1958 and 1959, it has been observed that soon after sunset the level of the cosmic noise goes through a number of prominent maxima. Fig. 1 shows the records obtained on September 12, 16 and 22, 1958. These records typically exhibit this phenomenon. The middle record obtained on September 16 is an undisturbed one, given for comparison. The number of maxima usually lies between four and six, generally occurring between sunset and midnight. The duration of each maximum is between 20 and 50 min.

Hewish[11], using a radio interferometer with phase switching arrangement, has studied the radio star scintillations on wavelengths of 6·7 and 8 m. and deduced that the size of the ionospheric irregularities is about 5 km. in the E–W direction. Wild and Roberts[9] have used the swept frequency interferometer to study the ionospheric irregularities. From the nature of dynamic spectra obtained by them, they conclude that the fluctuations are due to focussing effects by single lens-like formations rather than due to diffraction at a large number of irregularities. The size of the pattern on the ground is found to be lying in the range 1–6 km. during night in the E–W direction with a prevailing W–E motion of about 80 m./sec. Whitehead has shown that short-lived increases in the mean amplitude of the waves reflected from the F region of the ionosphere are the result of focussing effects caused by large scale distortions of the order of 15 km., moving horizontally. He has obtained an average value of 100 m./sec. for the velocity of these distortions which is of the same order as that for small scale irregularities reported by other workers.

The fluctuations in the level of the cosmic noise observed in the present work have to be regarded as focussing effects of travelling ionospheric irregularities of very large dimensions. The large scale irregularities observed here will have to cover most of the aerial beam to produce such pronounced effects as the magnitude of the maxima indicate. It is not possible to calculate the dimensions of the irregularities unless an assumption is made regarding their velocities and vice versa. Assuming, however, that (i) the irregularities are located at a height of 400 km. above ground and (ii) the irregularity has sufficient size to cover the entire beam area of the aerial array, the velocity of the irregularity can be estimated. The aerial beam covers a distance of about 60 km. in the E–W direction at a height of 400 km. If we assume the irregularity to have its linear dimension as 60 km. in the E–W direction and if it is travelling with a velocity V km./sec. in this direction, then the time T for which its effect can be observed will be given by $(60+60)/V = T$. Using this expression, and values of T ranging from 20 to 50 min., V is calculated to be in the region 40–100 m./sec. This compares well with velocities for smaller irregularities determined by other workers. On the other hand, assuming the velocity V to be 100 m./sec. the sizes of the irregularities come out to be in the range 60–240 km., for the observed times. It can, however, be seen that having three similar aerial arrays several kilometres apart in a triangle both the sizes of the irregularities and their velocities can be determined. This seems to be the most convenient method for the study of such large scale irregularities.

The occurrence of these irregularities only in winter months seems to be correlated with the behaviour of f_0F_2 at low latitudes during these months. Fig. 2 shows graphically the variation of mean f_0F_2 values during the night for the month of September 1958, at Delhi, Ahmedabad, Madras and

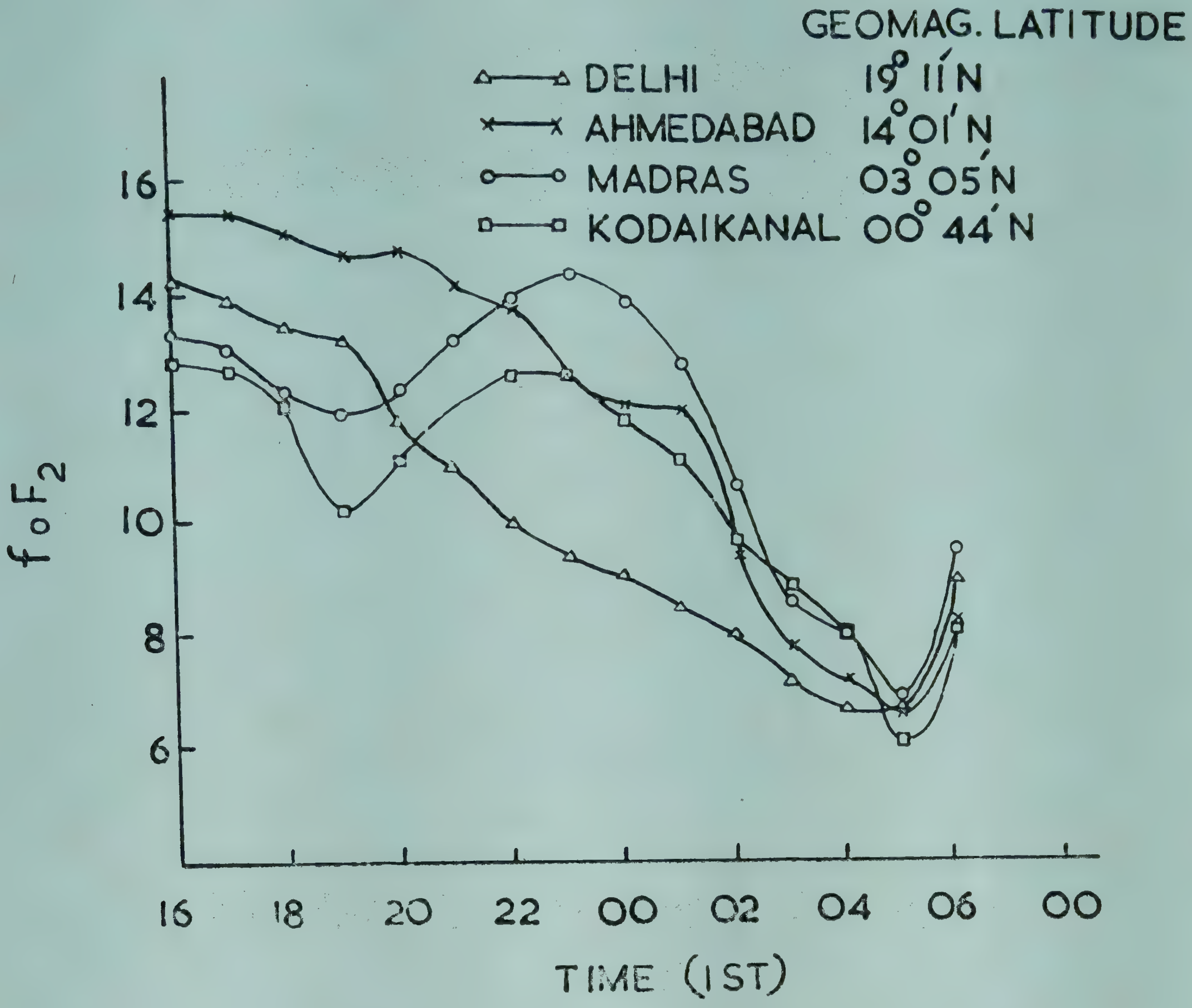

Fig. 2 — Variation of average values of f_0F_2 with time

Kodaikanal (taken from *Ionospheric Data* published by the Radio Research Committee). Both at Madras and Kodaikanal (low geomagnetic latitudes) these values go through a minimum between sunset and midnight, while at Delhi and Ahmedabad there is a regular decrease with time throughout the night. The time variations in f_0F_2 values with large gradients observed at the low latitudes indicate the corresponding large fluctuations in electron density leading to huge lens-like formations. Although such rapid fluctuations occur at the time ofs unrise the actual values of f_0F_2 are quite low and hence the electron densities are also too low to influence the high frequency radio waves. The focussing effects are generally found to occur on days when there are rapid fluctuations in f_0F_2 values. No quantitative correlation could, however, be made due to lack of data on f_0F_2 values at closer intervals.

References

1. Mitra, S. N., *J. Inst. elect. Engrs*, **96** (1949), 441.
2. Bramley, E. N. & Ross, W., *Proc. roy. Soc.*, **207A** (1951), 251.
3. Bramley, E. N., *Proc. roy. Soc.*, **220A** (1953), 39.
4. Whitehead, J. D., *J. atmos. terr. Phys.*, **9** (1956), 269.

5. Ryle, M. & Hewish, A., *Mon. Not. R. astr. Soc.*, **110** (1950), 381.
6. Little, C. G. & Maxwell, A., *Phil. Mag.*, **42** (1951), 267.
7. Little, C. G. & Maxwell, A., *J. atmos. terr. Phys.*, **2** (1952), 356.
8. Maxwell, A. & Dagg, M., *Phil. Mag.*, **45** (1954), 551.
9. Wild, J. P. & Roberts, J. A., *J. atmos. terr. Phys.*, **8** (1956), 55.
10. Booker, H. G., *Proc. Inst. Radio Engrs, N.Y.*, **46** (1958), 298.
11. Hewish, A., *Proc. roy. Soc.*, **214A** (1952), 494.

* * *

Ionospheric Propagation of Atmospherics. M. W. Chiplonkar & M. S. Hattiangadi, Department of Physics, Poona University, Poona.

The results of measurements of a number of waveforms of atmospherics in the frequency region 50 c/s. to 30 kc/s. observed at this station during April 1957 to December 1958 are analysed and presented. A large number of these waveforms show a multihop propagation. Though the height of the reflecting layer varies from 55 to 120 km., it lies most frequently between 80 and 90 km.

Similarly, the distance of the source of atmospherics varies from about 200 to 2000 km. The frequency distribution curve shows principal peaks at about 750 and 1750 km. with subsidiary peaks on either side of these. This trend is also shown by the individual monthly histograms for distances. Further, when separate histograms are drawn for distances which are associated with a height of 60 km. and those that are associated with a height of 90 km. it is found that the two principal peaks at 750 and 1700 km. are prominently shown by the 90 km. group alone and only the first peak is shown by the 60 km. group, thus indicating a preponderating role of the upper layer.

This statistical distribution of distances has been interpreted qualitatively with the help of Holingworth interference pattern of field strength.

When heights of the reflecting layers are plotted against the corresponding source distances, it is seen that the height of reflecting layer increases rapidly at first and then gradually reaches a limiting value around 95 km. However, there is evidence also to show the existence of two reflecting layers, one at about 60 km. and the other at about 90 km.

The reflection coefficient of the ionosphere varies from 0·4 to 0·9 or more. Occasionally, even smaller values up to 0·25 are also observed. It is higher in winter than in summer. (*Abstract*)

A Directional Study of Atmospherics for Climatology. M. W. Chiplonkar & T. A. Raju, Department of Physics, Poona University, Poona.

The direction of arrival of atmospherics at 0800, 1200, 1700 and 2100 hours in a small area around Sangli (about 400 miles) during July 1957 to December 1958 has been studied by means of a D.F. unit. The following results have been recorded:

(i) Very few atmospherics came from and around the bearings 0° and 180° except in December at 1700 hours.

(ii) A fairly large number of atmospherics came from the eastern bearings predominantly from 60 to 130° and only a few came from the western bearings.

(iii) There is a general increase in atmospherics arriving from northerly directions, especially from land masses, during the summer months; the most northerly pointing peak was obtained in August 1958.

(iv) A low percentage of noises is observed from the fourth quadrant (270–360°) during summer and a notable increase from directions in winter and rainy seasons.

(v) All the 2100 hours' curves show similarities of their maxima, and the seasonal changes in the positions of these maxima are only slight.

The studies have led to the conclusion that Sangli and areas to its west are less conducive to the formation of the convectional type of thunderstorms and that Sangli lies on a demarcation line which separates the areas to its west from those to its east perhaps because of the difference in the climates of these areas. In this connection attention is drawn to Koppen's work regarding the temperature zones of this part of the country which supports the above conclusion. (*Abstract*)

On the Law of Propagation of Atmospherics on 175 kc/s. M. W. Chiplonkar & T. A. Raju, Department of Physics, Poona University, Poona.

Studies made during 1959 and 1960 at Sangli with a D.F. unit working on 175 kc/s. seem to show that the variation of the field strength of atmospherics with the distance of their sources from Sangli during day-time follows three characteristics depending on whether the sources are near, at medium distance or very far from the D.F. The law followed in all these ranges seems to be a linear one, when the field strength is plotted on a logarithmic scale against the distance on a linear scale. They seem to correspond to the ground wave — the sky wave — and the diffraction wave range of the normal propagation of E.M. waves during day-time. The attenuation, in particular, in the near region is heavy. Considerable attenuation in the farthest region and less in the middle are exhibited. However, substantial variation in the field of the noises from similar distances in this region are noticed and are believed to be due to changes in the reflection coefficient of the ionosphere. (*Abstract*)

Flutter Fading of Short Wave Radio Signals in Equatorial Regions and its Connection with Spread Echoes, Magnetic Storms and the Radiation Belt. CHAMAN LAL, All India Radio, New Delhi [*J. Instn Telecomm. Engrs*, **6** (1960), 223].

The phenomena of spread echoes on vertical incidence ionospheric soundings and flutter fading on short wave C.W. transmissions are of frequent occurrence in low equatorial latitudes. Marked increase in the height of the F region of the ionosphere is almost a daily occurrence immediately after sunset, the height often ascending beyond 500–1000 km.

A physical explanation is offered for the origin of these two phenomena in terms of the Allen radiation belt, recently discovered from satellite explorations. This belt reaches down to a level of 500 miles or so from the surface of the earth. During its upward ascent, the F layer is likely to touch the lower fringe of this radiation belt and since this belt consists of high energy charged particles, turbulence and patchiness in ionization may set in in the ionospheric layer. The irregular ionization and the turbulence may manifest itself as spread echoes and flutter fading of radio waves reflected from the disturbed portions of the F region. The explanation receives additional support from the fact that both spread echoes and flutter fading are conspicuously absent at these latitudes during severe magnetic storms when the increase in the height of the F layer is inhibited and at times the F layer actually goes down appreciably. Various other observed characteristics of flutter fading and its relation to spread echoes have also been explained in terms of the Allen radiation belt in the exosphere. (*Abstract*)

APPENDIX 1

INDIAN IONOSPHERIC STATIONS AND THEIR PROGRAMME

STATION No.	STATION	VERTICAL INCIDENCE SOUNDINGS	ABSORPTION MEASUREMENTS		IONOSPHERIC WINDS	ATMOSPHERICS		SPECIAL IONOSPHERIC AND IONOSPHERIC TIDAL STUDIES
			Local transmitter	Extra terrestrial		Wave-form of atmospherics	Atmospheric radio noise	
E498	Delhi	×	×	×	×	×	×	—
E507	Banaras	×	—	—	×	×	—	×
E518	Ahmedabad	×	×	—	×	—	—	—
E521	Calcutta	×	×	—	×	—	—	—
E536	Bombay	×	—	—	—	—	—	—
E539	Poona	—	—	—	—	×	×	—
E541	Visakhapatnam-Waltair	×	×	—	×	—	—	—
E557	Madras	×	×	×	—	—	—	—
E565	Tiruchirapalli	×	—	—	—	—	—	—
E566	Kodaikanal	×	—	—	—	—	—	—
E603	Trivandrum	×	—	—	—	—	—	—

Note: × denotes stations where specific programmes given in column heads have been carried out.

APPENDIX 2

INDIAN IGY PUBLICATIONS ON IONOSPHERE

1. Aggarwal, K. K., Statistical analysis of fading on shortwave transmission. *J. Instn Telecomm. Engrs*, **5** (1959), 232.
2. Aiya, S. V. C., Atmospheric noise interference to shortwave broadcasting. *Proc. Inst. Radio Engrs, N.Y.*, **46** (1958), 580.
3. Aiya, S. V. C., Atmospheric noise interference to medium wave broadcasting. *Proc. Inst. Radio Engrs, N.Y.*, **46** (1958), 1502.
4. Aiya, S. V. C., Average power of impulsive atmospheric radio noise. *Proc. Inst. Radio Engrs, N.Y.*, **47** (1959), 92.
5. Aiya, S. V. C., Conversion data for atmospheric noise interference measurements. *J. sci. industr. Res.*, **17B** (1958), 337.
6. Aiya, S. V. C., Measurement and description of the characteristic of atmospheric radio noise. *J. sci. industr. Res.*, **18B** (1959), 44.
7. Aiya, S. V. C., Phadke, R. K., Padmanabhan, S. V. & Sane, C. K., Atmospheric radio noise levels at Poona in 2·5–20 Mc/s. band. *J. sci. industr. Res.*, **18B** (1959), 47.
8. Aiya, S. V. C. & Khot, C. G., Atmospheric noise interference in the standard broadcast band at Poona. *J. sci. industr. Res.*, **18B** (1959), 54.
9. Aiya, S. V. C., H.F. noise radiators in ground flashes of tropical lightning. *Proc. Inst. Radio Engrs, N.Y.*, **48** (1960), 955.

10. Aiya, S. V. C., Some aspects of tropical lightning. *J. Instn Telecomm. Engrs,* **4** (1958), 81.

11. Bandopadhyay, P., Electron distribution in the F layer of ionosphere over Haringhata (Calcutta) on quiet and disturbed days. *J. atmos. terr. Phys.,* **18** (1960), 132.

12. Bandopadhyay, P., Early morning E_2 layer and some evidence of pre-sunrise F layer "splitting". *J. atmos. terr. Phys.,* **16** (1959), 84.

13. Bandopadhyay, P. & Chatterjee, S. K., Decay of ionization below the F layer at night. *Indian J. Phys.,* **35** (1961), 240.

14. Bandopadhyay, P. & Chatterjee, S. K., Vertical transport of electron during pre-sunrise F layer "splitting". *Indian J. Phys.,* **45** (1962), 124.

15. Bhargava, B. N. & Subrahmanyan, R. V., Geomagnetic disturbance effects in equatorial E_s. *J. atmos. terr. Phys.,* **20** (1961), 81.

16. Bhargava, B. N. & Subrahmanyan, R. V., Movement in the F region of the ionosphere during solar eclipses. *Indian J. Met. Geophys.,* **11** (1960), 363.

17. Bhargava, B. N., Annual wave in the worldwide F region ionization. *Indian J. Met. Geophys.,* **10** (1959), 69.

18. Bhargava, B. N. & Gopala Rao, Y. V., Ionospheric disturbances associated with magnetic storms at Kodaikanal. *Indian J. Met. Geophys.,* **10** (1959), 203.

19. Bhonsle, R. V. & Ramanathan, K. R., Studies of cosmic radio noise at 25 Mc/s. at Ahmedabad. *J. sci. industr. Res.,* **17A** (1958), 40.

20. Chatterjee, B., Effects of obstacles and reflections on the propagation of VHF television signals. *J. Instn Telecomm. Engrs,* **6** (1959), 47.

21. Chiplonkar, M. W., Karekar, R. N., Raju, T. A. & Hattiangadi, M. S., A preliminary report on the nature and origin of atmospherics. *J. sci. industr. Res., Suppl.,* **17A** (1958), 3.

22. Das Gupta, P. & Vij, K. K., Statistical analysis of fading of a single downcoming wave. *J. atmos. terr. Phys.,* **18** (1960), 265.

23. Datta, S., On the electron production rate in the F_2 region of the ionosphere. *Indian J. Phys.,* **32** (1958), 483.

24. Datta, S. & Datta, R. N., Gyrofrequency in the ionospheric regions. *Indian J. Phys.,* **38** (1959), 316.

25. Datta, S., Bandopadhyay, P. & Datta, R. N., Ionospheric observations on the F region during the eclipse of April 19, 1958. *J. atmos. terr. Phys.,* **16** (1959), 182.

26. Datta, S., On the F_2 region of the ionosphere. *Indian J. Phys.,* **34** (1960), 66.

27. Ghosh, B. B. & Mitra, S. N., Thunderstorm activity and atmospheric noise in India. *Tech. Conv. Instn Telecomm. Engrs (India),* Dec. 1959.

28. Ghosh, S. N. & Nand, S., Ionization of E layer by X-rays. *Indian J. Phys.,* **34** (1960), 516.

29. Khastgir, S. R., Abnormal polarization of the atmospheric pulses reflected successively from the ionosphere. *Nature, Lond.,* **181** (1958), 1679.

30. Kotadia, K. M., Meteors and E_s ionization. *J. sci. industr. Res.,* **17A** (1958), 46.

31. Kotadia, K. M., Sporadic F over Ahmedabad during the half sunspot cycle 1953–57. *Proc. Indian Acad. Sci.,* **50A** (1959), 259.

32. Kotadia, K. M. & Ramanathan, K. R., Geomagnetic and ionospheric disturbances in the lower latitudes. *Ann. IGY,* **11** (1961), 68.

33. Krishnamurthi, M., Sastry, G. S. & Rao, T. S., Radio emission from the sun at 30 Mc/s. *J. sci. industr. Res.,* **17A** (1958), 71.

34. Kundu, M. R., Time relationship of metre-wave and 3 cm. wave bursts. *Nature, Lond.,* **183** (1959), 1047.

35. Kundu, M. R., A new high resolution interferometers for solar studies. *J. Instn Telecomm. Engrs,* **5** (1959), 77.

36. Lakashmi Bai, C., Effect of thickness of ionospheric layer on the separation of magneto-ionic split echoes. *J. sci. industr. Res.,* **17B** (1958), 83.

37. Mathur, S. B. & Mitra, A. P., The upper atmosphere and outer space: Part I — Densities, temperature and concentration of atmospheric constituents from 130 to 1000 km. *J. sci. industr. Res.*, **19A** (1960), 311.
38. Mazumdar, S. C., An automatic recorder for measuring ionospheric absorption. *J. Instn Telecomm. Engrs*, **4** (1958), 81.
39. Mitra, A. P., Night-time ionization in the lower ionosphere: Part I — Recombination process. *J. atmos. terr. Phys.*, **10** (1957), 140.
40. Mitra, A. P., Night-time ionization in the lower ionosphere: Part II — Distribution of electrons and positive ions and negative ions. *J. atmos. terr. Phys.*, **10** (1957), 153.
41. Mitra, A. P., The International Geophysical Year — the world programme, 1957–58. *J. sci. industr. Res.*, **16A** (1957), 327.
42. Mitra, A. P., The International Geophysical Year — the world programme. *J. Instn Telecomm. Engrs*, **3** (1957), 198.
43. Mitra, A. P., The Indian programme for the International Geophysical Year: Part I — Some results of the programme on ionosphere. *J. sci. industr. Res.*, **17A** (1958), 395.
44. Mitra, A.P., Sarada, K. A., Sarma, N. V. G. & Joshi, M. N., Radio patrol of solar flares. *J. sci. industr. Res.*, **17A** (1958), 74.
45. Mitra, A. P., Ionospheric disturbances at low latitudes. *J. sci. industr. Res.*, **17A** (1958), 34.
46. Mitra, A. P., Time and height variations of the day-time dissipative processes in the ionosphere: Part I — A noon-time model of the ionosphere loss coefficient from 60 to 600 km. over middle latitudes. *J. geophys. Res.*, **64** (1959), 733.
47. Mitra, A. P., Ionospheric effects of solar flares: Part I — Evaluation of experimental data. *Sci. Rep. ionos. Res. Lab. Pensyl. St. Univ.*, No. 112, 1958.
48. Mitra, A. P. & Sarada, K. A., Determination of the electron content of the outer ionosphere from measurements of cosmic radio noise absorption. *Radio Res. Com. Sci. Rep.* (Council of Scientific & Industrial Research, New Delhi), 1961, No. 147.
49. Mitra, A. P., Ionospheric effects of solar flares: Part II — Ionization model. *Sci. Rep. ionos. Res. Lab. Pensyl. St. Univ.*, No. 142, 1960.
50. Mitra, A. P., Recombination processes in the ionosphere. *Sci. Rep. ionos. Res. Lab. Pensyl. St. Univ.*, No. 147, 1961.
51. Mitra, A. P., IGY symposium. *J. sci. industr. Res.*, **20A** (1961), 409.
52. Mitra, S. N. & Rao, B. C. N., Effect of annular solar eclipse of April 19, 1958 (at sunrise) on the F_2 region of the ionosphere. *Indian J. Phys.*, **33** (1959), 540.
53. Mitra, S. N. & Vij, K. K., Geomagnetic field and ionospheric drift. *J. Instn Telecomm. Engrs*, **6** (1959), 90.
54. Mitra, S. N., Vij, K. K. & Dass Gupta, P., Horizontal drift in the ionosphere and Delhi. *J. atmos. terr. Phys.*, **19** (1960), 172.
55. Mitra, S. N. & Ghosh, B. R., Measurement of atmospheric noise. *J. Instn Telecomm. Engrs*, **5** (1958), 2.
56. Mitra, S. N., Some investigations on longwave propagation. *J. Instn Telecomm. Engrs*, **5** (1959), 121.
57. Mitra, S. N. & Ghosh, B. B., On the need for revision of noise grades for India. *J. Instn Telecomm. Engrs*, **5** (1959), 194.
58. Murty, Y. S. N., Polarization characteristics of radiowave propagation in the ionosphere. *Sci. & Cult.*, **25** (1959).
59. Murty, Y. S. N. & Khastgir, S. R., Polarization characteristic of downcoming radiowaves. *Proc. nat. Inst. Sci. India*, 1959.
60. Murty, Y. S. N., Singh, R. N. & Khastgir, S. R., Ionospheric absorption and electronic collisional frequency in the F region. *J. sci. industr. Res.*, **18A** (1959), 507.

61. Murty, Y. S. N. & Khastgir, S. R., General expression for the group refractive index of the ionosphere. *J. atmos. terr. Phys.*, **21** (1960), 65.

62. Parthasarthy, R., The effect of mutual impedance due to the neighbouring elements on the driving point impedances of a linear array. *J. Instn Telecomm. Engrs*, **5** (1957), 242.

63. Parthasarthy, R. & Sarada, K. A., A high sensitive frequency receiver for galactic noise (study development news), I.T.E., March 1958.

64. Ramana, K. V. V. & Rao, B. R., Investigation of ionospheric absorption on 5–6 Mc/s. at Waltair. *J. atmos. terr. Phys.*, **22** (1961), 1.

65. Ramanathan, K. R. & Bhonsle, R. V., Cosmic radio noise at 25 Mc/s. and F scatter at Ahmedabad. *J. geophys. Res.*, **64** (1959), 1635.

66. Rao, B. R. & Rao, E. B., Investigation of ionospheric drifts in F region over Waltair. *C.R. du* 3^e congress *de la F.*1 *G.S.A., Tanarive*, **A** (1957), 71.

67. Rao, B. R. & Rao, E. R., Horizontal ionospheric drifts in the F_2 region at equatorial latitudes. *Nature, Lond.*, **181** (1958), 1612.

68. Rao, B. R. & Ramana, K. V. V., Diurnal variation of absorption on 5–6 Mc/s. at Waltair during IGY. *J. sci. industr. Res.*, **17A** (1958), 56.

69. Rao, B. R. & Rao, E. R., Study of horizontal drifts in the F_1 and F_2 regions of the ionosphere at Waltair (17°43′N : 88°18′E, mag. lat. 9°30′N). *J. atmos. terr. Phys.*, **14** (1959), 94.

70. Rao, B. R., Rao, E. B. & Pant, P. R. R., Effects of magnetic activity on drifts of the F_2 region. *Nature, Lond.*, **183** (1959), 667.

71. Rao, B. R. & Ramana, K. V. V., Variation in height of anisotropy and random drift velocity of the irregularities in the ionosphere. *Nature, Lond.*, **190** (1961), 706.

72. Rao, B. R. & Rao, R. R., A new type of ionospheric drift recorder. *J. atmos. terr. Phys.*, **21** (1961), 208.

73. Rao, B. R., Rao, M. G. S. & Murty, D. S., Periodic fading in oblique incidence shortwave transmission. *Indian J. Phys.*, **35** (1961), 475.

74. Rao, B. V. T. & Rao, M. K., Ionospheric absorption over Delhi. *J. Instn Telecomm. Engrs*, **4** (1958), 205.

75. Rao, C. S. R. & Bhargava, J. C., M.U.F. factor and solar activity. *Indian J. Phys.*, **34** (1960), 85.

76. Rao, C. S. R. & Ranganathan, T. N., Ionosphere over Trivandrum: Part I. *J. Instn Telecomm. Engrs*, **6** (1960), 161.

77. Rao, C. S. R. & Bose, S. C., Ionosphere over Trivandrum: Part III. *J. Instn Telecomm. Engrs*, **7** (1961).

78. Rao, C. S. R. & Sain, M., Total electronic content of the F_2 layer at Madras during 1959. *J. Instn Telecomm. Engrs*, **8** (1962), 177.

79. Rao, C. V. S. & Mitra, S. N., Spread F and geomagnetic activity. *J. geophys. Res.*, **67** (1962), 127.

80. Rao, C. V. S., Ionosphere over Trivandrum: Part IV — Spread F over Trivandrum.

81. Rao, E. B. & Rao, B. R., Diurnal variation of F region drifts at Waltair. *Curr. Sci.*, **30** (1961), 9.

82. Rao, E. B. & Rao, B. R., Travelling disturbances in the F region over Waltair. *J. atmos. terr. Phys.*, **20** (1961), 296.

83. Rao, E. B. & Rao, B. R., Horizontal drifts in the ionosphere in relation to random fading. *J. sci. industr. Res.*, **20B** (1961), 301.

84. Rao, M. K., A wireless remote control unit. *J. Instn Telecomm. Engrs*, **6** (1960), 265.

85. Rao, M. K., Mazumdar, S. C. & Mitra, S. N., Ionospheric absorption over Delhi during IGY and IGC. *J. atmos. terr. Phys.*, **24** (1962), 245.

86. Rao, M. N. & Mitra, A. P., Effect of vertical drifts on the nocturnal ionization of the lower ionosphere. *J. atmos. terr. Phys.*, **18** (1958), 271.

87. Rao, M. S. V. G., Rao, B. R. & Pant, P. R. R., Correlation of spread F activity with F region height changes. *J. atmos. terr. Phys.*, **17** (1960), 345.

88. Rao, M. S. V. G., Rao, B. R. & Pant, P. R. R., Fading of C.W. signals as a means of spread F study. *Curr. Sci.*, **9** (1960), 304.

89. Rao, M. S. V. G. & Rao, B. R., Effect of equatorial spread F on C.W. transmission. *Canad. J. Phys.*, **39** (1961), 396.

90. Rao, M. S. V. G. & Rao, B. R., Equatorial spread F in relation to post-sunset height changes and magnetic activity. *J. geophys. Res.*, **66** (1961), 2113.

91. Rao, M. S. V. G. & Rao, B. R., Nocturnal and seasonal variation of equatorial spread F. *J. atmos. terr. Phys.*, **22** (1961), 12.

92. Rao, R. R. & Rao, B. R., Horizontal drifts in the E region at Waltair. *Nature, Lond.*, **185** (1960), 27.

93. Rao, R. R. & Rao, B. R., Study of horizontal drifts in the E region at Waltair. *J. atmos. terr. Phys.*, **22** (1961), 81.

94. Rao, R. R. & Rao, B. R., Height gradient of horizontal drifts in the E region over Waltair. *J. atmos. terr. Phys.*, **22** (1961), 158.

95. Reddy, C. A. & Rao, B. R., Polarization characteristics of E_s echoes at Waltair. *J. atmos. terr. Phys.*, **24** (1962), 401.

96. Rastogi, R. G., A study of noon-time critical frequencies of E and F_1 layers of the ionosphere. *Geofis. pur. appl.*, **40** (1958), Part II, 145.

97. Rastogi, R. G., Geomagnetic effects in F_1 and F_2 layers of the ionosphere. *J. atmos. terr. Phys.*, **14** (1959), 33.

98. Sachdev, D. K., Study of the atmosphere radio noise at 27 and 100 kc/s. at Delhi. *J. sci. industr. Res.*, **17A** (1958), 262.

99. Sachdev, D. K., Low frequency atmospheric radio noise over Delhi, a preliminary report. *Radio Res. Com. Sci. Rep.* (Council of Scientific & Industrial Research, New Delhi), No. 7.

100. Saha, A. K., Ionospheric irregularities and propagation at frequencies above the classical M.U.F. *J. Instn Telecomm. Engrs*, **5** (1959), 136.

101. Sarada, K. A., Sudden cosmic noise absorption associated with the solar event of March 23, 1958. *J. atmos. terr. Phys.*, **13** (1958), 192.

102. Sarada, K. A. & Mitra, A. P., Measurement of cosmic noise absorption at Delhi at 22·4 Mc/s. URSI Monograph No. 1, URSI Secretariat (Elsevier Publishing Co., Amsterdam), 1960, 270.

103. Satyanarayan, S., Bhakru, K. & Khastgir, S. R., Triple splitting of the F echoes. *J. atmos. terr. Phys.*, **13** (1959), 201.

104. Sethuraman, R., Measurement of ionospheric drift at Ahmedabad on 2·6 Mc/s. and 4·0 Mc/s. *Proc. Indian Acad. Sci.*, **42A** (1958), 84.

105. Sethuraman, R., Rates of fading of reflected pulses of electromagnetic waves at Ahmedabad on 2·6 Mc/s. and 4·0 Mc/s. *J. sci. industr. Res.*, **17A** (1958), 50.

106. Shirke, J. S., Ionospheric absorption on 2·5 Mc/s. at Ahmedabad. *Proc. Instn Telecomm. Engrs*, **5** (1959), 115.

107. Singh, R. N. & Murty, Y. S. N., Dispersion, absorption and polarization curves for radio wave propagation through the ionosphere. *J. sci. Res., Banaras Hindu Univ.*, **9** (1959).

108. Singh, R. N. & Khastgir, S. R., Study of winds in the F region of the ionosphere during the unusual days in the IGY calendar. *J. atmos. terr. Phys.*, **16** (1959), 376.

109. Singh, R. N. & Murty, Y. S. N., Limiting polarization curves for radio wave propagation in ionosphere. *Curr. Sci.*, **27** (1958), 161.

110. Somayjulu, Y. V. & Rao, N. N., Observations on galactic radiation at 30 Mc/s. *J. sci. industr. Res.*, **17A** (1958), 54.

111. SRIVASTAVA, R. S. & KHASTGIR, S. R., Studies of the waveforms of atmospherics during the regular world days and world meteorological intervals. *J. sci. industr. Res.*, **18A** (1959), 426.

112. SURYANARYANA, R. K., Effect of radio fade-out on the F_2 layer. *J. atmos. terr. Phys.*, **24** (1961), 57.

113. TANDON, J. N., Oscillations of rotating cosmical bodies in the presence of magnetic field. *Indian J. Phys.* (1958).

114. TANTARY, B. A. P. & SRIVASTAVA, R. S., Waveforms of atmospherics showing smooth wave train of nearly constant quasi-period. *Sci. & Cult.*, **23** (1958), 373.

115. TANTARY, B. A. P., Automatic recorder of the waveforms of atmospherics. *Indian J. Phys.*, **32** (1958), 267.

116. TANTARY, B. A. P. & SRIVASTAVA, R. S., Waveforms of atmospherics. *Proc. nat. Inst. Sci. India*, **24A** (1958), 217.

117. TANTARY, B. A. P. & SRIVASTAVA, R. S., Waveforms of atmospherics with superimposed pulses recorded with the automatic atmospherics recorder. *J. atmos. terr. Phys.*, **13** (1958), 38.

118. TANTARY, B. A. P. & SRIVASTAVA, R. S., Preliminary studies of the energy spectrum of near atmospherics over the frequency range 3–15 kc/s. *J. sci. industr. Res.*, **17B** (1958).

119. VENKATESWARLU, P. & SATYANARAYAN, R., Some studies on sporadic E. *J. sci. industr. Res.*, **20B** (1961), 8.

120. VENUGOPAL, V. R., Sunrise effect in the F region of the ionosphere over Kodaikanal. *Indian J. Met. Geophys.*, **10** (1959), 325.

121. VENUGOPAL, V. R., Variation of the F_2 layer ionization with solar activity at Kodaikanal on magnetically disturbed and quiet days. *Bull. Kodaikanal Obs.*, **51** (1959), 1.

AUTHOR INDEX

Banerjee, S. S.— 221
Bhagiratha Rao, E.— 96, 205
Bhargava, B. N.— 197
Bhonsle, R. V.— 117, 220
Bose, S. C.— 70

Chaman Lal — 239
Chiplonkar, M. W.— 218, 237, 238

Dasgupta, P.— 95, 97
Degaonkar, S. S.— 218

Hattiangadi, M. S.— 237

Kamal, I. R.— 64
Karekar, R. N.— 218
Kotadia, K. M.— 176
Krishnamurthi, M.— 212, 233

Mahajan, K. K.— 57
Mazumdar, S. C.— 132
Mitra, A. P.— 1, 57, 98, 158
Mitra, S. N.— 95, 132, 219
Mukherjee, P. K.— 221

Raghava Rao, R.— 72, 96, 171, 202
Raju, T. A.— 238
Ramachandra Rao, B.— 72, 80, 96, 149, 155, 157, 171, 202, 205
Ramakrishna, S.— 212
Ramana, K. V. V.— 80, 149, 155, 157
Ramana Murty, Y. V.— 155, 205
Ramanathan, K. R.— 176, 220
Ranganathan, T. N. — 70
Rangaswamy, S.— 40
Rao, C. S. R.— 40, 70
Rao, C. V. S.— 219
Rao, M. K.— 132

Sarada, K. A.— 98, 158
Satyanarayanmurthy, Ch.— 48
Seshagiri Rao, T.— 233
Setty, C. S. G. K.— 64
Shirke, J. S.— 142
Singh, R. N.— 85
Sivarama Sastry, G.— 233
Subrahmanyan, R. V.— 197

Vij, K. K.— 95, 97, 219

Scientific & Research Library
No. 271
7 JAN 1985
C.F.T.R.I. Experiment Station. LUDHIANA-6

C.F.T.R.I. LIBRARY, MYSORE – 13

Acc.No. 271

Call No. A (F) N62·1

Please return this publication on or before the last DUE DATE stamped below to avoid incurring overdue charges.

Due date	*Return Date*	*Due Date*	*Return Date*

Acc. No. ૨૭૧